

1995

## The synthesis, characterization, and application of ether-containing polyimides

Catharine Croall Fay  
*College of William & Mary - Arts & Sciences*

Follow this and additional works at: <https://scholarworks.wm.edu/etd>

 Part of the [Polymer Chemistry Commons](#)

---

### Recommended Citation

Fay, Catharine Croall, "The synthesis, characterization, and application of ether-containing polyimides" (1995). *Dissertations, Theses, and Masters Projects*. Paper 1539623875.  
<https://dx.doi.org/doi:10.21220/s2-j7ep-4j35>

This Dissertation is brought to you for free and open access by the Theses, Dissertations, & Master Projects at W&M ScholarWorks. It has been accepted for inclusion in Dissertations, Theses, and Masters Projects by an authorized administrator of W&M ScholarWorks. For more information, please contact [scholarworks@wm.edu](mailto:scholarworks@wm.edu).

## **INFORMATION TO USERS**

**This manuscript has been reproduced from the microfilm master. UMI films the text directly from the original or copy submitted. Thus, some thesis and dissertation copies are in typewriter face, while others may be from any type of computer printer.**

**The quality of this reproduction is dependent upon the quality of the copy submitted. Broken or indistinct print, colored or poor quality illustrations and photographs, print bleedthrough, substandard margins, and improper alignment can adversely affect reproduction.**

**In the unlikely event that the author did not send UMI a complete manuscript and there are missing pages, these will be noted. Also, if unauthorized copyright material had to be removed, a note will indicate the deletion.**

**Oversize materials (e.g., maps, drawings, charts) are reproduced by sectioning the original, beginning at the upper left-hand corner and continuing from left to right in equal sections with small overlaps. Each original is also photographed in one exposure and is included in reduced form at the back of the book.**

**Photographs included in the original manuscript have been reproduced xerographically in this copy. Higher quality 6" x 9" black and white photographic prints are available for any photographs or illustrations appearing in this copy for an additional charge. Contact UMI directly to order.**

# **UMI**

**A Bell & Howell Information Company  
300 North Zeeb Road, Ann Arbor, MI 48106-1346 USA  
313/761-4700 800/521-0600**



THE SYNTHESIS, CHARACTERIZATION, AND APPLICATION OF ETHER-  
CONTAINING POLYIMIDES

---

A Dissertation

Presented to

The Faculty of the Department of Applied Science  
The College of William and Mary in Virginia

In Partial Fulfillment

Of the Requirements for the Degree of  
Doctor of Philosophy

---

by

Catharine Croall Fay

1995



**UMI Number: 9616919**

---

**UMI Microform 9616919**  
**Copyright 1996, by UMI Company. All rights reserved.**

**This microform edition is protected against unauthorized  
copying under Title 17, United States Code.**

---

**UMI**  
**300 North Zeeb Road**  
**Ann Arbor, MI 48103**

APPROVAL SHEET

This dissertation is submitted in partial fulfillment of  
the requirements for the degree of

Doctor of Philosophy

Catharine Croall Fay  
Author

Approved, December 1995

Robert A. Orwoll

Robert A. Orwoll, Professor of Chemistry

Terry L. St. Clair

Terry L. St. Clair, Adjunct Professor of Applied Science, NASA-LaRC

Richard L. Kiefer

Richard L. Kiefer, Professor of Chemistry

Dorothy Silver Reilly

Dorothy Silver Reilly, Assistant Professor of Biology

Jeffrey A. Hinkley

Jeffrey A. Hinkley, Adjunct Assc. Professor of Applied Science, NASA-LaRC

Daniel P. Henkel

Daniel P. Henkel, Adjunct Assc. Professor of Applied Science

***This dissertation is dedicated to my husband Jim, for his love, support, and confidence throughout this endeavor.***

## Table Of Contents

	Page
Acknowledgments.....	x
List Of Tables.....	xii
List Of Figures.....	xiii
Abstract.....	xx
Chapter 1: Introduction.....	2
1.1 References.....	8
Chapter 2: Statement Of Research.....	11
Chapter 3: Literature Review.....	14
3.1 Introduction.....	14
3.2 Two-Step Method For Polyimide Synthesis.....	15
3.3 Rate Of Polymerization.....	17
3.4 Factors Influencing The Molecular Weight Of Poly (Amic Acids).....	18
3.5 Side Reactions.....	18
3.6 Chain-Chain Interactions.....	19
3.7 Thermal Imidization Of Poly (Amic Acids).....	22
3.8 Chemical Conversion Of Poly (Amic Acids) To Polyimides	24
3.9 One-Step Method For Polyimide Synthesis.....	26
3.10 Other Synthetic Routes To Polyimides.....	26
3.11 Structure-Property Relationships Of Polyimides.....	27
3.11.1 Thermal Stability.....	27
3.11.2 Hydrolytic Stability.....	29
3.11.3 Radiation Resistance.....	30
3.11.4 Glass Transition Temperature.....	31
3.11.5 Crystallinity.....	34

## Table of Contents

	<b>Page</b>
3.11.6 Solubility. ....	35
3.11.7 Polyimide Color. ....	36
3.11.8 Dielectric Constant. ....	37
3.11.9 Coefficient Of Thermal Expansion. ....	39
3.12 Molecular Orientation (Film Stretching). ....	39
3.12.1 Introduction. ....	39
3.12.2 Film Preparation And Drawing Techniques. ....	40
3.12.3 Stretching Parameters. ....	41
3.12.4 Properties Influenced By Stretching.. ....	42
3.13 Molecular Modeling. ....	44
3.14 Properties And Applications Of Some Commercial Polyimide Films. ....	45
3.15 Potential Liquid Crystalline Polyimides As Processing Aids. ....	50
3.15.1 Introduction. ....	50
3.15.2 Liquid Crystalline Mesophases. ....	50
3.15.3 Molecular Architecture. ....	53
3.15.4 Rheology. ....	56
3.15.5 Characterization Of Liquid Crystalline Polymers. . .	57
3.15.6 Properties Of Liquid Crystalline Polymers. ....	60
3.15.7 General Applications. ....	62
3.15.8 State-Of-The-Art Liquid Crystalline Polymers. ....	63
3.16 Liquid Crystalline Polyimides. ....	67
3.17 Polyimides For Microelectronic Applications. ....	68
3.17.1 Encapsulants. ....	69

## Table of Contents

	Page
3.17.2 Polyimides As Interlayer Dielectrics. . . . .	71
3.18 Polyimides For Harsh Environments . . . . .	73
3.18.1 Wire And Cable Insulation. . . . .	73
3.18.2 Radiation-Resistant Polyimides . . . . .	74
3.18.3 Squaric Acid Containing Polyimides. . . . .	76
3.19 References . . . . .	77
Chapter 4: Experimental. . . . .	85
4.1 Potential Liquid Crystalline Polyimides. . . . .	85
4.1.1 Starting Materials . . . . .	85
4.1.2 Preparation Of Dimethoxy Compounds. . . . .	89
4.1.3 Preparation Of Bisphenols By Demethylation. . . . .	92
4.1.4 Preparation Of Bisphenols Via Hydrolysis. . . . .	93
4.1.5 Synthesis Of Diether Dianhydrides . . . . .	99
4.1.6 Two-Step Polyimide Synthesis. . . . .	110
4.1.7 Preparation Of BMDEDA/ <i>p</i> -PDA Polymer Powders. . . . .	111
4.1.8 Extruded Ribbons And Rods. . . . .	111
4.1.9 Molecular Orientation (Film Stretching). . . . .	112
4.2 Polyimides For Microelectronic Applications. . . . .	113
4.2.1 Low Dielectric, Fluorinated Polyimides. . . . .	113
4.2.1.1 Starting Materials . . . . .	113
4.2.1.2 Preparation Of Monomers For Low Dielectric Fluorinated Polyimides. . . . .	114
4.2.1.3 Polymer Synthesis. . . . .	119
4.2.1.4 Films . . . . .	119
4.2.2 Polyimides As Encapsulants . . . . .	120

## Table of Contents

	<b>Page</b>
4.2.2.1 Starting Materials. . . . .	120
4.2.2.2 Polymer Synthesis . . . . .	121
4.2.2.3 Films. . . . .	122
4.2.2.4 Solubility . . . . .	122
4.3 Polyimides For Harsh Environments.. . . .	123
4.3.1 Hydrolytically Stable Polyimides. . . . .	123
4.3.1.1 Polymer Synthesis . . . . .	125
4.3.1.2 Films. . . . .	125
4.3.1.3 Alkaline Solution Exposure. . . . .	125
4.3.2 Electron Radiation-Resistant Polyimides . . . . .	128
4.3.2.1 Starting Materials. . . . .	128
4.3.2.2 Polymer Synthesis . . . . .	129
4.3.2.3 Polymer Films. . . . .	130
4.3.2.4 Electron Radiation Exposure . . . . .	130
4.4 References. . . . .	132
Chapter 5: Characterization. . . . .	133
5.1 Elemental Analysis. . . . .	133
5.2 Melting Point Determination. . . . .	133
5.3 Mass Spectrometry. . . . .	134
5.4 Inherent Viscosity. . . . .	134
5.5 Thermal Analysis. . . . .	136
5.6 Melt Viscosity. . . . .	136
5.7 Transmission UV-VIS Spectra. . . . .	137
5.8 Dielectric Constant. . . . .	137

## Table of Contents

	<b>Page</b>
5.9 Tensile Properties .....	137
5.10 Density .....	139
5.11 X-Ray Diffraction. ....	139
5.12 Saturation Moisture Content Measurements. ....	141
5.12.1 Polyimides As Encapsulants. ....	141
5.12.2 Hydrolytically Stable Polyimides. ....	141
5.13 Positron Lifetime Measurements. ....	142
5.14 Molecular Orientation (Film Stretching). ....	142
5.15 References. ....	144
Chapter 6: Results And Discussion. ....	145
6.1 Potential Liquid Crystalline Polyimides. ....	145
6.1.1 Introduction. ....	145
6.1.2 Synthesis. ....	146
6.1.3 Characterization Of Potential Liquid Crystalline Polyimides. . ....	148
6.2 Polyimides for Microelectronic Applications. ....	183
6.2.1 Low Dielectric, Fluorinated Polyimides. ....	183
6.2.2 Polyimides as Interlayer Dielectrics and Encapsulants. ....	189
6.3 Polyimides for Harsh Environments. ....	210
6.3.1 Hydrolytically Stable Polyimides. . ....	210
6.3.2 Radiation-Resistant Polyimides. ....	227
6.4 References. ....	245
Chapter 7: Applications. ....	249



## Table of Contents

	Page
7.1 Potential Liquid Crystalline Polyimides. . . . .	249
7.1.1 Repairable Adhesives. . . . .	249
7.2 Polyimides For Microelectronic Applications. . . . .	250
7.2.1 Stress Relief Layers, Dielectrics, and Encapsulants. . . . .	251
7.2.2 Pacemakers. . . . .	252
7.3 Polyimides For Harsh Environments. . . . .	254
7.3.1 Hydrolytically Stable Polyimides. . . . .	254
7.3.2 LaRC™-IA Wire Insulation. . . . .	255
7.3.3 Capacitance Humidity Sensor. . . . .	255
7.4 Radiation-Resistant Polymers. . . . .	260
7.5 References. . . . .	262
Chapter 8: Conclusions. . . . .	264
8.1 Potential Liquid Crystalline Polyimides As Processing Aids. . . . .	264
8.2 Polyimides For Microelectronic Applications. . . . .	266
8.3 Polyimides For Harsh Environments. . . . .	268
8.4 Papers And Presentations . . . . .	269
8.5 References. . . . .	273
Appendix. . . . .	274

## Acknowledgments

I would like to express my sincere gratitude to my dissertation advisor, Bob Orwoll, for accepting me into the program and into his research group and for his technical support, guidance, and encouragement. My graduate experience has been very memorable. I would like to thank my director of research, Terry St. Clair, for encouraging me to go back to school, helping me develop a research project, and for the opportunity to work on many projects because of my association with the Composites and Polymers Branch at NASA's Langley Research Center. This experience has been very valuable. My appreciation is also extended to my committee members, Dan Henkel, Dorothy Silver Reilly, Jeffrey Hinkley, and Dick Kiefer for their support and contributions to my dissertation.

I would like to thank Lockheed Engineering and Sciences Company for tuition reimbursement during 1991-1993 and NASA's Langley Research Center for funding this research. I also wish to acknowledge the companies who provided free chemicals for this research: Occidental Chemical Corporation (NY), Kwoya Hakko Kogyo (Japan), Central Glass Co., Ltd (Japan), and Mitsui Toatsu Chemicals (Japan).

Further thanks are extended to the Composites and Polymers Branch personnel at NASA's Langley Research Center and the supporting technicians and contractors for making their facilities and technical expertise available, as well as the many words of encouragement received. I have enjoyed working with you all, and have appreciated your assistance. In particular, I would like to express my sincere appreciation to John Connell and Steve Havens, who took the time early in my chemistry career and graduate studies to help me gain confidence and acquire good techniques to conduct research. I would like to

also thank some of my other co-workers for their assistance throughout the years: James Dezern, Joe Smith, Brian Jensen, Trish McDaniel, and Anne St. Clair. Special thanks are extended to James Dezern, Gilda Miner, and Scott Warrington for all their computer assistance. I would like to thank Will Schwartz (Occidental Chemical Corporation, NY) for developing the novel synthetic route for diether dianhydrides used in my research as well as his willingness to share information or make suggestions.

In closing, I wish to thank my husband, Jim, for the extra efforts he made over the past five years so I could continue my education. Thank you for fixing wonderful dinners, and taking care of the house and yard so I could concentrate on my studies. I wish to thank my family, especially my parents, Marion and Patrick Croall, who were with me in spirit every step of the way. Even though my siblings (all ten of them: Stephen, Mary Margaret, Bridget, Paul, Gregory, Michael, Marian, Patrick, Thomas, and Matthew) and my husband's family have been very supportive, I wish to especially thank my sister, Bridget Quinby, for her unconditional emotional support. I will always remember your encouragement and I hope you know how much it meant to me.

## List Of Tables

<b>Table</b>		<b>Page</b>
4.1	Structures And Acronyms Of Monomers Used In The Synthesis Of Potential Liquid Crystalline Polyimides . . . . .	88
4.2	Monomers Used For The Synthesis Of Polyimides As Encapsulants. . . . .	121
4.3	Commercially Available Films For Hydrolytically Stable Polyimides. . . . .	123
4.4	Dianhydrides And Diamines For Potential Hydrolytically Stable Polyimides. . . . .	124
4.5	Structures And Acronyms Of Monomers Used For Synthesis Of Radiation-Resistant Polyimides. . . . .	129
6.1	Physical Properties Of Polyimides. . . . .	211
6.2	Thermal Analysis Data Of Polyimide Films. . . . .	211
6.3	Thermal Analysis Of LaRC™ Squaric Acid Polyimides. . . . .	232
8.1	Best Candidates For Interlayer Dielectrics And Encapsulant Applications. . . . .	267

## List Of Figures

Figure		Page
3.1	Synthesis Of The First Aromatic Polyimide. . . . .	14
3.2	Polyimide Synthesis By Heat Fusion Of Salt Type Intermediates. . . . .	15
3.3	Reaction Mechanism For Two-Step Polyimide Synthesis . .	16
3.4	Formation Of The Polyimide Precursor. . . . .	17
3.5	Electron Affinities Of Commercial Dianhydrides. . . . .	20
3.6	Ionization Potentials Of Selected Diamines. . . . .	21
3.7	Reaction Mechanism For Thermal Imidization Process. . . .	23
3.8	Mechanism For Chemical Imidization. . . . .	25
3.9	Stress-Strain Curve For Amorphous PET Film. . . . .	43
3.10	Kapton®. . . . .	46
3.11	Upilex® R. . . . .	47
3.12	Upilex® S. . . . .	48
3.13	Apical®. . . . .	48
3.14	Novax®. . . . .	49
3.15	Ultem®. . . . .	49
3.16	Polymer Conformations In Solid And Liquid Phases. . . . .	52
3.17	Three Liquid Crystalline Structures. . . . .	53
3.18	Main Chain And Side Chain LC Configurations. . . . .	55
3.19	LC Material DSC Thermogram. . . . .	58
3.20	Kevlar® LCP. . . . .	64
3.21	Nomex® LCP. . . . .	65
3.22	Xydar® LCP. . . . .	66
3.23	Three Basic Polymers Of Vectra® LCP. . . . .	67

## List Of Figures

Figure		Page
4.1	General Preparation Of Aromatic Dimethoxy Compounds By Friedel-Crafts Acylation. . . . .	89
4.2	General Method For Preparation Of Bisphenols By Demethylation Reaction. . . . .	92
4.3	Hydrolysis Of Aromatic Dihalides. . . . .	94
4.4	General Synthesis Of Aromatic Diether Dianhydrides. . . . .	99
4.5	Two-Step Polyimide Synthesis. . . . .	110
4.6	Normal And Rolled Configurations For Chemical Exposure Of Polyimide Films . . . . .	126
4.7	Twisted Configuration For Chemical Exposure Of Polyimide Films. . . . .	127
5.1	Ostwald Type Viscometer. . . . .	135
5.2	Density Gradient Column. . . . .	140
6.1	Polymer Characterization Of 1,3-BBBDA/ <i>p</i> -PDA. . . . .	149
6.2	Polymer Characterization Of 1,4-BBBDA/ <i>p</i> -PDA. . . . .	149
6.3	BMDEDA/ <i>p</i> -PDA Polyimides. . . . .	153
6.4	Polymer Characterization Of LC-PI From Mitsui Toatsu. . . . .	154
6.5	Mechanical Properties Of BMDEDA/ <i>p</i> -PDA And The Analogous LC-PI. . . . .	155
6.6	Annealing Evaluation Of BMDEDA/ <i>p</i> -PDA. . . . .	157
6.7	Polymer Characterization Of BMDEDA/ <i>p</i> -PDA Powders. . . . .	159
6.8	Characterization Of 1,3-BAPDBB/PMDA. . . . .	160
6.9	Molecular Modeling Data For Bisphenol M Derivative PIs. . . . .	161
6.10	Other Bisphenol M Diether Dianhydride Films. . . . .	163

## List Of Figures

Figure		Page
6.11	Bisphenol M Diamine Polyimide Films. . . . .	164
6.12	Mechanical Properties Of Other Bisphenol M Dianhydride Polyimides. . . . .	165
6.13	Characterization Of Random Copolymers Containing BMDEDA. . . . .	168
6.14	Characterization Of Random Copolymers Containing BMDEDA. . . . .	169
6.15	Characterization Of Random Copolymers Containing BMDEDA. . . . .	170
6.16	Characterization Of Bisphenol M Diamine Copolymers. . .	171
6.17	Tensile Properties Of BMDEDA Copolymers . . . . .	172
6.18	Tensile Properties Of BMDEDA Copolymers . . . . .	173
6.19	Tensile Properties Of BMDEDA Copolymers . . . . .	173
6.20	Thin Film Properties Of Bisphenol M Diamine Copolymers.	174
6.21	Preliminary Screening Of LC-PI By Hot Stage Polarizing Microscopy . . . . .	175
6.22	Polyimide Blend Properties Of Extruded Ribbons. . . . .	177
6.23	Polyimide Blend Properties Of Extruded Ribbons. . . . .	178
6.24	Characterization Of <i>m</i> -Benzoyl Benzene Derivative Polyimides . . . . .	180
6.25	Solubilities Of BFDA:BPDA + DABTF Copolymers. . . . .	185
6.26	Characterization Of BFDA:BPDA + DABTF Copolymers. .	186
6.27	Mechanical Properties Of BFDA:BPDA + DABTF Copolymers . . . . .	186

## List Of Figures

Figure		Page
6.28	Properties Of BFDA:BPDA + DABTF .....	187
6.29	Characterization Of HQDEA + 4,4'-ODA:SAPPD Copolymers .....	192
6.30	Mechanical Properties Of HQDEA + 4,4'-ODA:SAPPD Copolymers .....	193
6.31	Moisture Uptake Of HQDEA + 4,4'-ODA:SAPPD Copolymers .....	194
6.32	Characterization Of ODPA + 3,4'-ODA:SAPPD Copolymers .....	199
6.33	Mechanical Properties Of ODPA + 3,4'-ODA:SAPPD Copolymers .....	200
6.34	Moisture Uptake Of ODPA + 3,4'-ODA:SAPPD Copolymers .....	201
6.35	Characterization Of ODPA + 3,4'-ODA: <i>p</i> -PDA Copolymers .....	203
6.36	Mechanical Properties Of ODPA + 3,4'-ODA: <i>p</i> -PDA Copolymers .....	204
6.37	Moisture Uptake Of ODPA + 3,4'-ODA: <i>p</i> -PDA Copolymers .....	205
6.38	Characterization Of BTDA + 4,4'-ODA: <i>p</i> -PDA Copolymers .....	207
6.39	Tensile Properties Of BTDA + 4,4'-ODA: <i>p</i> -PDA Copolymers .....	208



## List Of Figures

Figure		Page
6.40	Moisture Uptake For BTDA + 4,4'-ODA; <i>p</i> -PDA Copolymers . . . . .	209
6.41	Moisture Absorption Of Polyimides. . . . .	213
6.42	Hydrolysis Of The Imide Moiety. . . . .	214
6.43	Effect Of Chemical Exposure On Tensile Strength Of Kapton®. . . . .	217
6.44	Effect Of Chemical Exposure On Tensile Strength Of Apical®. . . . .	217
6.45	Effect Of Chemical Exposure On Tensile Strength Of Upilex® R. . . . .	218
6.46	Effect Of Chemical Exposure On Tensile Strength Of Upilex® S. . . . .	219
6.47	Effect Of Chemical Exposure On Tensile Strength Of LaRC™-TPI. . . . .	220
6.48	Effect Of Chemical Exposure On Tensile Strength Of LaRC™-CPI. . . . .	220
6.49	Effect Of Chemical Exposure On Tensile Strength Of LaRC™-ITPI. . . . .	221
6.50	Effect Of Chemical Exposure On Tensile Strength Of HQDEA/4-BDAF. . . . .	222
6.51	Effect Of Chemical Exposure On Tensile Strength Of BPDA/3,5-DABTF. . . . .	223
6.52	Effect Of Chemical Exposure On Tensile Strength Of 6F/3,5-DABTF. . . . .	223

## List Of Figures

<b>Figure</b>		<b>Page</b>
6.53	Effect Of Chemical Exposure On Tensile Strength Of ODPA/p-PDA. ....	224
6.54	Effect Of Chemical Exposure On Tensile Strength Of ODPA/3,4-ODA. ....	225
6.55	Effect of Chemical Exposure On Tensile Strength Of PMDA Polyimides. ....	226
6.56	LaRC™ Squaric Acid Polyimides. ....	230
6.57	RT Tensile Strength Of Squaric Acid Polyimides After Exposure To Electron Radiation. ....	235
6.58	RT Moduli of Squaric Acid Polyimides After Exposure To Electron Radiation. ....	236
6.59	RT Elongation Of Squaric Acid Polyimides After Exposure To Electron Radiation. ....	237
6.60	177°C Tensile Strength Of Squaric Acid Polyimides After Exposure To Electron Radiation. ....	238
6.61	177°C Moduli Of Squaric Acid Polyimides After Exposure To Electron Radiation. ....	239
6.62	177°C Elongation Of Squaric Acid Polyimides After Exposure To Electron Radiation. ....	240
6.63	232°C Tensile Strength Of Squaric Acid Polyimides After Exposure To Electron Radiation. ....	241
6.64	232°C Moduli of Squaric Acid Polyimides After Exposure To Electron Radiation. ....	242

## List Of Figures

Figure		Page
6.65	232°C Elongation Of Squaric Acid Polyimides After Exposure To Electron Radiation. ....	243
7.1	Capacitance Humidity Sensor. ....	257
7.2	Capacitance As A Function Of Relative Humidity For Kapton® HN Film. ....	258
7.3	Capacitance As A Function Of Relative Humidity For Upilex® R Film. ....	259
7.4	Capacitance As A Function Of Relative Humidity For HQDEA/4-BDAF Film. ....	260

## ABSTRACT

Polyimides are a family of heterocyclic polymers that have received extensive evaluation as adhesives, fibers, films, moldings, composite matrices, insulators, coatings, membranes, and resists. Their outstanding thermal stability, excellent mechanical and electrical properties, and chemical resistance make them attractive for many applications.

The purpose of this research was to develop ether-containing polyimides for three applications: liquid crystalline polyimides as processing aids, polyimides for microelectronic applications, and polyimides for harsh environments. The approach consisted of three primary activities: (1) develop novel diether dianhydrides for polyimide fabrication, (2) develop, characterize, and evaluate polyimide architectures based on the material application requirements, and (3) provide extensive structure-property relationships utilizing a number of unique groups in the polymer backbone and their contributions to the resultant polymer features.

Several novel extended diether dianhydrides were synthesized. When these flexible dianhydrides were combined with rigid diamines, an alternating flexible/rigid polymer backbone resulted and hence the potential was created for liquid crystallinity. Incorporation of rigid groups such as naphthalene and biphenyl, or spacers containing  $-CH_2-$  groups like butane or hexane, provided the potential to achieve liquid crystallinity in the resultant polyimides. The potential liquid crystalline polyimides developed exhibited crystallinity and other desirable properties, but data were inconclusive regarding their liquid crystallinity. Extensive knowledge was gained in the synthesis of novel dianhydrides and their precursors. Additionally, structure-property relationships based on a variety of novel dianhydride moieties resulted.

High performance polymer film and coating materials are increasingly being used by the electronic circuit industry. Electrical behavior is critical for polymers used in these applications. Materials are needed with substantially lower dielectric constants. Fluorinated dianhydrides and polyimides therefrom were synthesized to achieve lower dielectric constants. Additionally, a series of copolyimides was developed, using commercial and experimental monomers, for use as interlayer dielectrics and encapsulants. Several combinations were achieved that optimized mechanical, physical, and chemical properties required for the applications.

Polyimides for use in harsh environments were developed and evaluated. Two medium of particular interest were high pH to determine the polyimide's hydrolytic stability, and high-energy radiation, to determine utility of the polyimides in geosynchronous orbit. New and existing polyimides were evaluated through physical, mechanical, and chemical means to determine possible substitutes for wire and cable insulators that were degrading in the presence of alkaline cleaners. These candidates also have other utility in applications requiring hydrolytic stability. Also, squaric acid containing polyimides were developed and evaluated for potential space applications. These polyimides exhibited a combination of attractive properties, especially their resistance to the radiation component of geosynchronous orbit.

**THE SYNTHESIS, CHARACTERIZATION, AND APPLICATION OF ETHER-  
CONTAINING POLYIMIDES**

## Chapter 1: Introduction

Bogert and Renshaw synthesized the first aromatic polyimide in 1908 by melt polycondensation[1]. High molecular weight polyimides were not prepared until the 1950's, when DuPont researchers attempted to fabricate molding resins and hot-pressed films[2-4]. The polyimide film was code named "SP" for its "superlative properties". The film properties were similar to polyester films but had excellent retention of properties at high temperature, and resistance to ignition. This polyimide became commercially available under the trade name Kapton® in 1966.

As a class of polymers, polyimides offer a unique versatility among macromolecules. They can be prepared from a variety of starting materials by a variety of synthetic routes. Their architectures can be tailored to meet the wide range of material requirements for moldings, adhesives, composite matrices, coatings, interlayer dielectrics, insulators, encapsulants, resists, and membranes. Polyimides are thermally and chemically stable, and possess good mechanical and electrical properties.

This research developed ether-containing polyimides and their monomer precursors for three application areas: potential liquid crystalline polyimides as processing aids, polyimides for microelectronic applications, and polyimides for harsh environments.

## Potential Liquid Crystalline Polyimides

During the past two decades, liquid crystal polymers (LCPs) have become very popular due to the discovery that mesomorphism (liquid crystallinity) may lead to very interesting and useful new material property capabilities in macromolecular systems[5-10]. LCPs consist of molecules with stiff lath-shaped segments that possess a unique architecture which lies between that of the perfect order in crystals and the complete disorder in liquids. The most common liquid crystals (LC) are elongated cylindrical molecules whose aspect ratio (length/diameter) is high, leading to a tendency of the molecules to maintain a preferred orientation at temperatures higher than the melting point. LCPs have many properties which differentiate them from most other thermoplastics: low coefficient of thermal expansion (CTE), low gas permeability, high unidirectional strength and modulus of elasticity, high service temperature, and good fatigue and solvent resistance. In addition, the low melt viscosity of LCPs allows for their use as processing aids for conventional thermoplastics and as raw materials with very high filler loadings.

A review of reports and references has revealed the difficulty in developing thermotropic liquid crystalline polyimides[11-17]. Very few thermotropic liquid crystalline polyimides free of ester or carbonate groups have been developed to date. Mitsui Toatsu Chemicals, Inc., Central Research Institute (Japan)[18-20] has developed a thermotropic liquid crystalline polyimide which has neither an ester linkage nor a carbonate linkage. When this liquid crystalline polyimide was mixed with a high melting thermoplastic (i.e. Aurum®), the melt viscosity decreased. Kricheldorf and Linzer[21] developed thermotropic liquid crystalline polyimides free of ester groups by synthesizing polyimides prepared from  $\alpha, \omega$ -bis(4-aminophenoxy)

alkanes with various aromatic tetracarboxylic anhydrides. These two research efforts have concentrated on the synthesis of novel flexible diamines combined with rigid dianhydrides to afford favorable components of liquid crystalline polymers. No efforts appear to have been made to incorporate favorable components of liquid crystallinity into novel flexible dianhydrides combined with rigid diamines.

### **Polyimides For Microelectronic Applications**

Polyimides are finding increased applications in microelectronics due to their heat resistance, chemical resistance, dimensional stability, low dielectric constant, and planarization properties. As cited by Senturia[22], polyimides are widely used for four primary applications in the area of microelectronics: (1) as fabrication aids such as photoresists, planarization layers, and in implants, (2) as passivant overcoats and interlevel insulators, (3) as adhesives, and (4) as substrate components. Due to the availability of monomers for polyimide synthesis, molecular designs can meet the needs of the application.

Electrical behavior is critical for polymers used in these applications. Dielectric constants of state-of-the-art materials generally range from 3.2 to 4.0. Materials are needed with substantially lower dielectric constants. Reduction in the dielectric constants have been achieved by incorporating fluorine into the polymer backbone[23-26].

Material requirements for microelectronic applications are changing every day. New materials with improved performance, processability, and price are desired.



## **Polyimides For Harsh Environments**

The combination of properties such as thermo-oxidative stability, chemical stability, and good mechanical properties make polyimides particularly attractive for use in harsh environments. Two medium of particular interest are those with high pH and those with high-energy radiation such as in geosynchronous orbit.

Polyimide insulated electrical wire has been used in the aerospace industry in commercial, military, and to a lesser degree, general aviation aircraft since the early 1970's. The insulation offers benefits in terms of compact physical size, its ability to maintain good mechanical strength at high temperatures, and good dielectric strength.

Electrical insulating materials are known to deteriorate by a number of chemical and physical mechanisms which can be related to the polymer structure and the intensity of the various service stresses acting upon it. The predominant mechanism for deterioration is believed to be hydrolysis, a chemical reaction of water or aqueous fluids with the polymer chain where chain scission reduces the average chain length resulting in loss of strength and other properties. The rate of deterioration has been shown to be dependent upon the mechanical stresses from bending and stretching[27-28].

Wiring failures linked to insulation damage have drawn much attention in the media, and concerns have developed regarding the long term stability and safety of polyimide insulated electrical wire. The mechanical durability and chemical stability of polyimide insulated wire are affected by hydrolysis, notch propagation, wet and dry arc tracking, topcoat flaking, and degradation due to high pH fluids[29-32]. Polyimide insulated electrical wire is routinely exposed to high humidity, alkaline cleaners, and paint removers while under

mechanical stresses, due to the nature of the wiring and its installation in aircraft. These conditions, commonly encountered during aircraft maintenance and operation, can cause degradation of the polyimide insulation, and result in electrical failure (short circuit), commonly referred to as carbon arc tracking. The heat from the electrical current passing through the conductor in the degraded material can lead to more insulation degradation and can propagate the arc to additional wiring. The presence of moisture can also accelerate the arc (wet arc tracking). In some cases, carbon arc tracking and subsequent electrical fires have been reported[33-34]. Although the cause is usually attributed to mechanical damage due to poor wiring installation, the actual phenomena leading to damage have not been satisfactorily explained.

Kapton® HN was the most widely used polyimide for electrical insulation in military and some commercial aircraft until the early 1990's. Kapton® HN was originally developed for use in printed circuits, an application that required the removal of the polyimide by sodium hydroxide. Because of its lack of resistance to the sodium hydroxide found in many cleaning solutions, degradation of the polyimide insulated wire occurred as a result of routine maintenance. Therefore, an insulator was needed that was hydrolytically stable in these environments.

Another harsh media requiring suitable materials is high-energy radiation. Certain high performance polymers offer attractive features such as low density, high strength, optical transparency, and low dielectric constant. These polymeric materials have exhibited good short-term (3-5 years) space environmental durability; however, future spacecraft are being designed with lifetimes projected to be 10-30 years. This gives rise to concern that material property changes brought about during operation may result in unpredictable spacecraft performance.

Materials are needed for long term space durability. It is also important to understand the effects of radiation exposure on the physical and mechanical properties of these polymers. Additionally, data relating the chemical structure to radiation resistance in polyimides are needed.

## 1.1 References

1. Bogert, T. M.; Renshaw, R. R. *J. Am. Chem. Soc.* **1908**, *30*, 1140.
2. E. I. du Pont de Nemours and Co., French Patent 1 239 491, 1960.
3. Edwards, W. M. U.S. Patents 3 179 631 and 31 179 634, 1965; Brit. Pat. 898 651, 1959.
4. Endrey, A. L. U.S. Patents 3 179 631 and 3 179 633, 1965; Can. Patent 659 328, 1963.
5. Paolo La Mantia, F. *Thermotropic Liquid Crystal Polymer Blends*; Technomic: Lancaster, PA, 1993.
6. Evans, D.; Morgan, J. T. *Cryogenics* **1991**, *31*, 220-222.
7. Collyer, A. A. *Materials Science and Technology* **April 1989**, *5*, 309-322.
8. *High Modulus Polymers: Approaches to Design and Development*, Zachariades, A. E.; Porter, R. S., Eds.; Marcel Dekker: New York, 1988.
9. *Liquid Crystallinity in Polymers: Principles and Fundamental Properties*, Ciferri, A. , Ed.; VCH Publishers: New York, 1991.
10. *Polymeric Liquid Crystals*; Blumstein, A., Ed.; Plenum: New York, 1983.
11. Cassidy, P. E. In *Thermally Stable Polymers*; Marcel Dekker Inc: New York, 1982; Chap. 5.
12. Sillion, B. In *Comprehensive Polymer Science*; Allen, G.; Bevington, J. C., Eds.; Pergamon Press: Oxford, 1989; Vol. 5, Chap. 30.
13. Alam, S.; Kandpal, L.; Varma, I. K. *J. Macromol. Sci., Res. Macromol. Chem. Phys.* **1993**, *33*, 291.
14. Sroog, C. E. *Prog. Polym. Sci.* **1991**, *16*, 561.
15. *Polyimides*; Wilson, D.; Stenzenberger, H. D.; Hergenrother, P. M., Eds.; Blackie: Glasgow and London, 1990.

16. Bessonov, M. I.; Koton, M. M.; Kudryavtsev, V. V.; Laius, L. A. *Polyimides: Thermally Stable Polymers*, 2nd Ed.; Plenum: New York, 1987.
17. Critchley, J. P.; Knight, G. J.; Wright, W. W. *Heat Resistant Polymers, Technologically Useful Materials*; Plenum Press: New York and London, 1983; p 185-321.
18. Aranuma, T.; Oikawa, H.; Ookawa, Y.; Yamaguchi, A. *Polym. Prepr.* **1993**, *34* (2), 827.
19. Yamaguchi, K.; Urakami, U.; Tanabe, Y.; Yamazaki, M.; Tamai, S.; Yamaya, N.; Ohta, M.; Yamaguchi, A. Eur. Pat Appl. EP 425 265, May 2, 1991; *Chem. Abstr.* **1992**, *115*, 93782n.
20. Asanuma, T.; Oikawa, H.; Ookawa, Y.; Yamasita, W.; Matsuo, M. *J. Polymer Science Part A: Polymer Chemistry* **1994**, *Vol. 32*, 2111-2118.
21. Kricheldorf, H. R.; Linzer, V. L. *Polymer* **1995**, *Vol. 36*, No. 9, 1893.
22. Senturia, S. D. *Proc. of the ACS Div. of Polym. Mat.: Sci. and Eng.* **1986**, *55*, 385.
23. Stoakley, D. M.; St. Clair, A. K.; Baucom, R. M. Presented at the SAMPE Electronic Conference, Los Angeles, CA, June 19-22, 1989.
24. St. Clair, A. K.; Slem, W. S. *SAMPE Journal* **1985**, *Vol. 21*(4), 28-33.
25. Research Triangle Institute, "NASA Langley's Colorless and Low Dielectric Polyimide Thin Film Technologies", May 1994.
26. St. Clair, A. K.; St. Clair, T. L.; Winfree, W. P. Presented at the National Meeting of the American Chemical Society, Los Angeles, CA, Sept. 25-30, 1988; *Proceeding of the Division of Polymeric Materials: Science and Engineering* **1988**, *Vol. 59*, 28.
27. Campbell, F. J., "Hydrolytic Deterioration of Polyimide Insulation on Naval Aircraft Wiring", *Proceedings, IEEE Conference on Electrical Insulation and Dielectric Phenomena* **1988**, 180-188.

28. Campbell, F. J., "Temperature Dependence on the Hydrolysis of Polyimide Wire Insulation", *IEEE Transactions on Electrical Insulation* **1985**, E1-20, 111-116.
29. O'Neill, J. F., "The Kapton® Question", *Aviation Equipment Maintenance* **February 1989**, 26-32.
30. Hartman, R. V., "Unsafe Aircraft Wiring Poses Expensive Problem", *Defense Electronics* **January 1983**, 34-38.
31. Doherty, R., "Magellan Blaze Linked to Kapton®", *Electronic Engineering Times* **November 1988**, 6.
32. Pedley, M. D.; Leger, L. J., "Considerations in Using Kapton® Wire Insulation in Shuttle Systems"; NASA, Johnson Space Center, August 1988.
33. Jones, S., "NASA Wondering if Shuttle is Wired for Disaster", *Fort Worth Star-Telegram* **Sept. 21, 1988**, 1-2.
34. Campbell, F. J., Naval Research Lab, Washington, D. C., 20375-5000, personal communication.

## Chapter 2: Statement Of Research

The goals of this research are to synthesize, characterize, and evaluate ether-containing polyimides and their monomer precursors for three applications: thermotropic liquid crystalline polyimides as processing aids, polyimides for microelectronic applications, and polyimides for harsh environments.

### Potential Liquid Crystalline Polyimides

Very few thermotropic liquid crystalline polyimides free of ester or carbonate groups have been developed to date. Ester and carbonate groups in the polymer backbone decrease the thermal and hydrolytic stability. These thermotropic liquid crystalline polyimides have been synthesized using flexible diamines and rigid dianhydrides to afford the liquid crystalline characteristics.

The results of this study were the development of potential thermotropic liquid crystalline polyimides free of ester and carbonate groups. The work required to develop these materials included the synthesis and characterization of novel flexible dianhydrides, which when combined with "rigid" diamines would afford an alternating flexible/rigid backbone. Other favorable components of liquid crystallinity would also be incorporated into the dianhydrides and polyimides therefrom, such as flexible spacers, rigid units, or bulky groups, in *meta* and/or *para* catenations. No efforts are known that have

incorporated favorable components of liquid crystallinity into novel flexible dianhydrides combined with rigid diamines.

Polyimides and copolyimides were synthesized, characterized, and evaluated by physical and mechanical means. Polymer forms included films, powders, and melt extruded ribbons. Characterization and evaluation of a known thermotropic liquid crystalline polyimide, synthesized in-house, and provided by Mitsui Toatsu (Japan), was also performed, and comparisons of this polymer system to the polymers developed in this research were made.

### **Polyimides For Microelectronic Applications**

Polyimides are finding increased applications in microelectronics due to their high thermal stability, processability, chemical resistance, low coefficient of thermal expansion, and low dielectric constant. The results of this study were the development of polyimides as interlayer dielectrics and encapsulants. The work required for interlayer dielectric development included the synthesis and characterization of fluorinated diether dianhydrides and polyimides therefrom. Incorporation of fluorine into the polymer backbone has been shown to reduce the dielectric constant, making these materials more suitable for interlayer dielectrics than commercial materials possessing dielectric constants greater than 3.2. A low dielectric material is required to minimize propagation delay, interconnect capacitance, and crosstalk between lines.

The work required for encapsulant development included the design of copolyimides that exhibited the right combination of mechanical properties, electrical properties, and dimensional stability. Polyimides and copolyimides from commercial and experimental monomers were synthesized, characterized, and evaluated for application based on the material property requirements.



## **Polyimides For Harsh Environments**

Due to their high thermal, thermo-oxidative stability and chemical stability coupled with good mechanical properties, polyimides are particularly attractive for use in harsh environments. Two harsh medium were evaluated: high pH to determine the hydrolytic stability and high-energy radiation, which is the radiation component of geosynchronous orbit.

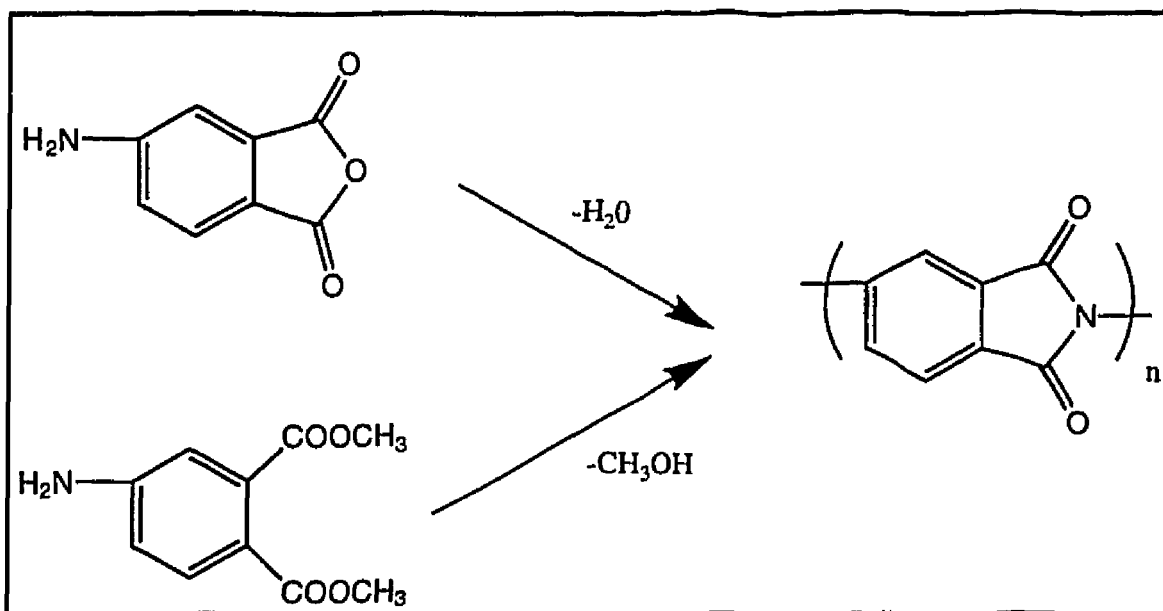
Polyimide insulated electrical wire has been used in the aerospace industry in commercial, military, and to a lesser degree, general aviation aircraft since the early 1970's. Polyimide insulated wire is routinely exposed to high humidity, alkaline cleaners, and paint removers while under mechanical stresses due to the nature of the wiring and its installation into the aircraft. This research evaluated commercial and experimental polyimides through chemical, physical, and mechanical means to determine alternate insulators for wire and cable applications. These materials would also be suitable for other applications requiring hydrolytic stability. The work required included the synthesis of polyimides, and evaluation of experimental and commercial polyimides in high pH solutions with various induced stresses.

Better materials are required with increased resistance to high-energy radiation. Certain polymeric materials have exhibited good short term (3-5 years) space environmental durability; however, future spacecraft are being designed with lifetimes projected to be 10-30 years. Polyimides were synthesized and subsequently exposed to 1 MeV electrons under high vacuum at total dosages representing 5-30 years. The effects of different exposures on the physical and mechanical properties were investigated using a variety of techniques.

## Chapter 3: Literature Review

### 3.1 Introduction

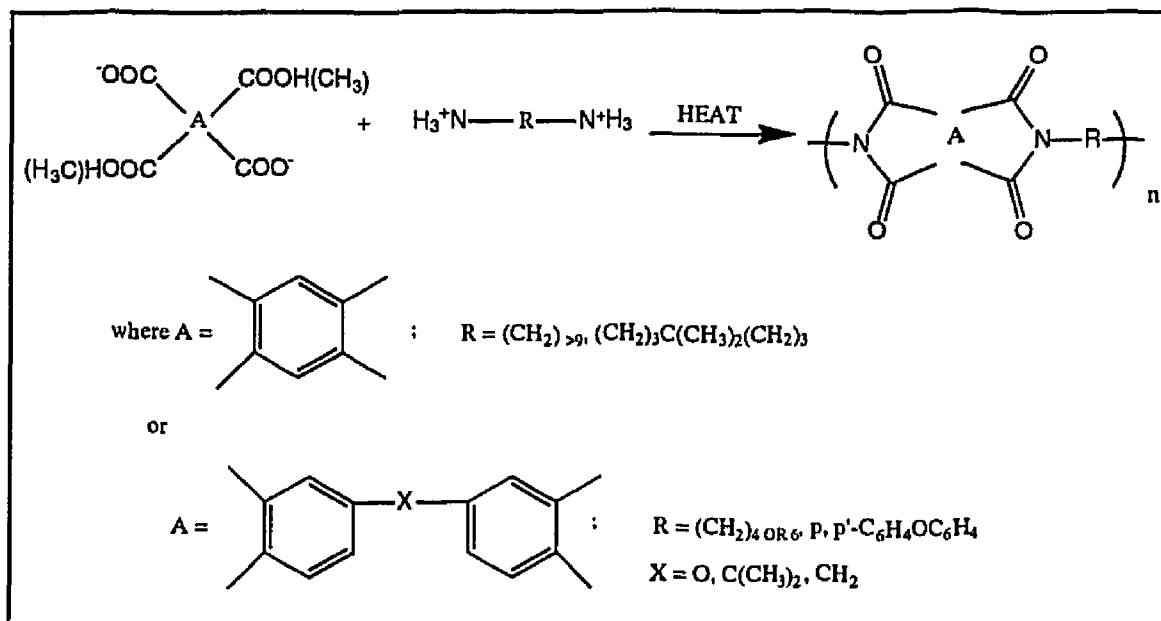
In 1908, Bogert and Renshaw[1-2] reported on the intramolecular melt polycondensation (A-B polymerization) of 4-aminophthalic anhydride, or dimethyl 4-aminophthalate, to afford the first aromatic polyimide (Figure 3.1). This prompted more research efforts to synthesize polyimides.



**Figure 3.1 Synthesis Of The First Aromatic Polyimide**

In the early 1950's, DuPont researchers, in an attempt to fabricate molding resins and hot-pressed films, produced moldable aliphatic/aromatic

polyimides by fusion of salt type intermediates[2-3]. The reaction mechanism is shown in Figure 3.2.



**Figure 3.2 Polyimide Synthesis By Heat Fusion Of Salt Type Intermediates**

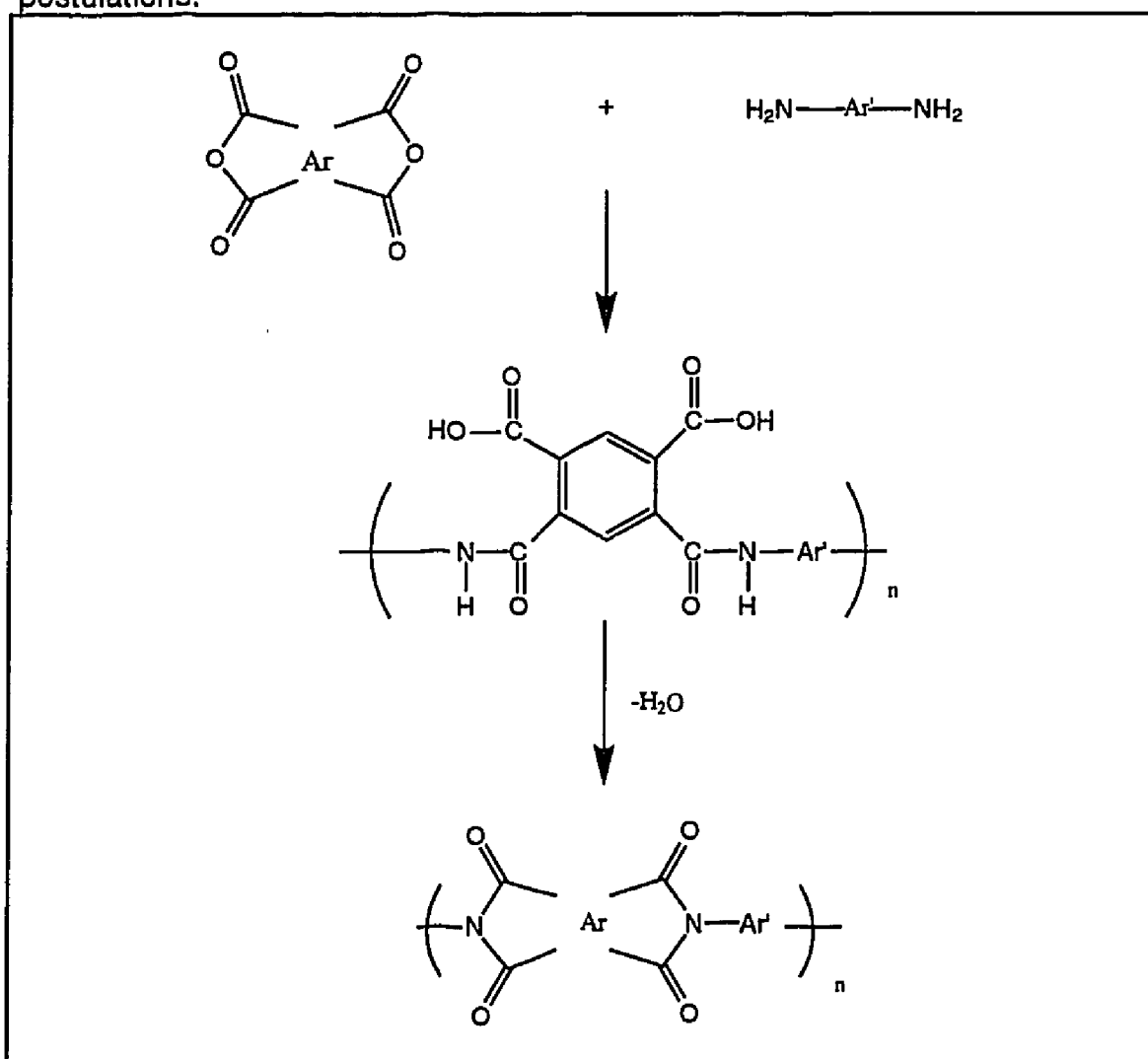
Researchers later discovered that these aromatic systems could be synthesized from dianhydrides and diamines in two stages to produce a soluble poly (amic acid) (PAA) solution that could be cyclodehydrated to the polyimide. This led to the classic two-step method for polyimide synthesis.

### 3.2 Two-Step Method For Polyimide Synthesis

Polyimides are formed by the condensation reaction of dianhydrides with diamines. In the classic, two-step method for polyimide synthesis, a tetracarboxylic dianhydride is added to a solution of diamine in a polar aprotic solvent at 15-57°C[4-8]. Commonly used solvents include N,N-methylpyrrolidone (NMP), N,N-dimethylacetamide (DMAc), or

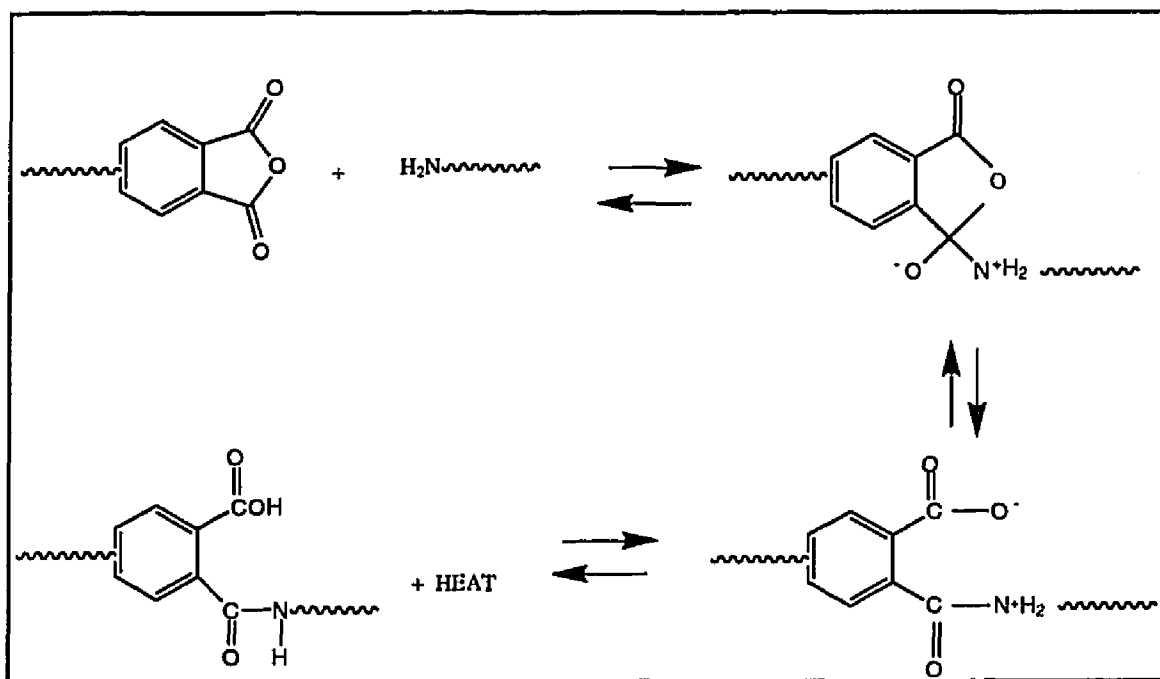
dimethylformamide (DMF). The resultant PAA solution is then cyclodehydrated to the corresponding polyimide by stage curing to elevated temperatures, or by treatment with chemical dehydrating agents.

The reaction mechanism for the two-step method for polyimide synthesis is shown in Figure 3.3[9]. Ar and Ar' represent aromatic units. The reaction of a tetracarboxylic acid dianhydride and an aromatic diamine is not completely understood. However, much evidence has been reported to support certain postulations.



**Figure 3.3 Reaction Mechanism For Two Step Polyimide Synthesis**

Figure 3.4 illustrates the formation of the polyimide precursor[9]. The reactants and products are in equilibrium[9-11]. The forward reaction is believed to begin with charge complex formation between the dianhydride (electron acceptor) and the diamine (electron donor). Propagation occurs via nucleophilic substitution at one of the dianhydride's carbonyl carbon atoms. The amine nucleophile attacks the  $sp^2$  carbon and displaces the adjacent carboxylate moiety.



**Figure 3.4 Formation Of The Polyimide Precursor**

### 3.3 Rate Of Polymerization

The rate of polymerization is dependent on the solvent. The rate increases with more polar and more basic solvents. Results by Russian scientists indicate the rate of acylation increases with solvent in the following order: tetrahydrofuran (THF) < acetonitrile < DMAc < *m*-cresol[9]. The large

rate of polymerization in *m*-cresol indicates that the solvent also serves as an acid catalyst.

### **3.4 Factors Influencing The Molecular Weight Of Poly (Amic Acids)**

As with all condensation polymerizations, the starting materials must be pure and the functional groups present in equal amounts in order to obtain high molecular weight polymers. In preparing poly (amic acids), several factors have been shown to influence the molecular weight[4,9]. Higher concentrations of monomers have produced higher molecular weights, since less solvent, and therefore less solvent impurities, were present. Molecular weight can be influenced by the order and mode of monomer addition. Higher molecular weights have been obtained by adding a solid dianhydride to a solution of diamine. Aromatic dianhydrides in amide solvents form complexes which are sensitive to moisture, impurities, or light[9]. Addition of the dianhydride as a solid minimizes these reactions. Temperature also influences molecular weight, where the highest molecular weights were obtained between -20 and 70°C. Above this temperature range, release of water with concurrent precipitation of the polyimide results.

### **3.5 Side Reactions**

Side reactions in the formation of the PAA can be eliminated by using pure monomers and solvents, under anhydrous conditions. However, these perfect conditions are not always possible and side reactions can occur.

Possible side reactions include reverse propagation, hydrolysis of the dianhydride, complexing with impurities, and reaction with the *o*-

carboxycarboxamide functionality[9]. The reverse propagation is possible since the reactants and products are in equilibrium. Fortunately, this side reaction does not greatly affect the molecular weight of the PAA because of the magnitude of the equilibrium constant ( $K_{eq}$ ). Studies[9] have shown that if no other reactions occurred, the number average degree of polymerization ( $X_n$ ) for most poly (amic acids) would be greater than 300 by the approximation  $X_n = (K_{eq})^{0.5}$ . Most PAAs have degrees of polymerization ranging from 25-275, which correlates to a number average molecular weight range between 10,000 and 100,000 g/mole.

The dianhydride can react with water, which, when present, competes with the propagation step. This removes the dianhydride from the equilibrium and causes an imbalance in the stoichiometry. This can affect the molecular weight of the poly (amic acid), but does not necessarily prevent the formation of high molecular weight. When the PAA is thermally imidized, the dicarboxylic acid produced by the hydrolysis can undergo dehydration and regenerate the anhydride.

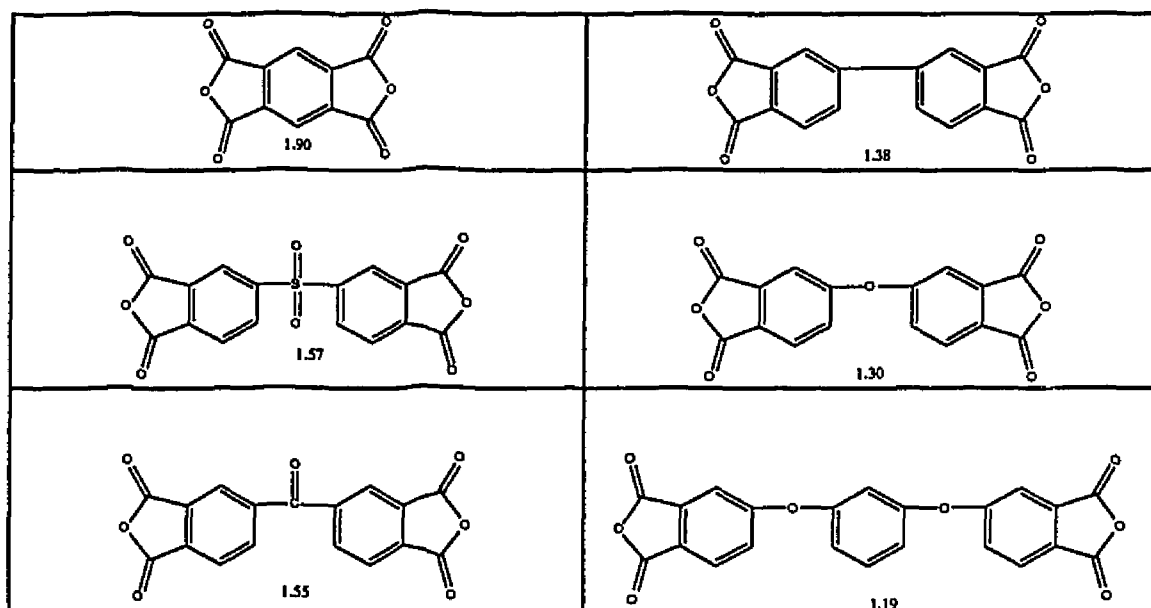
A reaction may occur involving solvent impurities. Amide solvents may contain amine impurities which can compete with the diamine. The stoichiometry is unbalanced and unreacted chain ends may result.

A side reaction can occur with the *o*-carboxycarboxamide generated by the addition of amine to the anhydride. The *o*-carboxycarboxamide can cyclize to the dianhydride, the isoimide, or the imide.

### **3.6 Chain-Chain Interactions**

Polyimide chain-chain interactions occur via charge transfer or electronic polarization[12]. The primary interaction should depend on the

electron affinity of the dianhydride moiety and the electron affinity of the diamine moiety. The more electrophilic the dianhydride, the more susceptible it is to nucleophilic attack. The electron affinity ( $E_a$ ) is a good measure of an anhydride's acceptor properties, and can be measured by polarographic reduction data. Figure 3.5[4, 13] shows the electron affinities in electron volts (eV) of some commercially available dianhydrides. The strong electron withdrawing moieties in this molecule activate each other towards nucleophilic attack.

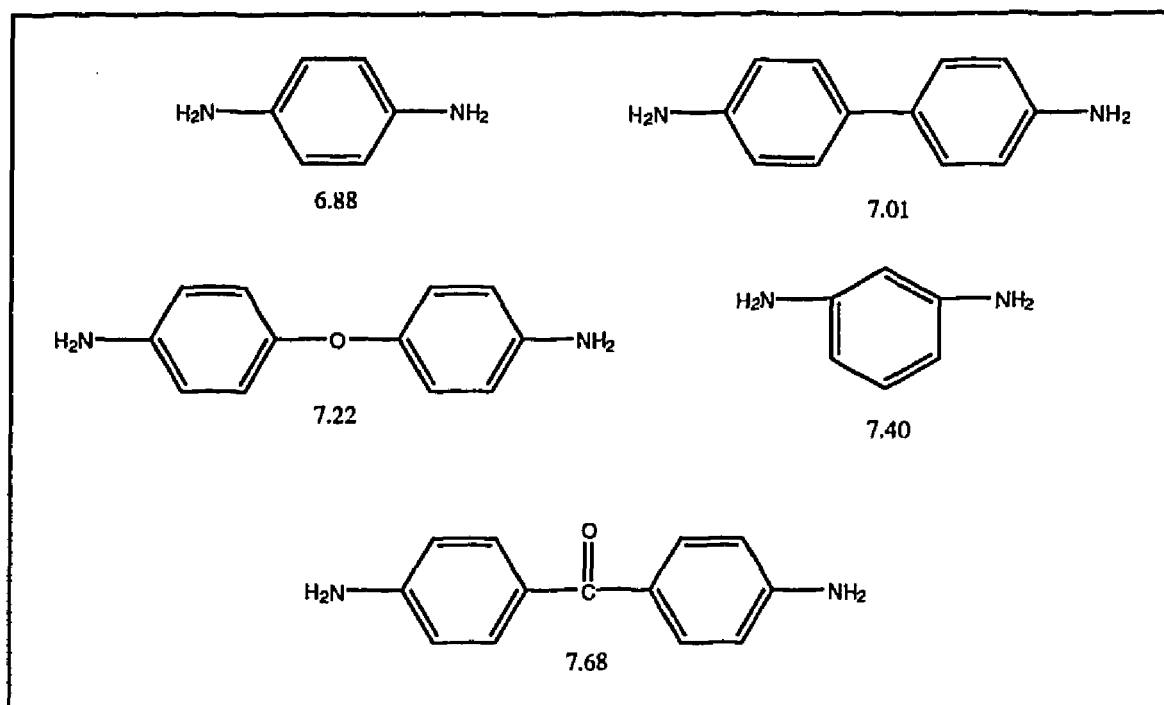


**Figure 3.5 Electron Affinities Of Commercial Dianhydrides in eV[4,13]**

The electron affinity of bridged monomers is strongly dependent on the electron-withdrawing capability of their bridge group. The values and rate constants decrease as the ability of the bridge group to withdraw electrons decreases.



Reactivity of the diamines has been correlated to their ionization potential, a measure of their electron-donating ability. Ionization potentials of selected diamines in electron volts (eV) are shown in Figure 3.6[4, 14].



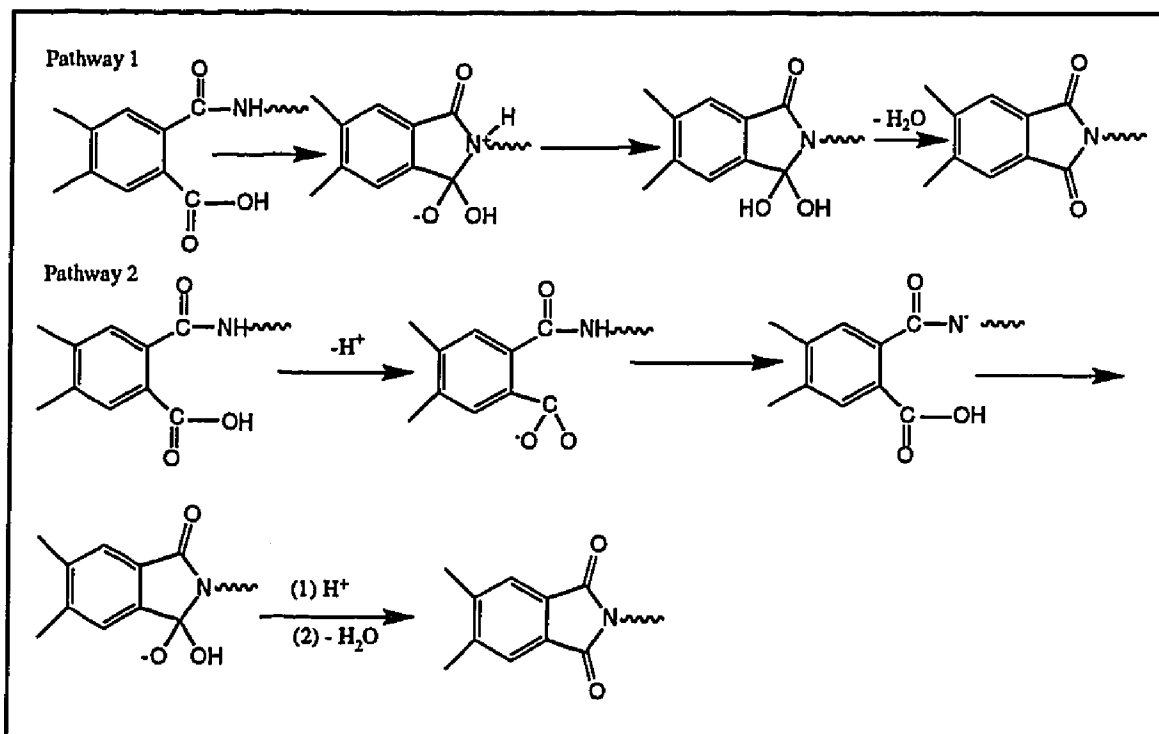
**Figure 3.6 Ionization Potentials Of Selected Diamines in eV[4, 14]**

These values are useful in correlating interactions between selected diamines and dianhydrides. For example, a polymer segment derived from pyromellitic dianhydride will have more tendency to react with an electron-rich amine derived center than one derived from an oxydiphthalic dianhydride[15]. Conversely, an oxydianiline derived diamine would be more likely to interact with an electron-deficient aromatic ring system than would a benzophenone containing diamine.

### 3.7 Thermal Imidization Of Poly (Amic Acids) (PAA)

The second step of the classic polyimide synthesis is the cyclodehydration of the PAA to the polyimide by heating at 200 to 400°C. The PAA solution is typically cast onto a glass plate, heated, and removed in its final thin film form. A standard polyimide cure cycle is 100, 200, and 300°C for one hour each[9, 16]. However, work done by Baise[17] showed that temperatures between 230 and 250°C (for 10 min or less) were adequate for the imidization of thin films of PMDA/ODA poly (amic acid) solutions. Additionally, Baise determined that heating at lower temperatures could lead to incomplete cures because loss of solvent at 150 and 200°C prevents complete cure at higher temperatures. The plasticizing effect of the solvent, which promotes the cyclization process, was no longer present.

During thermal imidization, an *o*-carboxycarboxamide group can cyclize intramolecularly to regenerate the anhydride, or it can cyclize to the isoimide or imide[9]. Two possible reaction mechanisms for the imidization process were proposed by Kreuz *et. al.*[18] and are shown in Figure 3.7.



**Figure 3.7 Reaction Mechanism For Thermal Imidization Process**

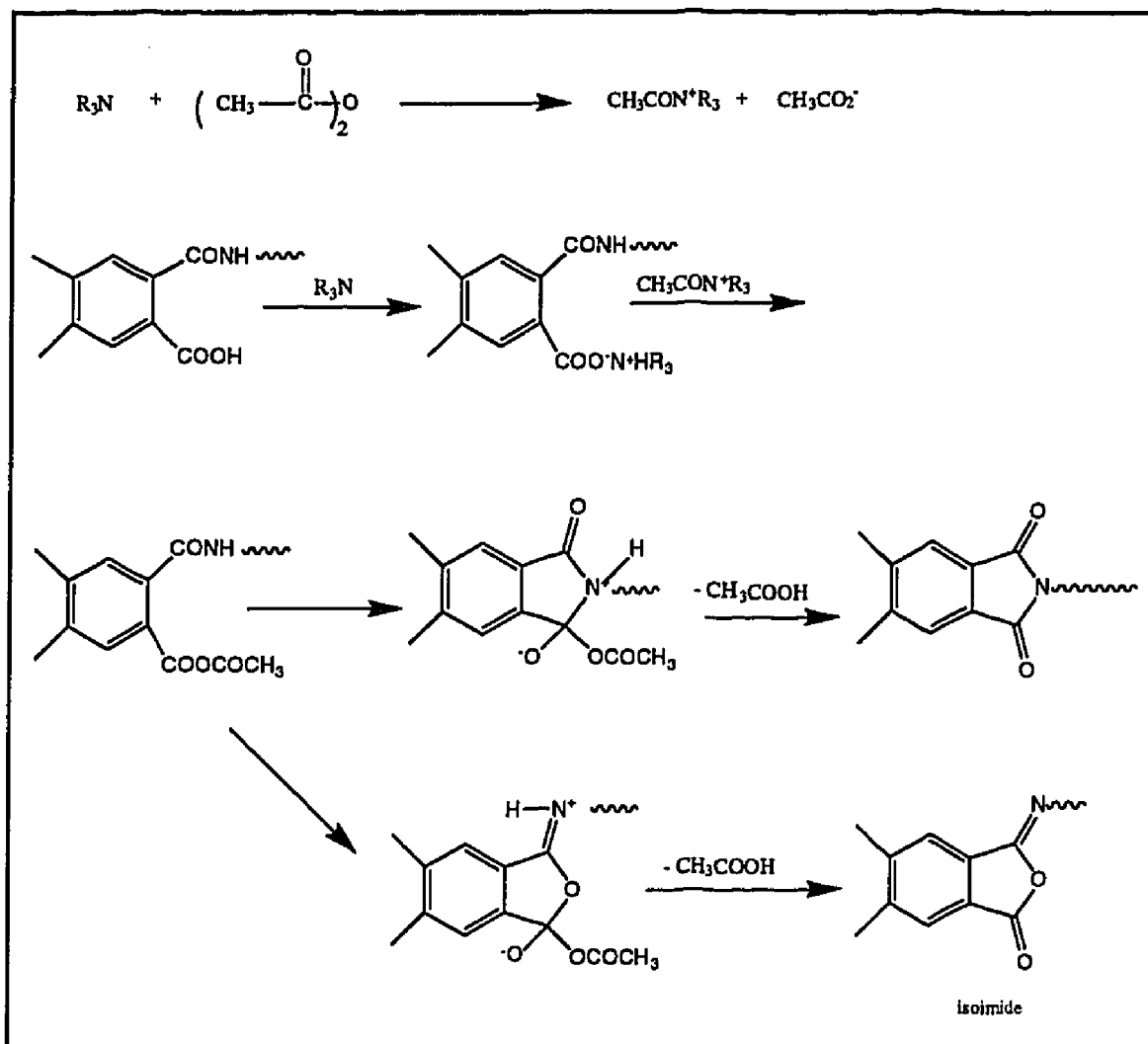
In the first reaction, the proton attached to the nitrogen is lost after cyclization whereas, in the second reaction, the proton is lost prior to ring closure. Ring closure should occur faster where the proton is lost prior to cyclization since the conjugate base of the amide is a stronger nucleophile than the amide.

PAA solutions in amide solvents imidize faster because the solvent molecules allow the reacting species to attain favorable conformations for cyclization[18]. Amide solvents may also facilitate cyclization because they form strong bond complexes with carboxyl groups and assist in the loss of the carboxyl proton.

### 3.8 Chemical Conversion Of Poly (Amic Acids) To Polyimides

Poly (amic acids) can be chemically converted to polyimides by treatment with a mixture of a dehydrating agent such as an aliphatic dianhydride, ketene, N,N-dialkylcarboimide, or a strong Lewis acid ( $\text{PCl}_3$ ), and a basic catalyst, such as pyridine or triethylamine. The mechanism is illustrated in Figure 3.8[9] using a mixture of acetic anhydride and a tertiary amine. First, the reaction of the tertiary amine and the dianhydride produces a salt, which is more susceptible to nucleophilic attack. The carboxylic acid group reacts with the tertiary amine to form its conjugate base, which is a better nucleophile. The dianhydride salt reacts with the conjugate base and forms the acetate group, which is a better leaving group.

Ring closure proceeds via nucleophilic substitution. Cyclization can occur by nitrogen attack of the amide group to form the isoimide, or oxygen attack to form the imide. Although both products are formed, the isoimide subsequently rearranges to the imide.



**Figure 3.8 Mechanism Of Chemical Imidization**

Insignificant amounts of isoimide are sometimes detected after thermal imidization, compared to significant amounts evidenced by the chemical imidization process. One postulation for this is that isoimides formed during thermal imidization may rearrange to the imide. Another possibility is that attack by the amides' oxygen group is enhanced by conditions used in the chemical imidization. The acetate group is a much better leaving group than the hydroxyl group that is eliminated during thermal imidization.

### 3.9 One-Step Method For Polyimide Synthesis

Polyimides are also prepared by a one-step method in which the dianhydride and diamine are stirred in a high boiling solvent at 180-220°C[9, 19-20]. Chain growth and imidization occur spontaneously. The water generated can be distilled from the reaction, but its removal is not usually required since the equilibrium is driven towards the product. Commonly used solvents are  $\alpha$ -chloronaphthalene, nitrobenzene, and *m*-cresol containing isoquinoline. However, these solvents are extremely toxic and use of them for large scale reactions is generally not desired. Gamma-butyrolactone (GBL) and acetic acid have been used to imidize poly (amic acid) solutions at temperatures between 110-130°C[21]. Imitec, Inc. has used Bisphenol A as a solvent in their synthesis of polyimides. Additionally, melt polymerizations are one-step reactions in which the monomers are heated above their melting points; no solvents or catalysts are required. The one-step method is useful in polymerizations of unreactive diamines and dianhydrides, and sterically hindered monomers.

Higher degrees of crystallinity can be obtained with these methods because the high temperature and the solvent may permit more mobility of the polymer chains, and hence the greater ability for packing[9].

### 3.10 Other Synthetic Routes To Polyimides

There are many other synthetic routes to polyimides: aromatic nucleophilic displacement polymerizations, exchange reactions, reactions of di-isocyanates and dianhydrides, vapor deposition directly from monomers, Diels-Alder reactions, and reactions of tetracarboxylic acids and diamines.

Takekoshi[22] and Sroog[23] have reviewed these methods and provided details and references.

### **3.11 Structure-Property Relationships Of Polyimides**

#### **3.11.1 Thermal Stability Of Polyimides**

The chemical factors which influence heat resistance include primary bond strength, secondary forces such as van der Waals forces or hydrogen bonding, resonance stabilization, molecular symmetry, rigid interchain structure, crosslinking, and branching[24]. The bond dissociation energy of aromatic systems is higher than that of single or double carbon bonds. Secondary or van der Waals bonding provides additional strength and thermal stability. Polar groups such as -CO- participate in strong intermolecular association and contribute to heat resistance in polymers. Molecular symmetry or regularity of the chemical structure arises when the moieties are joined in the same position in each repeat unit (e. g. *para* linkages).

Thermal stability has been measured with a variety of techniques. Weight loss in air indicates thermo-oxidative instability; whereas, weight loss in an inert atmosphere indicates thermal degradation. Studies by Adrova[23, 25] and St. Clair[23, 26] determined weight loss measurements in helium at 450°C for various polyimides based on oxydianiline (ODA). The order of decreasing stability based on the dianhydride moiety was pyromellitic dianhydride (PMDA) > oxydiphthalic dianhydride (ODPA) > benzophenone tetracarboxylic dianhydride (BTDA) > sulphonyl dianhydride (SO<sub>2</sub>DA). Other research has shown PMDA, biphenyl dianhydride (BPDA), and hexafluoropropane dianhydride (6FDA) to possess the same thermal stability[23].

Polyimides can be viewed as having electron-poor and electron-rich segments resulting from the dianhydride and diamine monomers. The commonly used dianhydrides such as PMDA, BTDA, ODPA, and 6FDA are electron-deficient and are not easily oxidized. However, since many diamines are electron-rich, and more susceptible to oxidation, it was proposed that thermo-oxidative instability was generally related to the diamine segment in the polymer backbone[15]. The general order of proposed stability for diamines was: benzidine > diaminobenzophenone (DABP) > *m*- or *p*-phenylene diamine (PDA) > oxydianiline (ODA) > diphenylmethane diamine (MDA). The stability of the diamine moiety using pyromellitimides indicated generally the same trend: benzidine > *p*-PDA > *m*-PDA > ODA > 3,3'-dimethylbenzidine > MDA[23].

Dine-Hart and Wright[27] studied the effect of variation of the chemical structure on the thermo-oxidative stability of polyimides using polyimides based on PMDA and a variety of diamines, and concluded the following: (1) *p*-linked polyimides were more thermally stable than *m*-linked polyimides, (2) the stability decreased as the number of fused rings in the diamine increased, (3) ring substitution in the diamine decreased stability, and (4) using the diamine structure,  $\text{H}_2\text{NC}_6\text{H}_4\text{-X-C}_6\text{H}_4\text{NH}_2$ , stability decreased in the order X equals single bond > S >  $\text{SO}_2 \geq \text{CH}_2 > \text{CO} > \text{SO} \geq \text{O}$ . However, it is important to note that with polyimides containing -S-, -SO-, and -CH<sub>2</sub>-, one has to be concerned with weight gain followed by weight loss. Also, no mention was made indicating the molecular weight of the polyimides in the series. Molecular weight can affect the thermo-oxidative stability of polymers.



### 3.11.2 Hydrolytic Stability

Chemical reactions of water or aqueous fluids with the polymer chain can lead to chain scission with resulting loss of strength and other properties. There is limited information available relating hydrolytic stability to chemical structure, or the void content, crystalline perfection, and related physical characteristics in test films. However, there are several studies that may provide some insight to this phenomenon[4, 23].

Resistance to hydrolysis greatly depends on the dianhydride component[4]. Of the polyimides studied[4], those based on PMDA were found to be the least resistant to hydrolysis. The speed of hydrolysis using various diamines was also determined. As the number of oxyphenylene groups in the diamine increased, the hydrolytic stability increased because the concentration of the imide bond decreased[4]. Imide bonds were not found to be hydrolytically stable.

Sroog *et. al* reported the loss of film flexibility on exposure of polyimide films to boiling water[8]. Polyimides derived from PMDA and a series of diamines were evaluated for retention of film flexibility. Films possessing high thermal stability were not as hydrolytically stable as those possessing moderate thermal stability. Results indicated the hydrolytic stability of the diamines as follows: *p*-ODA > diaminodiphenylsulfone (SDA) > *m*-PDA = *p*-PDA.

Androva *et. al.*[28] reported hydrolysis rates of some polypyrometallitimides in 0.5M sodium hydroxide at 90°C. De Iasi and Russell[29] evaluated the degradation of Kapton® immersed in water at 25-100°C and established activation energies for the loss of tensile strength and elongation. De Iasi also noted that the hydrolyzed film could, upon reheating to

310°C, regain essentially all the tensile properties lost on hydrolysis, the heated product showing improved stability versus the original.

Heacock[30] examined the hydrolytic stability of Kapton® as a function of exposure to relative humidity (22.9-100%) and temperature (23-100°C). Mudhenke and Schwartz[31] compared hydrolytic stability of polyimides utilizing ODA and *p*-PDA with PMDA, BTDA, BPDA, and ODA. ODA based polyimides exhibited the highest resistance to hydrolysis of the polyimides evaluated.

### 3.11.3 Radiation Resistance

Chemical reactions such as chain scission, crosslinking, formation of small molecular products, and modification of the molecular structure may result from high-energy radiation exposure[32]. Chain scission and crosslinking can decrease or increase the molecular weight. Outgassing of small molecules such as H<sub>2</sub>, CO, CO<sub>2</sub>, and CH<sub>4</sub> (depending on the chemical composition of the polymer) can occur and subsequently contaminate the environment for the polymeric material. Molecular composition and structure of the polymer can change because the loss and formation of unsaturation. Understanding these mechanisms, in addition to the kinetics of degradation, and the relationship between the chemical structure and radiation resistance, are critical in the development and selection of polymeric materials for space applications.

Many polyimides exhibit excellent resistance to radiation[4, 23]. Bessonov *et. al.*[4] attribute the resistance of polyimides to radiation to their ability to disperse large doses of absorbed energy and to their structure. Greater amounts of energy are required to break the heterocyclic bond. Their

studies also indicated that the thermal stability and electrical properties were not generally affected by radiation exposure, and mechanical properties were affected only slightly for the exposed polyimides.

Some PMDA based polyimides are noted for their excellent resistance to radiation. PMDA/MDA films retained good mechanical and electrical properties after exposure to high-energy electrons and PMDA/ODA remained tough after 45 day exposures to thermal neutrons at 175°C[23]. However, much data are still needed relating the chemical structure in polyimides to radiation resistance and the extent to which certain moieties enhance this resistance.

#### **3.11.4 Glass Transition Temperature**

The glass transition temperature ( $T_g$ ) is the temperature below which the various groups and atoms in the polymer chain have insufficient rotational energy to overcome the forces which restrict torsional oscillations and hinder their transition to free rotation.  $T_g$  is significantly affected by a number of variables: molecular weight (MW), nature of the end groups, extent and method of imidization, processing atmosphere and temperature profile, presence of absorbed moisture or retained solvent, and finally, the measurement and rate used by the investigator (i.e. Differential Scanning Calorimetry (DSC), Torsional Braid Analysis (TBA), and Thermomechanical Analysis (TMA)).

Data collected over the years have allowed several conclusions regarding the  $T_g$  of aromatic polyimides. Bridging groups such as O, CH<sub>2</sub>, SO<sub>2</sub>, and CO between rings increase the opportunity for bond rotation and lower the  $T_g$ . The  $T_g$  decreases because the polymer backbone flexibility

increases. Work by Dezern and Croall[33-34] showed that glass transition temperatures were generally higher for keto-bridged polyimides over corresponding ether-bridged systems and increased from *meta* to *para* catenation in the diamine portion of the backbone.

Structural disorder resulting from increased nonsymmetry of chains decreases  $T_g$ . The tendency is for the  $T_g$  to decrease as the polymer goes from all *para* catenation to all *meta* catenation. Lee[35] predicted that *ortho* and *meta* orientation in phenylene would be more effective than *para* in decreasing the  $T_g$  in aromatic polymers. Work by Bell and Gager[36], with limited exceptions, showed that the use of diamines with *ortho*-oriented amine groups failed to improve the flexibility of their polyimides since their  $T_g$  values were usually as high as those of polymers made from *para*-diamines.

Other researchers reported the effect of the diamine moiety on the glass transition temperature. Gibbs and Breder[37] and St. Clair *et. al.*[38] studied the effect of the diamine structure on the glass transition temperature in 6FDA containing polyimides. Results indicated the order of increasing  $T_g$  occurred with the following diamines: 4,4'-MDA < 4,4'-ODA < *m*-PDA < 4,4'-DABP < *p*-PDA < 1,5-naphthalene diamine (NDA). Polyimides from BTDA and *meta*-linked diamines showed the following trends regarding the  $T_g$ : 3,3'-MDA < 3,3'-ODA < 3,3'-DABP < 3,3'-diaminodiphenyl sulphone (DADPS).

The effect of isomers of ODPDA and selected diamines was reported by Gerber *et. al.*[39]. The  $T_g$  was not effected as much by isomeric attachment in the dianhydride moiety as the diamine moiety.

Intermolecular interactions in polyimides also affect the glass transition temperature. Polyimides can be viewed as polymeric chains with alternating donor and acceptor elements which can interact with each other to form interchain charge transfer complexes (CTC). Several researchers[27, 40] are

credited with the suggestion that polyimides form charge transfer complexes. Dine-Hart and Wright compared the functionality, solubility, and color of model aromatic imides, and Gordina *et. al.* investigated the relationship between color and chemical structure in polyimides.

Fryd[41] proposed that the  $T_g$  of polyimides was lowered by decreasing the chain rigidity with flexible linkages, or by reducing the charge transfer complex (CTC) formation. The strength of the CTC was defined by the electron affinity of the dianhydride and the ionization potential of the diamine. The strength of the CTC increased or decreased depending on whether the hinge group was electron-withdrawing or electron-donating. However, the hinge group in the dianhydride always reduced the strength of the CTC because it isolated the electron-withdrawing anhydride groups. Fryd[41] also proposed that *meta*-catenation distorted the linearity of the polymer chain, and therefore interfered with the chain packing and charge transfer formation. The energy of rotation was lowered and therefore, the  $T_g$  was lowered.

An extensive study by Lee[42] indicated some inconsistencies with the correlations between the  $T_g$  and CTC formation proposed in previous works. Lee studied approximately 250  $T_g$ -structure data to establish a universal set of relative bridging group effects for repeating units in polymers. These studies indicated that the bridging effect was not unique to polyimides and could be applied to the repeat units of polyquinolines and polyquinoxalines. The effect of the bridging group on the  $T_g$  was linked to the rotational barrier energies of the hinge group. Additionally, Lee did extensive work regarding the applicability of the Hayes' empirical equation, correlations between the  $T_g$  and the ether linkage density of repeat units, and the group contribution to the heat capacity jump. Lee concluded that the  $T_g$  was a function of the classic van der

Waals' forces and chain flexibility, not charge transfer complex formation or dipolar carbonyl-carbonyl attraction.

### 3.11.5 Crystallinity

Crystalline polyimides contain microcrystallites embedded in a matrix of amorphous polymer. The microcrystalline regions are composed of individual chains (or different segments of the same chain) packed side by side in a regular manner.

Polymers crystallize to attain a lower free energy. The regular packing of chains means closer packing and enhanced opportunities for intermolecular attractions. This is the driving force behind crystallization. In microcrystalline regions, the chains are held together by dipolar, hydrogen bonding, or van der Waals forces. Crystalline domains function as crosslinks for amorphous regions. The crystalline crosslinks can stiffen and toughen the polymer and reduce the swelling in solvents. However, in some cases, crystallinity can cause the polymers to be brittle.

Degree of crystallinity can be increased in polymers by stretching. Stretching pulls the chains into a roughly parallel orientation. This enhances regular packing of adjacent chains. Additional crystallization can also be introduced by heating and cooling the tensioned polymer in an annealing process. Crystallization which results from orientation can lead to significant increases in such properties as tensile strength, tensile modulus, and toughness.

Melting occurs when the free energy process,  $\Delta G$ , equals zero:

$$\Delta G = \Delta H_m - T_m \Delta S_m = 0$$

$$T_m = \Delta H_m / \Delta S_m$$

where  $\Delta H_m$  is the free enthalpy of melting and  $\Delta S_m$  is the free entropy of melting. With few exceptions, polymer structure influences the  $T_g$  and  $T_m$  similarly. Similar considerations of cohesive energy and molecular packing apply to amorphous and crystalline regions respectively, in accounting for the temperature at which transitions occur. As a result, the  $T_m$  and  $T_g$  are related for many polymers by the Beaman relationship where  $T_g$  (in Kelvin) is approximately  $1/2$  to  $2/3 T_m$  (in Kelvin). Exceptions that have been noted involve a polymer's tendency to crystallize or hydrogen bonding. Additionally, copolymers do not follow the same ratio[43]. The Beaman relationship[15, 44] is accurate in predicting the melting transition ( $T_m$ ) of aromatic polyimides which exhibit a  $T_g$ :

$$T_m = 1.3 T_g$$

where  $T_g$  and  $T_m$  are Kelvin temperatures. When a polymeric material is heated towards the melting point, the smaller and less perfect crystals melt first followed by the melting of the larger or more perfectly formed areas. Therefore, the  $T_m$  is usually a median of the temperature range. The 1.3 is an empirical constant that has been found for polyimides.

### 3.11.6 Solubility

A number of approaches[45] have been taken to attain solubility in polyimides while maintaining their high temperature characteristics: (1) the

incorporation of flexible or non-symmetrical, thermally stable linkages in the backbone, (2) the introduction of large, polar or non-polar substituents along the polymer backbone, and (3) the disruption of symmetry and recurrence of regularity through copolymerization of two dianhydrides or two diamines. Some highlights of this review will be presented.

Incorporating perfluoroisopropyl groups in both the diamine and dianhydride produced a soluble polyimide that is commercially available from DuPont[45]. Perfluoromethylene groups have been reported to enhance solubility but a minimum of three groups per repeat unit were required. Solubility was achieved by incorporating ether links in both the diamine and dianhydride. Introduction of siloxane groups also imparted solubility.

St. Clair and St. Clair[46] showed that the perfluoroisopropylidene unit in the 6FDA derived system imparted considerable solubility. Additionally, in this work, flexibility was shown to impart solubility through *meta* catenation and ether linkages.

### 3.11.7 Polyimide Color

Color in polyimides may result from chromophoric units, impurities from starting materials, side reaction products such as isoimides, and charge transfer complexing[15, 47].

Studies by St. Clair *et. al.*[48] were designed to reduce the color intensity of polyimide films by separating or removing chromophores, eliminating conjugation, and reducing overall electronic interactions between polymer chains. Introduction of oxygen or sulfur "separator" groups, incorporation of bulky groups such as  $-CF_3$  or  $-SO_2$ , use of *meta* isomerism in the aromatic diamine portion of the polymer, and removal of chromophores such as  $-CO$



groups have all contributed to the reduction of color intensity of polyimide films compared to conventional bright to dark yellow polyimide films. Additionally, evaluation of the effect of monomer purity, casting solvents, and cure atmosphere on the optical transparency of the films was determined.

Results of their study[48] indicated that the introduction of bulky groups such as  $-CF_3$  or  $-SO_2$  in conjunction with *meta*-linked diamines were the most effective in reducing CTC, affording colorless films. The use of separator groups such as  $-O-$  or  $-S-$  in both the diamine and the dianhydride reduced the overall color intensity, but not to the same degree. The purity of the aromatic diamine and dianhydride had a direct effect on the transparency of the resulting polyimide film. For example, the use of impure BTDA with its high acid content reduced optical transparency in polyimide films in additional studies. Additional experiments were conducted to determine the effects of the casting solvent and cure atmosphere on the transparency of the polyimide film. Poly(amic acid) solutions using identical monomers in DMAc, 1-methyl-2-pyrrolidinone (NMP), and a 20:80 mixture of NMP and diglyme were compared. No change in the optical transparency was observed by varying the solvent, or the cure environment of air or nitrogen.

### 3.11.8 Dielectric Constant

Electrical behavior is critical for polymers used as insulators or as the dielectric material in an electrical condenser. The dielectric constant of commercially available polyimides ranges from 3.2 to 4.0 depending on the frequency and moisture content of the polymer. Materials are needed with lower dielectric constants.

Structure/property relationship studies at NASA's Langley Research Center have shown that the introduction of fluorine atoms into the polymer backbone lowers the dielectric constant. The polyimide with the lowest dielectric constant contained the bulky fluorinated  $-C(CF_3)_2$  group in both the diamine and dianhydride[15]. Additionally, further reductions in the dielectric constant were achieved by physically incorporating selected diamine acid additives into low dielectric polyimide systems[49].

Dielectric data provided by St. Clair[15] showed the following trends: (1) *meta*-linked diamine polyimides afforded lower dielectric constants than the corresponding *para*-linked polyimides, (2) the carbonyl bridge in BTDA polymers resulted in higher dielectric constants than the oxy bridge in ODPDA polymers, and (3) 6F containing polyimides had the lowest dielectric overall. Policastro *et. al.*[50] reported that tetramethyldisiloxane units in the dianhydride segment lowered the dielectric constant to approximately 2.7 at 100kHz. St. Clair *et. al.*[51] synthesized aromatic fluorinated polyimides using dimethyl silane dianhydride (SiDA) or isopropylidene dianhydride (IPAN). Dielectric constants using SiDA with various diamines ranged from 2.56 to 2.87 with the lowest dielectric constant resulting from SiDA and 2,2-bis[4-(4-aminophenoxy) phenyl] hexafluoropropane (4-BDAF). Dielectric constants of polyimides containing IPAN and various diamines ranged from 2.49 to 2.80 with the lowest dielectric constant obtained from IPAN and 2,2-bis (3-aminophenyl) hexafluoropropane (4,4'-6F).

Auman *et. al.*[52] have added fluoroalkyl groups pendant to the polymer backbone to introduce a high level of fluorine without generally effecting the backbone stiffness and resulting high  $T_g$ . Dielectric constants, dry at 1MHz, ranged from 2.3 to 2.7 for the polyimides synthesized.

### 3.11.9 Coefficient Of Thermal Expansion

The coefficient of thermal expansion (CTE) is especially important because a mismatch of materials can generate stresses which may lead to device failure. This is especially true for small devices. Low CTE values are usually obtained by designing a rigid rodlike polymer backbone, such as BPDA combined with *p*-PDA. The CTE of this polymer is approximately 3-4 ppm/°C. This CTE value is close to that of silicon and therefore, the stress between this polyimide and a silicon substrate would be minimal.

Feiring *et. al.*[53] prepared polyimides from 2,2'-bis(fluoroalkoxy) benzidines and several dianhydrides that afforded a low moisture absorption, low dielectric constant, and a low CTE. Auman *et. al.*[54] synthesized rigid rodlike polyimides based on 4,4"-diamino-*p*-terphenyl (DATP), a monomer comprised of three aromatic rings between amino functions. Auman and Trofimenko[55] synthesized polyimides based on new fluorinated dianhydrides, 9,9-bis(trifluoromethyl)-2,3,6,7-xanthene-tetracarboxylic dianhydride and its 9-trifluoromethyl-9-phenyl analog, which have rigid, tricyclic structures, in an effort to lower the CTE.

## 3.12 Molecular Orientation (Film Stretching)

### 3.12.1 Introduction

Uniaxially and biaxially stretched films are all around us. They have utility as base films for audio, video, and computer tapes, among other uses. Oriented films are used as electrical wire insulators and in microelectronic

applications. They have enormous application potential; therefore, the understanding of the many aspects of the stretching process is important.

Oriented films are fabricated using two stage or multi-stage lines, blown film units, and uniaxial or biaxial film stretchers. The stretching rate, draw ratio, and temperature are optimized during stretching to produce the desired film properties. Different properties are obtained with uniaxial versus biaxial stretching. All of these parameters are key considerations when fabricating oriented films. Properties influenced by stretching include but are not limited to: (1) mechanical properties such as tensile strength, modulus, and elongation, (2) structural properties such as orientation, crystallinity, and birefringence, and (3) other properties such as electrical conductivity, coefficient of thermal expansion, creep, and surface roughness. The following are some general trends observed when films are oriented: (1) tensile strength and modulus increase with increased draw ratio, (2) elongation and creep strain decrease with increased draw ratio, (3) crystallinity increases with increased draw ratio and stretching rate, and (4) birefringence increases with increased stretching rate and draw ratio but decreases with increased stretching temperature.

### **3.12.2 Film Preparation And Drawing Techniques**

The condition of the film prior to stretching is a key consideration in the drawing process. There are several possible options: stretching films containing residual solvent, stretching films that have only been partially cured, stretching films swollen with an appropriate solvent, or stretching fully cured solvent-free films.

Kochi *et. al.*[56] investigated several drawing techniques to increase the strength and modulus in polyimides: drawing of swollen poly (amic acid) (PAA)

films, cold-drawing of as-cast PAA films[57], and hot drawing of polyimide (PI) films. A mixture of 20 vol% N,N-dimethylacetamide (DMAc) and 80 vol% ethylene glycol (EG) was chosen as the swelling solvent. Swollen films were stretched at 60°C in the swelling solvent using a monoaxial drawing machine[58]. The drawn film was then fixed in a metal frame and thermally imidized by incremental increases in temperature up to 250°C. The film was annealed at 450°C for 10 minutes.

The cold drawing technique utilized PAA solutions cast onto glass plates and subsequently cured for 1 hr at 50°C. The films were then removed from the glass and heated at 50°C under vacuum for 24 hr. The PAA films were cut into strips and drawn at room temperature (RT). The drawn specimens were mounted in a metal frame and thermally imidized at 250°C for 2 hr.

In the hot draw method, the PI films were drawn at their respective glass transition temperature regions. Films were heated to the draw temperature and held for 10 minutes prior to stretching.

### **3.12.3 Stretching Parameters**

There are several parameters that can be varied during stretching. These parameters influence the mechanical, physical, and structural properties of polymers to various degrees.

Stretching parameters include stretching rate, draw ratio, and temperature. The stretching rate is usually reported as a percent (100, 200, 300%, etc of the initial length of the specimen) per min, or as a speed, with units of length/time. Draw ratio is defined as the final length/original length before stretching. The draw ratio can be varied in one direction, or both directions simultaneously or sequentially.

Temperature is a key element in optimizing properties by stretching. Films can be stretched cold; some are stretched at or near their glass transition temperature ( $T_g$ ). Films can be stretched between their  $T_g$  and cold crystallization temperature, while others require higher temperatures near their respective melting points. The optimum stretching temperature can be determined by using thermal analysis information which generally can be obtained by differential scanning calorimetry (DSC), which determines the  $T_g$ , crystallization temperatures, and exotherms.

### **3.12.4 Properties Influenced By Stretching**

Mechanical properties of interest generally include, but are not limited to tensile modulus, tensile strength, yield strength, toughness, and elongation. Tensile modulus is a measure of the stiffness of the film. Tensile strength at break of stretched films is related to the perfection of orientation achieved through stretching. Yield strength is the resistance to initial plastic deformation. Elongation is representative of the mobility of the chains. Toughness is a measure of the energy required for mechanical failure. These properties are influenced by uniaxial and biaxial stretching.

Before discussing the change in tensile properties due to uniaxial or biaxial stretching, it is important to look at the molecular response of the polymer chains during processing. Orientation is induced by thermomechanical treatments at a particular temperature. By examining the stress-strain behavior of a polymer at the temperature of interest, one is able to better understand what is occurring during the stretching process[59-60]. Figure 3.9 shows the stress-strain curve for amorphous polyethylene terephthalate (PET) film,  $T_1 > T_2$  (for  $T > T_g$ ). Although this is specifically for

PET, this stress-strain behavior is typical for many polymers during stretching at the appropriate temperature. Up to the yield point (Region A), work is required to move the molecular segments from their equilibrium positions. This is called instantaneous elastic deformation or elastic extension. Deformation is not permanent at this point since the removal of stress returns the original form and properties. In Region B, the molecular chains rotate, translate, unfold, and become aligned in the direction of stretching. This is termed molecular alignment deformation. The molecular alignment is frozen into the structure upon cooling but deformation is partially recoverable upon heating. The final stage is unrecoverable viscous flow[60]. The polymer is highly ordered and the stress-strain behavior in Region C resembles strain-hardening that occurs in metals. The highest orientation is achieved by high stretching rates, followed by quenching to maintain orientation[60].

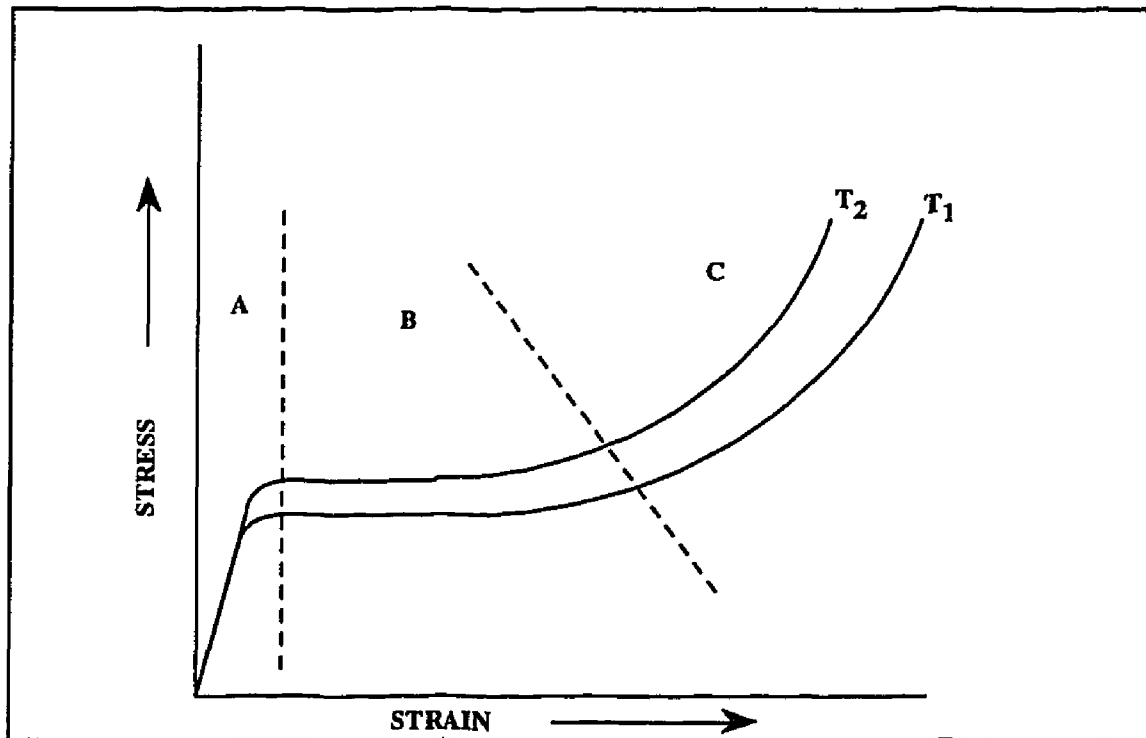


Figure 3.9 Stress-Strain Curve For Pet Film

Uniaxial stretching generally increases the tensile strength and modulus more than biaxial stretching. In a study by Heffelfinger and Schmidt[61], there was significantly higher machine direction tensile properties obtained from uniaxially stretched films compared to biaxially stretched films.

### **3.13 Molecular Modeling**

All chemists use models. Ball and stick models help explain atoms and compounds to children. Students can visualize structures and bond angles of compounds using models. Researchers use chemical drawing programs to assist them in understanding chemical phenomenon. Chemists also use models that are not pictorial, like chemical reactions. For example, the  $SN_2$  mechanism explains a lot of chemistry. Computational chemistry is also a useful model. It simulates chemical conformations and reactions based on the laws of physics. It allows chemists to run reactions on the computer. This could save time in the laboratory or help prioritize synthetic efforts in a study[62].

Computational chemistry is the study of chemistry assisted by computer resources. Computational chemistry, or molecular modeling, is fast emerging as an important research technique in the study of single chain behavior and bulk properties of amorphous, crystalline, and liquid crystalline polymers. Methods in theoretical and computational chemistry have been clearly demonstrated for obtaining geometric parameters, fundamental vibrational frequencies, and relative energies of small molecules. Interest in computational modeling of polymeric materials has greatly increased over the past decade. Structures and properties of polymers with 5000 to 10000 atoms have been investigated using computer simulations. In these simulations,



geometry optimizations are performed by minimizing the total energy under static or dynamic conditions. Much of this work uses empirical force fields based on molecular mechanics potential energy functions. The force field combines segmental vibrational interactions (bond stretching, angle bending, and inversion), van der Waals non-bonded interactions, and electrostatic interactions based on the charge of the atoms[62].

Molecular modeling can help chemists understand quantitative structure-property relationships and subsequently prioritize candidate polymers for synthesizing and testing. One such computer simulation is *Synthia®* by Biosym. *Synthia®* can calculate the following properties with an input of the chemical structure of the repeat unit: thermophysical properties, electrical, optical, and magnetic properties, mechanical properties, chain stiffness and entanglement properties, and transport properties[63].

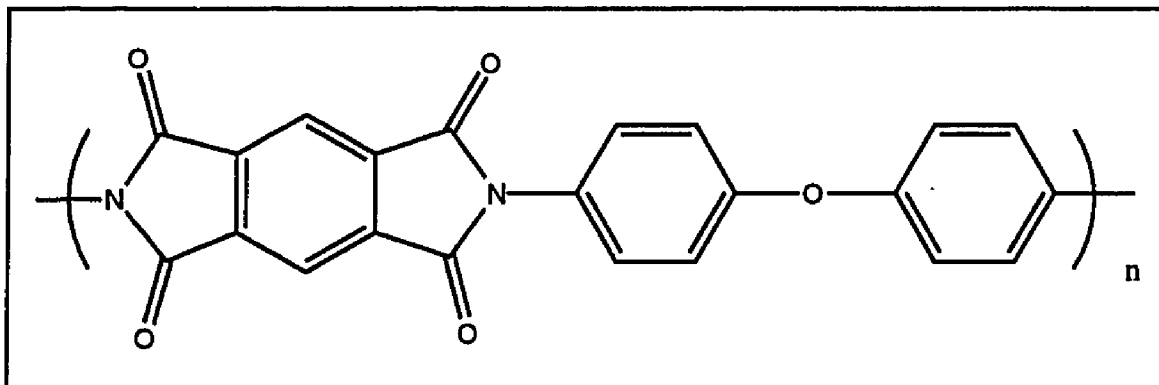
### **3.14 Properties And Applications Of Some Commercial Polyimide Films**

Hergenrother *et. al.*[64] reported on commercially available polyimides for adhesives, coatings, fibers, films, foams, powders and moldings, prepregs, and other applications. The following section will highlight on some of the commercially available films since films were the main product form of the research in this dissertation.

Aromatic polyimide films represent the largest end-use area for this class of polymers. DuPont, UBE, Allied Signal, and Mitsui Toatsu manufacture polyimide films for a variety of applications.

Kapton® polyimide film (Figure 3.10) possesses a unique combination of properties which makes it ideal for a variety of applications in many different industries[65]. The ability of Kapton® to maintain its excellent physical,

electrical, and mechanical properties over a wide temperature range has opened new design and application areas to plastic films.



**Figure 3.10 Kapton®**

Kapton® polyimide film can be used in a variety of electrical and electronic applications: wire and cable tapes, formed cable insulation, substrates for printed circuits, motor slot liners, magnet wire insulation, transformer and capacitor insulation, magnetic and pressure-sensitive tapes, and tubing. It is available in many types, each with unique properties.

Kapton® Type HN has been used successfully in applications at temperatures as low as  $-269^{\circ}\text{C}$  and as high as  $400^{\circ}\text{C}$ . It can be laminated, metallized, punched, formed, or adhesive coated. Kapton® HN is available in various thicknesses: 0.3 mil, 0.5 mil, 0.75 mil, 1 mil, 2 mil, 3 mil, and 5 mil.

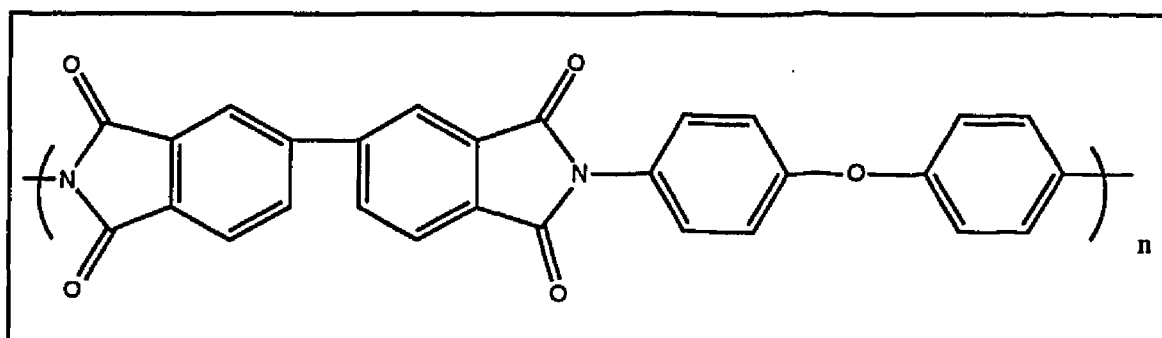
Kapton® Type VN has all the properties of HN film in addition to superior dimensional stability. Kapton® Type FN is a type HN film coated on one or both sides with Teflon® FEP fluoropolymer resin; it imparts heat sealability, provides a moisture barrier, and enhances chemical resistance.

Other Kapton® films are also available that are antistatic or thermally conductive. Kapton® film is available for applications requiring fine line

circuitry properties, cryogenic insulation capability, and corona resistance. Kapton® film can be pigmented for color.

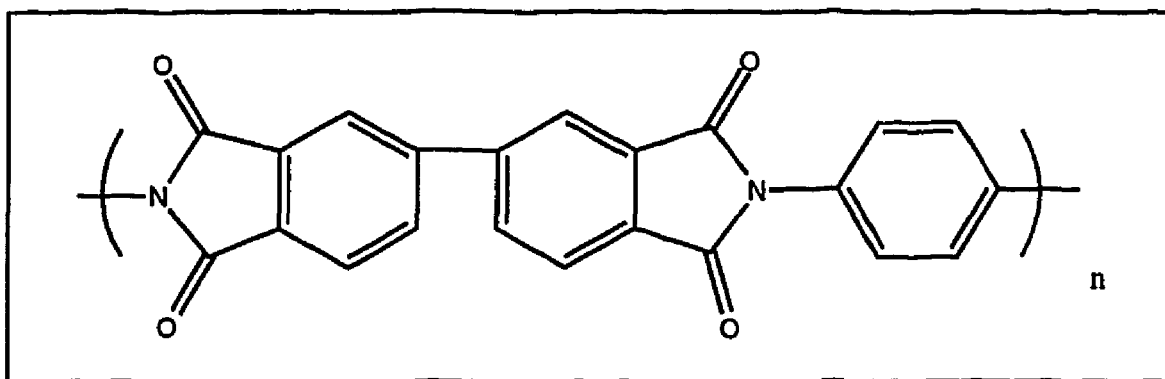
UBE Industries (and Uniglobe Kisco in the USA) manufacture Upilex® R and S polyimide film. They are available at a reasonable price, \$200/kg, and in a range of thicknesses: 0.8 mil, 1 mil, 2 mil, 3 mil, and 5 mil.

Upilex® R (Figure 3.11) is an uncoated, high heat resistant film with well balanced properties. Upilex® R is especially noted for its superior radiation resistance, consistent electrical properties over a wide range of conditions, good tensile strength combined with superior elongation, low water absorption and moisture permeability, and excellent tear initiation and propagation resistance[66].



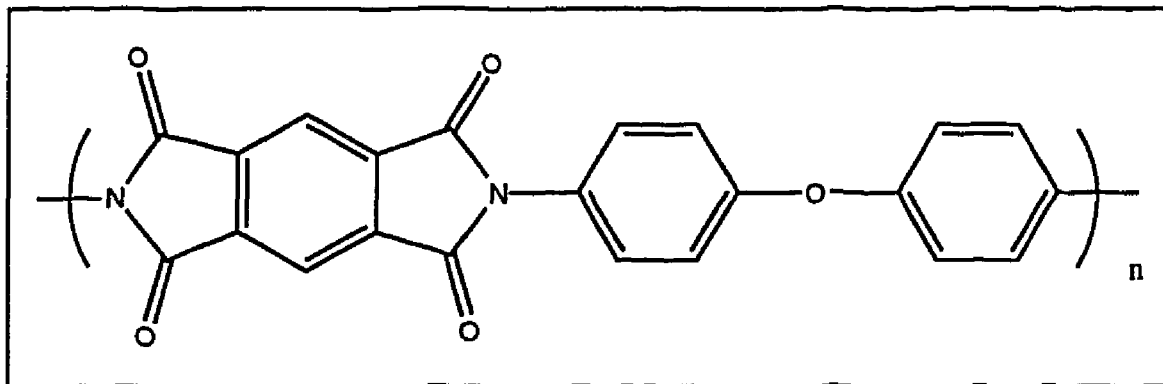
**Figure 3.11 Upilex® R**

Upilex® S (Figure 3.12) is an uncoated, ultra high heat resistant film with superior dimensional stability in chemical solutions, heat, and moisture. Upilex® S is especially noted for its high tensile strength and modulus, very low moisture absorption and moisture permeability, outstanding resistance to attack by chemicals or radiation, superior thermal and hygroscopic expansion characteristics, and consistent electrical properties over a wide range of conditions[66].



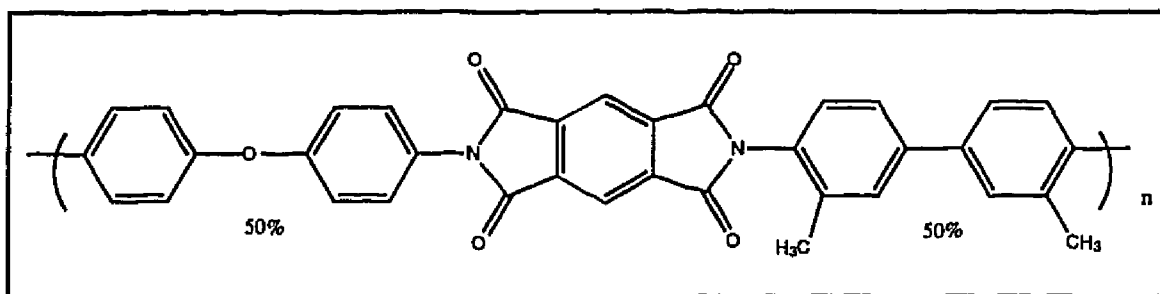
**Figure 3.12 Upllex® S**

Apical® (Figure 3.13), manufactured by Allied Signal, is believed to be the same chemical composition as DuPont's Kapton® and exhibits essentially the same material properties. It is available in 1 mil, 3 mil, and 5 mil thicknesses.



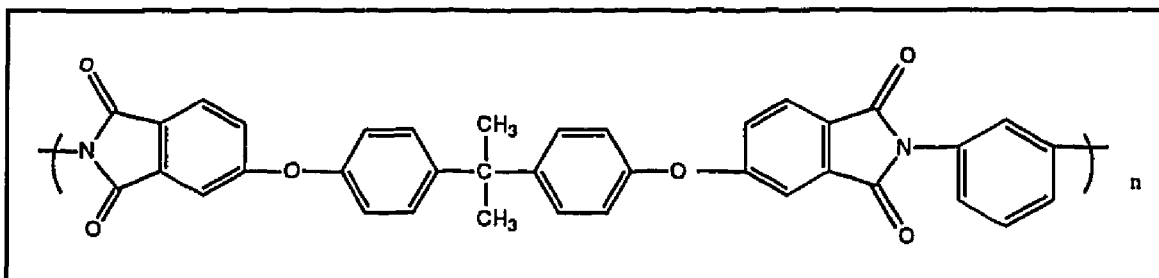
**Figure 3.13 Apical®**

Novax® (Figure 3.14), developed by Mitsubishi, is comprised of PMDA and 50% each of two diamines. It is stiffer than Kapton® and has a higher tensile strength. Its  $T_g$  is high and it possesses a lower CTE and moisture absorption than Kapton®[23].



**Figure 3.14 Novax®**

Ultem® (Figure 3.15) is a polyether imide that was developed at General Electric. It can be reinforced with a variety of materials such as glass or graphite. Ultem® can be injection-molded, compression-molded, or blow-molded. Ultem® is useful for applications in printed wiring boards, under the hood automotive uses, and in aerospace as both the neat resin polymer and in reinforced composites[23].



**Figure 3.15 Ultem®**

Thus far, the general review for polyimides has been presented. The following sections will focus on polyimides for the three particular application areas proposed in this dissertation: potential thermotropic liquid crystalline polyimides as processing aids, polyimides for microelectronic applications, and polyimides for harsh environments.

### **3.15 Potential Thermotropic Liquid Crystalline Polyimides As Processing Aids**

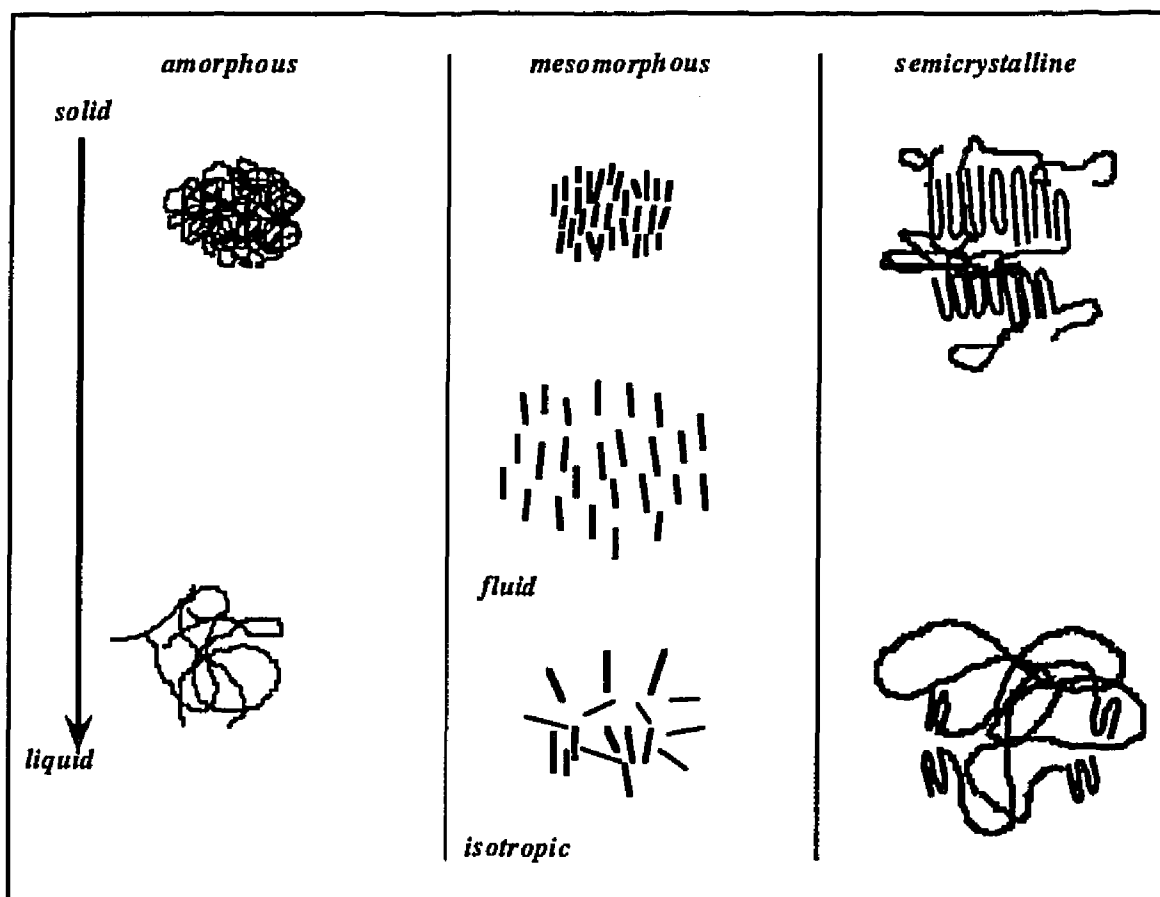
#### **3.15.1 Introduction**

Liquid crystallinity or mesomorphism is a highly desired phenomenon in materials since the molecules tend to orient and remain frozen in that orientation after solidification. This leads to a highly aligned system after processing, with a high degree of chain continuity and increased mechanical strength. Liquid crystalline polymers (LCPs) exhibit a unique balance of properties displayed by conventional amorphous and crystalline polymers. The main properties that differentiate them from the usual engineering thermoplastics (TPs) are their enhanced mechanical properties, chemical resistance, and low viscosity. LCPs are processed from solution by fiber spinning and in the melt by extrusion and injection molding. Enhancement of the material properties are obtained by controlling processing parameters, such as heat treatment, draw ratios, and extrusion rates. LCPs are currently used in tires as reinforcement, soft body armor, ropes, cookware, and chemical barriers. Potential applications of LCPs include other areas like electronics, automotive, and aerospace, to name only a few. LCPs continue to spark interest in both industry and academia and it is likely that more LCPs will find their way to the marketplace over the next few decades.

#### **3.15.2 Liquid Crystal Mesophases**

Liquid crystallinity exists in two forms: (1) lyotropic, in which the phenomenon occurs in solution and depends on concentration and (2) thermotropic, in which the phenomenon occurs in the melt phase and depends



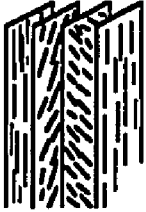
on temperature. The molecules in LCPs in solution or in the melt are not arranged in a random coil configuration like ordinary polymers but have a special architecture that lies between the perfect order in crystals and complete disorder in liquids. Figure 3.16[67] provides a schematic for the polymer conformations in solid and liquid phases for amorphous, mesomorphous, and semicrystalline polymers. The differences in the molecular arrangement as the polymer goes through phases to an isotropic liquid is shown. Amorphous polymers have a flexible, mobile chain in the solid state. In the melt, the molecules are assumed to be in a random coil configuration. In semicrystalline polymers, there are regions of ordered lamella (crystalline domains) between the tangled amorphous regions. These crystalline domains add order to the polymer which increases its strength and stiffness but decreases its elongation. Semicrystalline polymers exhibit better chemical resistance than amorphous polymers because it is difficult for solvents to penetrate the crystalline domains. However, low chain extension is exhibited by both the amorphous and semicrystalline polymers. Low mechanical properties, as compared to a highly aligned, ordered system, result. In LCPs, the mesomorphic domains are stretched and parallel to each other in the solid and liquid states. They exhibit greater order than conventional and semicrystalline polymers and therefore possess higher strengths and stiffnesses.



**Figure 3.16 Polymer Conformations In The Solid And Liquid Phases For Amorphous, Mesomorphous, And Semicrystalline Polymers**

Three major classes of liquid crystalline (LC) structures are known: the nematic, smectic, and cholesteric mesophases[68-69]. The nematic phase has molecules aligned in parallel along one axis (one dimensional order), with a low degree of long range order (periodicity) and low viscosity. The smectic phase has molecules arranged in layers and is highly viscous. The cholesteric mesophase is a chiral nematic structure and is highly viscous. Figure 3.17 shows the three LC structures and lists some structural characteristics[70].



	<ul style="list-style-type: none"> <li>• <b>Molecules Show Parallel One-Dimensional Order</b></li> <li>• <b>Turbid Liquid</b></li> <li>• <b>Low Viscosity</b></li> </ul>
	<ul style="list-style-type: none"> <li>• <b>Molecules Align Parallel And Stratified; Two-Dimensional Order</b></li> <li>• <b>Turbid Liquid</b></li> <li>• <b>Highly Viscous</b></li> </ul>
	<ul style="list-style-type: none"> <li>• <b>Shown By Optically Active Molecules Only</b></li> <li>• <b>Nematic Layers Arranged In Helical Structure</b></li> <li>• <b>Iridescent Liquid With Optical Rotatory Power</b></li> <li>• <b>Highly Viscous</b></li> </ul>

**Figure 3.17 Three Liquid Crystalline Structures And Some Of Their Structural Characteristics**

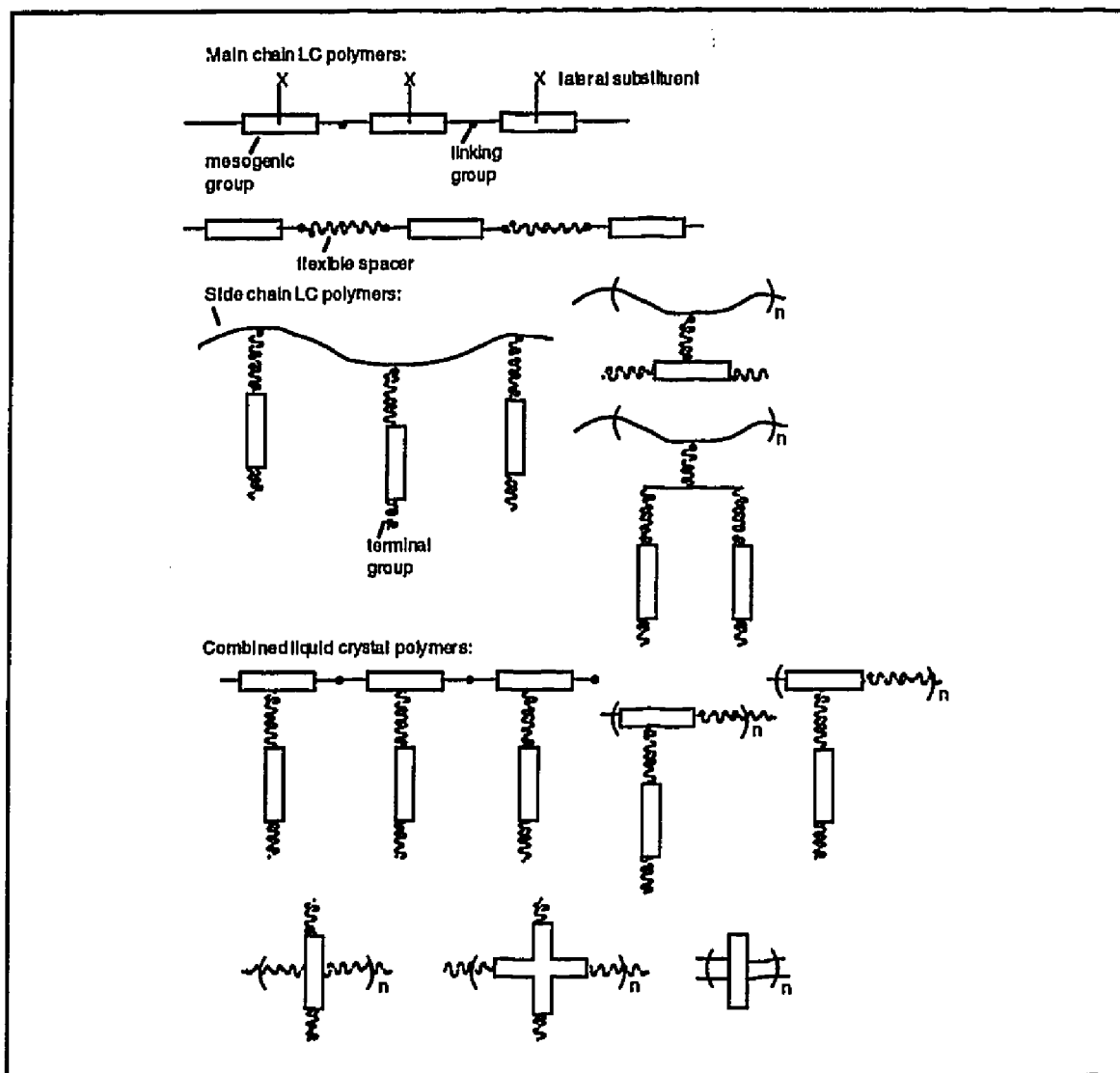
### 3.15.3 Molecular Architecture

Several factors must be taken into account when evaluating the potential LC behavior of polymers. The way in which the molecules pack together in an ordered arrangement and the thermal stability of that ordered arrangement

depend on the molecular structure, shape anisotropy (one molecular dimension is much smaller (disklike) or much larger (rodlike) than the other two), planarity of the mesogenic core, and the equilibrium flexibility of the substituents[71].

LCPs owe their properties to the liquid crystalline moieties that are incorporated into the backbone (main chain LCPs) or in side chains (side chain LCPs). Main chain LCPs have mesogenic building blocks in the polymer chain that are bound together by linking groups and flexible spacers. In side chain LCPs, mesogen units are attached laterally onto a flexible polymer chain through flexible spacers. Figure 3.18 shows a schematic representation of various main chain and side chain LCP configurations.

Configurations in Figure 3.18 depict linking groups and flexible spacers. Thermotropic rodlike materials tend to be infusible and intractable and often decompose below the melting point. In order to melt process these polymers, the melting point must be lowered without eliminating the LC formation. The transition temperatures are lowered by one or more of the following: introduction of flexible segments to separate the mesogenic groups, introduction of rigid kinks into straight polymer chains, substitution of the aromatic ring, or addition of an element of asymmetry to the main chain by copolymerizing mesogenic units of different shapes[71]. Flexible segments and spacers include polyethylene (-CH<sub>2</sub>-) and poly (ethylene oxide). The longer the -CH<sub>2</sub>- sequences, the higher the flexibility. Rigid kinks incorporated into the backbone include naphthalene and diphenyl ether units.



**Figure 3.18 Schematic Representation Of Various Main Chain And Side Chain LCP Configurations**

Some molecular features[72] that give rise to LC potential include:

1. high aspect ratio (length/diameter), generally 50-500
2. rigid units such as 1,4-phenylene, 1,4-bicyclooctyl, 1,4-cyclohexyl, etc.

3. rigid central linkages between rings such as -COO-, -CH=CH-,  
-N=NO-, -N=N-, etc.
4. anisotropic molecular polarization

#### 3.15.4 Rheology

The rheology of LCPs is very unusual. LCPs are more shear sensitive than ordinary polymers. Phenomena such as long relaxation times in the melt, low melt viscosities, shear thinning viscosity at low shear rates, negative first normal stress differences, and little or no die swell can influence the processing conditions[71-73].

Oriented LCPs relax very slowly due to rotation of whole molecules or the concurrent motion of many molecular units. This contributes to their retention of orientation after the solidification step.

The viscosity is inversely proportional to the rotational diffusivity of the rodlike polymers. When the rodlike polymers are parallel to each other, the rotational diffusivity is large and the resulting viscosity is small. LCPs have lower melt viscosities than isotropic polymer melts and therefore can be added to thermoplastics to improve their melt processability. The temperature range over which the LCP forms an anisotropic melt and which the thermoplastic is processed, must overlap. The LCP phase aligns along the flow direction and domains glide easily past each other and lubricate the melt. The reduction of melt viscosity allows a lower processing temperature and/or lower shear stresses to be used[71]. Also, polymers sensitive to degradation would benefit from a lower melt processing temperature.

The viscosity of LCPs is dependent on their shear rate. Shear thinning is when the viscosity decreases with increasing shear rate. The fundamental

reasoning for shear thinning is that the polymer molecules become more and more oriented in the shear direction. Shear thinning occurs at low shear rates.

Die swell values in LCPs are generally found to be smaller than ordinary polymers. The extrudate shrinks in diameter instead of swelling up. Low die swell is attributed to the long relaxation times resulting in nonrecoverable energy at the exit of the capillary[73].

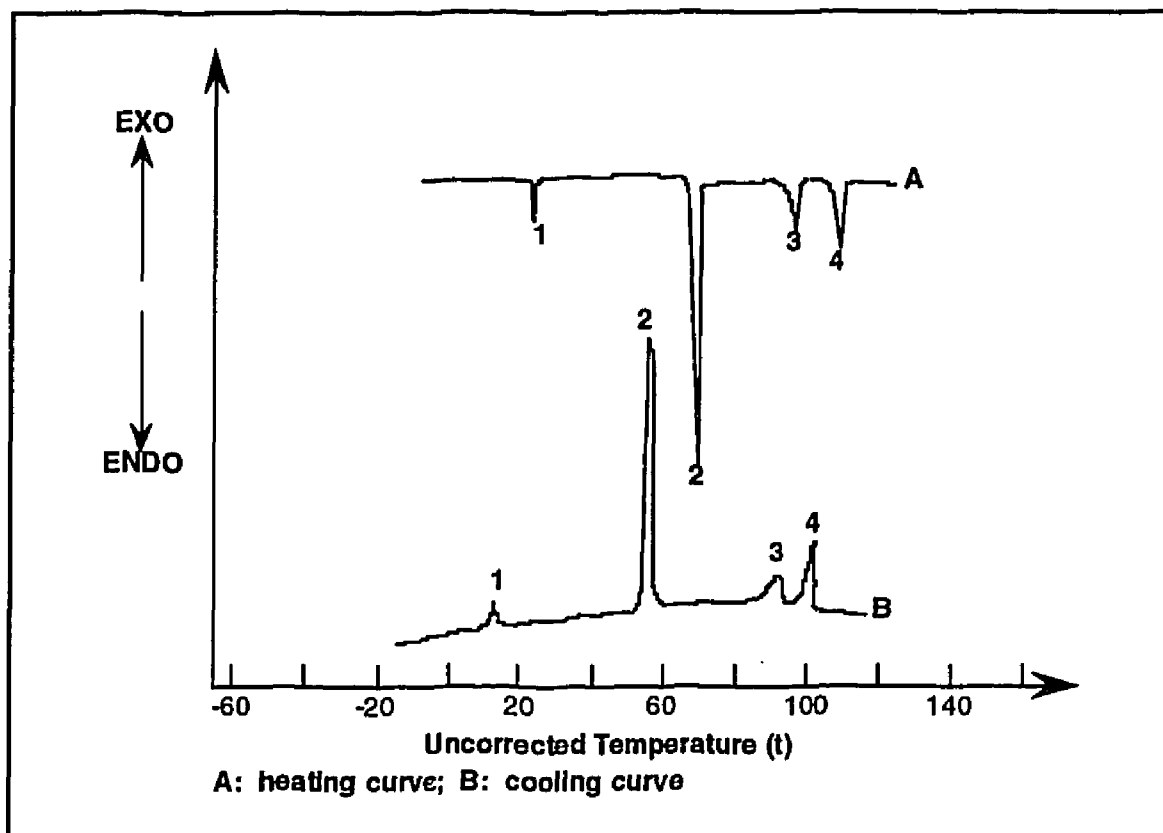
Ide and Ophir studied the orientation of thermotropic LCPs by shear and elongational flow[74]. Elongational flow results from a tensile stress during processing (e. g. drawing) while shear stresses are associated with shear flow. In the isotropic solution, rodlike molecules can be easily oriented in elongational flow; however, in shear flow, the molecules occasionally rotate. In liquid crystals, elongational flow stretches the domains and the molecules align in the flow direction, but shearing does not orient the molecules if the domains are stable.

### **3.15.5 Characterization Of Liquid Crystalline Polymers**

Several techniques available to characterize liquid crystallinity in polymers include: differential scanning calorimetry (DSC)[69, 75], optical microscopy, x-ray diffraction[69], infrared (IR) spectroscopy[72], and nuclear magnetic resonance (NMR).

DSC is a valuable tool in the measurement and calculation of the mesophase transition temperature, transition heats, and entropies. All peaks are reversible. A general liquid crystalline material DSC thermogram is shown in Figure 3.19[69]. A crystalline to crystalline transition occurs at peak 1. The crystalline to smectic B transition occurs at peak 2. Peak 3 denotes a transition phase from LC smectic B texture to a LC smectic A texture. Peak 4 results from

the transition from the smectic phase to an isotropic liquid. All peaks are recoverable as shown by the cooling diagram. LC thermograms may exhibit some or all of these peaks depending on the material. DSC can be used to distinguish between thermotropic nematic and smectic phases by the magnitude of the enthalpy change accompanying the transition to the isotropic phase.



**Figure 3.19 A Typical LC Material DSC Thermogram**

DSC thermograms are different for main chain and side chain LCPs since main chain LCPs are rodlike while side chain LCPs have mesogens attached laterally to the polymer backbone. A main chain LCP with one mesophase exhibits a high temperature exotherm (first order transition isotropic-

mesophase) and a lower temperature exotherm representing a first order transition mesophase crystal. The glass transition temperature may not be readily apparent. In side chain LCPs, a  $T_g$  is observed, followed by a transition from the mesophase to the isotropic melt.

When viewed under the cross polars of a polarizing microscope fitted with a heating stage, liquid crystals are often birefringent and beautiful optical textures can be seen[71, 76]. These textures change with temperature and concentration. Each polymorph shows different textures so it is possible to document the passage of a LC material through the different mesophases to an isotropic liquid.

X-ray diffraction of unoriented samples can be made using the Debye-Scherrer technique on powder samples. Nematic and smectic polymorphs give simple x-ray powder diffraction patterns. Wide angle x-ray diffraction gives interplanar atomic spacing data and the crystal structure of the unit cell. These data are equated to a fingerprint and are unique for each material. Therefore, this technique can be used for chemical identification of liquid crystals. Wide angle x-ray diffraction has also been used to determine the degree of orientation of molecules in processed products (from extrusion or injection molding) and to study how the degree of orientation varies across the flow. Wide angle x-ray diffraction is the most accurate method for measuring structural order in three dimensional systems but NMR and infrared dichroism are used more frequently.

Other techniques used to characterize LCPs include: IR, NMR, MW determination, and thermal optical analysis (TOA). IR spectroscopy and NMR have been used for identification of the chemical microstructure of LCPs. NMR aids in analysis of the polymer sequence distribution and has been used to measure the order parameter of the LCP mesophases[72]. MW determination

by solution viscosity yields information as to whether a sample is polymeric or oligomeric. The lack of solubility of rigid-rod polymers requires aggressive solvents such as sulfuric acid ( $\text{H}_2\text{SO}_4$ ), methane sulfonic acid ( $\text{CH}_3\text{SO}_3\text{H}$ ), and phenol/tetrachloroethane to be used. TOA, sometimes called depolarized light intensity (DLI), measures the intensity of light transmitted through a sample. The transmitted intensity from circularly polarized light can be directly related to sample crystallinity. TOA shows great potential for application in studying LCPs[75].

### **3.15.6 The Properties Of Liquid Crystalline Polymers**

LCPs are a new class of polymers possessing some unique properties that differentiate them from other thermoplastics. The properties of many LCPs include[67-68, 72, 75, 77-78]: high strength and modulus, excellent chemical resistance, low permeability, flame retardance, dimensional stability, and radiation resistance. Exceptions will be noted.

LCPs rodlike molecular structures provide strength and stiffness much like fiber reinforced composites. Modulus depends on chemical moieties and bonds comprising the molecular chain, conformation of the molecular chain, the orientation of the molecular chain, and the packing density of the molecular chains in the solid state[24]. LCPs and high performance thermoplastics are usually highly aromatic systems, which contributes to their high strength and stiffness. Tensile strength, modulus, and notch toughness are dependent on how strongly the molecules in the polymer are oriented in one direction. For a given molecular structure, the modulus increases as the rodlike character increases. LCPs possess higher flexural modulus values than poly (ether sulfone) (PES), poly (ether ether ketone) (PEEK), and many other TPs for



unfilled and glass fiber filled samples[79]. LCPs have excellent retention of mechanical properties at elevated temperature and often their properties at 200°C exceed room temperature (RT) properties of many engineering plastics. LCPs have good fatigue resistance. Toughness can be maintained even at cryogenic temperatures.

Due to their high crystallinity, LCPs exhibit excellent chemical resistance and are essentially unaffected by most solvents (e. g. acetone, chloroform, methylene chloride, methanol), fuels, grease, oil, and hydraulic fluid over a broad temperature range. Exposure to these chemicals results in no loss of mechanical properties, dimension, or weight after 30 days. However, highly concentrated acids and bases, and high pressure steam can attack LCPs at elevated temperatures. Thermotropic LCPs exhibit barrier properties superior to any other melt processable polymeric barrier material. The high degree of molecular order in the LCP molecules allows these materials to attain a very tight packing density similar to a log jam in a river; the tight packing makes it difficult for solvents to penetrate. Many thermotropic LCPs are nondripping and produce no halogens, cyanides, or nitrous oxides upon combustion.

LCPs have a coefficient of thermal expansion (CTE) close to that of glass because LCPs have a considerably lower heat of fusion compared to other conventional polymers; the CTE can be controlled by processing conditions, chemical composition of the LCP, and the use of fillers. The CTE of the LCP is lower than aluminum, copper, solder, PEEK, polyphenylene sulfide (PPS), and many other thermoplastics. LCPs have dimensional stability superior to other high performance engineering plastics, thermoset epoxies, and ceramics. LCPs can perform in the temperature range from cryogenic to 200°C with little dimensional change.

Thomas and Roth[80] claim that thermotropic LCPs are transparent to microwave energy and are virtually unaffected by exposure to 500 megarads of cobalt 60. Lyotropic LCPs are not resistant to ultraviolet (UV) radiation and exposure to visible radiation reduces their mechanical strengths[68]. Dielectric constant, dielectric strength, volume resistivity, and arc resistance of LCPs match or exceed those of other highly heat resistant polymers. Most LCPs have dielectric constants less than 3.0 and dissipation factors less than 0.01.

### **3.15.7 General Applications**

LCPs have a combination of the properties exhibited by conventional amorphous polymers and conventional crystalline polymers, making them good replacement candidates where metals, thermosets, ceramics, and other high performance thermoplastics are typically used[72]. Electrical and electronic markets currently employ PPS and phenolics for application in connecting and distribution devices, components, etc. The performance requirements for printed circuit boards (mechanical strength and toughness, good processability and molding to tight tolerances, dimensional stability, chemical resistance, and low CTE) can be better met with LCPs, but their high cost is a barrier despite their excellent properties.

Additional areas where LCPs may find application include the automotive, chemical, and medical industries. One driving force in the automotive industry to utilize LCPs is the weight reduction. Other applications include mechanical parts and fuel system components, due to their broad continuous temperature range, resistance to automotive fluids and solvents, and flame resistance. Competitors are PEEK and polyamide imides. In the chemical industry, LCPs can be used in pumps (bearings, rings, etc.) and in

distillation column packings to improve the separation efficiency. Bronze and fluoropolymers are currently used in these applications. LCPs have potential in the medical markets due to their compatibility with sterilization techniques (steam, cold chemical disinfection, dry heat, ethylene oxide sterilization, and gamma radiation).

LCPs have lower viscosities in general than conventional thermoplastics and therefore can be added to thermoplastic matrices to reduce the viscosity of the blend. Thus, LCPs serve as effective processing aids, even at low concentrations. However, the embrittlement problems have deterred this potential practical application from becoming a reality with thermotropic systems.

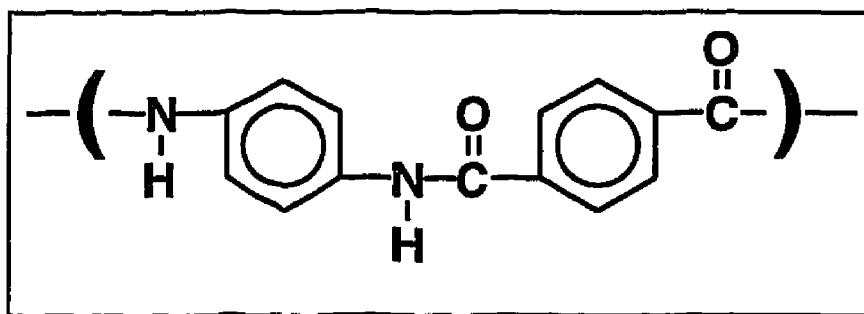
Potential areas for blends are the same as those for LCPs. Blends can be used in the electronics industry in molded interconnected devices and multilayer circuit boards. The automotive industry can use LCP blends in engine parts. LCP blends show promise for use in primary and secondary structural components.

### **3.15.8 State-of-the-art LCPs**

#### **Kevlar®**

Commercially available LCPs have found a wide variety of applications. One of the most well known lyotropic LCPs is Kevlar® (Figure 3.20). Kevlar®'s unique properties arise from crystal orientation that is not only parallel on the fiber axis but also has radial order, much like the spoke of a wheel. There are many grades of commercial and experimental Kevlar® available (e. g. 29, 49, 119, 149, etc). Each grade of Kevlar® is chemically the same, however, they differ in physical and mechanical properties, notably

in their moduli values. The difference in moduli results from proprietary variations in the processing conditions. Kevlar® fibers are five times as strong as steel on an equal weight basis. Kevlar® aramid fiber applications include [77, 81-83]: reinforcements in radial tires, replacement of asbestos in friction products, and ropes and cables for use on floating offshore oil drilling platforms. Additionally, Kevlar® is used in bullet-proof vests; it can stall a chain saw blade. Kevlar® combined with nylon has been used to manufacture an artificial foot. Kevlar® fibers are used in boat hulls and other structural components due to its high strength, light weight, and ability to dampen vibrations.



**Figure 3.20 Poly(*p*-phenylene terephthalate) (PPT) (Trade name Kevlar®)**

### Nomex®

Nomex® (Figure 3.21) possesses primary bond strength in its aromatic structure, hydrogen bonding, polar -CO groups, and molecular regularity in its all *meta* catenation; these characteristics contribute to the excellent flame retardance of Nomex®. Nomex® aramid blend structural sheet products are useful in thermal and electrical insulation and fire blocking layers due to its superior flame retardant properties. The high temperature resistance makes them suitable for asbestos replacement and in heat resistant workwear; both poly (benzamide) (PBA) and poly (*p*-phenylene terephthalate) (PPT) are used

in such applications. The service life of Nomex<sup>®</sup> is longer than for asbestos, and the wearing comfort is greater[68, 84].

Collyer[68] included Nomex<sup>®</sup> in his discussion of lyotropic liquid crystals; however, information received from the product information line stated that DuPont scientists believe the packing in Nomex<sup>®</sup> is not close enough for liquid crystallinity to occur.

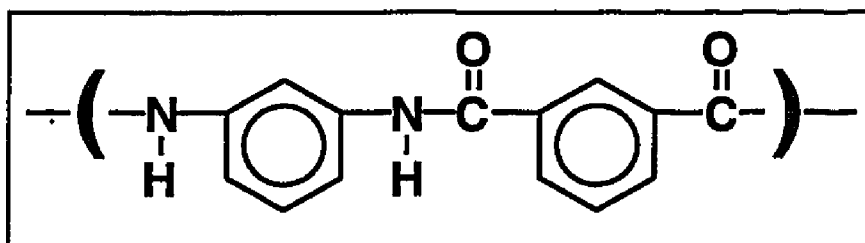
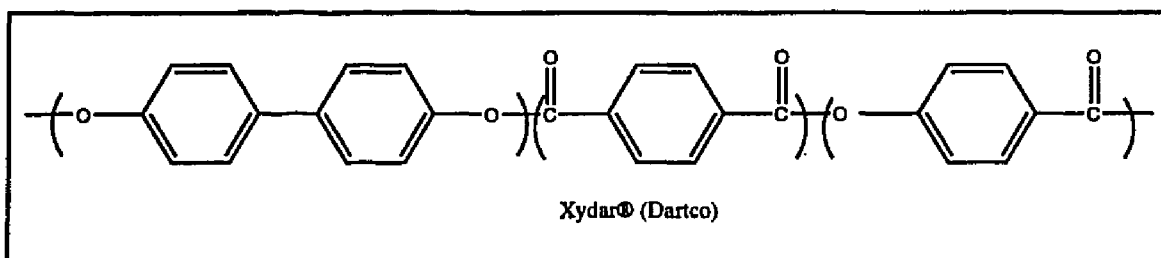


Figure 3.21 Poly (*m*-phenylene isophthalamide) (Trade name Nomex<sup>®</sup>)

### Xydar<sup>®</sup>

Xydar<sup>®</sup> (Figure 3.22) is comprised of *para*-oxybenzoyl and oxybiphenylene terephthaloyl units. Xydar<sup>®</sup> was developed as part of an effort to produce injection molded cookware for use in conventional and microwave ovens. Additional requirements of this potential cookware were nonstick properties similar to fluoropolymers, and resistance to thermal shock, impact, chemicals, and oxidation. The cookware also had to be superior to ceramic cookware. Xydar<sup>®</sup> has been evaluated more recently for application in commercial aircraft due to its exceptional flame retardance, high temperature strength, solvent resistance, and moldability[85].

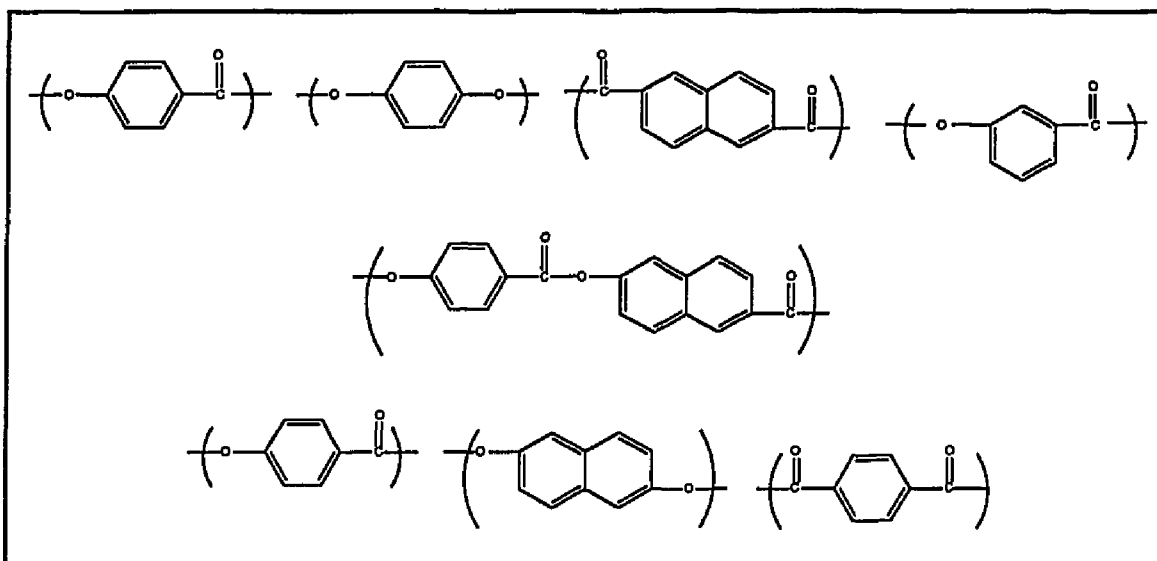


**Figure 3.22 Xydar®**

### Vectra®

Three basic polymers of Vectra® have been developed by Hoechst Celanese and are shown in Figure 3.23. Vectra® processes at a lower temperature than Xydar® but maintains equal or better properties. Its excellent chemical resistance has led to use as a replacement for the chemical saddles used in chemical processing towers and packed beds. LCP packing withstands splintering and fracture, thus resulting in lower maintenance costs. In particular, in an industrial scale column operating at 104°C for distillation of formic acid, the Vectra® saddles were still in outstanding condition after 12 months[67, 69, 86]. Vectra® is more expensive than the ceramic it replaces, however it has a much greater lifetime.

Vectra® can be used wherever high mechanical properties, good dimensional stability, high thermal resistance, low flammability, and outstanding chemical stability are required. The largest application area is electrical or electronic components: plug connectors, sockets, switches, relays, and other structural parts in which high dimensional stability and precision are required. Vectra® is used in fiber optics because of its low CTE, low flammability, and good barrier properties.



**Figure 3.23 Three Basic Polymers Of Vectra®**

### Polyimide and LCP Blends

The Foster-Miller company is examining melt blending of polyimides and thermotropic LCPs[87]. A wide variety of polymer blends containing LaRC™-TPI® (Thermoplastic Polyimide), New TPI®, and Xydar® LCP have been successfully processed by extrusion. Outstanding electrical properties are being obtained and potential application in the electronics industry is feasible.

### **3.16 Liquid Crystalline Polyimides**

Very few thermotropic liquid crystalline polyimides free of ester or carbonate groups have been developed to date. Mitsui Toatsu Chemicals, Central Research Institute (Japan)[88-90] has developed a thermotropic liquid crystalline polyimide which has neither an ester linkage nor a carbonate linkage. When this liquid crystalline polyimide is mixed with a high melting thermoplastic (i.e. Aurum®), the melt viscosity decreased. Kricheldorf and

Linzer[91] developed thermotropic polyimides free of ester groups by synthesizing polyimides prepared from  $\alpha, \omega$ -bis(4-aminophenoxy) alkanes with various aromatic tetracarboxylic anhydrides. These two research efforts have concentrated on the synthesis of novel diamines combined with rigid dianhydrides to afford favorable components of liquid crystalline polymers. No reports have been made describing the incorporation of favorable components of liquid crystallinity into novel flexible dianhydrides combined with rigid diamines.

### **3.17 Polyimides For Microelectronic Applications**

From the early 1950's, polymers have played a key role in the growth of the semiconductor industry. The polymer industry has furnished a variety of materials, ranging from radiation sensitive resists used to pattern the circuitry on chips and boards, to polymers used as insulators on chip carriers, and encapsulants, for protecting the electronic integrated circuit (IC) devices from an adverse environment and as well as increasing their long term reliability. These polymers play a "passive" role; they do not play an active part in the functioning of the device. Conversely, "active" polymers contribute significantly to the electronics industry, and include materials such as conducting polymers. Conducting polymers can be utilized as substitutes for known conductors, as polymer blends with high performance polymers, as non-linear optical materials to transmit or switch light for photonic applications, and as electrochemically active materials[92]. The following discussion will be limited to the passive roles of polymers for encapsulant and interlayer dielectric applications.



### 3.17.1 Encapsulants

The rapid development of IC technology from small-scale integration (SSI) to very large-scale integration (VLSI) has had a great technological and economic impact on the electronics industry. The growth of the number of components per chip, the decrease in device dimensions, and the increase in chip size have imposed stringent requirements on the IC physical design, fabrication, and the IC encapsulants.

Encapsulants are used in IC devices to protect them from an adverse environment and increase their long term reliability. Moisture, contaminants, mobile ions, hostile environmental conditions, and ultra-violet (UV), visible (VIS), and alpha-particle radiation can cause degradation and ultimately affect the performance or lifetime of the IC[93-96].

Moisture is the main cause of corrosion in IC devices. The diffusion rate of moisture is material dependent. Pure crystals and metals are most resistant to moisture, followed by glass. Organic polymers, such as fluorocarbons, epoxies, and silicones are inferior to glass but are still excellent candidates as moisture barriers.

Another source of corrosion in IC devices is mobile ions. Mobile ions, such as sodium and potassium, tend to migrate to the positive-negative (p-n) junction of the IC device, where they acquire an electron and deposit as the corresponding metal. This phenomenon destroys the device. Chloride ions in parts per million (ppm) levels could cause dissolution of aluminum metallization of complimentary semiconductor devices.

UV-VIS radiation can damage light sensitive optoelectrical devices. Protection from UV-VIS radiation is accomplished through the use of opaque encapsulants. Damage can also occur as the result of alpha-particle radiation

from small quantities of uranium in the device packaging. Even cosmic radiation as background radiation from the atmosphere can affect IC devices.

Other hostile environments are encountered during normal operating conditions of integrated circuits, including extreme cycling temperatures, high relative humidity, shock, and vibration.

### **Encapsulant Requirements**

Encapsulants for IC devices must provide a protective barrier for transport of chemical species that could attack the underlying device. They must adhere well to the substrate. Encapsulants must have sufficient mechanical, electrical, and physical properties to be effective in IC devices. They must possess a low dielectric constant to reduce the device propagation delay, and excellent thermal conductivity to dissipate heat produced by IC and high density packages. The encapsulant must be ultrapure since ion contaminants can destroy the device. From a processing standpoint, the encapsulant must be easy to apply over the package and repair in production and service.

### **Inorganic And Organic Encapsulants**

Commonly used inorganic encapsulants include silicon dioxide, silicon nitride, silicon-oxy-nitride, diamond, diamond-like materials, and silicon carbide[93]. Organic encapsulants commonly used in microelectronic applications include silicone, epoxies, polyimides, and benzocyclobutene[93]. Silicones have good temperature cycling qualities, good electrical properties, and a low modulus of elasticity. However, silicones do not exhibit good solvent

resistance and they have low mechanical strength. Epoxies have good mechanical strength and good solvent resistance, but only marginal electrical performance. Polyimides are thermally stable and have good solvent resistance, but usually require high cure temperatures. Benzocyclobutene has good solvent resistance, low moisture absorption, and a low dielectric constant, but requires high temperature curing.

### **3.17.2 Polyimides As Interlevel Dielectrics**

Insulating materials are used to isolate components of an electrical system from each other and from ground, as well as provide mechanical support for the components. Polyimides with the most nearly covalent bonding are the best insulators, and are also the best dielectrics because no carrier is free to conduct electricity. For insulation applications, electrical properties such as low dielectric constant, high electrical resistivity, low loss tangent (dissipation factor), high dielectric strength, and high arc resistance are critical. Electrical components can produce heat, thus the ability of the polyimide to dissipate heat may be important. Additionally, the insulators provide mechanical support, handle the thermal loads, and resist environmental impacts. Therefore, tensile strength, modulus, thermal stability, and toughness are important. Although many properties are important to the design consideration, these insulating properties can be weighted more heavily in the selection of potential candidates.

Polyimides are the first choice as material candidates for dielectrics because of their successful use in printed circuit boards, and planarization properties. Polyimides have to be comparable or better than inorganics to compete in the market. Additional properties necessary for dielectric

applications include[97]: ease of processing, good adhesion, planarization, chemical resistance, low moisture uptake, thermal stability, low CTE, and be cost effective.

Polyimides must possess high heat resistance because device processing may require sealing, packaging, die bonding, wirebonding, and soldering. Thermal stresses occur if there is a mismatch in the CTE of the polyimide and the substrate, resulting in peeling and cracking. A low CTE minimizes these effects. A low dielectric is required to minimize propagation delay, interconnect capacitance, and crosstalk between lines; this allows circuits to be run at a lower power input[98]. The dielectric constant changes with absorbed moisture, so low moisture uptake is required.

There are four possible interfaces when a polyimide is used as an interlayer dielectric[98]: metal on polyimide, polyimide on metal, polyimide on polyimide, and polyimide on substrate. Adhesion of metal on polyimide is poor, but can be enhanced by plasma treatments to the surface of the polyimide. Adhesion of polyimide to metal is dependent on the metal. Adhesion of polyimide to aluminum is excellent while the adhesion of polyimide to copper or nickel is good. Adhesion of polyimide to polyimide depends on the chemical structure. It is also enhanced by plasma treatment of the surface. Adhesion of the polyimide to the substrate is improved by coupling agents such as aminosilanes and aluminum chelates.

### **3.18 Polyimides For Harsh Environments**

#### **3.18.1 Wire And Cable Insulation**

Polyimide insulated electrical wire has been used in the aerospace industry in commercial, military, and to a lesser degree, general aviation aircraft since the early 1970's. The insulation offers benefits in terms of compact physical size, its ability to maintain good mechanical strength at high temperature, and good dielectric strength.

Electrical insulating materials are known to deteriorate by a number of chemical and physical mechanisms which can be related to the polymer structure and the intensity of the various service stresses acting upon it. The predominant mechanism for deterioration is believed to be hydrolysis, a chemical reaction of water or aqueous fluids with the polymer chain where chain scission reduces the average chain length resulting in loss of strength and other properties. The rate of deterioration has been shown to be dependent upon the mechanical stresses from bending and stretching[99-100].

Wiring failures linked to insulation damage have drawn much attention in the media, and concerns have developed regarding the long term stability and safety of polyimide insulated electrical wire. The mechanical durability and chemical stability of polyimide insulated wire are affected by hydrolysis, notch propagation, wet and dry arc tracking, topcoat flaking, and degradation due to high pH fluids[101-104]. Polyimide insulated electrical wire may be routinely exposed to high humidity, alkaline cleaners, and paint removers while under mechanical stresses, due to the nature of the wiring and its installation in aircraft. These conditions, commonly encountered during aircraft maintenance and operation, can cause degradation of the polyimide insulation, and result in

electrical failure (short circuit), commonly referred to as carbon arc tracking. The heat from the electrical current passing through the conductor in the degraded material can lead to more insulation degradation and can propagate the arc to additional wiring. The presence of moisture can also accelerate the arc (wet arc tracking). In some cases, carbon arc tracking and subsequent electrical fires have been reported[105-106]. Although the cause is usually attributed to mechanical damage due to poor wiring installation, the actual phenomenon leading to damage has not been satisfactorily explained.

Kapton® HN was the most widely used polyimide for electrical insulation in military and some commercial aircraft until the early 1990's. Kapton® HN was originally developed for use in printed circuits, an application that required the removal of the polyimide by sodium hydroxide. Because of its lack of resistance to the hydroxide ion found in many cleaning solutions, a more hydrolytically stable polyimide insulator was needed for this application.

### **3.18.2 Radiation-Resistant Polyimides**

The increased commitment from NASA and private industry to the exploration of outer space and the use of orbital instrumentation to monitor the Earth has focused attention on the organic polymeric materials for a variety of applications in space. Certain high performance polymers offer attractive features such as low density, high strength, optical transparency, and low dielectric constant. Polymeric matrix composites also offer weight savings, high strength, stiffness, and dimensional stability. Some polymeric materials have exhibited short-term (3-5 yr) space environmental durability; however, future spacecraft are being designed with lifetimes projected to be 10-30 years.

This gives rise to concern that material property change brought about during operation may result in unpredicted spacecraft performance[107].

Depending on the altitude and inclination, a spacecraft in orbit around the Earth can be subjected to the simultaneous effects of thermal cycling, atomic oxygen, ultraviolet radiation (UV), charged particles (electrons, protons, etc.), and high vacuum. To develop space durable polymeric materials, the mechanisms of environmentally induced degradation should be understood. This poses a difficult problem as no ground based simulation facility exists which can accurately reproduce all aspects of a particular space environment. Available facilities use either combined exposures (e.g. electrons and UV) or sequential exposures in an attempt to simulate a specific orbital environment. However, the use of sequential exposures may be misleading because of the absence of synergistic effects. In addition, simulation of 30 years of exposure in a reasonable amount of time requires high dose rates[107].

Material development for spacecraft applications has focused on three classes of materials: polymer films, coatings, and composites. Kapton® and Mylar® are currently used on spacecraft as thermal blankets[108]. Polymeric, metallic, and ceramic coatings are used to protect space structures, vehicles, or instrumentation from UV, electron, and proton radiation, and atomic oxygen. Composite materials such as graphite/polymer, graphite/aluminum, and graphite/glass are being evaluated for structural applications.

There are two space orbits to consider. In low Earth orbit (LEO), the primary effects include atomic oxygen, and micrometeoroid and space debris impacts. In geosynchronous orbit (GEO), the primary effects are electron and proton radiation. Long missions (25-30 years) may exceed the threshold for radiation damage for many polymeric materials, which is thought to occur at

$10^9$  rads. Changes in the mechanical and physical properties of these materials at these high dosages is a growing concern in the development and selection of material candidates.

Low Earth orbit (LEO) materials, such as those used for the Space Station, must have atomic oxygen stability, damage tolerance and toughness, stable optical properties, and low outgassing. Material requirements for geosynchronous orbit (GEO) include radiation stability (UV, electron, and proton), low expansion, high stiffness and damping capacity, and low outgassing.

### **3.18.3 Squaric Acid Containing Polyimides**

After an exhaustive literature search, no data were found on polyimides containing squaric acid derivatives. However, there are several articles discussing squaranes or squarylium dyes and their potential application in photovoltaics[109-110]. The squaric moiety is proposed to generate electrons and supply power, therefore making those materials useful in photovoltaic space power systems[111]. Photovoltaic space power and thin film solar cells are reviewed[112-113].



### 3.19 REFERENCES

1. Bogert, T. M.; Renshaw, R. R. *J. Am. Chem. Soc.* **1908**, *30*, 1140.
2. Critchley, J. P.; Knight, G. J.; Wright, W. W. *Heat Resistant Polymers, Technologically Useful Materials*; Plenum Press: New York and London, 1983; p 185-321.
3. Edwards, W. M.; Robinson, I. M. U.S. Patents 2 710 853, 1955; 2 867 609, 1959; 2 900 369, 1959.
4. Bessonov, M. I.; Koton, M. M.; Kudryavtsev, V. V.; Laius, L. A.; *Polyimides: Thermally Stable Polymers*, 2nd Ed.; Plenum: New York, 1987; p 1-95.
5. Bower, G. M.; Frost, L. J. *J. Polym. Sci.* **1963**, *A1*, 3135.
6. Dine-Hart, R. A.; Wright, W. W. *J. Appl. Polym. Sci.* **1967**, *11*, 609.
7. Frost, L. W.; Kesse, J. J. *J. Appl. Polym. Sci.* **1964**, *8*, 1039.
8. Sroog, C. E.; Endrey, A. L.; Abramo, S. V.; Berr, C. E.; Edwards, W. M.; Olivier, K. L. *J. Polym. Sci.* **1965**, *A3*, 1373.
9. Harris, F. W. In *Polyimides*, Wilson, D.; Stenzenberger, H. D.; Hergenrother, P. M., Eds.; Blackie: Glasgow and London, 1990; p 1-36.
10. Ardashnikov, A. Ya.; Kardash, I. Ye.; Pravednikov, A. N. *Polym. Sci. USSR* **1971**, *13(8)*, 2092.
11. Pravednikov, A. N.; Kardash, I. Ye.; Glukhoyedov, N. P.; Ardashnikov, A. Ya. *Polym. Sci. USSR*, **1973**, *15(2)*, 399.
12. Gordina, T. A.; Kotov, B. V.; Kolninov, O. V.; Pravednikov, A. N. *Vysok. Soyed 15B* **1977**, *237(3)*, 612.
13. Svelichnyi, V. M.; Kalinish, K. K.; Kudryavtsev, V. V.; Koton, M. M. *Dokl. Akad. Nauk* **1977**, *237(3)*, 612.
14. Zubkov, V. A.; Koton, M. M.; Kudryavtsev, V. V.; Svelichnyi, V. M. *Zh. Org. Khim.* **1981**, *17(8)*, 1682.

15. St. Clair, T. L. In *Polyimides*; Wilson, D.; Stenzenberger, H. D.; Hergenrother, P. M., Eds.; Blackie: Glasgow and London, 1990; p 58-78.
16. Takekoshi, T. U.S. Patent 3 847 870, 1974.
17. Baise, A. I. *J. Appl. Polym. Sci.* **1986**, *32*, 4043.
18. Kreuz, J. A.; Endrey, A. L.; Gay, F. P.; Sroog, C. E. *J. Polym. Sci. A-1* **1967**, *4*, 2607.
19. Beck & Co., French Patent 1 373 383, 1964.
20. Vinogradova, S. V.; Vygodskii, Ya., S.; Korshak, V. V.; *Polym. Sci. USSR* **1970**, *12(9)*, 2254.
21. St. Clair, T. L.; Chang, A. U. S. Patent Application Case Number LAR 15020-1, 1993.
22. Takekoshi, T. In *Polyimides*; Wilson, D.; Stenzenberger, H. D.; Hergenrother, P. M., Eds.; Blackie: Glasgow and London, 1990, p 38-57.
23. Sroog, C. E. *Prog. Polym. Sci.* **1991**, *Vol. 16*, 561-694.
24. *Polymers: An Encyclopedia Source Book of Engineering Properties*, John Wiley and Sons: New York, 1987; p 319-364, 427-476, 509-569.
25. Adrova, N. A. Israel program for Scientific Translation, Jerusalem, 1968.
26. St. Clair, T. L. Presented at the Symposium on Recent Advances in Polyimides and Other High Performance Polymers, Reno, NV, July 13-16, 1987.
27. Dine-Hart, R. A.; Wright, W. W. *Makromol. Chem.* **1971**, *143*, 189.
28. Androva *et. al.*, *Vysokomol. Soedin* **1979**, *B17(5)*, 409.
29. De lasi, R.; Russell, J. J. *J. Appl. Polym. Sci.* **1971**, *15*, 2965.
30. Heacock, J. F. In *Proc. 2nd Int. Conf. on Polyimides*, Ellenville, NY, Oct. 30-Nov. 1, 1985; p 174 .

31. Mundhenke, R. F.; Schwartz, W. T. *High Performance Polymers* **1990**, *2(1)*, 57.
32. O'Donnell, J. In *Radiation Effects on Polymers*; Clough, R. L.; Shalaby, S. W., Eds.; ACS Symposium Series, 1991; Chapter 24, p 402-413.
33. Dezern, J. F.; Croall, C. I., "Structure-Property Study of Keto-ether Polyimides"; NASA Technical Memorandum 104178, Dec. 1991.
34. Dezern, J. F.; Croall, C. I. In *Advances in Polyimide Science and Technology: Proceedings of the Fourth International Conference on Polyimides*; Ellenville, NY, Oct. 30-Nov 1, 1991; p 468-481.
35. Lee, W. A. Royal Aircraft Establishment Technical Report 66409, August 1966.
36. Bell, V. L.; Gager, H. J. *J. Polym. Sci.: Polymer Chem. Ed.* **1976**, *Vol. 14*, 2275-2292.
37. Gibbs, H. H. ; Breder, C. V. *ACS Polymer Preprints* **1974**, *15(1)*, 775.
38. St. Clair, T. L.; St. Clair, A. K.; Smith, E. N. In *Structure-Solubility Relationships in Polyimides*; Harris, F. W., Ed.; Academic Press, 1977; p 199.
39. Gerber, M. K.; Pratt, J. R.; St. Clair, T. L. In *Proceedings of the Third Conference on Polyimides*, 1988; p 101.
40. Gordina, T. A.; Kotov, B. V.; Kolniov, O. V.; Pravednikow, A. N. *Vysokomol Soed*, **1973**, *B15*, 378.
41. Fryd, M. In *Polyimides: Synthesis, Characterization, and Applications*; Mittal, K. L., Ed.; 1984; p 377-383.
42. Lee, Chung-jen Submitted to the Technical Volume Committee of the Society of Plastics Engineering, 1987; *Macromol. Chem. Phys.* **1989**, *C29(4)*, 431-560.
43. Billmeyer, Jr., F. W. *Textbook of Polymer Science*; John Wiley and Sons, NY; 1984.

44. Beaman, R. G. *J. Polym. Sci.* **1955**, *9(5)*, 470.
45. Harris, F. W.; Lanier, L. H. In *Structure-Solubility Relationships in Polymers*; Academic Press, 1977; p 183.
46. St. Clair, A. K.; St. Clair, T. L. In *Polymers for High Technology, American Chemical Society Symposium Series*, Bowden, M. J.; Turner, S. R., Eds.; 1987; p 437.
47. St. Clair, A. K.; St. Clair, T. L. U.S. Patents 4 595 548 and 4 603 061, 1986.
48. St. Clair, A. K.; St. Clair, T. L.; Stemp, W. S. In *Recent Advances in Polyimide Science and Technology, Proceedings of the 2nd International Conference on Polyimides*, Weber, W.; Gupta, M., Eds.; Society of Plastic Engineers, Poughkeepsie, NY, 1987; p 16-36.
49. Stoakley, D. M.; St. Clair, A. K.; Baucom, R. M. Presented at the SAMPE Electronic Conference, Los Angeles, CA, June 19-22, 1989.
50. Policastro, P.P.; Lupinski, J. H.; Hernandez, P. K. *Preprints Polymer Mat. Sci., and Eng.* **1988**, *59*, 209.
51. St. Clair, A. K.; St. Clair, T. L.; Pratt, J. R. Presented at the SPE ANTEC Conference, New Orleans, LA, May 1993.
52. Auman, B. C.; Higley, D. P.; Scherer, K. V. *Polymer Preprints* **1993**, *34(1)*, 389-90.
53. Feiring, A. E.; Auman, B. C.; Wonchoba, E. R. *Macromolecules* **1993**, *26(11)*, 2779-84.
54. Auman, B. C. *Polymer Preprints* **1993**, *34(1)*, 443-444.
55. Auman, B. C.; Trofimenko, S. *Polym. Mater. Sci. Eng.* **1992**, *66*, 253-254.
56. Kochi, M.; Yonezawa, T.; Yokata, R.; Mita, I. In *Advances in Polyimide Science and Technology*, Feger, C.; Kojasteh, M. M.; Htoo, M. S., Eds.; Technomica Publishing: Lancaster, PA, 1991; p 375-387.

57. Kochi, M.; Yokata, R.; Iizuka, T.; Mita, I. *J. Polym. Sci.: Part B: Polymer Physics* **1990**, Vol. 28, 2463-2472.
58. Yonezawa, T. Masters Thesis, The University of Tokyo, 1990, 71 (reference not obtainable).
59. Heffelfinger, C. J. *Polym. Eng. and Sci.* **Nov. 1978**, Vol. 18, No. 15, 1163-1173.
60. Siegmann, A.; Nir, Y. *Polymer Eng. and Sci.* **Mid Feb. 1987**, Vol. 27, No. 3, 225-230.
61. Heffelfinger, C. J.; Schmidt, P. G. *J. Appl. Polym. Sci.* **1965**, Vol. 9, 2661-2680.
62. Foresman, J. B.; Frisch, A. *Exploring Chemistry with Electronic Structures*, Gaussian, Inc: Pittsburgh, PA; p 1-7.
63. Biosym Technologies, Inc., "Computational Techniques for Solving Polymer Problems"; 1994.
64. *Polyimides*; Wilson, D.; Stenzenberger, H. D.; Hergenrother, P. M., Eds.; Blackie: Glasgow and London, 1990; Appendix.
65. "DuPont High Performance Films, Kapton® Polyimide Films Summary of Properties"; DuPont, Delaware.
66. "Upilex® Polyimide Films, Technical DataSheet", ICI Films.
67. Brinegar, W. C.; Fleischer, D.; Kirsch, G. *Hoechst High Chem Magazine* **1992**, 6, 36-45.
68. Collyer, A. A. *Material Science and Technology* **Oct. 1990**, 6, 981-992.
69. Collyer, A. A. *Materials Science and Technology* **April 1989**, 5, 309-322.
70. Calundann, Gordon W. Presented at the The Robert A. Welch Foundation Conferences on Chemical Research, XXVI, Synthetic Polymers, Houston Texas, Nov. 15-17, 1982.
71. *Liquid Crystallinity in Polymers*; Ciferri, A., Ed.; VCH: New York, 1991; Chapters 3-5, 10-11.

72. La Mantia, F. P. *Thermotropic Liquid Crystalline Polymer Blends*, Technomic: Lancaster, PA, 1993; Chapters 1-6.
73. Dutta, D.; Fruitwala, H.; Kohli, A; Weiss, R. A. *Polym. Eng. Sci.* **Mid-Sept. 1990**, Vol. 30, No. 17, 1005-1018.
74. *High Modulus Polymers: Approaches to Design and Development*, Zachariades, A. E.; Porter, R. S., Eds.; Marcel Dekker: New York, 1988; p 1-36, 145-168.
75. Collins, P. J. In *Liquid Crystals: Nature's Delicate Phase of Matter*, Princeton University Press: Princeton, NJ, 1990; p 162-180.
76. Brown, G. H.; Crooker, P. P. *Chemical and Engineering News* **Jan. 31, 1983**, 24-37.
77. Kwolek, S.; Memeger, W.; Van Trump, J. E. In *International Union of Pure and Applied Chemistry*; Lewin, M. ,Ed.; VCH Publishers, 1988; p 421-454.
78. Evans, D.; Morgan, J. T. *Cryogenics* **April 1991**, 31, 220-222.
79. Cox, M. K. *Mol. Cryst. Liq. Cryst.* **1987**, 153, 415.
80. Thomas, L. D.; Roth, D. D. *ChemTech* **Sept. 1990**, 546-550.
81. Magat, E. E. *Phil. Trans. R. Soc. Lond. A* **1980**, Vol. 294A, 453-469.
82. Graff, G. *High Technology* **1985**, 62-63.
83. DuPont's Kevlar®, product information booklet.
84. DuPont's Technical Information, Properties of Nomex® Aramid Filament yarns, Bulletin NX-17, 1981.
85. Fein, M. *17th National SAMPE Conference Proceedings* **1985**, Vol. 17, 563-570.
86. Sarlin, J.; Tormala, P. J. *J. Appl. Polym. Sci.* **1990**, Vol. 40, 453-469.
87. Blizzard, K.; Haghghat, R. R. *Polym. Eng. Sci.* **1993**, Vol. 33, No. 13, 799-808.
88. Aranuma, T.; Oikawa, H.; Ookawa, Y.; Yamaguchi, A. *Polym. Prepr.* **1993**, 34 (2), 827.

89. Yamaguchi, K.; Urakami, U.; Tanabe, Y.; Yamazaki, M.; Tamai, S.; Yamaya, N.; Ohta, M.; Yamaguchi, A. *Eur. Pat Appl. EP 425 265*, May 2, 1991; *Chem. Abstr.* **1992**, *115*, 93782n.
90. Asanuma, T.; Oikawa, H.; Ookawa, Y.; Yamasita, W.; Matsuo, M. *J. Polymer Science Part A: Polymer Chemistry* **1994**, *Vol. 32*, 2111-2118.
91. Kricheldorf, H. R.; Linzer, V. L. *Polymer* **1995**, *Vol. 36*, No. 9, 1893.
92. *Science and Applications of Conducting Polymers*; Salaneck, W. R.; Clark, D. T.; Samuelsen, E. J., Eds.; Adam Higler Publishers, 1991.
93. Wong, C. P., "Recent Advances in IC Passivation and Encapsulation" In *Polymers for Electronic and Photonic Applications*, Wong, C. P., Ed.; Academic Press, Inc., 1993; p 167-220.
94. *Encyclopedia of Polymer Science and Engineering*, John Wiley and Sons, 1987; Vol. 5; p 638-641.
95. Kinjo, N.; Ogat, M.; Nishi, K.; Kaneda, A., "Epoxy Molding Compounds as Encapsulation Materials for Microelectronic Devices", In *Specialty Polymers/Polymer Physics*; Springer-Verlag: New York, 1989; p 1-83.
96. Wong, C. P., "Application of Polymer in Encapsulation of Electronic Parts", In *Electronic Applications*; Springer-Verlag, 1988; p 63-83.
97. Rothman, L. B. *J. Electrochem. Soc.* **1980**, *127*, 2216.
98. Monk, D. J.; Soane, D. S. In *Polymers for Electronic and Photonic Applications*; Wong, C. P., Ed.; Academic Press, Inc., 1993; p 119-165.
99. Campbell, F. J., "Hydrolytic Deterioration of Polyimide Insulation on Naval Aircraft Wiring", *Proceedings, IEEE Conference on Electrical Insulation and Dielectric Phenomena* **1988**, 180-188.
100. Campbell, F. J., "Temperature Dependence on the Hydrolysis of Polyimide Wire Insulation", *IEEE Transactions on Electrical Insulation* **1985**, *E1-20*, 111-116.

101. O'Neill, J. F., "The Kapton® Question", *Aviation Equipment Maintenance* **February 1989**, 26-32.
102. Hartman, R. V., "Unsafe Aircraft Wiring Poses Expensive Problem", *Defense Electronics* **January 1983**, 34-38.
103. Doherty, R., "Magellan Blaze Linked to Kapton®", *Electronic Engineering Times* **November 1988**, 6.
104. Pedley, M. D.; Leger, L. J., "Considerations in Using Kapton® Wire Insulation in Shuttle Systems"; NASA, Johnson Space Center, August 1988.
105. Jones, S., "NASA Wondering if Shuttle is Wired for Disaster", *Fort Worth Star-Telegram* **Sept. 21, 1988**, 1-2.
106. Campbell, F. J., Naval Research Lab, Washington, D. C., 20375-5000, personal communication.
107. Connell, J. W.; Siochi, E. J.; Croall, C. I. *High Performance Polymers* **1993**, 5, 1-14.
108. Tenney, D. In NASA Conference Publication 3035, Part 1, 1989; p 25-52.
109. Scott, G. W.; Tran, K. *J. Phys. Chem.* **1994**, 98, 11563-11569.
110. Morel, D. L.; Ghosh, A. K.; Feng, T.; Stogryn, E. L.; Purwin, P. E.; Shaw, R. F.; Fishman, C. *Appl. Phys. Lett.* **1978**, 32(8), 15.
111. Scott, Gary W., "Development of Organic Thin Film Solar Cells for Space Applications", CalSpace Proposal CS-11-92, April 1992; p 3-9.
112. Landis, G. A.; Bailey, S. G.; Flood, D. J. *Space Power* **1989**, Vol. 8, No. 1/2, 31.
113. Ralph, E. *Space Power* **1989**, Vol. 8, Nos. 1/2, 3.



## Chapter 4: Experimental

### 4.1 Potential Liquid Crystalline Polymers

#### 4.1.1 Starting Materials

##### Solvents

Methylene chloride, potassium hydroxide (KOH) pellets, dimethylsulfoxide (DMSO), concentrated hydrobromic acid (HBr, 48%), and dimethylformamide (DMF) were used as received from Aldrich. Glacial acetic acid was used as received from Mallinckrodt. Tetramethylene sulfone (sulfolane) was vacuum distilled prior to use (Aldrich, Phillips 66). N,N-Dimethylacetamide (DMAc) and  $\gamma$ -butyrolactone (GBL) were used as received from Fluka.

##### Dimethoxy and bisphenol synthesis

Anisole (99%, bp 154°C), aluminum chloride (AlCl<sub>3</sub>, 97%), and terephthaloyl chloride (99%) were used as received from Aldrich. Isophthaloyl chloride (98%) was used as received from Fluka. 1,4-Bis(4-fluorobenzoyl) benzene was synthesized as previously reported and recrystallized from toluene (mp 218-219°C)[1]. 1,4-Dihydroxynaphthalene was recrystallized from water (mp 160-161°C, 198-199°C). 4,4'-Bis(4-fluorobenzoyl) biphenyl was synthesized as previously reported (mp 264-265.5°C)[2]. 1,4-Bis(4-fluorobenzoyl) hexane was prepared as previously reported (mp 123-

124°C)[3]. 3,3'-Bis(4-fluorobenzoyl) biphenyl was prepared as previously reported (mp 161-162°C)[4]. 1,4-Bis(4-fluorobenzoyl) butane was synthesized as previously reported (mp 165-167°C)[5].

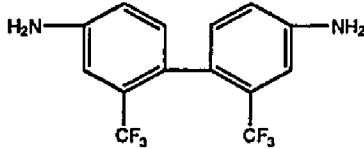
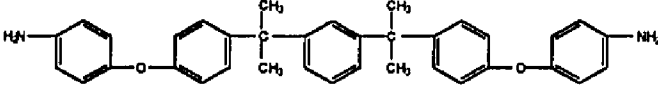
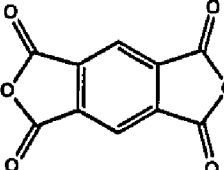
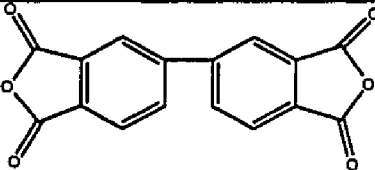
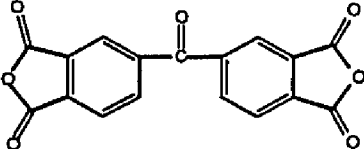
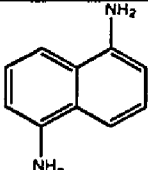
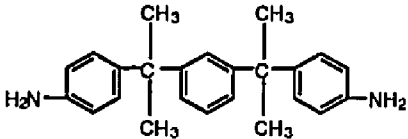
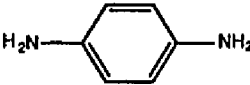
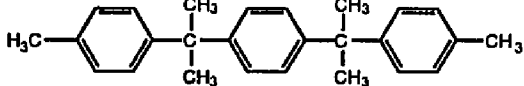
### Dianhydride Synthesis

1,3-Bis(4-hydroxyphenyl-2-propyl) benzene (Bisphenol M) was used as received from Ken Seika Corp (mp 138-139°C). 4-Fluorophthalic anhydride was used as received from Occidental Chemical Corp (mp 77-78°C). Spray-dried potassium fluoride (KF, 99%) was used as received from Aldrich. 1,4-Bis(4-hydroxy-2-propyl) benzene (Bisphenol P) was used as received from Ken Seika Corp (mp 194-195°C).  $\alpha,\alpha$ -Bis(4-hydroxy-3,5-dimethylphenyl)-4-diisopropyl benzene was used as received from Shell Development Co.

### Polymer Synthesis

1,5-Diaminonaphthalene (1,5-DAN) was recrystallized from ethanol (Aldrich, mp 190-191°C). 2,2'-Bis(trifluoromethyl) benzidine (ABL-21) was used as received from Central Glass (Japan) (mp 182-183°C). 1,4-Phenylenediamine (*p*-PDA) was recrystallized from ethanol and then sublimed (Aldrich, mp 142-143°C). 1,3-Bis[4-aminophenoxy-4-( $\alpha,\alpha$ -dimethylbenzyl)] benzene (1,3-BAPDBB) was prepared as previously described[6-7]. Phthalic anhydride (PA) was sublimed prior to use (Aldrich, mp 129-130°C). 1,3-Bis(4-amino-2-propyl) benzene (Bisaniline M, (BAM)) was used as received from Mitsui (Japan). 1,4-Bis(4-amino-2-propyl) benzene (Bisaniline P, (BAP)) was used as received from Air Products. Pyromellitic dianhydride (PMDA) was sublimed prior to use (mp 283-284°C). 3,3',4,4'-Benzophenone tetracarboxylic dianhydride (BTDA) was sublimed prior to use (mp 222-223°C). 3,3',4,4'-Biphenyl tetracarboxylic dianhydride (BPDA) was used as received from

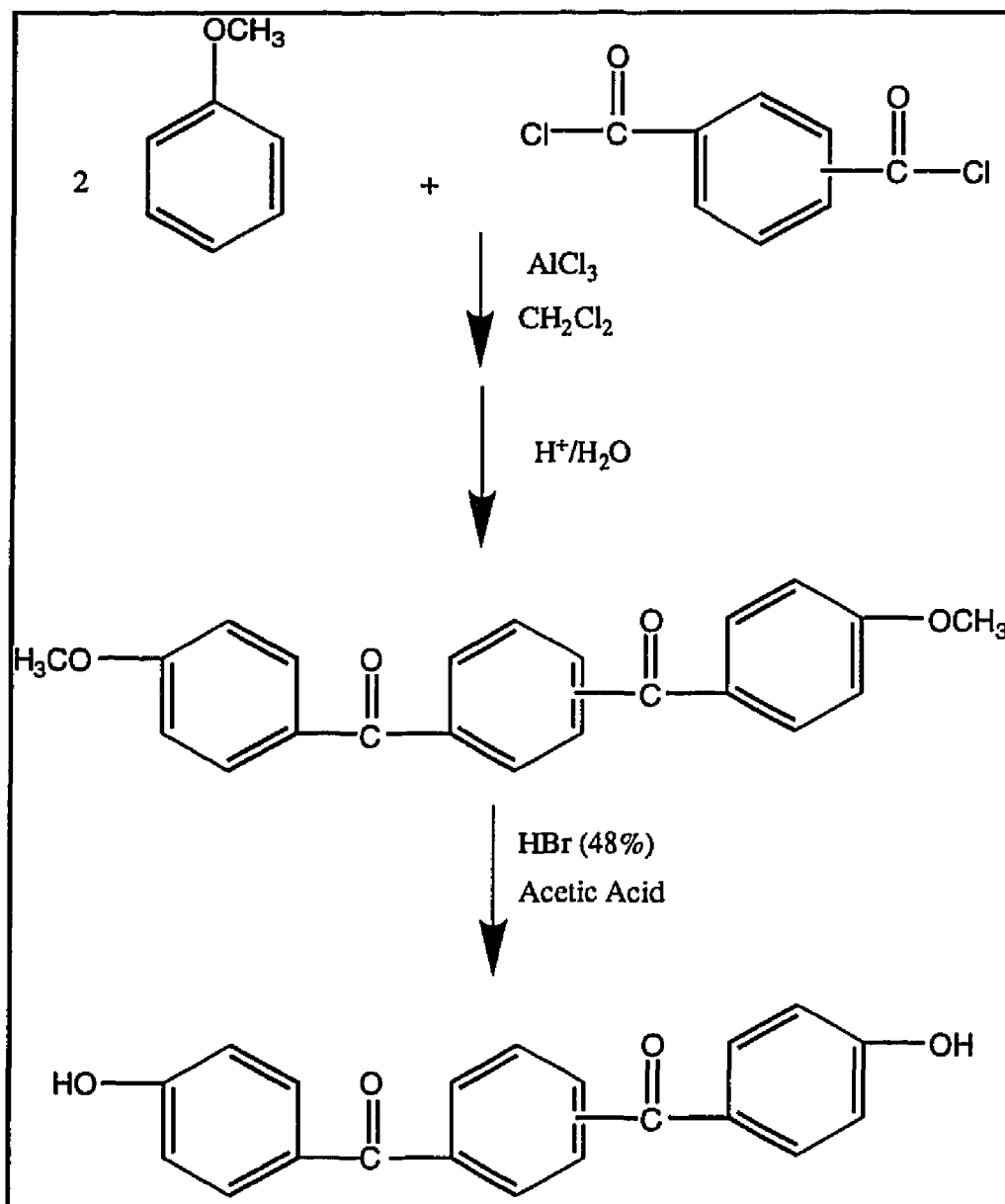
Chriskev Company, Inc. (mp 300-301°C). Structures and acronyms are illustrated in Table 4.1.

STRUCTURE	ACRONYM
	ABL-21
	1,3-BAPDBB
	PMDA
	BPDA
	BTDA
	1,5-DAN
	BAM
	<i>p</i> -PDA
	BAP

**Table 4.1 Structures And Acronyms Of Monomers Used In The Synthesis Of Potential Liquid Crystalline Polyimides**

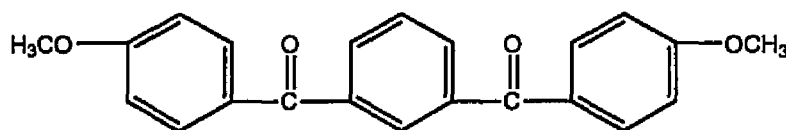
### 4.1.2 Preparation Of Dimethoxy Compounds

The general scheme for the synthesis of the aromatic dimethoxy compounds is shown in Figure 4.1 below. A representative sample procedure for each compound follows.



**Figure 4.1 General Preparation Of Aromatic Dimethoxy Compounds By Friedel-Crafts Acylation**

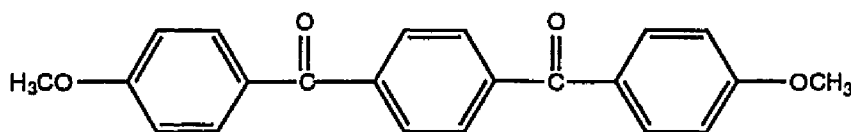
### Preparation Of 1,3-Bis(4-Methoxybenzoyl) Benzene



Into a 1-L, three-neck round bottom flask equipped with addition funnel, mechanical stirrer, Claisen adapter, thermometer, condenser, gas trap, and ice bath were placed aluminum chloride (181.99 g, 1.36 mol) and methylene chloride (350 ml). Isophthaloyl chloride (125.95 g, 0.62 mol) and anisole (134.85 ml, 1.24 mol) were heated in an Erlenmeyer flask until all the solid dissolved. The isophthaloyl chloride/anisole solution was then placed into the addition funnel and added slowly (1.5 hr) to the reaction vessel. The temperature was maintained between 10-20°C by regulating the addition of the isophthaloyl chloride/anisole solution. The solution was then stirred for 16 hr at room temperature (RT). The solution was poured slowly into a 4 L beaker of ice and concentrated HCl (250 mL), and stirred until it reached RT. The water layer was decanted and the solution was added to a 2-L separatory funnel and extracted with methylene chloride and water. The water layer (top layer) was discarded and the organic layer was washed two times with distilled water in the separatory funnel, again discarding the water layer. The organic layer was then washed two times with 5% sodium bicarbonate solution in a large flask so that the carbon dioxide formed did not build up in the separatory funnel. The organic layer was washed with distilled water and subsequently washed with magnesium sulfate (MgSO<sub>4</sub>). MgSO<sub>4</sub> was collected through a gravity funnel. The methylene chloride was removed from the solution by vacuum distillation. The remaining yellow solid was air-dried in the ventilation hood overnight and

subsequently dried at 130°C under vacuum. Differential scanning calorimetry (DSC) showed a broad melt at 132°C. The yield was 186.9 g (87%). The solid was recrystallized from 1 L of toluene to afford a yield of 86.2 g (40%, mp 135-138°C). Elemental analysis calculated for C<sub>22</sub>H<sub>18</sub>O<sub>4</sub>: C, 76.29%; H, 5.24%. Found: C, 76.08%; H, 5.27%.

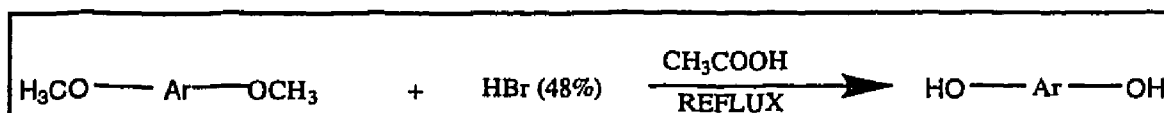
### Preparation Of 1,4-Bis(4-Methoxybenzoyl) Benzene



Aluminum chloride (169.43 g, 1.27 mol) and methylene chloride (350 ml) were placed into a 1-L, three-neck round bottom flask equipped with addition funnel, mechanical stirrer, Claisen adapter, thermometer, condenser, gas trap, and ice bath. Terephthaloyl chloride (117.27 g, 0.58 mol) and anisole (124.30 ml, 1.15 mol) were heated in an Erlenmeyer flask until all the solid dissolved. The terephthaloyl chloride/anisole solution was then placed into the addition funnel and added slowly (45 min) to the reaction vessel. The temperature was maintained between 10-20°C by regulating addition of the isophthaloyl chloride/anisole solution. The solution was stirred for 16 hr at RT, poured into a 4-L beaker of ice and concentrated HCl (250 mL), and allowed to reach RT. The water was decanted, and methylene chloride (1000 ml) and water (1500 ml) were added to the beaker. The water was decanted; the solid was filtered, and subsequently air-dried at 100°C. The yield was 162.5 g (81%, mp 230°C). The solid was recrystallized from DMAc to afford a light yellow solid (mp 235°C). Elemental analysis calculated for C<sub>22</sub>H<sub>18</sub>O<sub>4</sub>: C, 76.29%; H, 5.24%. Found: C, 76.33%; H, 4.87%.

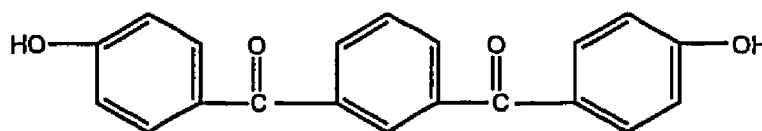
### 4.1.3 Preparation Of Bisphenols By Demethylation

Bisphenols were synthesized by the demethylation reaction shown in Figure 4.2. A representative sample procedure for each compound follows.



**Figure 4.2 General Method For Preparation Of Bisphenols By The Demethylation Reaction**

#### Preparation Of 1,3-Bis(4-Hydroxybenzoyl) Benzene

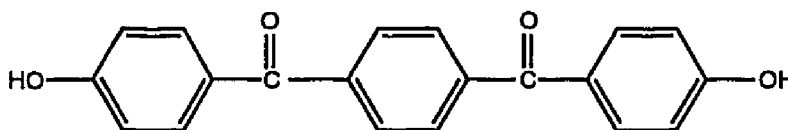


Into a 2-L, three-neck round bottom flask equipped with nitrogen inlet, mechanical stirrer, thermometer, condenser, gas trap, and heating mantle were placed 1,3-bis(4-methoxybenzoyl) benzene (86.10 g, 0.25 mol) and acetic acid (344 ml). The solution was stirred and heated until all the solid dissolved. Concentrated HBr (430 mL, 48%) was added gradually to the stirred solution. After refluxing for 16 hr, the solution was cooled and poured slowly into a 4-L beaker of ice water to afford a pink solid. The solution was allowed to warm to RT and the solid was collected through a medium porosity sintered glass funnel. The filtrate was neutralized to pH 7 before discarding. The solid was washed three times with distilled water to remove any residual acid, then air-dried in the ventilation hood for 64 hr. The solid was vacuum-dried at 130°C for



16 hr to afford a yield of 76.8 g (97%, mp 210-211°C). Elemental analysis calculated for  $C_{20}H_{14}O_4$ : C, 75.49%; H, 4.43. Found: C, 74.85%; H, 4.61%.

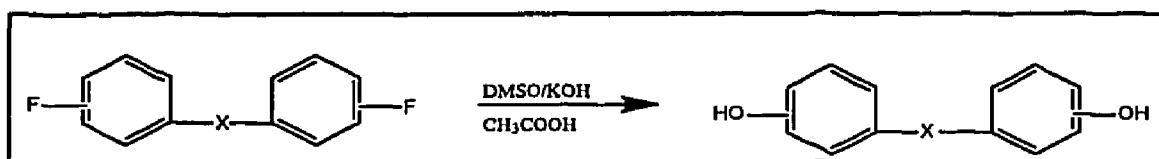
#### Preparation Of 1,4-Bis(4-Hydroxybenzoyl) Benzene



1,4-Bis(4-methoxybenzoyl) benzene (68.00 g, 0.20 mol) and acetic acid (700 ml) were placed into a 2-L, three-neck round bottom flask equipped with nitrogen inlet, thermometer, mechanical stirrer, condenser, gas trap, and heating mantle. The solution was heated to reflux for 1 hr. Some solid remained undissolved. Concentrated HBr (700 ml, 48%) was added slowly to the warm solution; a precipitate formed immediately. The heat was maintained at 120°C for 16 hr. All solids dissolved. The cooled reaction mixture was poured into distilled water (2 L), collected, and subsequently washed four times in distilled water until the filtrate had a pH of 7. The yellow solid was dried for 4 hr at 100°C. The solid was recrystallized from DMAc (mp 226°C and 294°C).

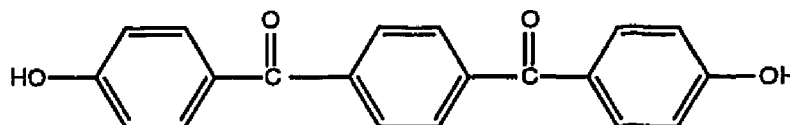
#### 4.1.4 Preparation Of Bisphenols Via Hydrolysis

Bisphenols were also synthesized by the hydrolysis of aromatic dihalides as shown in Figure 4.3[8]. The X group represents various aromatic segments and will be illustrated in the following sections. A representative sample procedure for each compound follows.

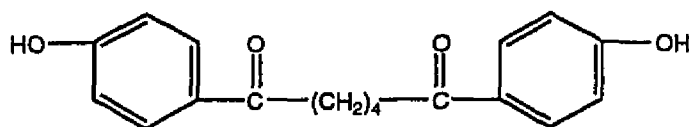


**Figure 4.3 Hydrolysis Of Aromatic Dihalide Compounds**

### Preparation Of 1,4-Bis(4-Hydroxybenzoyl) Benzene

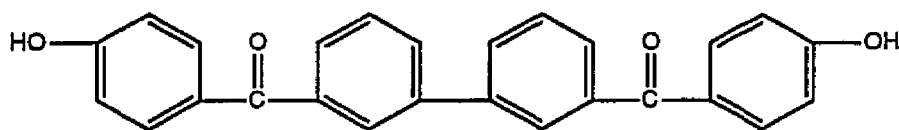


1,4-Bis(4-fluorobenzoyl) benzene (39.1 g, 0.12 mol), 2.0 N potassium hydroxide (KOH, 240 ml), and dimethylsulfoxide (DMSO, 460 ml) were placed into a 1-L, three-neck round bottom flask equipped with mechanical stirrer, nitrogen inlet, thermometer, condenser, and heating mantle. The reaction was maintained at 110-120°C for 20 hr. Distilled water (240 ml) was added to the solution and the solution was cooled to RT. The solution was filtered to remove any unreacted monomers or salts. The collected solid was discarded and the remaining filtrate was added dropwise through an addition funnel into a flask of hot glacial acetic acid (800 ml). A light yellow precipitate formed immediately. Once the filtrate was added, the solution was cooled to RT. The solid was collected and washed two times in hot distilled water. The yellow solid was collected by filtration through a medium porosity sintered glass funnel and dried under vacuum for 8 hr at 100°C. The yield was 31 g (82%, mp 301-302°C). The solid was recrystallized from DMF, air-dried in the hood overnight, and vacuum-dried for 8 hr at 150°C. Elemental analysis calculated for C<sub>20</sub>H<sub>14</sub>O<sub>4</sub>: C, 75.46%; H, 4.43%. Found: C, 75.32%; H, 4.47%.

**Preparation Of 1,4-Bis(4-Hydroxybenzoyl) Butane**

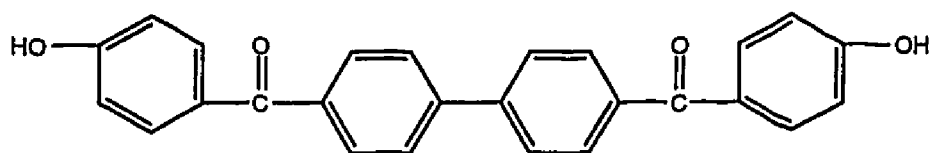
1,4-Bis(4-fluorobenzoyl) butane (25.4 g, 0.084 mol), 2.0 N potassium hydroxide (240 ml), and dimethylsulfoxide (300 ml) were placed into a 1-L, three-neck round bottom flask equipped with mechanical stirrer, nitrogen inlet, thermometer, condenser, and heating mantle. The reaction was maintained at 110-120°C for 20 hr. Distilled water (150 ml) was added to the solution and the solution was cooled to RT. All solids were removed by filtration and the filtrate was added dropwise through an addition funnel into a flask of hot glacial acetic acid (800 ml). Once all the filtrate was added, the solution was cooled to RT. The solid was collected and washed two times in hot distilled water. Water (1000 ml) was added to the filtrate and more solid was collected. The solid was dried under vacuum for 8 hr at 110°C. The solid was recrystallized from ethanol. The melting point by DSC was 255°C. Elemental analysis calculated for  $C_{18}H_{18}O_4$ : C, 72.47%; H, 6.08%. Found: Crop 1, C, 72.14%; H, 6.06%; Crop 2, C, 72.28%; H, 6.07%.

### Preparation Of 3,3'-Bis(4-Hydroxybenzoyl) Biphenyl

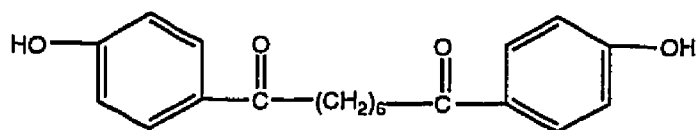


Into a 1-L, three-neck round bottom flask equipped with mechanical stirrer, nitrogen inlet, thermometer, condenser, and heating mantle were placed 3,3'-bis(4-fluorobenzoyl) biphenyl (35.0 g, 0.09 mol), 2.0 N potassium hydroxide (240 ml), and dimethylsulfoxide (300 ml). The reaction was maintained at 110-120°C for 20 hr. Distilled water (200 ml) was added to the dark red solution and the solution was cooled to RT. The solid material was removed by filtration. The filtrate was then added dropwise through an addition funnel into a flask of hot glacial acetic acid (750 ml). An orange precipitate formed immediately. Once the filtrate was all added, the solution was cooled. The solid was collected and washed two times in hot distilled water. The orange solid was collected by filtration through a medium porosity sintered glass funnel and dried at 100°C for 17 hr. The yield was 36 g (91%, mp 264°C). Elemental analysis calculated for C<sub>26</sub>H<sub>18</sub>O<sub>4</sub>: C, 79.17%; H, 4.60%. Found: C, 76.22%, H, 4.21%. Twenty grams was converted to a diether dianhydride and 16 g was recrystallized from ethanol/water (1:1). The yellow crystals were collected by filtration and heated under vacuum at 150°C for 8 hr. The yield was 12 g (75%, mp 264-265°C). Elemental analysis calculated for C<sub>26</sub>H<sub>18</sub>O<sub>4</sub>: C, 79.17%; H, 4.60%. Found: C, 78.57%, H, 4.52%.

### Preparation Of 4,4'-Bis(4-Hydroxybenzoyl) Biphenyl



Into a 1-L, three-neck round bottom flask equipped with mechanical stirrer, nitrogen inlet, thermometer, condenser, and heating mantle were placed 4,4'-bis(4-fluorobenzoyl) biphenyl (20.67 g, 0.05 mol), 2.0 N potassium hydroxide (180 ml), and dimethylsulfoxide (500 ml). The reaction was maintained at 110-120°C for 20 hr. Distilled water (300 mL) was added to the solution and the reaction mixture was cooled to RT. The resulting orange solution contained undissolved solid material which was filtered and discarded. The yellow filtrate was placed in an addition funnel and added slowly to a flask of hot glacial acetic acid (800 mL). Once filtrate had all been added to the hot glacial acetic acid, the solution was cooled in an ice bath. The solid was collected, subsequently washed two times with hot distilled water, and collected. The yellow solid was dried under vacuum at 110°C for 6 hr. The yield was 17.4 g (85%, mp 283-284°C). Elemental analysis calculated for  $C_{26}H_{18}O_4$ : C, 79.17%; H, 4.60%. Found: C, 78.72%; H, 4.33%. The solid was recrystallized from ethanol/water (3:1) to afford a light yellow solid after drying under vacuum at 100°C for 8 hr. The yield was 14.42 g (70%, mp 286-287°C). Elemental analysis calculated for  $C_{26}H_{18}O_4$ : C, 79.17%; H, 4.60%. Found: C, 78.93%; H, 4.34%.

**Preparation Of 1,4-Bis(4-Hydroxybenzoyl) Hexane**

1,6-Bis(4-fluorobenzoyl) hexane (22.47 g, 0.07 mol), 2.0 N potassium hydroxide (120 ml), and dimethylsulfoxide (200 ml) were placed into a 500-mL, three-neck round bottom flask equipped with mechanical stirrer, nitrogen inlet, thermometer, condenser, and heating mantle. The reaction was maintained at 110-120°C for 20 hr. Most of the solid was consumed after that time. Distilled water was added to the solution (100 mL) and a precipitate formed immediately. The solution was cooled to RT. The solid was filtered and discarded. The filtrate was poured slowly into a beaker of hot acetic acid (450 mL) and collected. After drying in air for 64 hr in the ventilation hood, the white solid was dried under vacuum at 100°C for 7 hr. A very small second crop formed and was collected, washed two times in hot water, and dried at 100°C for 7 hr. Combined yields were 73%. The crops were combined and recrystallized from ethanol/water (2:1), collected, and vacuum dried at 100°C for 8 hr to afford a yield of 14.2 g (64%, mp 178°C and 212°C). Elemental analysis calculated for C<sub>20</sub>H<sub>22</sub>O<sub>4</sub>: C, 73.60%; H, 6.79%. Found: C, 73.58%; H, 6.74.

#### 4.1.5 Synthesis Of Diether Dianhydrides

Aryl diether diphthalic dianhydrides were prepared by the reaction of a bisphenol (1 mole) with 4-fluorophthalic anhydride (2.2 mole) and potassium fluoride (3 mole) in the presence of tetramethylene sulfone (sulfolane)[9-10] as shown in Figure 4.4. A representative sample procedure for each compound follows.

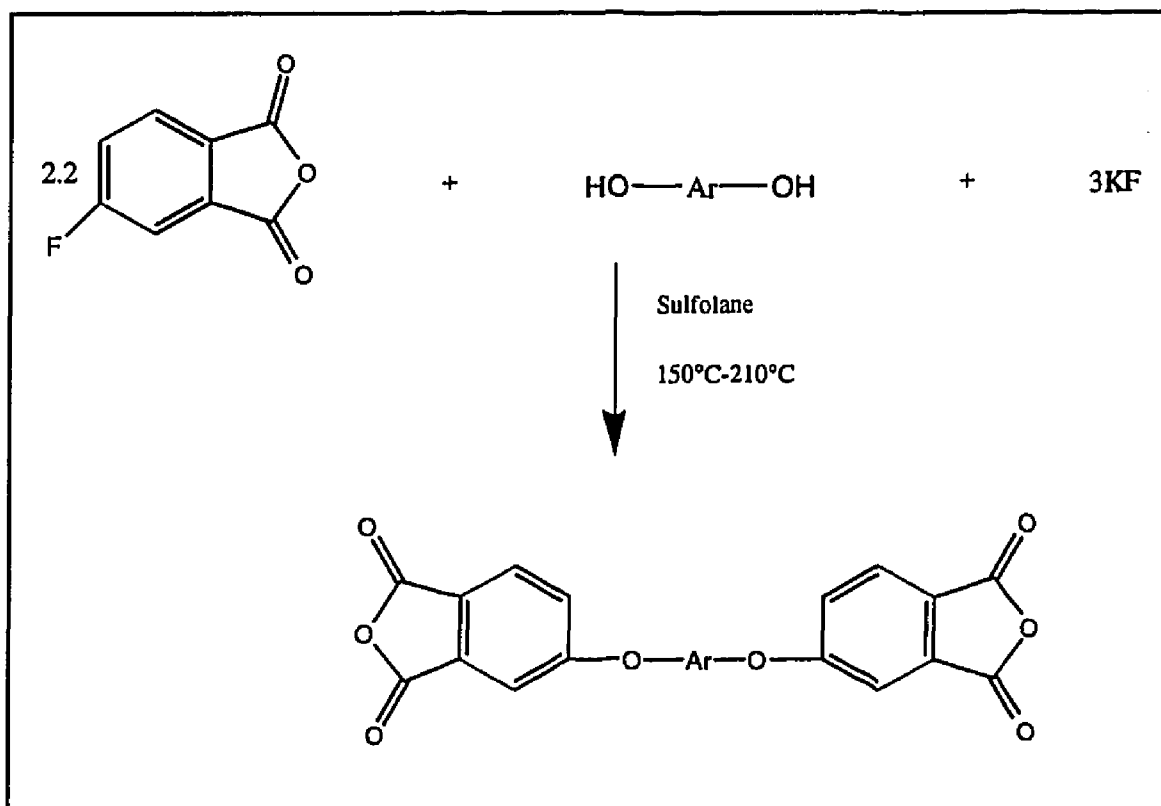
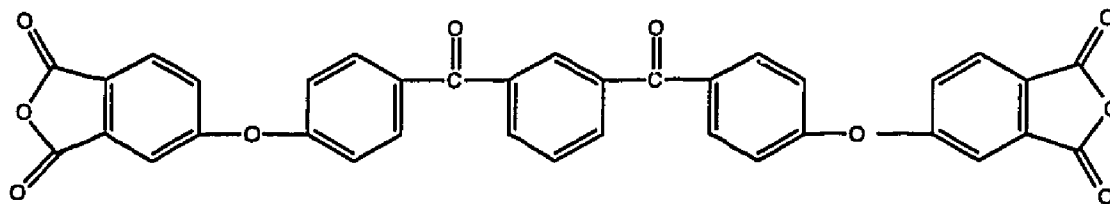


Figure 4.4 General Synthesis Of Aromatic Diether Dianhydrides

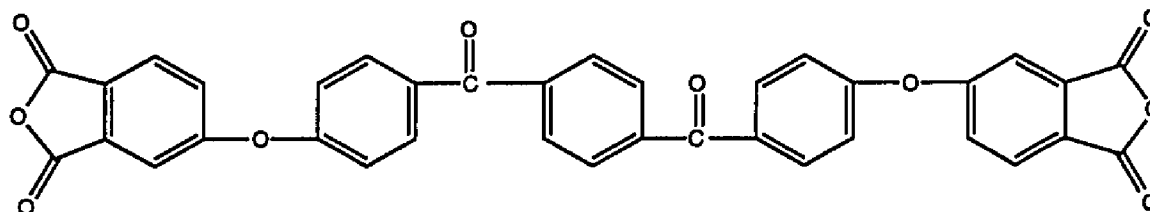
**Preparation Of 1,3-Bis(3,4-Dicarboxyphenoxy-4-Benzoyl) Benzene Dianhydride (1,3-BBBDA)**



Into a 500-ml, three-neck round bottom flask equipped with nitrogen inlet, condenser, mechanical stirrer, thermometer, and heating mantle were placed 1,3-bis(4-hydroxybenzoyl) benzene (24.15 g, 0.08 mol), 4-fluorophthalic anhydride (28.75 g, 0.17 mol), spray-dried KF (13.72 g, 0.24 mol), and sulfolane (211 g, as received from Aldrich, 99%). The reaction mixture was heated to 155°C and maintained for 3 hr. The cooled reaction mixture was poured into a large beaker of saturated sodium chloride (NaCl) solution. The solid was collected, washed two times with distilled water, and collected to afford a yield after drying of 36 g (75%). The solid was placed in hot acetic acid, and charcoal filtered. The volume of acetic acid in the solution was decreased by vacuum distillation. Crystals formed in remaining viscous solution after 30 days. Two crops formed. Crop 1 showed a melting point of 142°C and crop 2 had a melting point of 134°C. Elemental analysis calculated for C<sub>36</sub>H<sub>18</sub>O<sub>10</sub>: C, 70.82%; H, 2.97%. Found: Crop 1, C, 67.67%; H, 2.74%. A mass spectrum was not obtained because the sample was not volatile during the GC-MS analysis.

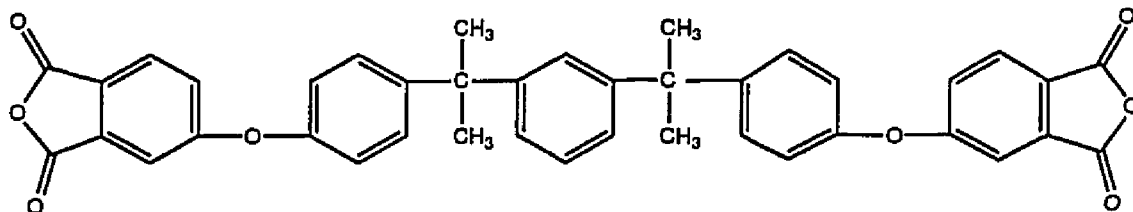


**Preparation Of 1,4-Bis(3,4-Dicarboxyphenoxy-4-Benzoyl) Benzene Dianhydride (1,4-BBBDA)**



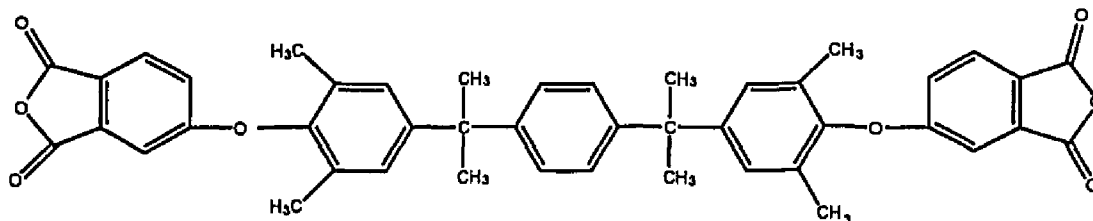
Into a 500-ml, three-neck round bottom flask equipped with nitrogen inlet, condenser, mechanical stirrer, thermometer, and heating mantle were placed 1,4-bis(4-hydroxybenzoyl) benzene (27.00 g, 0.08 mol), 4-fluorophthalic anhydride (31.00 g, 0.19 mol), spray-dried KF (15.00 g, 0.25 mol), and vacuum distilled sulfolane (202 g). The reaction mixture was heated to 160°C and maintained for 3 hr. The reaction was cooled and the mixture was poured into a large beaker of saturated NaCl solution. The solid was collected by suction, washed in NaCl solution, collected, and washed with distilled water. The solid was stage-dried to 175°C for 8 hr. The yield was 51 g (100%). The solid was recrystallized from acetic anhydride/acetic acid (4:1) (mp 216-217°C). Elemental analysis calculated for C<sub>36</sub>H<sub>18</sub>O<sub>10</sub>: C, 70.82%; H, 2.97%. Found: C, 70.28%; H, 3.05%. A mass spectrum was not obtained because the sample was not volatile during the GC-MS analysis.

**Preparation Of 1,3-Bis(3,4-Dicarboxyphenoxy-4-Phenyl-2-Propyl) Benzene Dianhydride [Bisphenol M Diether Dianhydride (BMDEDA)]**



A mixture of Bisphenol M (34.65 g, 0.10 mole), 4-fluorophthalic anhydride (36.54 g, 0.22 mole), spray-dried KF (17.43 g, 0.30 mole), and vacuum distilled sulfolane (328 g) was heated under a nitrogen atmosphere for 4 hr at 180°C. The cooled reaction mixture was precipitated into a blender of 20% (w/v) sodium chloride solution, collected, washed with distilled water, and stage-dried under vacuum to 150°C to afford a 90% yield of a light orange solid. The crude solid was recrystallized from acetic anhydride/acetic acid (4:1) and vacuum dried at 167°C to afford a light yellow solid (mp 174-175°C). The recrystallized yield was approximately 52%, but recovery from subsequent crops increased the overall yield 10-15%. Elemental analysis calculated for C<sub>42</sub>H<sub>30</sub>O<sub>8</sub>: C, 75.22%, H, 4.73%. Found: C, 75.19%, H, 4.83%. A mass spectrum was not obtained because the sample was not volatile during the GC-MS analysis.

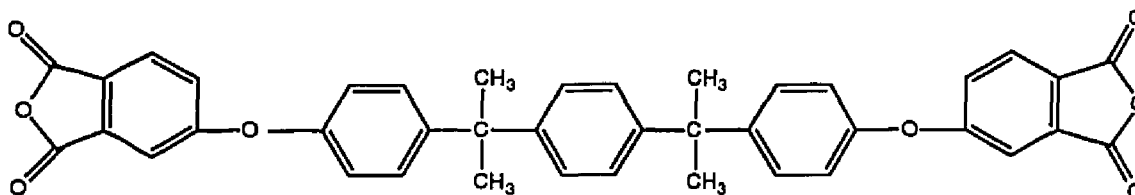
**Preparation Of  $\alpha,\alpha$ -Bis(3, 4-Dicarboxyphenoxy-3,5-Dimethylphenyl)-4-Diisopropyl Benzene Dianhydride**



$\alpha,\alpha$ -Bis(4-hydroxy-3,5-dimethylphenyl)-4-diisopropyl benzene (20.33g 0.05 mol), 4-fluorophthalic anhydride (19.62 g, 0.12 mol), spray-dried KF (8.72 g, 0.17 mol), and freshly distilled sulfolane (182 g) were placed into a 250-ml, three-neck round bottom flask equipped with mechanical stirrer, nitrogen gas inlet, heating mantle, and reflux condenser. The reaction mixture was heated to 230°C for 2 hr and maintained at 190°C for 16 hr. The cooled reaction mixture was poured into a blender of salt water and collected. The solid was subsequently washed two times with deionized water, and collected. Recrystallization from acetic anhydride/acetic acid (4:1) was attempted, but no crystals formed. The volume of acetic acid/acetic anhydride was reduced by vacuum distillation and the resultant taffy-like material was vacuum-dried at 100°C for 16 hr. DSC showed peaks at 150°C and 245°C. The glass-like material was pulverized and the solid was recrystallized from acetic anhydride/acetic acid (4:1). DSC indicated melting points at 88°C and 254°C. Sublimation of the material was attempted but was not successful. Elemental analysis calculated for  $C_{44}H_{38}O_8$ : C, 76.06%; H, 5.51%. Found: C, 62.68%; H, 5.89%. Elemental analysis indicated that either the dianhydride was not very pure or the reaction produced a free acid or another compound. A mass

spectrum was not obtained because the sample was not volatile during the GC-MS analysis.

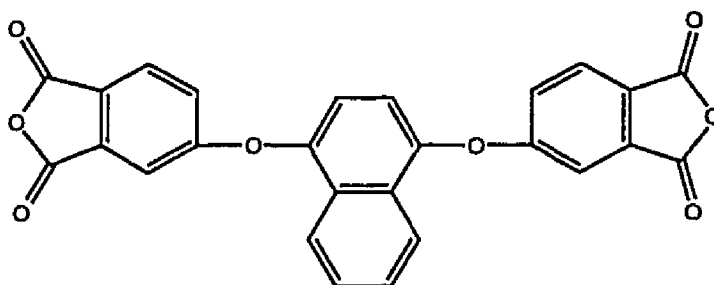
**Preparation Of 1,4-Bis(3,4-Dicarboxyphenoxy-4-Phenyl-2-Propyl) Benzene Dianhydride [Bisphenol P Diether Dianhydride (BPDEDA)]**



Bisphenol P (34.64 g, 0.10 mol), 4-fluorophthalic anhydride (36.54 g, 0.22 mol), spray-dried KF (17.43 g, 0.30 mol), and freshly distilled sulfolane (285 g) were placed into a 500-ml, three-neck round bottom flask equipped with mechanical stirrer, nitrogen gas inlet, heating mantle, and reflux condenser. The reaction mixture was heated to 170°C for 4 hr. The mixture was then cooled slowly, poured into a blender of water, collected, and dried at 125°C. The compound began to gum at approximately 50°C in the vacuum oven. The yield was 63.9 g (99%). The solid was broken up, pulverized, and recrystallized from acetic anhydride/acetic acid (4:1). The solution was vacuum distilled to remove the acetic acid/acetic anhydride and the remaining gum-like material was vacuum-dried. DSC showed a broad peak at 177°C. Recrystallization from acetic anhydride/acetic acid (4:1) was attempted again. Two crops formed. Both crops were dried at 160°C. DSC indicated a melting point at 184°C with a broad shoulder for Crop 1. DSC indicated a melting point at 193°C with a broad shoulder for Crop 2. Both crops were dried further at 180°C under vacuum. Elemental analysis calculated for C<sub>42</sub>H<sub>30</sub>O<sub>8</sub>: C,

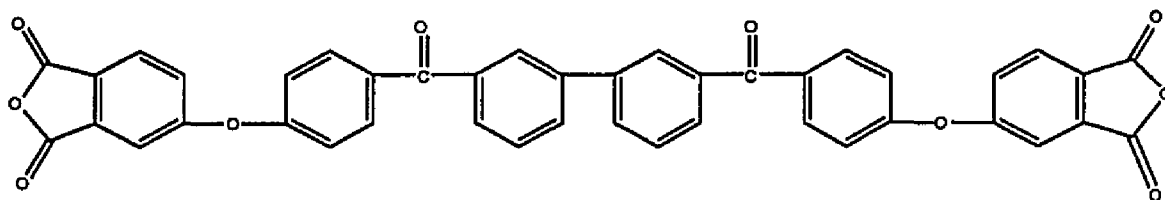
75.22%; H, 4.73%. Found: Crop 1, C, 74.18%; H, 5.03%; Crop 2, C, 74.92%; H, 4.90%. The crops were combined and recrystallized from 1,2,4-trichlorobenzene. Elemental analysis calculated for  $C_{42}H_{30}O_8$ : C, 75.22%; H, 4.73%. Found: C, 76.41%; H, 5.19%.

### Preparation Of 1,4-Bis(3,4-Dicarboxyphenoxy) Naphthalene Dianhydride



1,4-Dihydroxy naphthalene (11.2 g, 0.07 mol), 4-fluorophthalic anhydride (25.50 g, 0.15 mol), spray-dried KF (12.20 g, 0.21 mol), and freshly distilled sulfolane (156 g) were placed into a 500-ml, three-neck round bottom flask equipped with mechanical stirrer, nitrogen gas inlet, heating mantle, and reflux condenser. The reaction mixture was heated to 170-180°C for 4 hr. The mixture was then cooled slowly, poured into a blender of NaCl solution, and collected. The solid was washed with deionized water, collected, and dried at 150°C. The solid was recrystallized from acetic anhydride/acetic acid (4:1). DSC showed melting peaks at 177°C and 238°C. Elemental analysis calculated for  $C_{26}H_{12}O_8$ : C, 69.03%; H, 2.84%. Found: C, 69.12%; H, 2.84%. A mass spectrum was not obtained because the sample was not volatile during the GC-MS analysis.

### Preparation Of 3,3'-Bis(3,4-Dicarboxyphenoxy-4-Benzoyl) Biphenyl Dianhydride

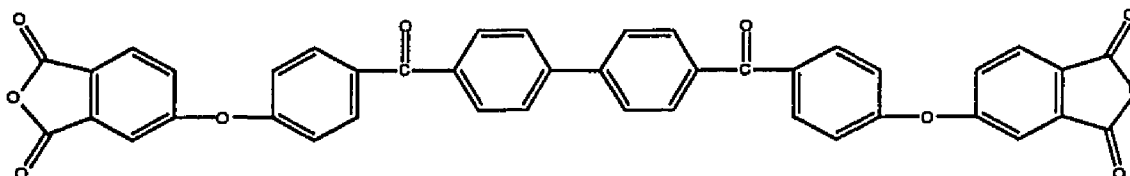


Into a 500-ml, three-neck round bottom flask equipped with nitrogen inlet, condenser, mechanical stirrer, thermometer, and heating mantle were placed 3,3'-bis(4-hydroxybenzoyl) biphenyl (20.00 g, 0.05 mol), 4-fluorophthalic anhydride (16.84 g, 0.10 mol), spray-dried KF (8.84 g, 0.15 mol), and vacuum distilled sulfolane (160 g). The reaction mixture was heated to 180°C and maintained at 150°C for 4 hr. The reaction was cooled and the green mixture was poured into a blender of distilled water, collected, and washed two times with distilled water. The solid was dried at 100°C for 11 hr. The yield was 36 g (99%, mp 138°C and 187°C). The solid was placed in acetic anhydride/acetic acid (4:1), charcoal filtered, and allowed to crystallize. An oil formed in the flask initially, but crystals began forming in the flask after 24 hr. The solution was stirred an additional 24 hr to induce more crystallization. The solid was collected and vacuum-dried at 160°C for 6 hr. Elemental analysis calculated for C<sub>42</sub>H<sub>22</sub>O<sub>10</sub>: C, 73.47%; H, 3.23%. Found: C, 73.18%; H, 3.16%.

The reaction was repeated using purified 3,3'-bis(4-hydroxybenzoyl) biphenyl and a higher temperature of 165°C. One-half of the dianhydride was dried in the vacuum oven at 170°C and the other half was sublimed. Sublimation was not successful. The solid was recrystallized again from acetic anhydride/acetic acid (4:1). Elemental analysis calculated for C<sub>42</sub>H<sub>22</sub>O<sub>10</sub>: C,

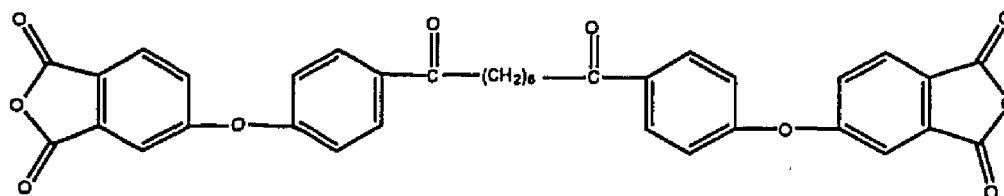
73.47%; H, 3.23%. Found: C, 73.28%; H, 2.97%. A mass spectrum was not obtained because the sample was not volatile during the GC-MS analysis.

#### Preparation Of 4,4'-Bis(3,4-Dicarboxyphenoxy-Benzoyl) Biphenyl Dianhydride



A mixture of 4,4'-bis(4-hydroxybenzoyl) biphenyl (14.40 g, 0.04 mole), 4-fluorophthalic anhydride (12.13 g, 0.07 mole), spray-dried KF (6.36 g, 0.11 mole), and vacuum distilled sulfolane (127 g) was heated under a nitrogen atmosphere for 4 hr at 160°C. The cooled reaction mixture was precipitated into a blender of distilled water, collected, washed with distilled water, and stage-dried under vacuum to 150°C to afford a light tan solid (98%, no mp detected). The solid was recrystallized from acetic anhydride/acetic acid (4:1). Three crops were formed. Crop 1 formed within 4 hr; Crop 2 crystallized overnight and was collected; Crop 3 was recovered when the acetic anhydride/acetic acid was removed by vacuum distillation. Crops 2 and 3 were vacuum dried at 117°C to afford light orange solids. Crop 1 yielded 1.17 g with no apparent melting point to 325°C. Crop 2 yielded 12.4 g with a melting point of 163-164°C. Crop 3 yielded 7.73 g with melting peaks at 164°C, 214°C, and 303°C. Elemental analysis calculated for C<sub>42</sub>H<sub>22</sub>O<sub>10</sub>: C, 73.47%; H, 3.23%. Found for Crop 1: C, 73.37%; H, 2.99%. Found for Crop 2: C, 72.42%; H, 3.18%. Found for Crop 3: C, 69.14%; H, 2.90%. A mass spectrum was not obtained because the sample was not volatile during the GC-MS analysis.

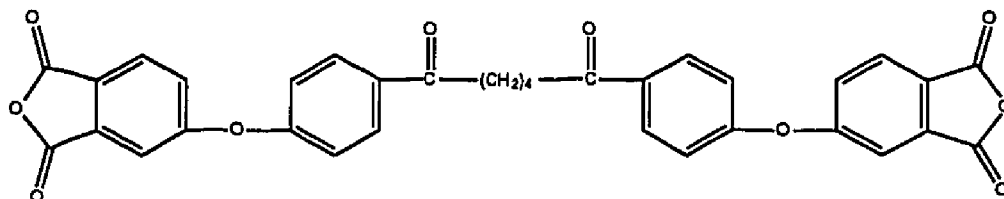
### Preparation Of 1,6-Bis(3,4-Dicarboxy-Phenoxy-Benzoyl) Hexane Dianhydride



A mixture of 1,6-bis(4-hydroxybenzoyl) hexane (14.13 g, 0.04 mole), 4-fluorophthalic anhydride (14.62 g, 0.09 mole), spray-dried KF (6.97 g, 0.12 mole), and vacuum distilled sulfolane (133 g) was heated under a nitrogen atmosphere for 4 hr at 160-170°C. The cooled reaction mixture was precipitated into a blender of distilled water, collected, washed with distilled water, and stage-dried under vacuum to 150°C. The yield was 22.23 g (90%, mp 153°C and 245°C). Elemental analysis calculated for C<sub>36</sub>H<sub>26</sub>O<sub>10</sub>: C, 69.90%; H, 4.24%. Found: C, 62.27%; H, 4.23%. The crude solid was recrystallized from acetic anhydride/acetic acid (4:1). The acetic anhydride/acetic acid was recovered by vacuum distillation and the remaining tacky material was vacuum dried at 120°C. The yield was 9.94 g (40%, mp 253°C). Elemental analysis calculated for C<sub>36</sub>H<sub>26</sub>O<sub>10</sub>: C, 69.90%; H, 4.24%. Found: C, 68.78%; H, 4.02%.



### Preparation Of 1,4-Bis(3,4-Dicarboxyphenoxy-Benzoyl) Butane Dianhydride



A mixture of 1,4-bis(4-hydroxybenzoyl) butane (2.91 g, 0.0049 mole), 4-fluorophthalic anhydride (2.36 g, 0.0142 mole), spray-dried KF (1.3 g, 0.0223 mole), and vacuum distilled sulfolane (31 g) was heated under a nitrogen atmosphere for 6 hr at 120-130°C. The cooled reaction mixture was precipitated into distilled water, collected, washed with salt water, and subsequently washed with distilled water. The dark solid was stage-dried under vacuum to 120°C. The yield was 2.23 g (80%, mp 313°C). Elemental analysis calculated for  $C_{34}H_{22}O_{10}$ : C, 69.15%; H, 3.76%. Found: C, 67.21%; H, 4.22%. The crude solid was recrystallized from acetic anhydride/acetic acid (4:1). Brown crystals formed and were collected by filtration. The yield was 0.7 g (31%, mp 257°C and 354°C). Elemental analysis calculated for  $C_{34}H_{22}O_{10}$ : C, 69.15%; H, 3.76%. Found: C, 68.64%; H, 3.78%.

### 4.1.6 Two-Step Polyimide Synthesis

Figure 4.5 represents the reaction of an aromatic dianhydride with an aromatic diamine to afford the poly (amic acid). The poly (amic acid) is then thermally imidized to afford the polyimide film.

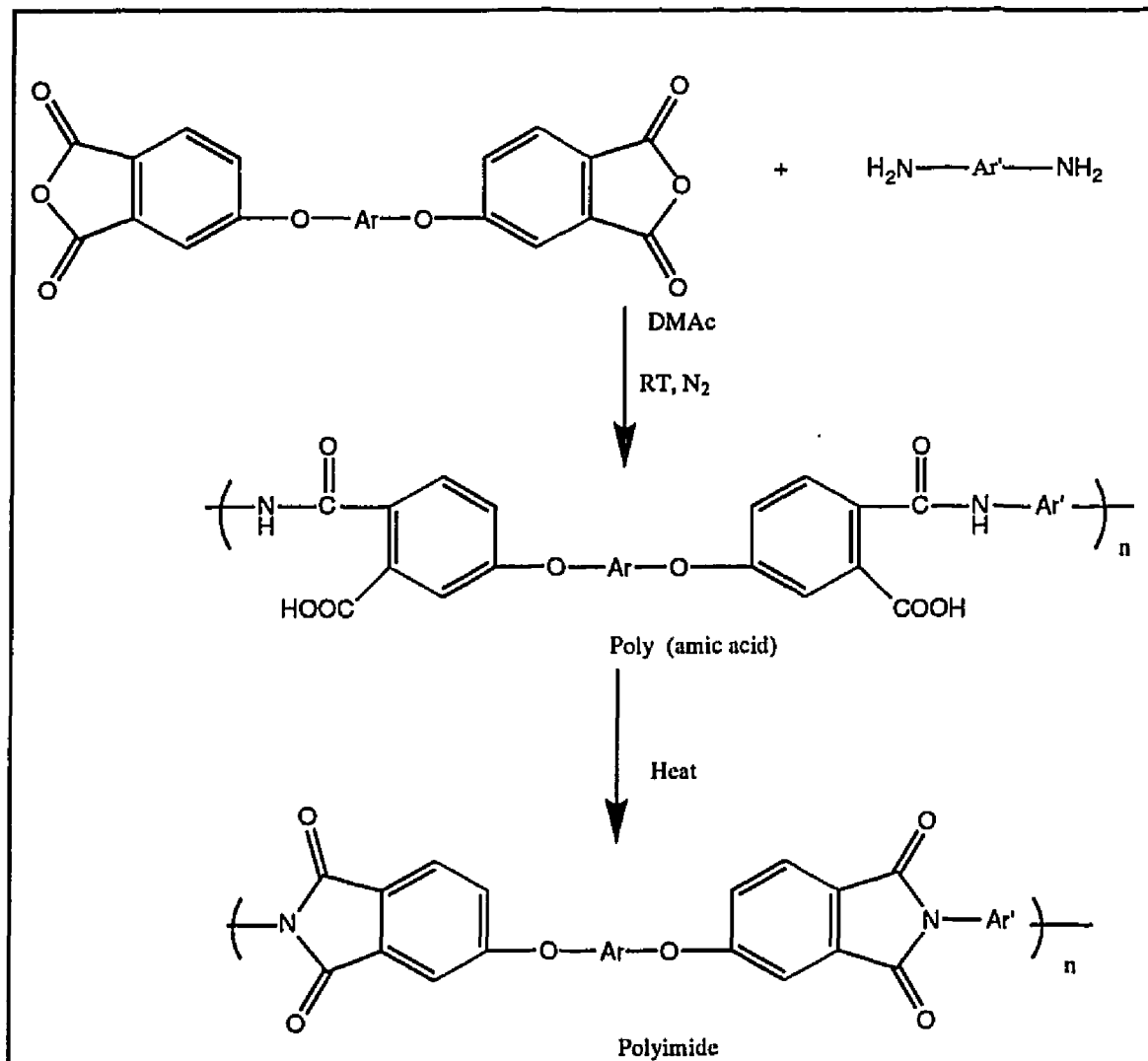


Figure 4.5 Two-Step Polyimide Synthesis

DMAc solutions (~15-20% solids) of the poly (amic acid)s (PAA) were centrifuged, the decantate doctored onto clean, dry plate glass and dried to a tack-free form in a low humidity chamber. The films on glass were dried at 100, 200, and 240-250°C for 1 hr each in flowing air. Additional cure temperatures were employed to evaluate the effects of temperature on the polymer properties.

#### **4.1.7 Preparation Of BMDEDA/*p*-PDA Polymer Powders**

Polymer powders were prepared by reacting Bisphenol M diether dianhydride (BMDEDA) and *p*-PDA in GBL at 23°C under a N<sub>2</sub> atmosphere at 10-15% solids. Powders using stoichiometric amounts of diamine and dianhydride were synthesized as well as polymers with the stoichiometry upset by 2, 2.5, and 3 mole%, and endcapped with phthalic anhydride. The phthalic anhydride endcap was added to the reaction after stirring for ~16 hr and the mixture was then stirred for an additional 4 hr. Glacial acetic acid (10% of solvent weight) was subsequently added, and the mixtures were heated to 120°C for ~20 hr. The polymer powder precipitated from the reaction mixtures after 1 hr at 120°C. The cooled mixtures were poured into methanol, collected, washed in hot methanol, and dried at 120°C under vacuum to afford the polymers in >95% yields.

#### **4.1.8 Extruded Ribbons And Rods**

Polymer powders and blends were extruded using a Brabender PL-2000 Plastic-Corder® designed for mixing and compounding polymers in a melted state. The mixer was preheated, and at 330°C, the polymers or polymer blends

were rapidly added to the cavity using a 5 kg mass to pack the material if necessary. The ribbons were extruded at a rate of 20-100 rpm over a 30 minute period.

#### **4.1.9 Molecular Orientation (Film Stretching)**

Installation of the T. M. Long Film Stretcher began in 1993. Since the film stretcher is not yet fully operational, results and discussion of the progress made towards this effort will be included in the Appendix.

## **4.2 Polyimides For Microelectronic Applications**

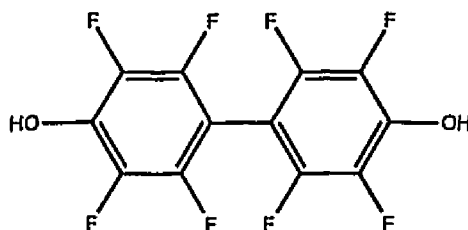
### **4.2.1 Low Dielectric, Fluorinated Polyimides**

#### **4.2.1.1 Starting Materials**

3,3',4,4'-Biphenyl tetracarboxylic acid dianhydride (BPDA) was obtained from Mitsui Toatsu Chemicals and Ube Industries, Japan, and was vacuum-dried at 150°C before use. 2,2-Bis(3,4-dicarboxyphenoxy-phenyl) hexafluoropropane dianhydride (6FDA) was used as received from Hoechst Celanese Corp. 3,5-Diaminobenzotrifluoride (DABTF) was synthesized in-house by hydrogenation of 3,5-dinitrobenzotrifluoride (Aldrich)[11]. Dimethoxyoctafluorobiphenyl was used as received from Aldrich (mp 82-83°C). Bis(4-hydroxyphenyl) hexafluoropropane (Bisphenol AF) was recrystallized from toluene (DuPont, mp 162-164°C). Spray-dried potassium fluoride (KF) was used as received from Aldrich (99% purity). 3,3'-Methylene diphenol was synthesized as previously described (mp 101-103°C)[12]. 1,3-Bis(2-hydroxyhexafluoroisopropyl) benzene was used as received from Central Glass (Japan). 4-Fluorophthalic anhydride was used as received from Occidental Chemical Corp. Tetramethylene sulfone (sulfolane) was obtained from Phillips 66 and vacuum distilled prior to use. Methylene chloride was used as received from Aldrich.

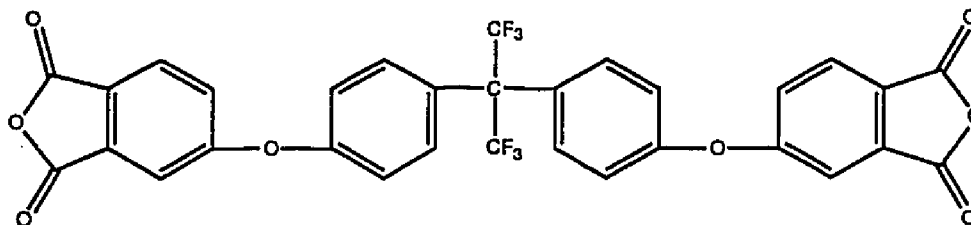
#### 4.2.1.2 Preparation Of Monomers For Low Dielectric, Fluorinated Polyimides

##### Preparation Of 4,4'-Dihydroxyoctafluorobiphenyl



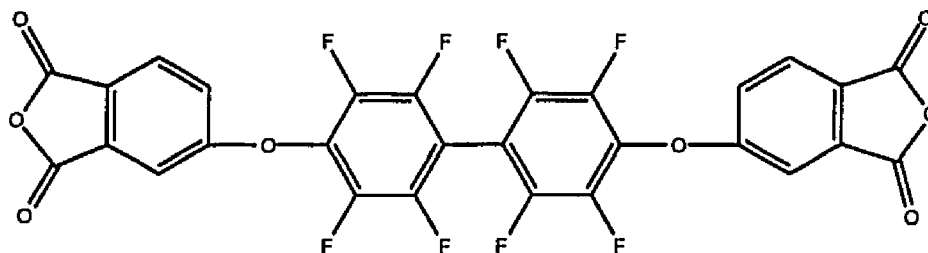
Into a 2-L, three-neck round bottom flask equipped with nitrogen inlet, thermometer, mechanical stirrer, condenser, gas trap, and heating mantle were placed 4,4'-dimethoxyoctafluorobiphenyl (55.00 g, 0.15 mol) and acetic acid (200 ml). The solution was heated to 50°C and maintained until all solids dissolved (30 min). Concentrated hydrobromic acid (48%, 500 ml) was added slowly to the warm solution; a precipitate formed immediately. The heat was increased to 120°C and maintained for 16 hr. All solids dissolved. The solution was cooled in an ice bath. The white crystals were collected through a medium porosity funnel, subsequently washed two times in water, collected, and vacuum-dried at 70°C (16 hr) to afford a yield of 40 g (80%). DSC showed the melting point of the dimethoxy starting material. The reaction was run again using 1 L of HBr and 200 ml of acetic acid. The solid was collected by filtration, washed two times in water, and dried at 80°C for 8 hr. The visual melting point was 210°C. The yield was 33 g (65%, mp 210-212°C). Elemental analysis calculated for C<sub>12</sub>H<sub>2</sub>O<sub>2</sub>F<sub>8</sub>: C, 43.66%; H, 0.59%; F, 46.04%. Found: C, 43.29%; H, 0.61%; F, 45.96%.

**Preparation Of Bis[4-(3,4-Dicarboxyphenoxy)Phenyl] Hexafluoropropane Dianhydride (BFDA)**



Bisphenol AF (33.62g 0.10 mol), 4-fluorophthalic anhydride (38.44 g, 0.23 mol), spray-dried KF (17.43, 0.30 mol), and freshly distilled sulfolane (315 g) were placed into a 500-ml, three-neck round bottom flask equipped with mechanical stirrer, nitrogen gas inlet, heating mantle, and reflux condenser. The reaction mixture was heated to 180°C and maintained at this temperature for 3 hr. The mixture was then cooled slowly, poured into a blender of ice water, and collected. The solid was subsequently washed with deionized water, collected, and stage-dried under vacuum to 215°C to afford a light tan solid (mp 229-231°C). Elemental analysis calculated for  $C_{31}H_{14}O_8F_6$ : C, 59.25%; H, 2.25%; F, 18.14%. Found: C, 58.94%; H, 2.35%; F, 18.09%. A mass spectrum was not obtained because the sample was not volatile during the GC-MS analysis.

### Preparation Of 1,4-Bis(3,4-Dicarboxyphenoxy) Octafluorobiphenyl Dianhydride (8FDA)

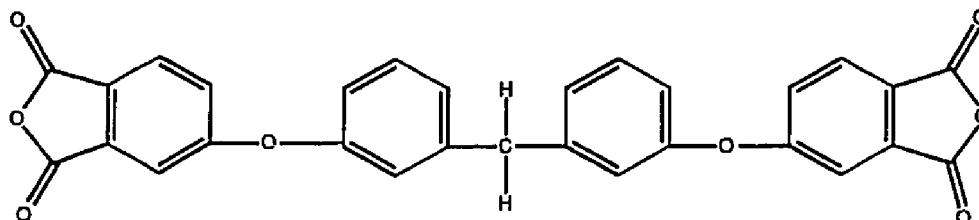


Into a 500-ml, three-neck round bottom flask equipped with nitrogen inlet, thermometer, mechanical stirrer, condenser, and heating mantle were placed 4,4'-dihydroxyoctafluorobiphenyl (20.00 g, 0.06 mol), 4-fluorophthalic anhydride (22.15 g, 0.1333 mol), spray-dried potassium fluoride (10.57 g, 0.18 mol), and vacuum distilled sulfolane (168 g). The reaction was heated to 150°C-180°C for several hours. The yellow solution turned dark brown as the reaction proceeded. The reaction mixture was cooled and the solution was precipitated into a 10% (w/v) solution of NaCl. The solid was collected and washed in distilled water. Filtration was slow due to the small particle size. The liquid layer was decanted and the solid was vacuum-dried overnight at RT to remove the water and residual sulfolane. The solid was then stage-dried to 150°C to afford a yield of 27 g. DSC showed a broad melt at 300°C. The solid was placed in n-hexane (300 ml) and stirred for 1 hr to remove any sulfolane. The solution was placed in an uncovered crystallizing dish and placed in the ventilation hood to evaporate the n-hexane. The solid was then dried at 180°C. The yield was 24.7 g. The solid was placed in a sublimator and heated to 230°C. The sublimed material had a sharp melting point at 217°C. The solid was recrystallized from 1,2,4-trichlorobenzene, charcoal filtered, collected, and stage-dried to 150°C for 8 hr. Elemental analysis calculated for



$C_{28}H_6O_8F_8$ : C, 54.03%; H, 0.97%; F, 24.42%. Found: C, 50.46%; H, 0.90%; F, 30.30%. A mass spectrum was not obtained because the sample was not volatile during the GC-MS analysis.

### Preparation Of 3,3'-Bis(3,4-Dicarboxyphenoxy) Diphenyl Methane Dianhydride



The following reaction was not successful. Inclusion of the procedure and structure is important to illustrate the systematic approach proposed for the structure-property study. In contrast to the compound described above, this proposed compound was not fluorinated. Since the *meta*-catenated methylene group was expected to impart solubility and lower the dielectric constant in the resultant polymers, its synthesis was attempted.

Into a 250-ml, three-neck round bottom flask equipped with nitrogen inlet, thermometer, mechanical stirrer, condenser, and heating mantle were placed 3,3'-methylene diphenol (10.36 g, 0.05 mol), 4-fluorophthalic anhydride (19.87 g, 0.12 mol), spray-dried potassium fluoride (9.06 g, 0.16 mol), and vacuum distilled sulfolane (102 g). The reaction was heated to 150°C-160°C and maintained for 2 hr. The reaction mixture was cooled and the solution was precipitated into a 20% (w/v) solution of NaCl. An oil formed. The salt solution was decanted and the oil was again mixed with a NaCl solution. After several washes in salt water, the solution was decanted and hexanes were added to the oil. The hexanes were decanted and the oil dried under vacuum at RT

overnight. The oil was then placed in 500 mL of toluene and refluxed for 4 hr. The toluene was decanted and the material was refluxed in acetic anhydride for 4 hr. The acetic anhydride was removed by vacuum distillation and the brown solid was dried under vacuum at RT for 16 hr and subsequently stage-dried at 120°C for 8 hr. Elemental analysis calculated for  $C_{29}H_{16}O_8$ : C, 70.73%; H, 3.28%. Found: C, 15.14%; H, 1.49%.

### Preparation Of 3,3'-Bis(3,4-Dicarboxyphenoxy Hexafluoroisopropyl) Benzene Dianhydride (12FDA)



The following reaction was not successful. Inclusion of the procedure and structure was important to illustrate the systematic approach proposed for the structure-property study. This proposed compound contained two hexafluoroisopropylidene groups.

Into a 250-ml, three-neck round bottom flask equipped with nitrogen inlet, thermometer, mechanical stirrer, condenser, and heating mantle were placed 1,3-bis(2-hydroxyhexafluoroisopropyl) benzene (20.51 g, 0.05 mol), 4-fluorophthalic anhydride (18.27 g, 0.11 mol), spray-dried potassium fluoride (8.72 g, 0.15 mol), and vacuum distilled sulfolane (95 g). The reaction was heated to 150°C-160°C and maintained for 2 hr. The reaction mixture was cooled and precipitated into a beaker of water. An oil formed. The water was decanted and tetrahydrofuran (THF) was added to the oil. The oil and THF

were miscible. Water was added to return the oil. The THF was decanted and the oil allowed to air dry in the ventilation hood. Diethyl ether was then added to the oil. They were miscible. The diethyl ether was removed by vacuum distillation. Methylene chloride and  $\text{MgSO}_4$  were added to the oil. The  $\text{MgSO}_4$  was removed by filtration and the methylene chloride was removed by vacuum distillation. Hexanes were added to the oil but no crystallization occurred. The hexanes were removed by vacuum distillation. The oil was vacuum distilled. A clear solvent distilled at approximately  $60^\circ\text{C}$  and 0.3 mm Hg. Sulfolane usually distilled at  $90^\circ\text{C}$  and 0.3 mm Hg. NMR of the oil indicated sulfolane and possibly a phenol.

#### **4.2.1.3 Polymer Synthesis**

The poly (amic acid) solutions were prepared at a concentration of 20% solids (w/w) by the slow addition of a stoichiometric amount of the dianhydride or a combination of dianhydrides in powder form to a magnetically stirred solution of the diamine or a combination of diamines in N,N-dimethylacetamide (DMAc) under a nitrogen atmosphere at room temperature. Polymer solutions were stirred 8-24 hr.

#### **4.2.1.4 Films**

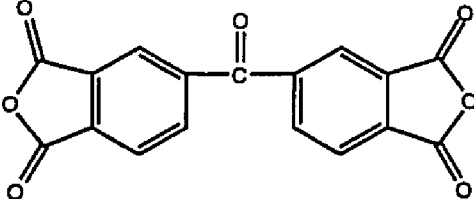
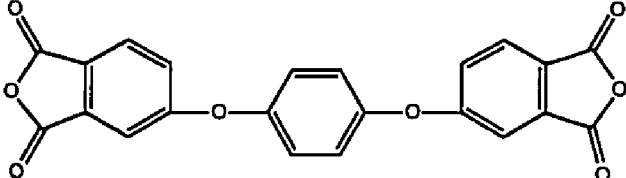
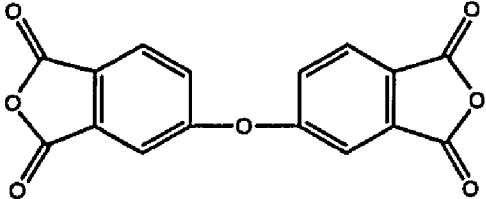
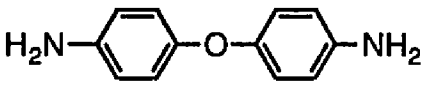
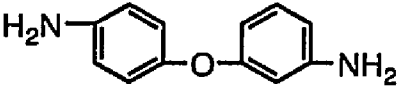
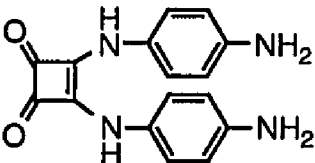
The poly (amic acid) solutions were centrifuged, the decantate cast onto plate glass using a doctor blade, and allowed to dry to a tack-free form in a dust-free chamber at room temperature, continually purged with dry air. The films on glass were then thermally converted to the polyimide by heating in a

forced air oven at 100, 200, and 300°C for 1 hr at each temperature. Cooled films were removed from the glass plates by immersion in warm water.

## 4.2.2 Polyimides As Encapsulants

### 4.2.2.1 Starting Materials

4,4'-Oxydiphthalic anhydride (ODPA) was recrystallized from acetic anhydride/acetic acid (4:1) (Occidental Chemical Corporation, mp 226-227°C). Hydroquinone diether dianhydride (HQDEA) was used as received from Occidental Chemical Corporation (mp 267-268°C). Squaric acid derivative diamine (SAPPD) was vacuum-dried at 150°C prior to use (Kwoya Hakko Kogyo Co., Ltd, mp 287-288°C). *Para*-phenylene diamine (*p*-PDA) was recrystallized from ethanol and then sublimed (mp 143°C). 3,3',4,4'-Benzophenone tetracarboxylic dianhydride (BTDA) was sublimed prior to use (mp 222-223°C). 4,4'-Oxydianiline (4,4'-ODA) was sublimed prior to use (mp 186-187°C). 3,4'-Oxydianiline (3,4'-ODA) was recrystallized from ethanol/water (mp 80-81°C). *N,N*-Dimethylacetamide (DMAc) was used as received from Fluka. Structures and acronyms of the monomers are shown in Table 4.2.

STRUCTURE	ACRONYM
	BTDA
	HQDEA
	ODPA
	4,4'-ODA
	3,4'-ODA
	SAPPD

**Table 4.2 Monomers Used For Synthesis Of Polyimides As Encapsulants**

#### 4.2.2.2 Polymer Synthesis

The poly (amic acid)s were prepared at a concentration of 8-20% solids (w/w) by the slow addition of a stoichiometric amount of the dianhydride in powder form to a mechanically stirred solution of the diamine or a combination

of diamines in *N,N*-dimethylacetamide (DMAc) under a nitrogen atmosphere at room temperature. Polymer solutions were stirred 16-24 hr.

#### **4.2.2.3 Films**

The poly (amic acid) solutions were centrifuged, the decantate cast onto plate glass using a doctor blade, and allowed to dry to a tack-free form in a dust-free chamber at room temperature, continually purged with dry air. The films on glass were then thermally converted to the polyimide by heating in a forced air oven at 100, 200, and 300°C for 1 hr at each temperature. Polymers were also cured at 100 and 200°C for 1 hr each and subsequently cured at 250°C for 2 hr. The properties of the two cure cycles were compared. All data reported are the result of films cured by the standard imidization cure cycle of 100, 200, and 300°C for 1 hr at each temperature. Cooled films were removed from the glass plates by immersion in warm water.

#### **4.2.2.4 Solubility**

The solubility of some polyimides was examined using a 1% solids solution of the polyimide film in either NMP, DMAc, DMF, diglyme, or methylene chloride (CH<sub>2</sub>Cl<sub>2</sub>). The films in solution were placed in a closed vial at RT and were examined at intervals of 3 hr, 1 day, 3 days, and 5 days. Visual identification determined if the polyimide was insoluble, partially soluble, or soluble. Noted in the examinations were any discoloration of the solvent, swelling of the polymer, or other changes in the polymer film.

### 4.3 Polyimides For Harsh Environments

#### 4.3.1. Hydrolytically Stable Polyimides

Commercially available films used in this study are listed below.

Material	Manufacturer
KAPTON <sup>®</sup> 200HN	DuPont, Circleville, OH
UPILEX <sup>®</sup> R	UBE Industries, LTD, Japan
UPILEX <sup>®</sup> S	UBE Industries, LTD, Japan
APICAL <sup>®</sup> 300AV	Allied Signal, Des Plaines, IL
LaRC <sup>™</sup> -TPI	Mitsui Toatsu Chemicals, Tokyo, Japan

**Table 4.3 Commercially Available Films For Hydrolytic Stability Evaluation**

The materials used to make the experimental polyimide films for hydrolytic stability evaluation are listed in Table 4.4, along with their acronyms, sources, and purification methods.

Material	Acronym	Source	Purification
4,4'-Isophthaloyl diphthalic anhydride	IDPA	NASA-LaRC[13]	Vacuum-dried at 125°C
4,4'-Oxydiphthalic anhydride	ODPA	Occidental Chemical Corporation	Sublimed at 200-210°C
Hydroquinone diether anhydride	HQDEA	Occidental Chemical Corporation	Used as received
2,2-Bis(3,4-dicarboxyphenyl)-hexafluoropropane dianhydride	6F	Hoechst Celanese	Used as received
Pyromellitic dianhydride	PMDA	Allco Chemical Corporation	Used as received
3,3',4,4'-Benzophenone tetracarboxylic dianhydride	BTDA	Allco Chemical Corporation	Sublimed at 200-210°C
3,3',4,4'-Biphenyl tetracarboxylic dianhydride	BPDA	Mitsubishi International Corp.	Used as received
1,3-Phenylenediamine	<i>m</i> -PDA	Fluka AG	Used as received
1,4-Phenylenediamine	<i>p</i> -PDA	Fluka AG	Recrystallized from ethanol and sublimed at 120°C
3,4'-Oxydianiline	3,4'-ODA	Kennedy and Klim, Inc.	Used as received
4,4'-Oxydianiline	4,4'-ODA	Kennedy and Klim, Inc.	Used as received
3,5-Diaminobenzotrifluoride	3,5-DABTF	Occidental Chemical Corporation and NASA-LaRC[11]	Used as received
2,2-Bis[4-(4-aminophenoxy)phenyl]hexafluoropropane	4-BDAF	Central Glass Company, LTD, Japan	Recrystallized from dichloromethane and hexane
1,3-Bis(4-aminophenoxy-4'-benzoyl)benzene	1,3-BABB	DayChem Laboratories, Inc.	Recrystallized from toluene

**Table 4.4 Dianhydrides And Diamines For Potential Hydrolytically Stable Polyimides**



#### **4.3.1.1 Polymer Synthesis**

The poly (amic acid)s were prepared at a concentration of 20% solids (w/w) by the slow addition of a stoichiometric amount of the dianhydride in powder form to a magnetically stirred solution of the diamine in N,N-dimethylacetamide (DMAc) under a nitrogen atmosphere at room temperature. Polymer solutions were stirred overnight.

#### **4.3.1.2 Films**

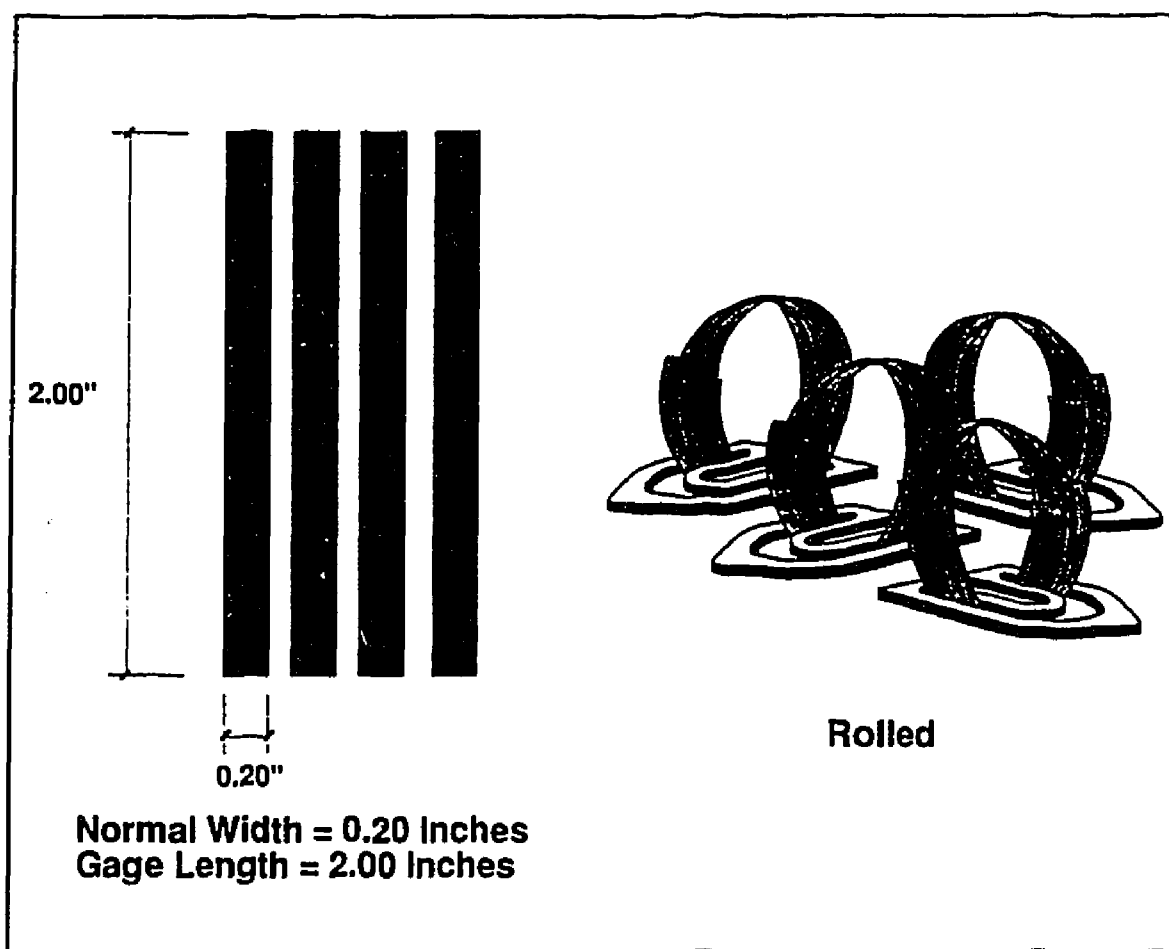
The poly (amic acid) solutions were centrifuged, the decantate cast onto plate glass using a 23 mil (0.023 in) doctor blade, and allowed to dry to a tack-free form in a dust-free chamber at room temperature, continually purged with dry air. The films on glass were then thermally converted to the polyimide by heating in a forced air oven at 100, 200, and 350°C for 1 hr at each temperature. LaRC™-CPI was heated to 300°C. Cooled films were removed from the glass plates by immersion in warm water.

#### **4.3.1.3 Alkaline Solution Exposure**

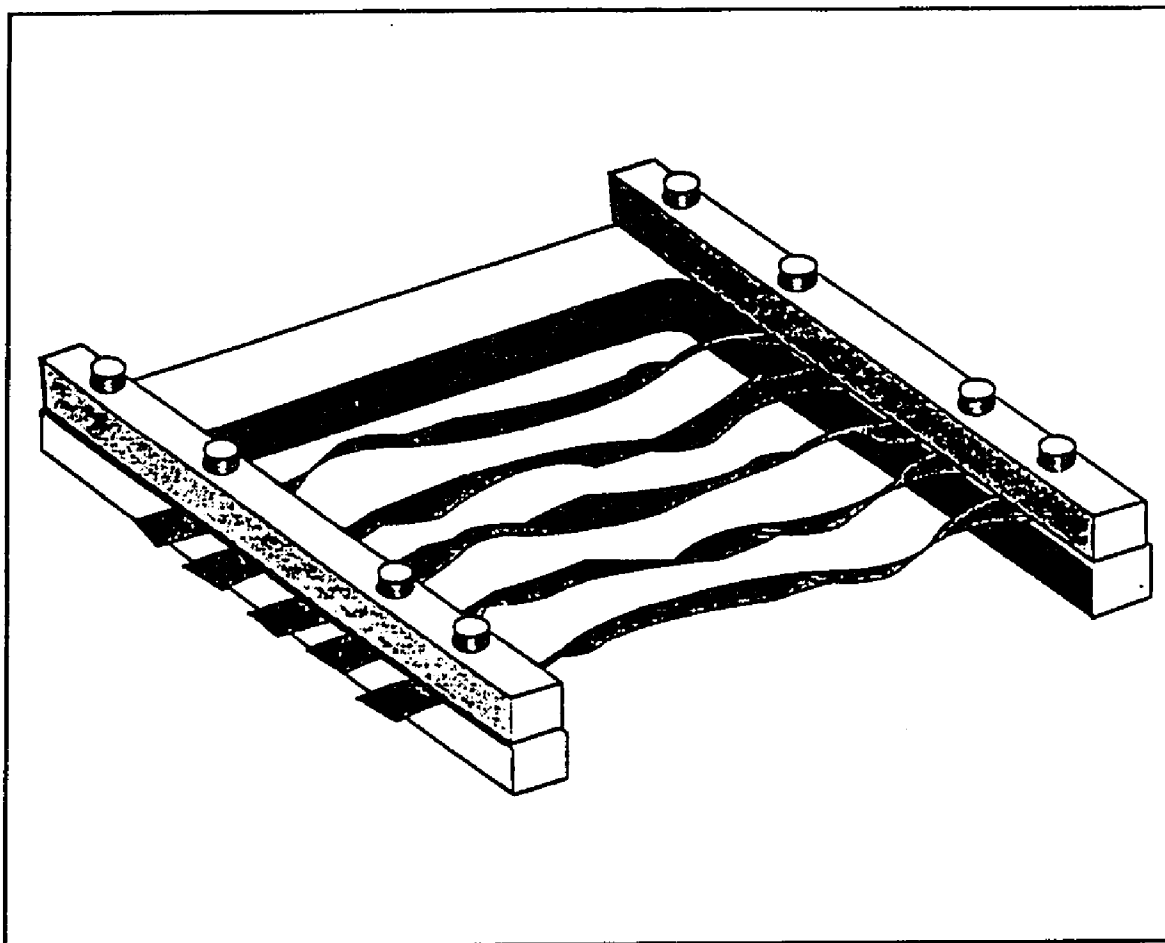
A baseline for exposed films was established for each of the three configurations shown in Figures 4.6 and 4.7. Normal (unstressed) configurations were placed in solvents, flat, horizontal, and parallel to each other. Rolled configurations were wrapped around a 0.25-in diameter glass tube and secured by a polyethylene paper clip. Twisted configuration specimens were clamped in a machined stainless steel device with four twists

per specimen over a length of four inches. All specimens were 0.20 in wide and approximately 4-6 in in length.

Films were immersed for 48 hr at RT in the following basic solutions: 1.0 M ammonium hydroxide (7% v/v, pH = 11), 1.0 M sodium carbonate (11% w/v, pH = 12), 0.5 M trisodium phosphate (19% w/v, pH = 13), and 1.0 M sodium hydroxide (4% w/v, pH = 14). After exposure, the specimens were removed, washed with tap water, and rinsed with distilled water. They were blotted dry and placed in a desiccator until tensile testing was performed.



**Figure 4.6 Normal And Rolled Configurations For Chemical Exposure Of Polyimide Films**

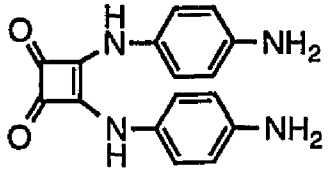
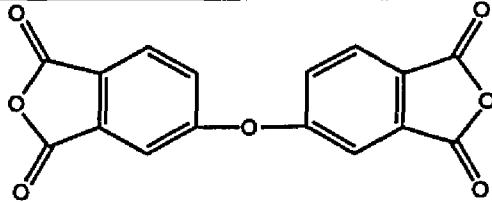
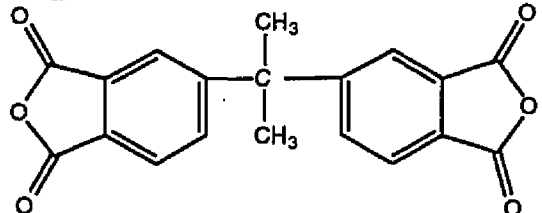
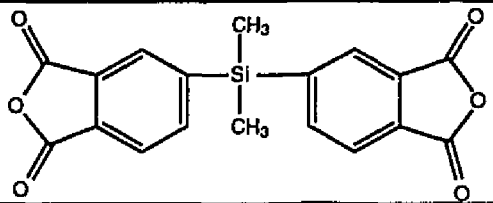


**Figure 4.7 Twisted Configuration For Chemical Exposure Of Polyimide Films**

## 4.3.2. Electron Radiation Resistant Polyimides

### 4.3.2.1 Starting Materials

4,4'-Oxydiphthalic anhydride (ODPA) was sublimed prior to use (Occidental Chemical Corp, mp 226-227°C). Squaric acid derivative diamine (SAPPD) was vacuum-dried at 150°C prior to use (Kwoya Hakko Kogyo Co., Ltd, mp 287-288). 3,3',4,4'-Benzophenone tetracarboxylic dianhydride (BTDA) was sublimed prior to use (mp 222-223°C). 2,2-Bis[4-(3,4-dicarboxyphenyl)] isopropylidene dianhydride (IPAN) was vacuum dried at 150°C prior to use (mp 187-188°C). 2,2-Bis[4-(3,4-dicarboxyphenyl)] silane dianhydride (Si(CH<sub>3</sub>)<sub>2</sub>DA) was used as received (mp 180-181°C). Structures and acronyms are shown in Table 4.5.

STRUCTURE	ACRONYM
	SAPPD
	ODPA
	IPAN
	Si(CH <sub>3</sub> ) <sub>2</sub> DA

**Table 4.4 Structures And Acronyms Of Monomers Used For Synthesis Of Radiation Resistant Polyimides**

#### 4.3.2.2 Polymer Synthesis

The poly (amic acid)s were prepared at concentrations between 8-15% solids (w/w) by the slow addition of a stoichiometric amount of the dianhydride in powder form to a mechanically stirred solution of the diamine in N,N-dimethylacetamide (DMAc) under a nitrogen atmosphere at room temperature. Polymer solutions were stirred overnight.

#### 4.3.2.3 Polymer Films

The poly (amic acid) (PAA) solutions were centrifuged, the decantate cast onto plate glass using a doctor blade, and allowed to dry to a tack-free form in a dust-free chamber at room temperature, continually purged with dry air. Three films on glass were then thermally converted to the polyimide by heating in a forced air oven at 100, 200, and 300°C for 1 hr at each temperature. The polymer designated Si(CH<sub>3</sub>)<sub>2</sub>DA/SAPPD adhered so well to the glass plate that it could not be removed by immersion in hot water. This PAA solution was synthesized again and cast onto a glass plate covered with 4 mil (0.004 in) aluminum. The aluminum had been treated with Frekote® release agent and dried at 100°C. Cooled films were removed from the glass or aluminum covered plate by immersion in warm water. A razor blade was required to remove the Si(CH<sub>3</sub>)<sub>2</sub>DA/SAPPD polymer film from the aluminum covered glass plate.

#### 4.3.2.4 Electron Radiation Exposure

Thin films (3.5 in x 6.5 in x 0.002 in) were exposed to 1 MeV electrons using a Radiation Dynamics Inc. Dynamitron Model 1000/10 accelerator. The specimens were secured around the perimeter and held flat against a temperature controlled aluminum plate positioned in the uniform area of the electron beam. The absorbed dose and dose rate were calculated from the current flux levels monitored with a Faraday cup mounted in the exposure area of the aluminum plate. The Faraday cup was calibrated using National Bureau of Standards calibrated polymeric dosimeter films. The exposure chamber operated at a pressure of  $2 \times 10^{-7}$  torr and the temperature of the films did not

exceed 40°C. The films received doses of  $5 \times 10^7$  rads and  $1 \times 10^9$  rads at a dose rate of  $5 \times 10^7$  rads/hr without interruption. After exposure, the specimens were stored in a desiccator until they were characterized.

#### 4.4 References

1. Havens, S. J., NASA Langley Research Center, Polymeric Materials Branch, Laboratory Notebook 121, July 1991; p 79.
2. Havens, S. J., NASA Langley Research Center, Polymeric Materials Branch, Laboratory Notebook 69, April 1989; p 46.
3. Havens, S. J., NASA Langley Research Center, Polymeric Materials Branch, Laboratory Notebook 39, December 1987; p 12.
4. Havens, S. J., NASA Langley Research Center, Polymeric Materials Branch, Laboratory Notebook 69, May 1989; p 46.
5. Havens, S. J., NASA Langley Research Center, Polymeric Materials Branch, Laboratory Notebook 39, October 1987; p 4.
6. Aranuma, T.; Oikawa, H.; Ookawa, Y.; Yamaguchi, A. *Polymer Preprint* **1993**, *34(2)*, 827.
7. Yamaguchi, K.; Urakami, U.; Tanabe, Y.; Yamazaki, M.; Tamai, S.; Yamaya, N.; Ohta, M.; Yamaguchi, A. European Patent Appl. EP 425 265, May 2, 1991; *Chem. Abst.* **1992**, *115*, 93782n.
8. Staniland, P. A.; Wilde, C. J.; Bottino, F. A.; Di Pasquale, G.; Pollicino, A.; Recca, A. *Polymer* **1992**, *Vol. 33 (9)*, 1976-1981.
9. Schwartz, Jr., W. T. *High Performance Polymers* **1990**, *Vol. 2, No. 2*, 189-196.
10. Schwartz, Jr., W. T. US Patent 4 868 316, September 1989.
11. Gerber, M. K.; Pratt, J. R.; St. Clair, A. K.; St. Clair, T. L. *Polym. Prepr.* **1990**, *31 (1)*, 340.
12. Havens, S. J., NASA Langley Research Center, Polymeric Materials Branch, Laboratory Notebook 974, August 1983; p 61.
13. Pratt, J. R.; Blackwell, D. A.; St. Clair, T. L.; Allphin, N. L. *Polymer Engineering and Science* **1989**, *31(1)*, 63-68.



## Chapter 5: Characterization

### 5.1 Elemental Analysis

Elemental analyses were performed by Galbraith Laboratories, Inc., Knoxville, TN and Oneida Research Services, Inc., Whitesboro, NY. The determinations from Oneida Research Services, Inc.[1] of percent carbon, hydrogen, and nitrogen (CHN) were performed using CEC Model 240-A CHN and Leco Model 932 CHNS Analyzers. The accuracy of results obtained were within 0.3% (absolute) for each element. Quality control sample checks were incorporated with each run. Fluorine analysis was performed using an ion selective electrode, where the sample was burned and then analyzed.

### 5.2 Melting Point Determinations

Melting points were determined using differential scanning calorimetry (DSC) conducted on a Shimadzu DSC-50 Thermal Analyzer or DuPont Differential Thermal Analyzer (DTA) at a heating rate of 10°C/min with the melting point taken at the peak minimum. Visual melting points were determined using a Thomas Hoover Capillary Melting Point Apparatus. Several batches of each compound were synthesized or attempted. A representative DSC thermogram or DTA plot for each compound can be found in the Appendix with its chemical name and structure included on each graph.

### 5.3 Mass Spectrometry

Mass spectra were obtained on a Finnigan 4500 Gas Chromatograph-Mass Spectrometer (GC-MS) equipped with a solid probe. The sample was held at 35°C for 5 min and then ramped to 350°C at a heating rate of 20°C/min. The scanning range was 35-700 atomic mass units (amu); the scanning rate was 2 sec/scan.

### 5.4 Inherent Viscosity

Inherent viscosities ( $\eta_{inh}$ ) of poly (amic acid) solutions were determined at a concentration of 0.5 g/dL using an Ostwald type viscometer manufactured by Cannon Instruments (Figure 5.1). A volume of 10 mL was introduced into B and drawn up by suction into A until the level of the liquid was above the mark  $m_1$ . The suction was released and the time required for the level to fall from  $m_1$  to  $m_2$  was measured. The time required for the standard reference solution was designated  $T_{solvent}$ . The time required for the polymer solution was designated  $T_{solution}$ . The average driving force during the flow of this volume of liquid through the capillary tube was proportional to the difference in heights of the liquids in tubes B and A. Inherent viscosities were measured at 25°C or 35°C and the values calculated using:

$$\eta_{inh} = \frac{\ln (T_{solution} / T_{solvent})}{0.5 \text{ g/dL}}$$

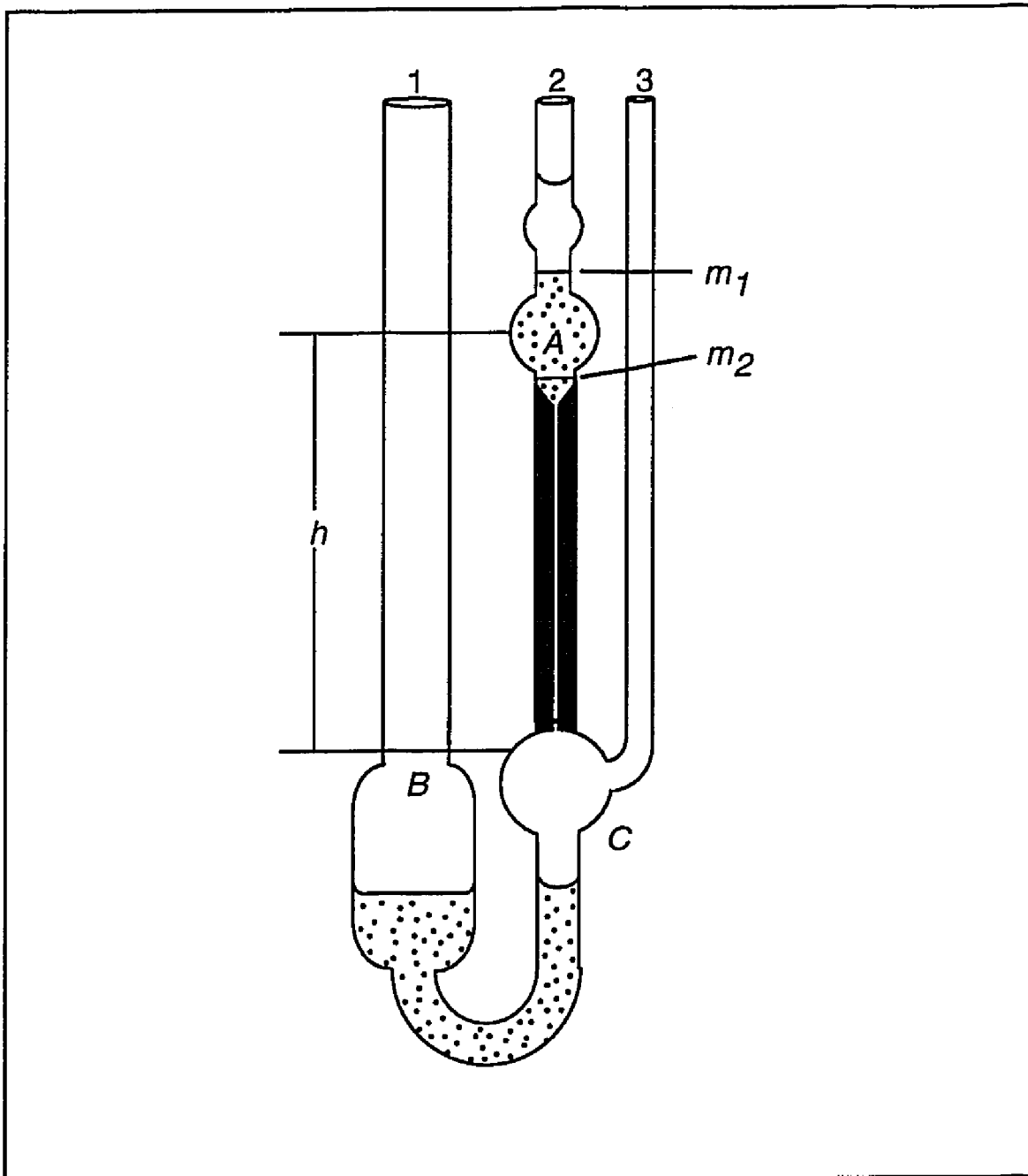


Figure 5.1 Ostwald Type Viscometer

## 5.5 Thermal Analysis

Glass transition temperatures ( $T_g$ ) were determined by differential scanning calorimetry (DSC) using a Shimadzu DSC-50 Thermal Analyzer or a Seiko DSC 210 at a heating rate of 20°C/min.  $T_g$ s were also obtained by thermomechanical analysis (TMA) obtained on a DuPont 9900 Computer Thermal Analyzer at a heating rate of 5°C/min. Dynamic thermogravimetric analyses (TGA) were obtained in flowing air (40 cc/min or 50cc/min) at a heating rate of 2.5°C/min after an initial 30 min hold at 100°C using a Seiko Model TG/DTA 220 or Seiko TGA Model 5200. Coefficients of thermal expansion (CTE) were obtained on either a Seiko TMA 120 at a heating rate of 5°C/min or a Seiko TMA Model 100 at a heating rate of 2°C/min.

## 5.6 Melt Viscosity

Melt viscosity measurements of the imidized powders and blends were performed on a C. W. Brabender Instruments Inc. PL2000 Plastic-Corder® operated at a shear rate of 74 sec<sup>-1</sup> with a torque range of 0-50 meter-gram at temperatures ranging from 300-360°C. Rheological properties were also measured using a parallel plate Rheometrics System Four. The polymer was placed between two parallel metal plates, and the specimen was heated until the polymer melted.

## **5.7 Transmission UV-visible (UV-VIS) Spectra**

Transmission UV-visible (UV-VIS) spectra were obtained on 0.013 mm (0.5 mil) thick films using a Perkin-Elmer Lambda 5 UV-VIS spectrometer in the reflectance mode with an integrating attachment.

## **5.8 Dielectric Constants**

Dielectric constants for the polyimides for microelectronic applications were determined using a Hewlett-Packard 8510 Automated Network Analyzer over the frequency range 8-12 GHz. The polymer films were desiccated overnight prior to the measurement. A stack of ten 0.025 mm (1 mil)-thick film specimens was inserted between flanges in an x-band waveguide and tested at 26°C in 25-35% relative humidity to obtain the dielectric data. The dielectric constants for the hydrolytically stable polyimide evaluation were obtained from various literature sources, and were not measured by the same instrument.

## **5.9 Tensile Properties**

A model 2000/2 table-top MTS Systems Corp. SINTECH load frame, equipped with CompuAdd Model 286 or Compaq Model 486 computer and HP graphics plotter, was used for measuring tensile properties. Pneumatically operated, one-inch rubber padded steel grips were used to clamp the films at RT. Approximately 40 psi was supplied to the grips. Elevated temperature properties were obtained using a clamshell model radiant heat furnace by Research Inc. Stainless steel machined clamps were used at elevated temperatures. The Micristar® temperature control unit was programmed for

tests temperatures at 93, 121, 150, 177, 202, and 232°C. The test program ramped to the set point in five minutes. A ten minute hold at that temperature allowed the film to equilibrate to  $\pm 1-2^{\circ}\text{C}$ , at which point the test was begun.

Tensile specimens were 0.200 in wide and varied in length from 4-6 inches. The gauge length was 2.00 in. Each specimen thickness was determined to within 0.0001 in using Testing Machines Inc. Models 549M and 49-70 electronic micrometers. Thickness measurements were made at every inch over the specimen length and the average was used for the calculation. Film thicknesses for the experimental films were approximately 1-3 mils and commercial films of the same thicknesses were obtained where available. Film strips for the hydrolytic stability study were initially cut to 0.200 in widths using a machined device that held a series of razor blades at 0.200 in intervals and was pulled on top of the guide rests over the polyimide film. Later in that study, and for all other polyimide films in this dissertation, the specimens were cut more accurately with a 0.200 in Thwing-Albert Precision Cutter. A minimum of five specimens was used for each condition. A crosshead speed of 0.200 in/min was used for determination of tensile strength, modulus, and elongation at break.

The tensile specimens used in this dissertation were smaller in size than recommended in the American Society of Testing and Materials (ASTM) Standard D882 but this standard was used as a guide. The ratio of length to width was 10:1 as suggested in ASTM D882. A data base using 0.200 in widths of Kapton® and ULTEM® compared to full sizes (10" x1") clearly indicated that for the measurements of changes in tensile properties, data obtained for smaller specimens were acceptable[2].

### 5.10 Density

Density measurements were made using the density gradient technique shown in Figure 5.2. This apparatus meets the temperature and dimensional requirements of ASTM D1505-60T. The column was calibrated using glass beads of known density. The liquid system for the density gradient column was  $\text{ZnCl}_2/\text{H}_2\text{O}$ . The temperature was maintained at  $25^\circ\text{C}\pm 1^\circ\text{C}$ .

### 5.11 X-ray Diffraction

X-ray diffraction was performed using a Philips APD 3600, XRG 3100 equipped with a flat sample holder and copper radiation source. The excitation energy settings (source energy) were 45kV and 40mA. Wide angle x-ray diffraction was determined using a graphite monochromator with a 2 second time increment every  $0.02^\circ\text{C}$  ( $2\theta$ ). The angular range was  $5-40^\circ$  ( $2\theta$ ). Small angle x-ray diffraction was determined using a Kratky camera with an angular range of  $0.5-5.0^\circ$  ( $2\theta$ ).

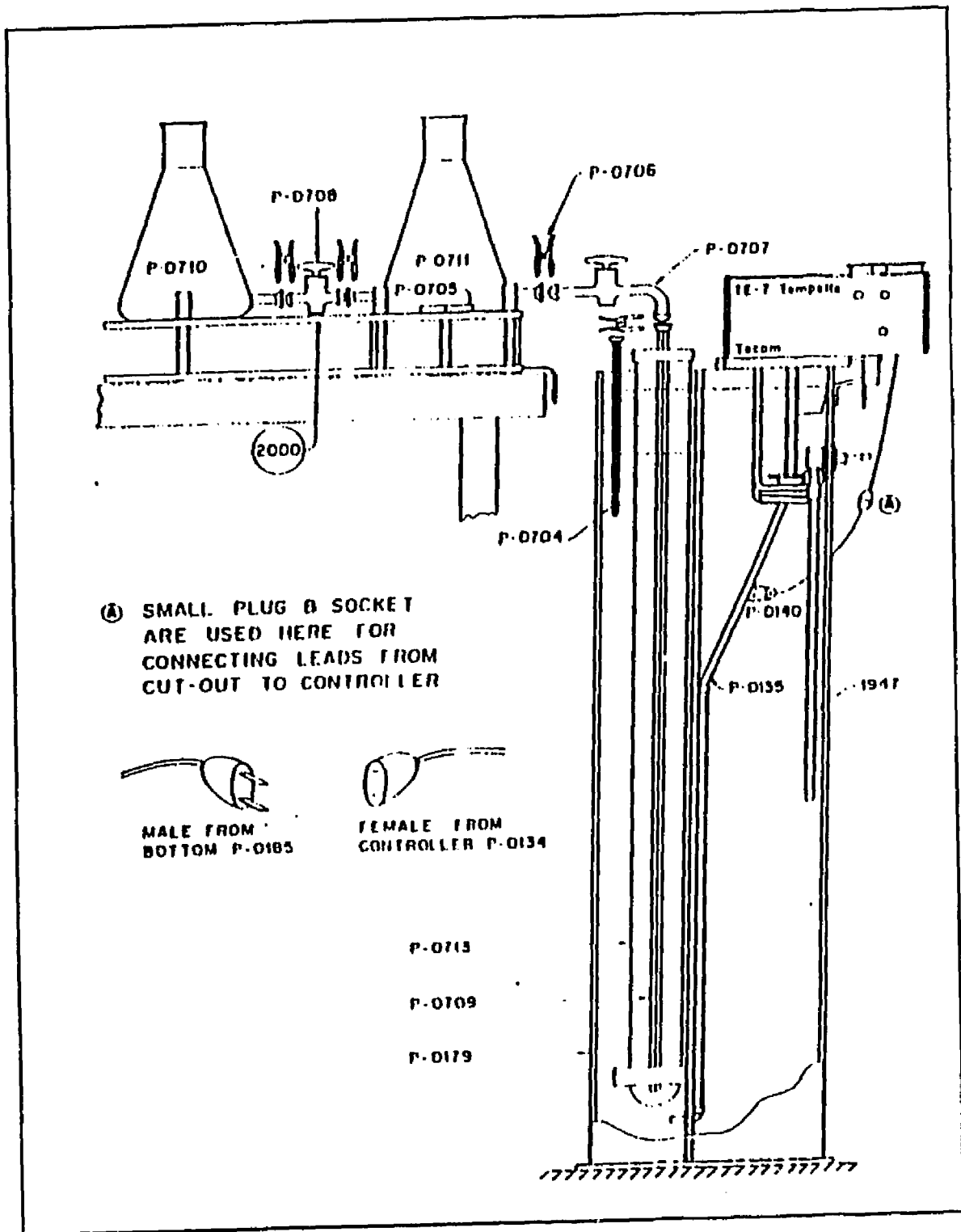


Figure 5.2 Density Gradient Column



## 5.12 Saturation Moisture Content Measurements

### 5.12.1 Polyimides As Encapsulants

The samples (approximately 2 in by 2 in) were first desiccated by heating them to 120°C in a vacuum oven until their weights became constant. An oven was used to maintain the water temperature between 90-93°C. The films were submerged in the water until their weights stabilized. The saturation moisture content by weight,  $w/o$ , was determined as:

$$w/o = ((w_{SS} - w_{DS}) / w_{DS}) \times 100$$

where  $w_{SS}$  was the saturated sample weight and  $w_{DS}$  was the desiccated sample weight. The saturation moisture fraction by volume ( $v/o$ ) was then calculated from the measured weight fraction as follows:

$$\text{Saturation moisture fraction by volume (v/o)} = \frac{100\rho(w/o)}{100 + \rho(w/o)}$$

where  $\rho$  is the density of the dry polymer sample relative to the density of water[3].

### 5.12.2 Hydrolytically Stable Polyimides

Moisture uptake measurements for hydrolytically stable polyimides were determined by first drying a film sample at 100°C overnight, weighing the sample, and then submersing it in water at RT for 30 days. Samples were then

removed, dried with a dust-free cloth, and re-weighed. The moisture uptake was calculated by the weight gain over the original weight of the polyimide film sample.

### **5.13 Positron Lifetime Measurements**

Positron lifetimes in the test films were measured using a low energy positron flux generation scheme in order to obtain free volume values in selected polymers[4]. The positron source holder was thin aluminized Mylar® film. It was sandwiched between two well-annealed polycrystalline, high purity, tungsten moderator strips. The test films were placed between the source holder and the moderator strips. The films electrically insulated the source holder from the moderator strips. Thermalized positrons diffused out of the moderator when a small negative potential (-V) was applied between the source holder and the moderator strips. The positrons were attracted to the source holder and therefore entered and annihilated in the test films. When a positive potential (+V) was applied, the outdiffusing positrons were forced back into the moderator strips. The difference in the two spectra from applied positive and negative potentials was entirely due to the positrons annihilating in the test films. The lifetime data was acquired using a 250 microcuries  $^{22}\text{Na}$  positron source and a standard fast-fast coincidence measurement system with a time resolution of approximately 225 picosecond[3].

### **5.14 Molecular Orientation (Film Stretching)**

Stretching of the polymer films was attempted using the T. M. Long Film Stretcher. The film stretcher[5] operated by the movement of two draw bars at

right angles to each other upon hydraulically driven rods. A fixed draw bar was located opposite each moving draw bar. Together, they made up the two axes at right angles along which the specimen was stretched. The stretch ratio was up to four times the original size. Film can be stretched in one or both directions independently, or in both directions simultaneously.

The constant stretch rate can be varied from 0.20 to 20 inches per minute. The constant force can be varied from 0 to 25 psi. Nominal specimen size was 4 x 4 inches between grips. Specimens were cut oversized to 4.4 x 4.4 inches to ensure the maximum gripping surface area for the film specimen.

Specimens can be heated rapidly in excess of 200°C and maintained during the stretching cycle. An automatic loading and quenching mechanism was provided which inserted the film and quenched it at the end of the stretch. Quenching was important so as to preserve polymer orientation and reduce relaxation.

There were 52 clips (13 on each draw bar) to hold the specimen in place. Each clip had a miniature air cylinder. The clips were connected to a high pressure nitrogen source. The O-rings on the pistons were rated for limited service to 248°C. Many polymers may require stretching above 248°C, and in those applications, a different O-ring material would be necessary.

The film was heated from both sides by streams of high velocity heated air from air heaters. The sample was placed on a vacuum plate and the loader was run in and dropped down to load the film. The loader was retracted and the cover lowered for stretching. After the completion of stretching, the loader was swung about on its carriage and another vacuum plate of stretched specimen size was run in to extract the film. This plate was at room temperature and was therefore used to quench the film as it was pulled into contact with the plate.

### 5.15 References

1. Maraio, Sharon, Oneida Research Services, Inc., Technical Representative, personal communication.
2. Long, Jr., E. R.; Long, S. A. T., NASA Technical Paper 2429 , 1985.
3. Eftekhari, A.; St. Clair, A. K.; Stoakley, D. M.; Sprinkle, D. R.; Singh, J. J. In *Polymers For Microelectronics, Resists And Dielectrics* ; ACS Symposium Series 537, 1994; Chapter 38, p 535-545.
4. Singh, J. J.; Eftekhari, A.; St. Clair, T. L. *Nucl. Instrum. Methods. Phys. Res.* **1991**, *B53*, 342-348.
5. T. M. Long Film Stretcher Manual.

## Chapter 6: Results And Discussion

### 6.1 Potential Liquid Crystalline Polyimides

#### 6.1.1 Introduction

The objective of this research was to synthesize dianhydrides that when combined with appropriate diamines would potentially afford liquid crystalline polyimides. All the dianhydrides proposed would contain flexible segments via an ether linkage (diether dianhydrides). When these flexible dianhydrides were combined with rigid diamines, an alternating flexible/rigid polymer backbone resulted and hence the potential was created for liquid crystallinity[1-6]. Groups such as isopropylidene, carbonyl, naphthalene, biphenyl, butane, and hexane in *meta* and/or *para* catenations would be incorporated into the aromatic diether dianhydride. Incorporation of rigid groups such as naphthalene and biphenyl, or spacers containing -CH<sub>2</sub>- groups like butane or hexane, would provide the potential to achieve liquid crystallinity in the resultant polyimides.

Aryl diether dipthalic dianhydrides can be synthesized from the corresponding bisphenol with fluorophthalic anhydride in the presence of sulfolane. In several cases, the bisphenols were not commercially available and therefore were synthesized. Two bisphenols were synthesized via Friedel-Crafts acylation followed by demethylation to the corresponding bisphenols.

Five bisphenols were synthesized via hydrolysis of the corresponding difluoro compounds in the presence of potassium hydroxide.

Bisphenols are also used in the synthesis of poly (arylene ether)s[7]. Poly (arylene ether)s are high performance engineering thermoplastics with attractive properties for applications such as adhesives, composites, and coatings. Some poly (arylene ether)s were synthesized from these novel bisphenol intermediates but will not be discussed here since this dissertation was limited to polyimides. Additional research could be conducted to develop poly (arylene ether)s using these novel bisphenols.

### 6.1.2 Synthesis

#### Dimethoxy Compounds

The aromatic dimethoxy compounds were synthesized by acylation of anisole with terephthaloyl or isophthaloyl chloride via the Friedel-Crafts reaction. A catalyst is nearly always needed and aluminum chloride is the most common. Other Lewis acids are used, and also proton acids such as hydrofluoric acid (HF) and sulfuric acid (H<sub>2</sub>SO<sub>4</sub>). Acylation usually requires a little more than 1 mole of catalyst per mole of reagent since the first mole coordinates with oxygen of the reagent. Therefore, a 10% excess of aluminum chloride was used in the synthesis. The mechanism of Friedel-Crafts acylation is not completely understood but in most cases, the attacking species is the acyl cation, either free or as an ion pair[8].

The dimethoxy compounds were then reacted with concentrated hydrobromic acid (HBr) to form the resultant bisphenols via ether cleavage. Heating dialkyl ethers with strong acids (HBr, hydroiodic acid (HI)) causes them to undergo reactions in which the C-O bond breaks. HBr causes fewer

side reactions than HI and was therefore was the better reagent. The mechanism for synthesis begins with the formation of the oxonium ion. Then, a  $S_N2$  reaction with the  $Br^-$  acting as a nucleophile produces a bisphenol and methylbromide[8].

### Bisphenols

Bisphenols were also synthesized by an alternate route. Aromatic dihalides were converted to bisphenols via hydrolysis using potassium hydroxide by nucleophilic substitution[9]. The  $OH^-$  nucleophile reacts with the halogenated compound by replacing the halogen, which leaves as a halide ion. This reaction eliminated the need to synthesize the intermediate dimethoxy compound. Additionally, although this research did not use commercially available dihalide compounds, many are available and could be used in the design of bisphenols and dianhydrides for poly (arylene ether) and polyimide synthesis'.

### Diether Dianhydrides

Aryl diether diphthalic anhydrides were prepared by the reaction of a bisphenol with 4-fluorophthalic anhydride and spray-dried KF in the presence of sulfolane. The KF acts as an HF acceptor and eliminates the need to prepare the bisphenol salt in a separate step[10-11]. The fluorine atom on the 4-fluorophthalic anhydride functions as the leaving group and becomes the site for the formation of the ether bridge. The KF complexes with the HF released to form  $KHF_2$ . Although the reaction mechanism is not completely understood, some evidence is available. Proton NMR showed that no phenoxide was present during the reaction of phenol and KF in the presence of sulfolane[10].

This evidence was important since phenol and 4-fluorophthalic anhydride have been shown to react in the same fashion as bisphenols.

Clark and Owen discovered that 4-cyanophenol in KF/nitro or chloro displacements yielded a strongly hydrogen-bonded fluoride complex[12]. The complex formed was believed to repress the nucleophilicity of the fluoride ion, and exclude formation of fluoride on the aromatic ring[10]. If used alone, fluoride is a strong nucleophile and is capable of rapidly replacing nitro or other halogen groups on an aromatic ring. The bisphenol/KF reactions should be equally effective with bromo-, chloro-, or nitrophthalic anhydride, although only 4-fluorophthalic anhydride was used in the synthesis of monomers for potential liquid crystalline polyimides.

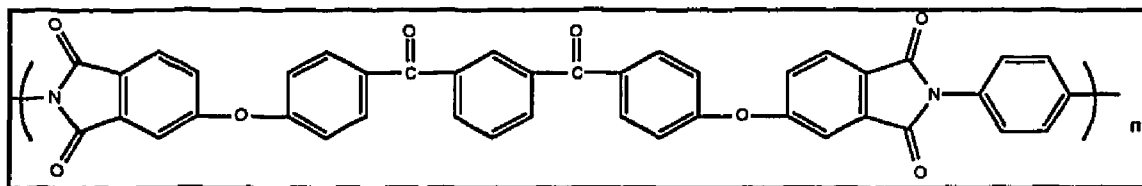
### **6.1.3 Characterization of Potential Liquid Crystalline Polyimides From Novel Diether Dianhydrides**

The first two dianhydrides synthesized contained a flexible phenoxy-isophthaloyl (1,3-BBBDA) or -terephthaloyl (1,4-BBBDA) segment. When combined with the rigid diamine *para*-phenylene diamine (*p*-PDA), an alternating flexible/rigid polymer resulted. Polymer characterization of the isophthaloyl- and terephthaloyl-segmented polyimides is shown in Figures 6.1 and 6.2. Structures of the repeat unit in the polymer backbone are provided in each figure.

Inherent viscosities for both polymers were low, most likely due to the lack of dianhydride purity. Both dianhydrides were difficult to recrystallize. The  $T_g$  by DSC for the 1,3-BBBDA/*p*-PDA polymer was 226°C; the  $T_m$  was 372°C; the  $T_g$  by the expansion probe method was 184°C; the  $T_g$  by TMA was 181°C. Thermal analysis for the 1,4-BBBDA/*p*-PDA polymer indicated a  $T_g$  by

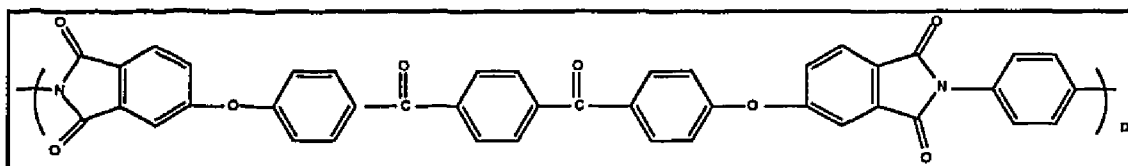


DSC of 287°C for the 1,4-BBBDA/*p*-PDA polymer. A  $T_m$  was exhibited at 434°C. The  $T_g$  by the expansion probe method not readily apparent, while the  $T_g$  by TMA was 311°C.



$\eta$ (inh), dL/g	$T_g$ ( $T_m$ ) by DSC, °C	$T_g$ by expansion probe, °C	$T_g$ by TMA, °C	5% Wt. Loss, °C
0.29	226 (372)	184	181	310
CTE, ppm/°C	Tensile Str., ksi	Tensile Mod., ksi	Elong., %	x-ray diffraction
70	16.0	468.8	7.90	crystalline

Figure 6.1 Polymer Characterization Of 1,3-BBBDA/*p*-PDA



$\eta$ (inh), dL/g	$T_g$ ( $T_m$ ) by DSC, °C	$T_g$ by expansion probe, °C	$T_g$ by TMA, °C	5% Wt. Loss, °C
0.24	287 (434)	ND	311	489
CTE, ppm/°C	Tensile Str., ksi	Tensile Mod., ksi	Elong., %	x-ray diffraction
51	brittle	brittle	brittle	crystalline

ND=Not Detected

Figure 6.2 Polymer Characterization Of 1,4-BBBDA/*p*-PDA

Temperature at which 5% weight loss occurred was low for the 1,3-BBBDA/*p*-PDA at 310°C, while the 1,4-BBBDA/*p*-PDA exhibited a much higher temperature at 489°C. Residual solvent may have been present in the 1,3-BBBDA/*p*-PDA, resulting in a low 5% weight loss temperature. The CTE was high for the 1,3-BBBDA/*p*-PDA polymer (70 ppm/°C) and moderate for the 1,4-BBBDA/*p*-PDA polymer (51 ppm/°C). The temperature range for the CTE measurement was 100 to 120°C.

Despite its low solution viscosity, the 1,3-BBBDA/*p*-PDA exhibited good mechanical properties. Tensile strength, modulus, and elongation were 16.0 ksi, 468.8 ksi, and 7.90% respectively. The 1,4-BBBDA/*p*-PDA was brittle, due to its crystallinity and low molecular weight, and mechanical properties could not be determined. Both films were crystalline by x-ray diffraction. No evidence of liquid crystallinity was noted by thermal analysis.

Due to the difficulty in the synthesis and purification of the intermediate products and the isophthaloyl- and terephthaloyl-segmented dianhydrides, the decision was made to continue with novel dianhydride syntheses rather than fabricate additional novel polyimides or copolyimides using rigid diamines other than *p*-PDA.

### **Bisphenol M Derivative Polyimides**

The next dianhydride synthesized contained the Bisphenol M unit and was designated Bisphenol M diether dianhydride (BMDEDA). A diamine synthesized from Bisphenol M, designated 1,3-BAPDBB, had shown evidence of liquid crystallinity by optical microscopy and thermal analysis[13-14] when combined with the rigid dianhydride PMDA. Thus, it was of interest to examine

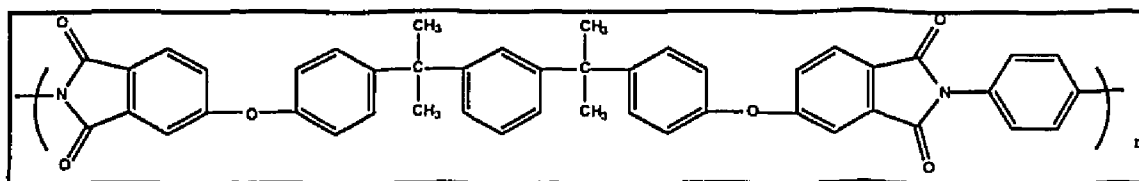
the effect on polymer properties of incorporating the same unit in a novel dianhydride.

Separation of the sulfolane reaction medium from the Bisphenol M diether dianhydride (BMDEDA) was difficult. Even small amounts caused the dianhydride product to "gum" when heat was applied. Heating the compound to 150°C under vacuum afforded a glass, which was subsequently ground to a fine powder prior to recrystallization. Recrystallization in acetic acid/acetic anhydride afforded a pure dianhydride, resulting in high MW polymers. Also, larger amounts of BMDEDA were synthesized than the previous two dianhydrides, and the characterization of the polymers herein was much more extensive than in the previous section. Polymers were prepared and characterized using the novel dianhydride containing the Bisphenol M unit and properties were compared to the analogous liquid crystalline polyimide (LC-PI) synthesized from Bisphenol M, designated PMDA/1,3-BAPDBB, and patented by Mitsui Toatsu, Japan.

The Bisphenol M diether dianhydride (BMDEDA) was combined with *p*-PDA in stoichiometric amounts and cured at various temperatures to afford polyimide films. Polymer powders of BMDEDA/*p*-PDA of controlled MW were also synthesized and characterized. BMDEDA was combined with other rigid diamines such as 1,5-diaminonaphthalene (1,5-DAN) and 2,2'-bis(trifluoromethyl) benzidine (ABL-21). These polymer properties were compared to the properties of an analogous liquid crystalline polyimide containing the Bisphenol M unit in the diamine segment of the polymer, synthesized at NASA's Langley Research Center[15] by the method previously described[13-14], and provided by Mitsui Toatsu (Japan) in film and powder form. New long diamines containing isopropylidene, carbonyl, and ether groups were also synthesized at NASA's LaRC[16]. These diamines were

combined with BMDEDA and other dianhydrides to investigate the potential contribution of the isopropylidene derivative and other flexible/rigid segments to the polyimide properties.

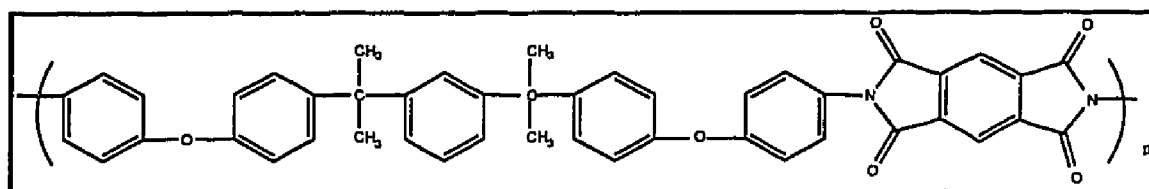
Characterization of Bisphenol M diether dianhydride/*p*-PDA polyimides is shown in Figure 6.3. Several batches of dianhydride and subsequent polyimides were synthesized. Inherent viscosities depended on dianhydride purity obtained with each batch. Polyimides were identified as high molecular weight (MW) (1.74 dL/g) or intermediate MW (0.74 dL/g). Cure temperatures of 200, 240, and 300°C were employed to determine differences in properties. The polyimide films possessed low color.  $T_g$ s were similar for all films (180-190°C).  $T_m$ s were only detected on the first heat for films cured at 200°C, and were not observed upon reheating. This may have resulted from a solvent induced crystallinity that was rendered amorphous after cooling. The temperature at which 5% weight loss occurred ranged between 407 and 455°C with lower temperatures exhibited by films cured at lower temperatures. Similar properties were obtained for films of intermediate and high inherent viscosities of the PAA solutions.



Polyimide Film	Cure Temp., °C	PAA $\eta$ (inh), dL/g	T <sub>g</sub> , °C	T <sub>m</sub> , °C	TGA, 5% Wt. Loss, °C
High MW	200	1.74	186	231	417
High MW	240	1.74	186	none	428
High MW	300	1.74	190	none	455
Intermediate MW	200	0.71	180	228	407
Intermediate MW	240	0.71	189	none	428

**Figure 6.3 Bisphenol M Dianhydride/*p*-Phenylene Diamine Polyimides**

Figure 6.4 illustrates the thermal properties of the analogous liquid crystalline polyimide (PMDA/1,3-BAPDBB) obtained from Mitsui Toatsu Chemicals, Inc., Japan. T<sub>g</sub>s were not detected for either film. Two melting transitions were observed for both films. Both melting points were recoverable upon reheating. The first peak was the liquid crystalline to crystalline transition (T<sub>lc</sub>) and the second peak was the crystalline to isotropic melting transition (T<sub>m</sub>). The T<sub>g</sub> and T<sub>m</sub> were significantly different from BMDEDA/*p*-PDA film properties illustrated in Figure 6.3, yet the elemental compositions were identical.



Polyimide	T <sub>g</sub> , °C	T <sub>m</sub> , °C	TGA, °C
PMDA/1,3-BAPDBB (LC-PI) <sup>1</sup>	ND <sup>3</sup>	276, 300	458
PMDA/1,3-BAPDBB (LC-PI) <sup>2</sup>	ND <sup>3</sup>	275, 294	-

<sup>1</sup>Polyimide film source: Mitsui Toatsu Chemicals, Inc.

<sup>2</sup>Melt press film, 330°C (30 min), 500 psi, powder source: Mitsui Toatsu Chemicals, Inc.

<sup>3</sup>ND=Not Detected

**Figure 6.4 Polymer Characterization Of Mitsui Toatsu Liquid Crystalline Polyimide (LC-PI)**

Mechanical properties at RT and 150°C are shown in Figure 6.5 for the BMDEDA/*p*-PDA intermediate (Inter.) and high MW polymers, and the PMDA/1,3-BAPDBB (LC-PI) polyimide film obtained from Mitsui Toatsu.

Tensile strengths at RT ranged from 10.4 to 14.2 ksi. Tensile strengths increased with decreasing cure temperature. Residual solvent induced crystallinity could contribute to higher strengths and moduli, and decreased elongations, as was seen with these polymers. RT moduli ranged from 342 to 454 ksi. Moduli decreased with increasing cure temperature. Crystallinity was decreased with higher cure temperatures, therefore decreasing the stiffness of the polymer backbone. RT elongations ranged from 2 to 48%. Tensile strengths at 150°C were low, retaining less than 50% of their RT value; however, 150°C was only 30 to 40°C below their respective T<sub>g</sub>s. Moduli at 150°C ranged from 206 to 378 ksi. Higher retentions of moduli were exhibited

by the intermediate MW films. Elongations at 150°C ranged from 3 to 94% with higher elongations obtained from the higher cure temperatures. Mechanical properties of the BMDEDA/*p*-PDA and PMDA/1,3-BAPDBB polymers were very similar.

Polyimide	Cure, °C	Tensile Str., ksi		Modulus, ksi		Elongation, %	
		RT	150°C	RT	150°C	RT	150°C
High MW	200	13.1	5.29	444	222	5	17
High MW	240	10.4	4.91	356	206	11	94
High MW	300	11.4	4.13	342	222	7	94
Inter. MW	200	14.2	8.55	454	378	5	3
Inter. MW	240	11.9	6.33	369	326	48	62
PMDA/1,3-BAPDBB	-	10.4	5.3	394	238	3	2

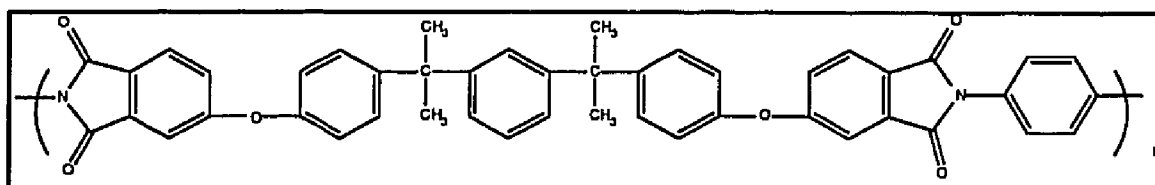
**Figure 6.5 Mechanical Properties Of BMDEDA/*p*-PDA And The Analogous Liquid Crystalline Polyimide (PMDA/1,3-BAPDBB)**

Another batch of BMDEDA/*p*-PDA polymer exhibited unusual melting characteristics. Additional cure studies were performed on this system to gain insight into the crystalline characteristics as well as study the effects of annealing. The BMDEDA/*p*-PDA PAA solution was cured to 250°C; the inherent viscosity, 5% weight loss temperature, and mechanical properties were very similar to the properties shown in Figures 6.3 and 6.5. However, the first heat using DSC showed a double melting point at 260°C and 292°C with a  $T_g$  at 185°C. These melting peaks were close in value to the melting peaks exhibited by the LC-PI. The second heat showed only a  $T_g$  at 186°C. The TMA analysis indicated that at 235 to 245°C, the material softened. It had no more

crystallinity above 245°C. Therefore, it was possible that the two transitions at 260 to 265°C and 285 to 290°C may not be crystalline melts. Evidence points to liquid crystallinity between 235 and 245°C and 285 and 290°C with two different LC forms. The transition between them could be the exotherm at 260 to 265°C. It may be that it takes a long time for the system to reorganize into a liquid crystalline phase after it has been heated to the isotropic phase above 285 to 290°C. After the first heat using DSC up to greater than 300°C, the isotropic phase was locked in upon quenching and the sample has not had sufficient time for the liquid crystal ordering to reform. Liquid crystalline characteristics were not supported by optical microscopy data. Up to 300°C, the sample did not exhibit any color or texture under crossed polars.

An annealing evaluation was conducted on this film sample. Annealing is a heat treating process designed to impart ductility, induce crystallinity, or relieve stresses, by allowing the polymer chains to re-arrange. Samples were annealed at 250°C (10°C below the first melting point), at 280°C (between melting points 1 and 2), and at 300°C (just above the second melting point). Figure 6.6 shows the annealing temperatures and times,  $T_g$ s by TMA, first and second heats using DSC, and x-ray diffraction results.



T<sub>g</sub> (T<sub>m</sub>) by DSC, °C

Anneal Temp., °C	Anneal Time, hr	T <sub>g</sub> by TMA, °C	TGA, 5% Wt. loss, °C	Run 1	Run 2	X-ray Diffr.
250	1	186	471	181 (266,292)	186	crystalline
250	16	188	438	184 (294)	188	crystalline
250	24	180	429	188 (293)	189	crystalline
280	1	181	441	188 (301)	187	crystalline
280	16	194	428	197 (303)	196	crystalline
280	24	201	430	210 (302)	207	semi-cryst.
300	1	180	464	190 (287,306)	189	amorphous
300	16	ND	431	234	232	ND
300	24	ND	429	263	270	ND

Figure 6.6 Annealing Evaluation Of BMDEDA/p-PDA

T<sub>g</sub>s by TMA and 5% weight loss temperatures were similar for the different annealing temperatures and times. Two crystalline peaks were exhibited on the first run after annealing for 1 hr at 250°C. After annealing for 16 hr at 250°C, only one crystalline form appeared on the DSC scan. Annealing at 280°C resulted in only one crystalline form on the DSC scan. However, when the temperature was increased to 300°C, two crystalline forms were seen on the DSC scan for the 1 hr hold. Both peaks disappeared after holding at 16 hr and 24 hr at 300°C. The second heat for all DSCs showed no crystalline melting points. Generally, the T<sub>g</sub> as evidenced by the second heat

of the DSC increased with the increasing anneal hold time and temperature due to chain extension and decreased molecular motion of the backbone.

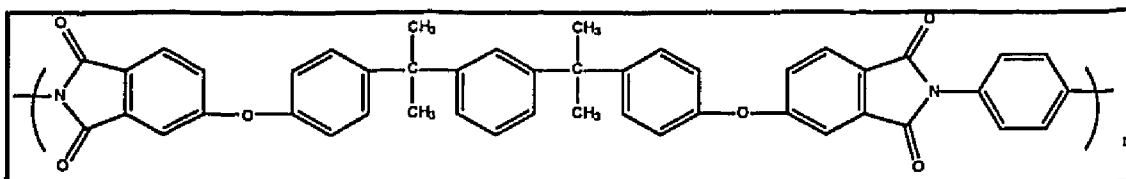
There was sufficient time (16 hr and 24 hr) and heat applied at 250°C for movement of the polymer chains so that only one crystalline form was exhibited on the first DSC scan. Likewise at 280°C, movement of the polymer chains was such that only one crystalline form was exhibited. At 300°C for 1 hr, two crystalline melting peaks were observed, yet the film was amorphous by x-ray diffraction. No melting peaks were observed for annealed films at 300°C for the 16 and 24 hr hold times. TMA and x-ray diffraction were not determined (ND) because the film pieces were too brittle for testing by these techniques.

### **Controlled MW Bisphenol M Derivative Polyimides**

Polyimides (PIs) were synthesized from BMDEDA combined with *p*-PDA and endcapped with phthalic anhydride (PA) using molar offsets of 2.0, 2.5, and 3.0% to give total PA amounts of 4.0, 5.0 and 6.0% as designated in Figure 6.7. Two solvents were used: DMAc and GBL. Inherent viscosities of the PAA solutions synthesized in GBL were not obtained due to the insolubility of the dianhydride at RT.  $T_g$ s ranged from 170 to 190°C with the lower  $T_g$ s resulting from the largest offsets (and lower MWs) as expected. Recoverable  $T_m$ s were exhibited by all the BMDEDA/*p*-PDA/PA polyimides. The PI containing 6% PA exhibited a recoverable  $T_{m1}$  and  $T_{m2}$ . Recoverable  $T_m$ s were not exhibited by the BMDEDA/*p*-PDA films previously described.

Melt press films were fabricated in a steel mold fitted to a hydraulic press at 340°C and 200 psi. Films were brittle so no mechanical properties were determined. However, pieces of films were adequate for thermal analysis and x-ray diffraction determination.

The temperature at which 5% weight loss occurred ranged from 393 to 406°C. Higher weight loss temperatures (432°C and 467°C) resulted from the melt-pressed films because higher temperatures and pressures can facilitate the removal of volatiles.



PI Powders	$\eta$ (inh), dL/g	$T_g$ , °C	$T_m$ , °C	5% Wt. Loss, °C
4% PA (GBL)	-	190	295	406
5% PA (GBL)	-	180	286	400
5% PA(DMAc)	0.65	178	291	403
6% PA (GBL)	-	170	276,356	-
6% PA (DMAc)	0.60	178	287	393
Melt-pressed Films				
5% PA (DMAc)	0.60	183	290	467
6% PA (GBL)	0.65	174	292	432

**Figure 6.7 Polymer Characterization Of BMDEDA/p-PDA Powders**

To provide for a direct comparison of the diamine and dianhydride containing the Bisphenol M unit, the diamine and corresponding PIs were prepared in-house by the method previously reported[13]. The PIs prepared from 1,3-BAPDBB and PMDA at stoichiometric offsets of 0, 2.5 and 5.0 mole% exhibited  $T_m$ s, which were recoverable (Figure 6.8)[15]. Two distinct  $T_m$ s were

observed for the uncontrolled molecular weight material. As the stoichiometric imbalance was increased, the  $T_m$ s coalesced to a single broad melt at 245°C. LC characteristics were observed for the PI film prepared from 1,3-BAPDBB and PMDA at no stoichiometric offset using optical microscopy after application of a shearing force to the material above its respective  $T_m$ [13].

Polyimide	PAA $\eta$ (inh), dL/g	$T_g$ , °C	$T_m$ , °C	5% Wt. Loss, °C
PMDA/1,3-BAPDBB	0.77	ND	269, 290	-
PMDA/1,3-BAPDBB/5% PA	0.50	235	268, 285	476
PMDA/1,3-BAPDBB/10% PA	0.39	236	245	464

ND=Not Detected

**Figure 6.8 Characterization Of 1,3-BAPDBB/PMDA Polyimide Films**

The elemental compositions are identical for the BMDEDA/*p*-PDA polymer and the Mitsui Toatsu Chemicals PMDA/1,3-BAPDBB (LC-PI) polymer. However, only one exhibited liquid crystalline characteristics by thermal analysis, optical microscopy, and melt viscosity measurements. Molecular modeling was used to investigate structural differences in the polymer backbone that may explain this phenomena.

#### Molecular Modeling of Bisphenol M Derivative Polyimides

The polymer backbones were drawn for each polyimide in order to calculate the aspect ratio. Next, bond lengths and angles were assigned based on the CHARM forcefield[17]. Typically, two or three bond lengths were available so the values were either averaged, or if two values were identical, that value was selected for the calculation. The fully extended chain length (L)

was calculated using the bond lengths and geometry. Next, the diameter was calculated by:

$$D=(MW/\rho N_A L)^{1/2}$$

where MW was the molecular weight of the repeat unit,  $\rho$  was the density of the polymer measured experimentally using the density gradient technique,  $N_A$  was Avogadro's number, and L was the fully extended chain length comprised of the segments of the backbone  $l_1, l_2$ , etc. The virtual bond lengths  $l_1, l_2$ , etc., are shown in the Appendix. The mean-end-to-end vector squared,  $r^2$ , to the Kuhn bond length  $L_K$ , was calculated using a computer program developed by Hinkley[18]. The Kuhn length,  $L_K$ , for the freely jointed chain was equal to  $r^2/L$ . The aspect ratio was then calculated by  $L_K/D$ .

Figure 6.9 compares the fully extended chain length (L), diameter (D),  $r^2/\text{bond}$ ,  $L_K$ , and aspect ratio ( $L_K/D$ ) for the BMDEDA/*p*-PDA and PMDA/1,3-BAPDBB polyimides.

	L, Å	D, Å	$r^2/\text{bond}$ , Å <sup>2</sup>	$L_K$ , Å	$L_K/D$
BMDEDA/ <i>p</i> -PDA	35	5	101	20.0	3.9
PMDA/1,3-BAPDBB	35	5	154	21.8	4.2

**Figure 6.9 Molecular Modeling Data For Bisphenol M Derivative Polyimides**

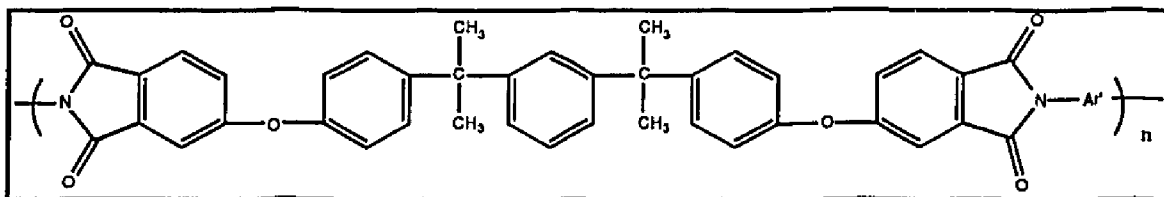
The fully extended chain lengths and diameters are very similar for both polymers. However, there are five virtual bond lengths for the LC-PI while the BMDEDA/*p*-PDA polymer is comprised of seven for approximately the same fully extended chain length. This indicates there are two additional hinge points in the BMDEDA/*p*-PDA polymer per repeat unit. It is not as rigid as the

LC-PI. There is a significant difference in the mean end-to-end chain vector to bond length (>33%). The  $r^2/\text{bond}$  value for the LC-PI is higher as might be expected for oriented molecules. The length  $L_K$  is not significantly different (22 Å compared to 20 Å). The aspect ratios only differ by less than 9%. According to Takahashi *et. al.*[19], the critical mean axial ratio  $L_K/D$  of the Kuhn length for the freely jointed chain equals 6.4, beyond which the ordered state is predicted to be stable at all temperatures. Alternatively, in terms of the wormlike chain model with limiting curvature (WCLC)[20], the ratio of  $r^2/L$  at an infinite temperature corresponds to the cutoff wavelength  $L_c$ , representative of the maximum allowed curvature at all temperatures. The critical axial ratio of the cutoff wavelength required for the absolute stability of an ordered state in the bulk is predicted to be approximately 4.45 in the limits of high molecular weights. The Mitsui Toatsu LC-PI does not exhibit a  $L_K/D$  ratio greater than 6.4. This suggests that the theory of Takahashi *et. al.* needs additional evaluation in its prediction of  $L_c/D$  or  $L_K/D$  values beyond which ordered states are predicted.

#### **Other Bisphenol M Derivative Alternating Flexible/Rigid Backboned Polyimides**

Other rigid diamines such as 1,5-DAN and ABL-21 were combined with BMDEDA to afford alternating flexible/rigid polymer backbones. Benzidine is a rigid diamine but is extremely toxic. Use of benzidine requires special permits. Therefore, a fluorinated benzidine, ABL-21, was used. It is less toxic, and was provided gratis by Central Glass, Japan, for this evaluation. Although the combination of the Bisphenol M dianhydride and Bisphenol M diamine did not afford an alternating rigid/flexible backbone, the polymer was synthesized and characterized for the structure-property database.

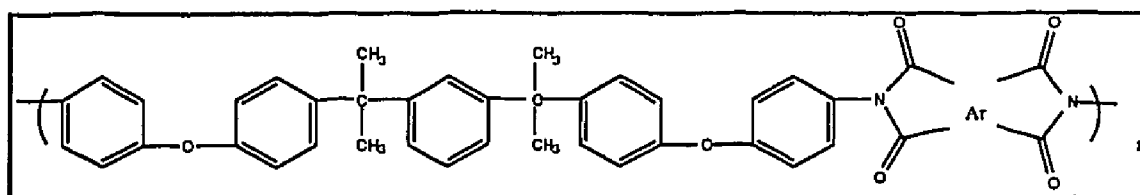
Poly (amic acid)s were prepared by the reaction of stoichiometric quantities of BMDEDA and aromatic diamines in DMAc under a nitrogen atmosphere at 23°C (Figure 6.10). The  $\eta_{inh}$  of the PAAs ranged from 0.38 to 0.53 dL/g. Unoriented thin films were cast from the PAA solutions and thermally imidized during a stage cure to 240°C in flowing air. The  $T_g$ s of the films ranged from 150 to 222°C. The polyimide film which contained the 1,3-BAPDBB group, exhibited a crystalline melt upon the initial DSC scan. Upon cooling to room temperature and rescanning the same sample, the  $T_m$  was not recovered.



Ar' (Diamine)	PAA $\eta$ (inh), dL/g	$T_g$ , °C	$T_m$ , °C	TGA, 5% wt loss, °C
1,5-DAN	0.38	222	none	441
ABL-21	0.53	188	none	438
1,3-BAPDBB	0.41	150	355	463

**Figure 6.10 Other Bisphenol M Diether Dianhydride Films**

For comparison, the diamine containing the Bisphenol M unit (1,3-BAPDBB) was combined with another rigid dianhydride, BPDA. The  $\eta_{inh}$  of the PAAs ranged from 0.53 to 0.76 dL/g (Figure 6.11). Thin films were cast from DMAc solutions of the PAAs and thermally imidized during a stage cure to 250°C in flowing air to afford the unoriented polyimide films.



Ar (Dianhydride)	PAA $\eta_{inh}$ , dL/g	$T_g$ , °C	$T_m$ , °C	TGA, 5% Wt Loss, °C
BPDA	0.76	183	none	-
0.975 BPDA/0.05 PA	0.53	179	none	479

**Figure 6.11 Bisphenol M Diamine Polyimide Films**

Combining the Bisphenol M diamine with a rigid dianhydride like BPDA did not afford a liquid crystalline polyimide, as characterized by a double melting point. No  $T_m$ s were observed.

The tensile properties of other Bisphenol M derivative polyimide films are shown in Figure 6.12. The ranges of tensile strength, modulus, and elongation at break of the Bisphenol M diether dianhydride films were from 12 to 15 ksi, 365 to 454 ksi, and 4 to 100% at 23°C, respectively, with good retention of properties at 150°C. The retention of tensile properties at 150°C for the PI film which contained 2,2'-bis(trifluoromethyl) benzidine (ABL-21) units was notable since the  $T_g$  of the polymer was 188°C.



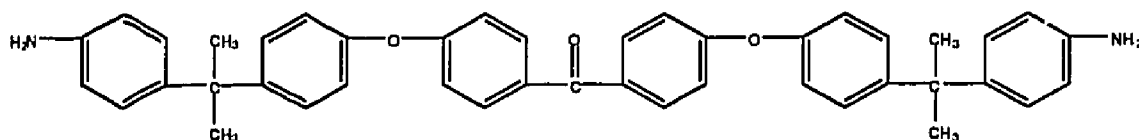
PI Film Designation	RT	150°C	RT	150°C	RT	150°C
BMDEDA/1,5-DAN	15.2	11.0	424	369	4	4
BMDEDA/ABL-21	13.1	6.43	389	330	100	>100
BMDEDA/1,3-BAPDBB	12.1	6.5 <sup>1</sup>	3.65	320 <sup>1</sup>	6	3 <sup>1</sup>

<sup>1</sup>Film tested at 121°C.

<sup>2</sup>Polyimide film source: Mitsui Toatsu Chemicals, Inc.

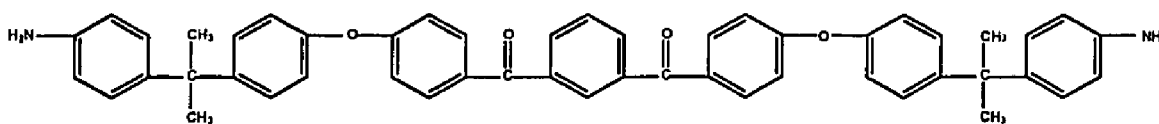
**Figure 6.12 Mechanical Properties Of Other Bisphenol M Dianhydride Polyimides**

Also included in the development of liquid crystalline polyimides was the synthesis of novel extended diamines[16] that contained six or seven aromatic rings with ether, carbonyl, and isopropylidene linkages as shown below.



When combined with BMDEDA, a good film formed. The inherent viscosity was 0.52 dL/g; the  $T_g$  was 171°C and the  $T_m$  was 342°C. The  $T_m$  was recoverable upon reheating. The CTE was 57 ppm/°C. Tensile strength, modulus, and elongation at RT were 13 ksi, 354 ksi, and 5.5%, respectively.

Another diamine synthesized for this project in collaboration with Smith and St. Clair[16] contained seven aromatic rings with different carbonyl, ether, and isopropylidene linkages as shown.



When combined with BMDEDA, the solution gelled and did not dissolve with subsequent dilution. The solution was poured onto plate glass and the solvent was allowed to evaporate for four days in a humidity controlled dry box. The film was cured at 100, 175, and 250°C for one hour each. No tensile properties were obtained due to the brittleness of the film. The first heat on the DSC scan indicated a melting point at 164°C and a  $T_g$  at 218°C. The second heat on the DSC scan showed only a  $T_g$  at 163°C.

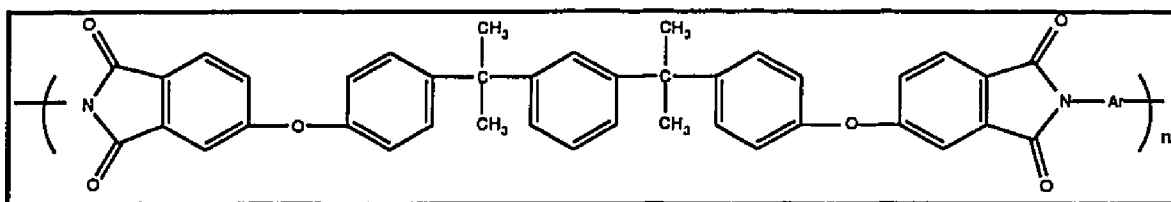
Thus far, uncontrolled and controlled molecular weight polyimides have been synthesized and characterized from BMDEDA and *p*-PDA. These polymers have been compared to the analogous LC-PI. Other polymers using the Bisphenol M derivative dianhydride and diamine with other rigid diamines or dianhydrides have been examined.

### Copolymers Of Bisphenol M Derivatives

The next stage in the research of potential liquid crystalline polyimides was the evaluation of copolymers using either the Bisphenol M diether dianhydride (BMDEDA) or the Bisphenol M diamine (1,3-BAPDBB)[21]. Incorporation of other segments in the polymer backbone could be achieved with copolymers, especially the isopropylidene group which appears to contribute liquid crystallinity to the LC-PI evaluated in the previous sections. Additionally, random copolymers disrupt the crystallinity.

Random copolymers containing BMDEDA were synthesized with a combination of *p*-PDA, and either Bisaniline M (BAM), Bisaniline P (BAP), or 1,5-DAN, in ratios of 25:75, 50:50, and 75:25. BAM and BAP were utilized to evaluate the potential unique characteristics of the aromatic isopropylidene groups in the polymer backbone. Random copolymers containing 1,3-BAPDBB were synthesized with a combination of PMDA and either BTDA or BPDA.

Figures 6.13-6.15 show the characterization of the random copolymers. Inherent viscosities ranged from 0.20 to 0.77 dL/g.  $T_g$ s by DSC ranged from 168 to 212°C with lower  $T_g$ s resulting from the *meta*-catenated Bisaniline M copolymers and the higher  $T_g$ s resulting from the more rigid 1,5-DAN copolymers. There were no significant differences in 5% weight loss temperatures (406 to 432°C). The CTEs were above average for polyimides, ranging from 61 to 85 ppm/°C. All films were amorphous by x-ray diffraction. Densities were low, ranging from 1.18 to 1.23 g/cm<sup>3</sup>. Kapton® HN film has a density of approximately 1.4 g/cm<sup>3</sup>.



Ar


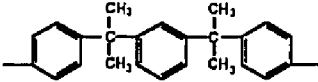
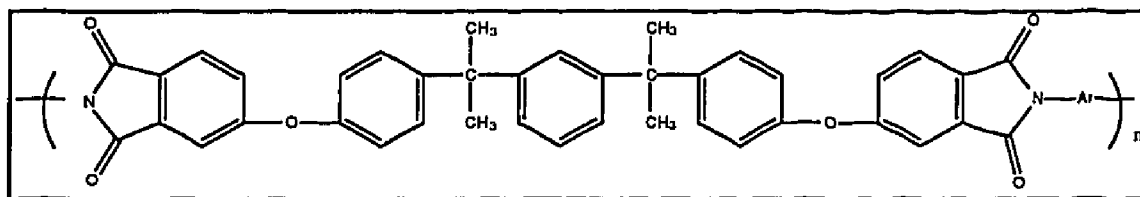
		$\eta$ (inh) (PAA), dL/g	$T_g$ by DSC, °C	$T_g$ by TMA, °C	5% Wt. Loss, °C
0.25	0.75	0.77	168	158	406
0.50	0.50	0.52	172	167	415
0.75	0.25	0.66	177	175	432
		CTE, ppm/°C	x-ray diffraction	density, g/cm <sup>3</sup>	
0.25	0.75	71	amorphous	1.18	
0.50	0.50	77	amorphous	1.19	
0.75	0.25	85	amorphous	1.21	

Figure 6.13 Characterization Of Random Copolymers Containing BMDEDA




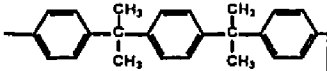
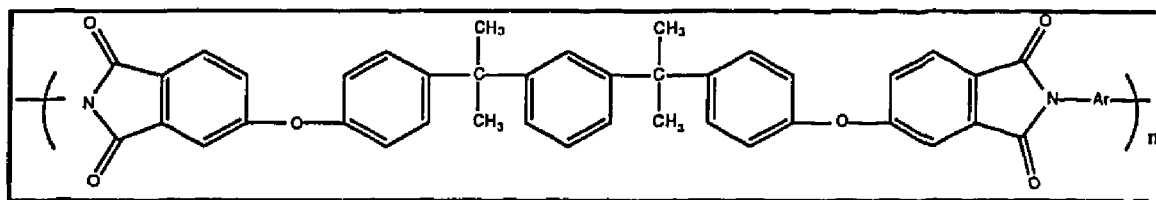

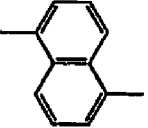
		$\eta$ (inh) (PAA), dL/g	$T_g$ by DSC, °C	$T_g$ by TMA, °C	5% Wt. Loss, °C
0.25	0.75	0.75	175	176	425
0.50	0.50	0.53	186	176	429
0.75	0.25	0.20	185	173	413
		CTE, ppm/°C	x-ray diffraction	density, g/cm <sup>3</sup>	
0.25	0.75	63	amorphous	1.18	
0.50	0.50	64	amorphous	1.20	
0.75	0.25	66	amorphous	1.19	

Figure 6.14 Characterization Of Random Copolymers Containing BMDEDA

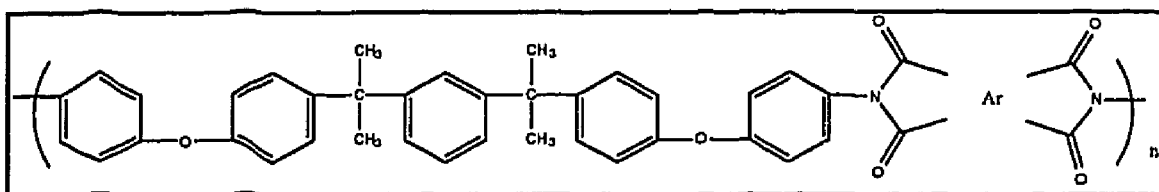


Ar

		$\eta$ (inh) (PAA), dL/g	$T_g$ by DSC, °C	$T_g$ by TMA, °C	5% Wt. Loss, °C
0.25	0.75	0.26	212	204	414
0.50	0.50	0.32	209	201	410
0.75	0.25	0.45	193	191	420
		CTE, ppm/°C	x-ray diffraction	density, g/cm <sup>3</sup>	
0.25	0.75	61	amorphous	1.22	
0.50	0.50	67	amorphous	1.22	
0.75	0.25	69	amorphous	1.23	

**Figure 6.15 Characterization Of Random Copolymers Containing BMDEDA**

Figure 6.16 shows the polymer characterization of random copolymers using the Bisphenol M diamine with dianhydride ratios of 25:75, 50:50, and 75:25 with PMDA, and either BTDA or BPDA.



Ar

				$\eta_{inh}$ (PAA), dL/g <sup>2</sup>	$T_g$ , °C <sup>3</sup>	$T_m$ , °C <sup>3</sup>	5% Wt. Loss, °C, air (N <sub>2</sub> ) <sup>4</sup>
1.0	-	-	-	0.25	-	(276, 295,301)	-
0.75	0.25	-	-	0.25	203	256	470 (477)
0.50	0.50	-	-	0.27	185	215	463 (473)
0.25	0.75	-	-	0.23	186	216	404 (473)
0.75	-	0.25	-	0.25	189	259	474 (481)
0.50	-	0.50	-	0.23	181	223	470 (470)
0.25	-	0.75	-	0.17	-	-	-

<sup>1</sup>3 mole % stoichiometric imbalance, phthalic anhydride endcapped.

<sup>2</sup>Determined on 0.5% (w/v) GBL solution at 25°C.

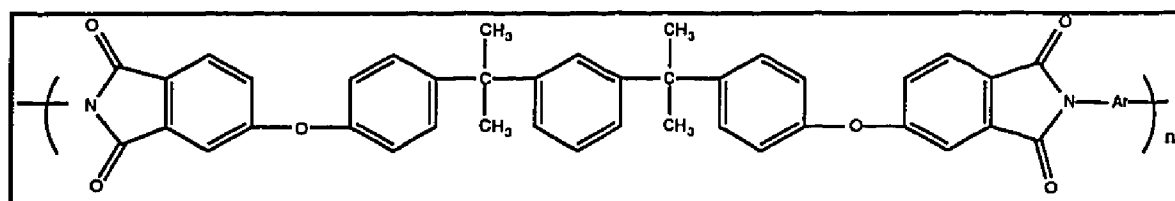
<sup>3</sup>Determined on as-isolated powders by DSC at 10°C/min.

<sup>4</sup>Determined on as-isolated powders by TGA at 2.5°C/min.


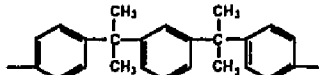
**Figure 6.16 Characterization Of Bisphenol M Diamine Copolymers<sup>1</sup>**

Inherent viscosities were low, ranging from 0.17 to 0.25 dL/g; however, the stoichiometric imbalance was 3%.  $T_g$ s ranged from 181 to 203°C. Only one  $T_m$  was observed for the copolymers. TGA indicated 5% weight loss temperatures between 404 and 474°C. Copolymers utilizing PMDA with BTDA or BPDA did not afford multiple melting peaks as was observed with the PMDA/1,3-BAPDBB homopolymer.

Film properties of the random copolymers utilizing BMDEDA at RT and 121°C are shown in Figures 6.17-6.19.

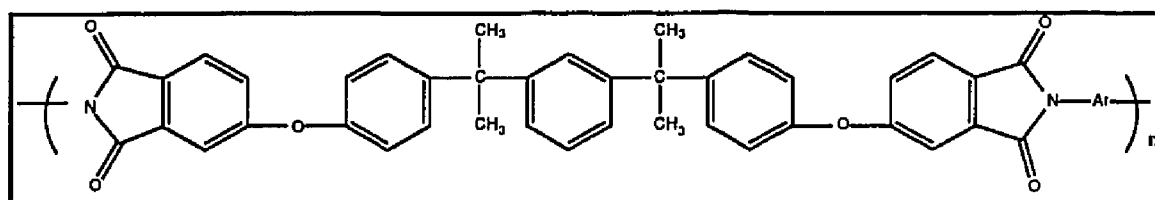


Ar

		<b>Tensile Str., ksi RT (121°C)</b>	<b>Modulus, ksi RT (121°C)</b>	<b>Elong., % RT (121°C)</b>
0.25	0.75	11.6 (4.25)	371.7 (250.5)	4.3 (22.4)
0.50	0.50	12.7 (5.71)	383.0 (262.6)	5.8 (27.7)
0.75	0.25	12.2 (5.34)	377.7 (254.7)	7.8 (87.2)

**Figure 6.17 Tensile Properties Of BMDEDA Copolymers**





Ar

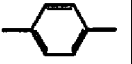
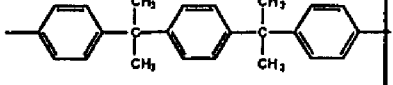
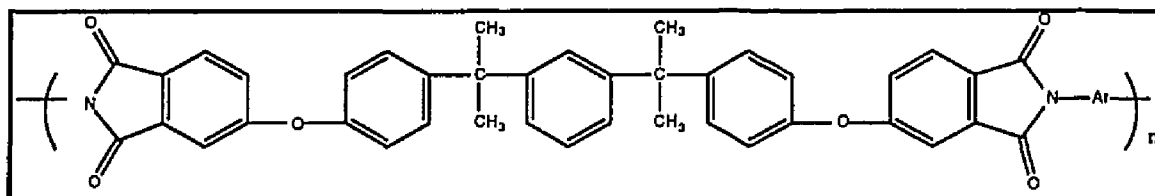
		Tensile Str., ksi RT (121°C)	Modulus, ksi RT (121°C)	Elong., % RT (121°C)
0.25	0.75	Brittle	Brittle	Brittle
0.50	0.50	11.4 (6.07)	345.9 (274.8)	8.1 (13.7)
0.75	0.25	12.0 (6.40)	362.1 (295.7)	9.9 (29.7)

Figure 6.18 Tensile Properties Of BMDEDA Copolymers



Ar


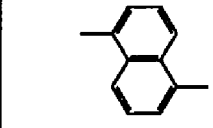
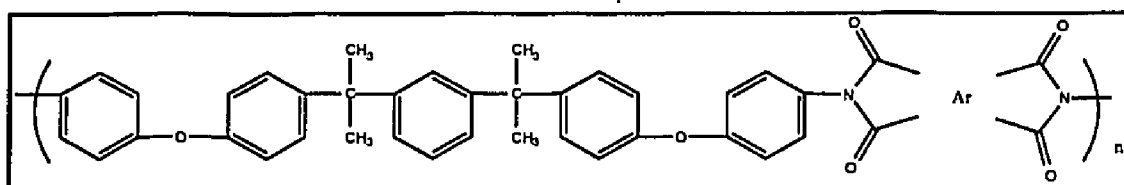
		Tensile Str., ksi RT (121°C)	Modulus, ksi RT (121°C)	Elong., % RT (121°C)
0.25	0.75	14.5 (10.7)	402.0 (334.8)	4.7 (4.4)
0.50	0.50	14.7 (9.95)	406.0 (324.5)	5.4 (5.4)
0.75	0.25	13.2 (7.59)	394.6 (264.4)	5.9 (5.8)

Figure 6.19 Tensile Properties Of BMDEDA Copolymers

Tensile strengths were similar to the homopolymer, BMDEDA/*p*-PDA, with values between 11.4 and 14.7 ksi at RT. Moduli ranged from 345.9 to 406.0 ksi at RT. Elongations at RT ranged from 4.3 to 9.9%. Ranges of properties at 121°C were 4.25 to 10.7 ksi, 250.5 to 334.8 ksi, and 4.4 to 87.2% for tensile strengths, moduli, and elongations at break, respectively.

A general trend observed was that higher retentions of tensile strengths and moduli were exhibited by the polyimides containing 1,5-DAN, a more rigid diamine than either BAM or BAP. No crystallinity as evidenced by x-ray diffraction was observed in any BMDEDA copolymers.

Mechanical properties of the Bisphenol M diamine copolymers at RT and 121°C are shown in Figure 6.20. Only three copolymers formed good films. Tensile strengths ranged from 10.7 to 12.3 ksi at RT and from 5.8 to 6.4 ksi at 121°C. Moduli ranged from 380 to 389 ksi at RT and 216 to 280 ksi at 121°C. Elongations ranged from 4 to 13% at RT and 7 to 76% at 121°C.

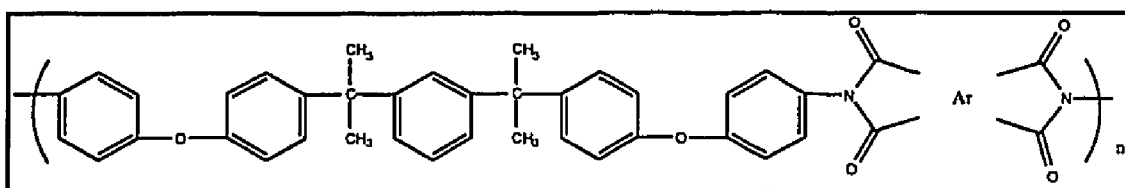


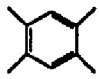
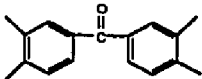
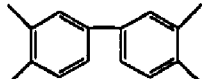
			Tensile Str., ksi RT (121°C)	Modulus, ksi RT (121°C)	Elong., % RT (121°)
			11.3 (5.8)	380 (216)	5 (33)
0.50	0.50	-	12.3 (6.4)	382 (280)	13 (76)
0.25	0.75	-	10.7 (6.2)	389 (268)	4 (7)

Figure 6.20 Thin Film Properties Of Bisphenol M Diamine Copolymers

Optical microscopy of the copolyimides containing BMDEDA did not show any colors or textures indicating liquid crystallinity. The copolymers utilizing the Bisphenol M diamine did show color and textures. Figure 6.21 shows the crystalline and isotropic melt temperatures for these copolymers. Photomicrographs of the Mitsui Toatsu Chemicals LC-PI and the copolymers designated in Figure 6.21 are exhibited in the Appendix.

Threaded or schlieren textures are indicative of nematic phases[22-23]. Cholesteric liquid crystals are usually exhibited by planar textures with oily streaks, moiré fringes, and/or Grandjean lines. These planar structures can show bright reflection colors. In the case of smectic polymers, observations of specific textures may be difficult. High viscosities of smectic melts often inhibit the observation of obscure textures. Smectic phases have been observed resembling focal conic or fan-shaped textures[24].



Ar			$T_{init}, ^\circ\text{C}$	$T_{isotropic}, ^\circ\text{C}$
				
0.75	0.25	-	236	282
0.50	0.50	-	249	281
0.25	0.75	-	252	270
0.75	-	0.25	236	247
0.50	-	0.50	234	246
0.25	-	0.75	269	283

**Figure 6.21 Preliminary Screening Of Liquid Crystalline Polyimides By Hot Stage Polarizing Microscopy**

Figure 6.21 shows the preliminary screening of potential liquid crystalline copolyimides by hot stage polarizing microscopy. The initial melting temperature,  $T_{init}$ , was the temperature at which the polymer first began to flow. After this temperature but prior to  $T_{isotropic}$ , color and texture were persistent.  $T_{isotropic}$  was the temperature at which there was a clear liquid and no more color or texture was present. The initial melting temperatures ranged from 234 to 269°C; the isotropic melting temperatures ranged from 246 to 283°C. Only one  $T_m$  was observed for each of these copolymers by DSC. However, evidence of liquid crystallinity was exhibited by the colors and textures observed by hot stage polarizing microscopy. As a result of these data, two polyimides were synthesized and sent to Zymet, Inc. for evaluation as a repairable adhesive. More discussion of this application follows in Chapter 7: Application.

### **Extruded Polymer Blends Containing The LC-PI**

The LC-PI powder obtained from Mitsui Toatsu was blended with a controlled MW high performance polymer, LaRC™-IA (3% offset), to determine the effects of the addition of the LC-PI on the melt viscosity, thermal properties, and mechanical properties. Weight loadings of 5-25% LC-PI were added to the LaRC™-IA (3% offset). The blends (27g) were extruded into one inch wide ribbons using a Brabender PL-2000 Plastic-Corder equipped with a 1.25 in slit die. The extrusion temperature was 330°C and the rate at which the material was pushed through the extruder was 20 revolutions per minute (rpm). The final thickness of the ribbon was approximately 10 mils (0.010 in).

Figures 6.22 and 6.23 illustrate the thermal and mechanical properties of the polyimide blend properties of the extruded ribbons.

Polymer Designation	T <sub>g</sub> , °C	T <sub>m1</sub> , T <sub>m2</sub> , °C	CTE <sup>3</sup> , ppm/°C
LaRC™-IA <sup>1</sup>	231	-	69
LaRC™-IA/5% LC-PI	231	278,295	37
LaRC™-IA/10% LC-PI	231	279,297	65
LaRC™-IA/15% LC-PI	228	277,297	61
LaRC™-IA/20% LC-PI	230	278,297	59
LaRC™-IA/25% LC-PI	233	279,298	44
LC-PI <sup>2</sup>	229	276,294	23

<sup>1</sup>LaRC™-IA was synthesized from ODA/3,4'-ODA with a molar offset of 3% and endcapped with phthalic anhydride.

<sup>2</sup>LC-PI was synthesized from PMDA/1,3-BAPDBB and was supplied by Mitsui Toatsu, Japan.

<sup>3</sup>Expansion temperature range was 100-120°C.

**Figure 6.22 Polyimide Blend Properties Of Extruded Ribbons**

The T<sub>g</sub>s were similar for both homopolymers, and therefore the T<sub>g</sub>s for the blends were essentially the same. Two melting points were exhibited by all blends and the LC-PI. The T<sub>m</sub>s for the blends were indicative of the LC-PI and were approximately the same value.

The temperature range for the CTE measurement was 100 to 120°C. CTEs were measured in the machine direction. CTEs did not follow the expected trend for the series. The CTE of the LC-PI was low (23 ppm/°C) and it was expected that as the weight loadings were increased, the CTE of the blends would decrease. However, the blend containing only 5% by weight LC-PI exhibited the lowest CTE of all the blends measured. The measurement was performed again and the same result was obtained. The blends using 10,

15, and 20% LC-PI had moderate CTEs (59-65 ppm/°C). The blend with 25% LC-PI had a CTE of 45 ppm/°C.

The temperatures at which 5% weight loss occurred were high and ranged between 480 and 505°C.  $T_g$ s by TMA ranged between 220 and 226°C for the LaRC™-IA and blends. No TMA was obtained for the LC-PI because the extruded ribbon was too brittle.

Figure 6.23 shows the apparent melt viscosities, and the mechanical properties at RT and 177°C for the polyimide blends.

Polymer Designation	Apparent Melt Viscosity, Poise	Tensile Str., ksi RT (177°C)	Modulus, ksi RT (177°C)	Elong., % RT (177°C)
LaRC™-IA <sup>1</sup>	54,700	14.5 (6.6)	356 (203)	44 (98)
LaRC™-IA/5% LC-PI	59,200	12.3 (5.1)	308 (198)	32 (89)
LaRC™-IA/10% LC-PI	36,000	14.3 (6.1)	350 (221)	48 (93)
LaRC™-IA/15% LC-PI	40,000	11.4 (5.5)	343 (189)	14 (70)
LaRC™-IA/20% LC-PI	30,400	12.0 (4.5)	334 (181)	5 (25)
LaRC™-IA/25% LC-PI	24,500	7.6 (ND)	287 (ND)	3 (ND)
LC-PI <sup>2</sup>	15,000	Brittle	Brittle	Brittle

<sup>1</sup>LaRC™-IA was synthesized from ODP/3,4'-ODA with a molar offset of 3% and endcapped with phthalic anhydride.

<sup>2</sup>LC-PI was synthesized from PMDA/1,3-BAPDBB and was supplied by Mitsui Toatsu, Japan.

**Figure 6.23 Polyimide Blend Properties Of Extruded Ribbons**

Generally, the apparent melt viscosity decreased with increasing amounts of LC-PI as expected because the LC-PI lubricated the melt. The tensile strength decreased 38% from the 5% blend to the 25% blend while the modulus decreased only 6% with increased weight loadings. Elongation

decreased with increasing amounts of the LC-PI blend because of the loss of flexibility with more crystallites present. All ribbons were crystalline by x-ray diffraction and are shown in the Appendix. These x-ray diffraction patterns do not exhibit any peaks pertaining specifically to liquid crystalline versus crystalline phenomena. The optimum weight loading was 10% of LC-PI. Mechanical properties were retained while the melt viscosity was reduced 34%.

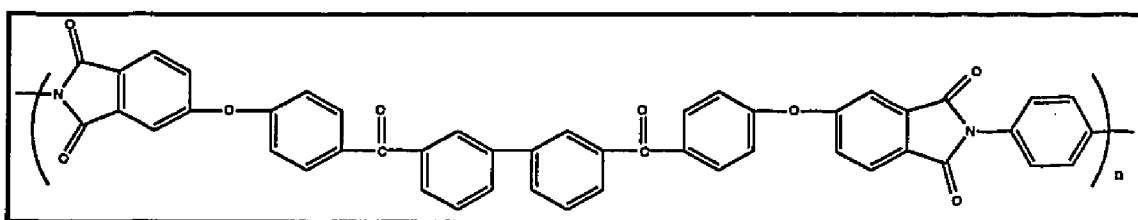
### **Polyimides From Novel Diether Dianhydrides**

The next dianhydride synthesized contained the Bisphenol P derivative (BPDEDA), the difference from Bisphenol M being the *meta* versus *para* catention of the isopropylidene groups. Although elemental analysis of the dianhydride indicated high purity, only low MW polymers were obtained. The PAA solution of the BPDEDA/*p*-PDA had an inherent viscosity of 0.12 dL/g. The solution was thermally imidized on glass by heating at 100, 200, and 240°C for one hour each. The  $T_g$  and  $T_m$  were 198°C and 273°C respectively. The  $T_m$  was not recoverable upon reheating the same sample. Additional batches of BPDEDA were synthesized but good films were not obtained. Further attempts were made to purify the BPDEDA, but were not successful.

The next dianhydride synthesized contained the Bisphenol P derivative but had pendant methyl groups *ortho* to the oxygen linkages in the diether dianhydride. The elemental analysis indicated that the carbon and hydrogen contents differed by approximately 18 and 6% from the theoretical values, respectively, indicating impurity of the dianhydride or that another compound was obtained such as the free acid. The dianhydride was synthesized two more times without successfully making a material useful for polymer synthesis.

The elemental analysis of 1,4-bis(3,4-dicarboxyphenoxy) naphthalene dianhydride indicated the reaction was successful. However, reaction of this dianhydride with *p*-PDA resulted in a very low viscosity solution. Attempts were made to thermally solution imidize the PAA solution to the imide powder but were not successful.

The next dianhydride synthesized contained the *meta* biphenyl linkage. Polymer characterization is shown in Figure 6.24.



$\eta$ (inh) PAA, dL/g	Cure Temp., °C	$T_g$ ( $T_m$ ), °C run 1	$T_g$ ( $T_m$ ), °C run 2	$T_g$ by TMA, °C	X-ray Diffr.	CTE, ppm/°C	TGA, 5% Wt. Loss, °C
0.57	250	217(269)	222(329)	219	cryst.	48	453
ND	200	(236)	219(326)	190	cryst.	48	444
ND	250	220(268)	231(335)	215	cryst.	52	450
		Tensile Str., ksi	Modulus ksi	% Elong.			
0.57	250	Brittle	Brittle	Brittle			
ND	200	17.2	456	8.1			
ND	250	17.7	448	8.8			

ND=Not Determined

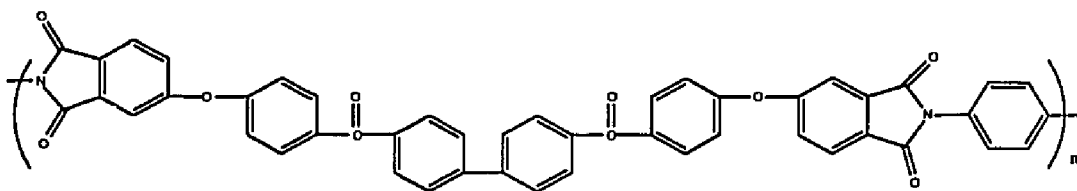
**Figure 6.24 Characterization Of *m*-Benzoyl Biphenyl Derivative Polyimides**



The polymer films were synthesized using two different batches of dianhydride. The first polymer synthesized had an inherent viscosity of 0.57 dL/g. The film was cured at 100, 175, and 250°C for one hour each. The film was opaque and the plate glass cracked in the oven. Mechanical properties could not be obtained. The polymer was synthesized again with another batch of dianhydride. The PAA solution gelled; addition of solvent did not dissolve the gel. The viscosity was not determined. The polymer solution was poured onto plate glass and the solvent was allowed to evaporate for four days in the dry box. Two films were fabricated using cures of 100, 150, and 200°C and 100, 200, and 250°C for one hour at each temperature. Both films were good quality despite the gelled solution from which they were cast.

All three polymer films had similar  $T_g$ s (219 to 231°C) and  $T_m$ s (326 to 335°C). All  $T_m$ s were recoverable upon reheating the sample. The polymer films were crystalline with low to moderate CTEs of 48 to 52 ppm/°C. TGAs ranged between 444 and 453°C. Film properties were obtained from the gelled PAA solution cured at different temperatures. Tensile strength, modulus, and elongation were approximately 17 ksi, 452 ksi, and 8%, respectively.

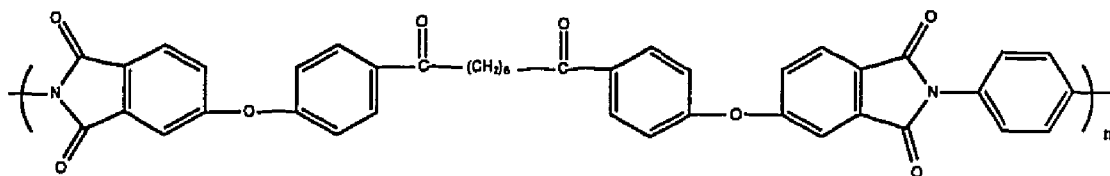
The next dianhydride synthesized contained the *para* biphenyl linkage. This dianhydride was combined with *p*-PDA and the structure is shown below.



The film was cured at 100, 200, and 250°C. The film was opaque and shattered on the plate glass. TMA and mechanical properties could not be performed due to the brittleness of the film. No  $T_g$  was detected up to 350°C for

two runs using DSC. A third DSC run showed a melting point at 365°C and what appeared to be the shoulder of another melting point. A fourth DSC run to 450°C showed a melting point at 420°C. The temperature at which 5% weight loss occurred was 479°C. It is likely that the film was crystalline since it was opaque, but no x-ray diffraction analysis was performed due to the small pieces of film obtained.

The next dianhydride synthesized contained the hexane group. This dianhydride was combined with *p*-PDA to afford the repeat unit shown below.



The polymer had an inherent viscosity of 0.19 dL/g, which indicated the dianhydride was not very pure. The film was cured at 100, 200, and 240°C for one hour at each temperature. The dark film was brittle and no mechanical tests were performed on this film sample. The  $T_g$  by DSC was 198°C. A  $T_m$  was exhibited on the first run at 263°C but was not recovered on the second run. A 5% weight loss occurred at 362°C. CTE, TMA, and mechanical properties were not obtained due to the brittleness of the film. An attempt, which turned out to be unsuccessful, was made to recrystallize the dianhydride to improve the monomer purity and afford a higher molecular weight film.

## 6.2 Polyimides For Microelectronic Applications

### 6.2.1. Low Dielectric, Fluorinated Polyimides

High performance polymer film and coating materials are increasingly being used by the electronic circuit industry. As cited by Senturia[25], polyimides are widely used for four primary applications in the area of microelectronics: (1) as fabrication aids such as photoresists, planarization layers, and in implants, (2) as passivant overcoats and interlayer dielectrics, (3) as adhesives, and (4) as substrate components. Electrical behavior is critical for polymers used in these applications. Dielectric constants of state-of-the-art materials generally range from 3.2 to 4.0. Materials are needed with substantially lower dielectric constants. Reductions in dielectric constant have been achieved by incorporating fluorine into the polymer backbone[26-29]; incorporation of *meta* linkages and bulky groups lower the free volume and therefore potentially lower the dielectric constant.

The polymers synthesized, characterized, and evaluated for potential microelectronic applications in the following sections are ether-containing polyimides.

Syntheses of three fluorinated diether dianhydrides were attempted: 2,2-bis[4-(3,4-dicarboxyphenoxy)phenyl] hexafluoropropane (BFDA), octafluorobiphenyl dianhydride (8FDA), and 3,3'-bis(dicarboxyphenoxy hexafluoroisopropyl) benzene (12FDA). BFDA contained one hexafluoropropylidene group (6F) resulting in 18% fluorine content. BFDA was synthesized previously[30] by reacting stoichiometric amounts of Bisphenol AF with sodium hydroxide to produce the disodium salt. This reaction produces an intermediate compound which is sufficiently active to enter a nucleophilic

displacement reaction with the chloro-substituent on 4-chloro-N-phenyl phthalimide to produce [3,4-(phenylphthalimide-phenoxy)phenyl] hexafluoropropane. Hydrolysis and subsequent dehydration of the compound to the corresponding dianhydride is accomplished by reacting the compound with aqueous sodium hydroxide followed by acidification and dehydration. The synthesis is time consuming and requires purification of the intermediates. The BFDA for the polymer synthesis described herein was synthesized successfully by the one-step method developed by Schwartz[10-11].

The incorporation of fluorine lowers the dielectric constant but can also increase the solubility in organic solvents. Copolymers were synthesized with the addition of BPDA to achieve insolubility and therefore make the resultant polyimides suitable as aircraft matrix resins[31]. Copolymers were prepared combining BPDA with BFDA and the fluorinated diamine 3,5-diaminobenzotrifluoride (DABTF) in an effort to impart insolubility to these polyimides while retaining their low dielectric constants. The solubilities are shown in Figure 6.25. The control BFDA/DABTF and 75:25 BFDA:BPDA/DABTF copolymer were soluble in all the solvents while the 60:40 BFDA:BPDA/DABTF copolymer was partially soluble in DMAc and chloroform and insoluble in diglyme and DMF. All copolymers with 55% or less BFDA were insoluble in all solvents.

BFDA:BPDA	Film Solubility in			
	DMAc	Chloroform	Diglyme	DMF
BFDA Control	S	S	S	S
75:25	S	PS	S	S
60:40	PS	PS	I	I
55:45	I	I	I	I
50:50	I	I	I	I
75:25	I	I	I	I
BPDA Control	I	I	I	I

S=Soluble; PS=Partially Soluble; I=Insoluble

**Figure 6.25 Solubilities Of BFDA:BPDA + DABTF Copolymers**

Figure 6.26 shows the inherent viscosities,  $T_g$ s by TMA, 10% weight loss temperatures, and densities of the BFDA:BPDA + DABTF series. Several trends were noted. As the amount of BPDA increased, the apparent  $T_g$  and the thermo-oxidative stability increased. This was expected due to the increasing amounts of the rigid biphenyl unit in the polymer backbone. Film densities were determined on the polyimide controls and the copolymers that contained the minimum concentration of the BPDA required to obtain insolubility. The densities of the BFDA and BPDA controls were essentially the same, and no change in density was seen in making the copolymers.

<b>BFDA:BPDA</b>	<b><math>\eta</math>(inh) dL/g</b>	<b>T<sub>g</sub> by TMA °C</b>	<b>TGA (10% wt loss), °C</b>	<b>Density (g/cc)</b>
BFDA Control	0.55	232	506	1.46
75:25	0.50	246	508	-
60:40	0.80	257	508	-
55:45	0.96	263	511	1.46
50:50	0.73	268	511	-
25:75	0.74	288	519	-
BPDA control	0.71	325	527	1.45

**Figure 6.26 Characterization Of BFDA:BPDA + DABTF Copolymers**

Mechanical properties are shown in Figure 6.27. Tensile strengths at RT ranged from 14.5 to 20.2 ksi and 6.8 to 11.6 ksi at 200°C. Higher retentions of strength at 200°C were exhibited by the BPDA control (57%) than the 55:45 BFDA:BPDA (52%) and the BFDA Control (47%). Moduli at RT ranged from 391.5 to 507.5 ksi at RT and from 290.0 to 391.5 ksi at 200°C. Retentions of moduli at 200°C ranged from 69 to 77%.

<b>Polymer</b>	<b>Tensile Str., ksi</b>		<b>Tensile Mod., ksi</b>	
	<b>RT</b>	<b>200°C</b>	<b>RT</b>	<b>200°C</b>
	BPDA/DABTF	20.2	11.6	507.5
55:45 BFDA:BPDA/DABTF	15.8	8.3	420.5	290.0
BFDA/DABTF	14.5	6.8	391.5	290.0

**Figure 6.27 Mechanical Properties Of BFDA:BPDA + DABTF Copolymers**

Additional properties of the BFDA:BPDA + DABTF series are shown in Figure 6.28. Several trends were noted. The CTEs and optical transparencies decreased with increasing BPDA content while the dielectric constant increased slightly. As expected, the addition of BPDA increased the cutoff and decreased the % transmission because of the decrease in the fluorine content.

<b>BFDA:BPDA</b>	<b>CTE (ppm/°C)</b>	<b>Dielectric constant at 10GHz</b>	<b>% Transmission at 500nm</b>	<b>UV Cutoff (nm)</b>
BFDA Control	52	2.6	91	368
75:25	51	2.7	90	368
60:40	49	2.7	91	369
55:45	47	2.7	88	365
50:50	48	2.7	90	375
25:75	45	2.8	89	379
BPDA Control	40	2.9	88	379

**Figure 6.28 Properties Of BFDA:BPDA + DABTF**

The octafluorobiphenyl dianhydride (8FDA) was synthesized successfully and contained 30% fluorine. Only two polyimides were attempted using the 8FDA. 8FDA was combined with 4,4'-ODA to afford an inherent viscosity of 0.47 dL/g. The poly (amic acid) solution was cast onto plate glass and subsequently thermally imidized at 100, 200, and 300°C for one hour each. Thermal analysis by DSC and TMA indicated a  $T_g$  at 252°C and 262°C respectively. The 5% weight loss temperature occurred at 493°C. Isothermal weight loss at 300°C for 100 hr was 1.3%. The dielectric constant was 2.7.

Tensile strength, modulus, and elongation were 19.0 ksi, 350 ksi, and 75% respectively.

The 8FDA/4,4'-ODA polyimide exhibited higher tensile strength than the fluorinated polyimides using BFDA with only a slight increase in the dielectric constant. The elongation was very high (75%) which is often desirable for microelectronic applications.

The synthesis of 8FDA combined with a fluorinated diamine, 4,4-oxy-bis(3-trifluoromethyl) benzidine, was unsuccessful. Based on the solution appearance, the inherent viscosity was extremely low. The reactivity was not sufficient for successful polymerization of an electron-rich dianhydride and an electron-rich diamine.

Polyimides containing the 8FDA showed good potential for microelectronics applications. Unfortunately, the starting material, dimethoxyoctafluorobiphenyl, has become very expensive. Bulk quantities may be purchased for future research because polyimides containing 8FDA also show promise for photorefractive polymer development.

The diphenyl methane dianhydride synthesis was not successful. Although it is not fluorinated, its synthesis was attempted to produce polyimides with potentially less charge transfer complexing, lower color, and a lower dielectric constant. The synthesis of 3,3'-bis(dicarboxyphenoxy hexafluoroisopropyl) benzene was not successful because the product could not be isolated. The hydroxy functional group was attached to an aliphatic carbon versus an aromatic ring as with the syntheses described previously.



### 6.2.2 Polyimides As Interlayer Dielectrics And Encapsulants

The copolymers synthesized, characterized, and evaluated for microelectronic applications described herein are all ether-containing polyimides; the homopolymers may not contain ether linkages but were required for the systematic study and database.

The recommended use of these proposed materials was encapsulants; however, other microelectronics applications, such as interlayer dielectrics, require many of the same material properties. Material requirements included glass transition temperatures ranging from 250 to 300°C; cure temperatures between 250 and 325°C; resistance to hydrolysis; resistance to adhesion loss after a water boil test at 120°C and 2 ATM; high toughness; electronically pure materials; inherent viscosities ( $\eta_{inh}$ ) between 0.9 and 1.2 dL/g or higher if there were no obvious gels; good mechanical properties; insoluble polymers after curing; an insoluble partially imidized poly (amide acid) in strip solvents (i.e. ketones, butyl acetate); and a coefficient of thermal expansion in the range of 30 to 35 ppm/°C with a maximum allowable value of 50 ppm/°C. Many of these parameters were determined and evaluated by the research conducted in this dissertation. External evaluations will be performed by a microelectronics company working with NASA's Langley Research Center Materials Division.

Polymers were synthesized using a equimolar amount of dianhydride and diamine or a combination of diamines. Ratios of diamines employed were 50:50, 75:25, and 90:10. Additional polymers were synthesized using diamine combinations such as 60:40 and 80:20 to optimize the desired properties once the original combinations were characterized. The polyimides were characterized by inherent viscosities of the poly (amic acid)s, glass transition

temperatures, thermogravimetric analysis reported as a temperature at which 10% weight loss occurred, CTE, tensile strength, tensile modulus, and elongation at break. Once the best candidates were selected from each series, moisture uptake and positron annihilation spectroscopy were performed to determine a weight percent moisture uptake and free volume fraction. Data determination is time consuming and therefore was not determined for each polymer. Atomic Force Microscopy (AFM) was performed on selected candidates to determine the potential planarity of the film. AFM determines the topography of the film surface. Scanning Electron Microscopy (SEM) was also performed on selected candidates to see if there were any obvious defects or impurities. Additional testing may be performed on candidates selected for further evaluation by interested microelectronics companies.

Four series of polyimide copolymers were synthesized and characterized: (1) HQDEA + 4,4'-ODA:SAPPD, (2) ODPA + 3,4'-ODA:SAPPD, (3) ODPA + 3,4'-ODA:*p*-PDA, and (4) BTDA + 4,4'-ODA:*p*-PDA.

### **Copolymers Of HQDEA + 4,4'-ODA:SAPPD**

Copolymers were prepared combining HQDEA with 4,4'-ODA and SAPPD in an effort to decrease the CTE and increase the  $T_g$ , while maintaining high tensile strength and elongation (flexibility). Figure 6.29 shows the inherent viscosities of the PAA's,  $T_g$ s determined by both DSC and TMA, 10% weight loss temperature (TGA), and CTE. The solution viscosities ranged from 0.93 to 2.72 dL/g. Glass transition temperatures by TMA ranged from 231 to 277°C. The homopolymer, HQDEA/SAPPD, outgassed and no  $T_g$  could be determined

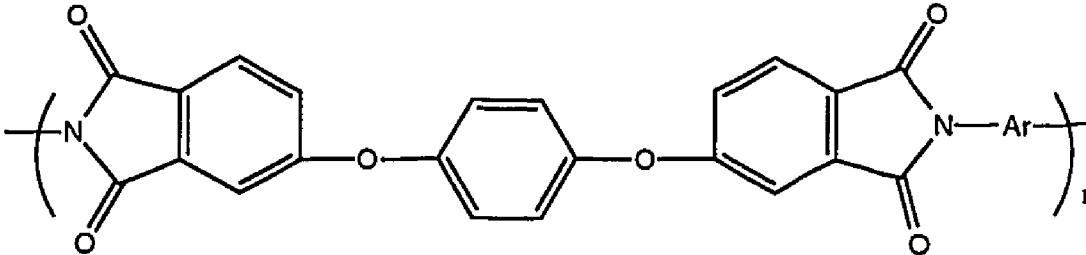
by DSC or TMA techniques. A weight loss of 10% occurred between 407 and 525°C for the polyimide series. CTEs ranged from 35.5 to 42.6 ppm/°C.

In general, several trends were noted in the HQDEA + 4,4'-ODA:SAPPD series. As the concentration of SAPPD increased, the inherent viscosity and apparent  $T_g$  increased while the temperature at which 10% weight loss occurred and CTE decreased. The higher  $T_g$ s are the result of the larger, stiffer SAPPD incorporated into the backbone. The more rigid the molecule, the more difficult the mobility becomes and consequently the greater the temperature required to give the polymer sufficient energy to move in a way appropriate to the rubber state. The temperature at which 10% weight loss occurred decreased with increasing SAPPD. The thermal instability was believed to be the result of partial degradation or complexing due to the squaric acid moiety. The size of the moiety will probably result in larger or smaller free volume, and this may help explain CTE values. CTE decreased nearly linearly with increasing amounts of SAPPD due to its rigidity and possibility its lower free volume.

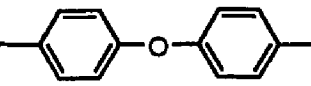
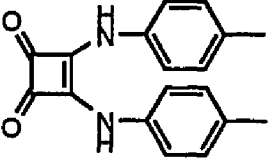
Thermo-oxidative stabilities should follow the rule that if a dianhydride and a diamine are electron-deficient, then the resultant polyimides should exhibit better oxidative resistance than other polymers of similar molecular weights. Electron-poor dianhydrides include BTDA, PMDA, ODPA, and 6FDA[32]. HQDEA is not listed but it is postulated that it is similar to ODPA. SAPPD is not a common diamine but data produced here indicated that its stability is not as good as the diphenyl ether. This is tentatively attributed to the -C-NH-phenylene bond which is not as stable as the -phenylene-O-phenylene bond.

Mechanical properties of HQDEA + 4,4'-ODA:SAPPD are shown in Figure 6.30. The tensile strengths ranged from 16.6 to 23.8 ksi. The tensile

moduli ranged from 370.2 to 666.4 ksi and the elongations at break were between 7.8 and 93.0%.



**Ar**

			$\eta_{inh}^1$ , dL/g	$T_g^2$ , °C	$T_g^3$ , °C
0	100		2.72	ND <sup>4</sup>	ND <sup>4</sup>
50	50		2.35	ND <sup>4</sup>	277
60	40		1.45	254	274
75	25		1.42	266	256
90	10		1.18	251	244
100	0		0.93	240	231

		10% wt. loss <sup>5</sup> , °C	CTE <sup>6</sup> , ppm/°C
0	100	407	ND <sup>4</sup>
50	50	470	35.5
60	40	474	37.0
75	25	503	38.9
90	10	516	42.6
100	0	525	40.0

<sup>1</sup>Determined on 0.5% (w/v) DMAc solutions at 25°C

<sup>2</sup>Determined by DSC at a heating rate of 20°C/min on film samples

<sup>3</sup>Determined by TMA at a heating rate of 5°C/min on film samples

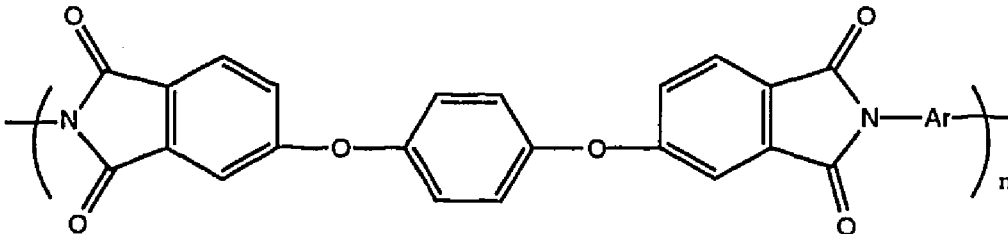
<sup>4</sup>ND = not detected due to decomposition or outgassing of the polymer sample

<sup>5</sup>Determined by TGA at a heating rate of 2.5°C/min in flowing air

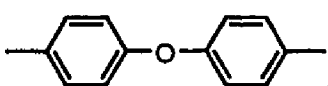
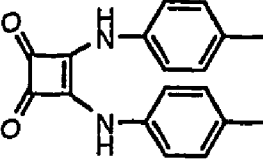
<sup>6</sup>Determined by TMA at a heating rate of 2°C/min

**Figure 6.29 Characterization Of HQDEA + 4,4'-ODA:SAPPD Copolymers**

Several observations were noted. The tensile strength changed very little with copolymer compositions up to 50% SAPPD. The strengths of the copolymers did not follow the rule of mixtures; tensile strengths for the copolymers were lower than both of the homopolymers. The modulus increased only slightly with compositions up to 40% SAPPD. Elongation decreased with increasing amounts of SAPPD and decreasing amounts of 4,4'-ODA. 4,4'-ODA contributed more flexibility to the polymer resulting in higher elongations.



**Ar**

			Tensile strength, ksi	Tensile modulus, ksi	Elong., %
					
0	100		21.4	666.4	7.8
50	50		17.6	456.1	11.3
60	40		17.2	387.2	11.1
75	25		17.8	387.6	42.7
90	10		16.6	376.9	42.2
100	0		23.8	370.2	93.1

**Figure 6.30 Mechanical Properties Of HQDEA + 4,4'-ODA:SAPPD Copolymers**

Solubility of these polyimide films was evaluated in NMP, DMAc, diglyme, DMF, and chloroform at intervals of 3 hr, 1 day, 3 days, and 5 days using a 1% solids concentration in a closed vial. Visual identification determined if the polyimides were soluble, partially soluble, or insoluble. Noted in the evaluations were discoloration of the solvent, swelling of the polymer, or other changes in the polymer film. All films in the HQDEA + 4,4'-ODA:SAPPD series were insoluble.

The best candidates from this series based on the material requirements were the 75:25 and 60:40 copolymers. The  $T_g$ s were 256°C and 274°C respectively. The CTEs were 38.9 ppm/°C and 37 ppm/°C respectively, i.e., only slightly higher than the optimum range of 30 to 35 ppm/°C. No outgassing occurred in these samples.

The polyimides in this series evaluated for moisture uptake and free volume fraction were the two homopolymers, HQDEA/SAPPD and HQDEA/4,4'-ODA, and the 75:25 copolymer. The 60:40 candidate would be evaluated at a later time should it be selected for scale-up. The moisture uptake by weight (w/o) and volume (v/o), cell size, free volume fraction, f(%), and inhibition factor are shown in Figure 6.31.

Polyimide	Moisture	Moisture	Cell Size Å <sup>3</sup>	Free	Inhibition Factor
	Uptake (w/o)	Uptake (v/o)		Volume Fraction, f(%)	
HQDEA/SAPPD	2.36	3.23	22	4.8	0.67
75:25	0.85	1.14	4	2.2	0.53
HQDEA/4,4'-ODA	0.83	1.11	18	3.7	0.30

Figure 6.31-Moisture Uptake Of HQDEA + 4,4'-ODA:SAPPD Polymers

A low moisture uptake is desired for microelectronics applications because electrical properties can change with absorbed moisture. To determine the moisture uptake for the polyimides, the samples were first desiccated by heating them to 120°C in a vacuum oven until their weights became constant. They were submerged in water in an oven maintained at 90-93°C until their weights stabilized. The moisture uptake by weight,  $w/o$ , was determined as:

$$w/o = ((w_{ss} - w_{ds}) / w_{ds}) \times 100$$

where  $w_{ss}$  was the saturated sample weight and  $w_{ds}$  was the desiccated sample weight. The saturation moisture fraction by volume ( $v/o$ ) was then calculated from the measured weight fraction as follows:

$$\text{Moisture uptake by volume (v/o)} = \frac{100\rho(w/o)}{100 + \rho(w/o)}$$

where  $\rho$  is the density of the dry polymer sample relative to the density of water measured experimentally by the density gradient technique[33].

Positron annihilation spectroscopy was used to determine the free volume fraction in the polymer films. Positrons, the anti-particles of electrons carrying a positive charge equal in magnitude to the negative charge carried by an electron, quickly thermalize when they enter polymeric solids. These thermalized positrons then destroy the molecular electrons. Three possibilities exist when the positron enters the test films: (1) they exist as free positrons, (2) they exist as positronium species (a bound state of electron and positron), and

(3) they exist as a trapped positron. The lifetime of each of these can then be used to calculate the cell size (void) and the free volume fraction.

The cell size is the average size of the microvoid. The cell size does not account for distributions of small or large voids, only a mean value. The free volume fraction is calculated from the mean size and number of cells, and is an indication of how much space is available for infiltration of the moisture. If the moisture uptake ( $v/o$ ) is lower than the free volume fraction, there is a chemical or geometrical factor inhibiting the penetration of the moisture into the polymer, such as polar groups, electrical factors, or geometric influences due to packing of the chains. The inhibition factor is a ratio of the moisture uptake by volume ( $v/o$ ) to the free volume fraction. Therefore, if the inhibition factor is close to 1.0, the majority of the free volume is being filled by water molecules. Conversely, if the number is closer to 0.0, the penetration of the water is being inhibited.

The moisture uptake by weight ( $w/o$ ) ranged from 0.83 to 2.36. The moisture uptake of the homopolymer was not greatly affected by the 25 molar percent addition of SAPPD to afford the 75:25 copolymer. Moisture uptake by volume ( $v/o$ ) ranged from 1.11 to 3.23. The cell size ranged from 4 to 22 Å<sup>3</sup>. The size of the microvoids was quite large for the two homopolymers compared to the 75:25 copolymer. The size of the microvoid is drastically reduced in the copolymer compared to the homopolymers. The free volume fraction ( $f\%$ ) ranged between 2.2 and 4.2%. The free volume was lowest for the 75:25 copolymer. The inhibition factors ranged between 0.30 and 0.67. The HQDEA/4,4-ODA has the lowest inhibition factor. This backbone structure imparted resistance to moisture.

AFM and SEM were used to characterize the HQDEA/4,4-ODA homopolymer and the 75:25 copolymer. AFM indicated that the surface



topography of the homopolymer HQDEA/SAPPD had islands (peaks), approximately 15 to 20 nm in height, in a directional pattern. The 75:25 copolymer had an average surface roughness of 15 to 20 nm with the same oval-shaped islands of 8 to 10 nm in height. These films had low surface roughness but were not planar as is optimum for microelectronics applications. SEM indicated that there was a lot of particulate matter on both surfaces of the films. These data indicated that filtering the PAA solutions may be required to obtain uniform surfaces on substrates or electronic device packages.

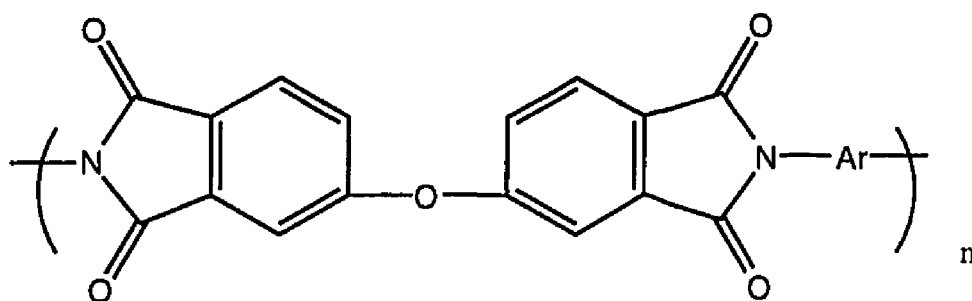
### **Copolymers of ODPA + 3,4'-ODA:SAPPD**

Copolymers were prepared combining ODPA with 3,4'-ODA and SAPPD. The polymer designated ODPA/3,4'-ODA is patented under the trademark LaRC<sup>TM</sup>-IA and is a well characterized polyimide with excellent thermal, chemical, and mechanical properties[34]. However, its  $T_g$  is too low and its CTE is too high for this application. Adding SAPPD to this homopolymer should impart a higher strength, modulus, and  $T_g$ , while lowering the CTE.

Figure 6.32 shows the characterization of the random ODPA + 3,4'-ODA:SAPPD copolymers. Inherent viscosities ranged from 1.12 to 1.34 dL/g.  $T_g$ s by DSC were not detected for several polymers due to outgassing or decomposition in polymers containing greater than 25 molar percent of SAPPD. Other  $T_g$ s ranged from 237 to 261°C. The temperature at which 10% weight loss occurred ranged from 422°C to 518°C. CTEs ranged from -2 to 39.5 ppm/°C. The homopolymer ODPA/SAPPD had a negative CTE. The larger the amount of SAPPD in the polymer backbone, the lower the CTE. SAPPD imparts dimensional stability but impairs thermo-oxidative stability.

The mechanical properties of the ODPA + 3,4'-ODA:SAPPD polymers are shown in Figure 6.33. Tensile strengths ranged from 16.9 to 25.9 ksi. Moduli ranged from 421.5 to 873.3 ksi. Elongations ranged from 4.2 to 63.4%. The general trends noted were that tensile strength and modulus increased with increasing amounts of SAPPD while the elongation decreased.

Solubility of these polyimide films was evaluated in NMP, DMAc, diglyme, DMF, and chloroform at intervals of 3 hr, 1 day, 3 days, and 5 days using a 1% solids concentration in a closed vial. All films in the ODPA + 3,4'-ODA:SAPPD series were insoluble.



Ar

		$\eta_{inh}^1$ , dL/g	$T_g^2$ , °C	$T_g^3$ , °C
0	100	1.12	ND <sup>4</sup>	ND <sup>4</sup>
50	50	1.14	ND <sup>4</sup>	ND <sup>4</sup>
75	25	1.19	ND <sup>4</sup>	261
80	20	1.23	252	254
90	10	1.30	249	250
100	0	1.34	238	237
		10% wt. loss <sup>5</sup> , °C	CTE <sup>6</sup> , ppm/°C	
0	100	422	-2 to 6 <sup>4</sup>	
50	50	456	30.8	
75	25	503	34.2	
80	20	505	36.0	
90	10	518	38.5	
100	0	511	39.5	

<sup>1</sup>Determined on 0.5% (w/v) DMAc solutions at 25°C

<sup>2</sup>Determined by DSC at a heating rate of 20°C/min on film samples

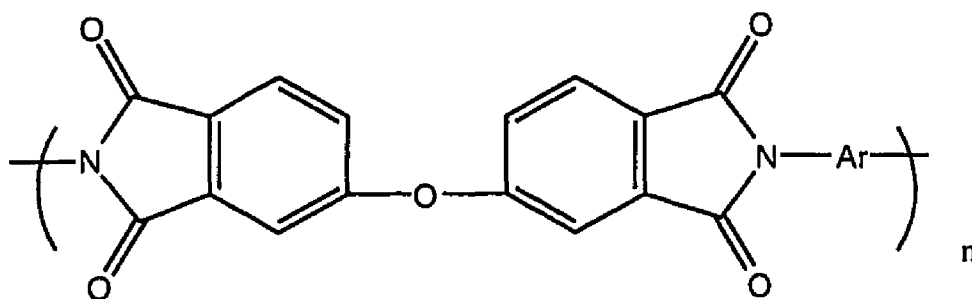
<sup>3</sup>Determined by TMA at a heating rate of 5°C/min on film samples

<sup>4</sup>ND = not detected due to decomposition or outgassing of the polymer sample

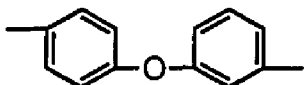
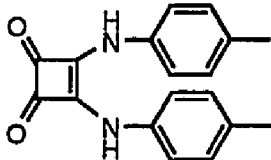
<sup>5</sup>Determined by TGA at a heating rate of 2.5°C/min in flowing air

<sup>6</sup>Determined by TMA at a heating rate of 2°C/min

**Figure 6.32 Characterization Of ODPA + 3,4'-ODA:SAPPD Copolymers**



Ar

			Tensile strength, ksi	Tensile modulus, ksi	Elong., %
0		100	25.9	873.3	6.4
50		50	18.8	601.4	4.2
75		25	18.5	494.4	9.6
80		20	20.7	463.2	10.6
90		10	18.6	439.0	63.4
100		0	16.9	421.5	28.1

**Figure 6.33 Mechanical Properties Of ODPA + 3,4'-ODA:SAPPD Copolymers**

Based on the material requirements for the target microelectronic applications, the best candidate from the ODPA + 3,4'-ODA:SAPPD series was the 80:20 polyimide. The  $T_g$  was 254°C with a 10% weight loss occurring at greater than 500°C. The CTE was low (36.0 ppm/°C) and mechanical properties were good.

AFM indicated a well distributed surface roughness of approximately 15 to 20 nm for the ODPA/SAPPD homopolymer. There were no distinct islands (peaks) on the surface as seen with the HQDEA +4,4'-ODA:SAPPD copolymer

candidate. The surface roughness of the 80:20 copolymer was lower, approximately 10 to 15 nm. SEM showed no particulate matter for the ODPA/SAPPD homopolymer and only a very small amount of particulate matter for the copolymer.

Moisture uptake and positron data for the 80:20 copolymer and homopolymers are shown in Figure 6.34. The w/o ranged from 0.88 to 3.07. The v/o ranged from 1.20 to 4.23. The cell size ranged from 9 to 17 Å<sup>3</sup>. The free volume fraction ranged from 3.5 to 4.4%. The inhibition factor ranged from 0.27 to 0.97. The 80:20 copolymer had the lowest moisture uptake, but the highest free volume fraction. This indicated that there was more space available for penetration of moisture but the moisture uptake was inhibited by some chemical or geometric factor.

Polyimide	Moisture	Moisture	Cell Size Å <sup>3</sup>	Free	Inhibition Factor
	Uptake (w/o)	Uptake (v/o)		Volume Fraction, f(%)	
ODPA/SAPPD	3.07	4.23	9	4.4	0.97
80:20	0.88	1.20	17	4.4	0.27
ODPA/3,4'-ODA	0.96	1.32	13	3.5	0.35

**Figure 6.34 Moisture Uptake For The ODPA + 3,4'-ODA:SAPPD Copolymers**

#### **Copolymers of ODPA + 3,4'-ODA:p-PDA**

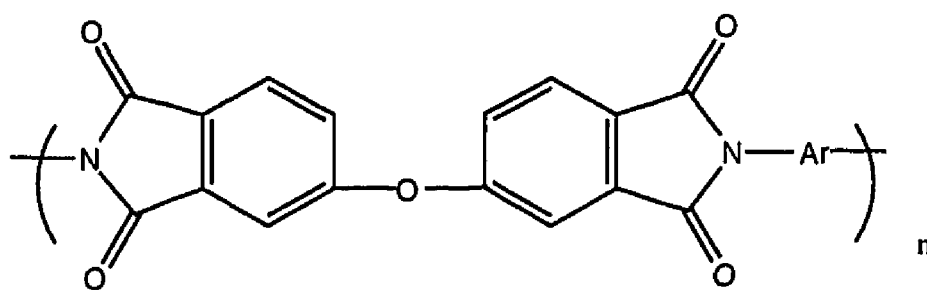
Copolymers were prepared combining ODPA with 3,4'-ODA:p-PDA in an effort to increase the T<sub>g</sub> and lower the CTE. Since ODPA/3,4'-ODA

possesses excellent chemical, physical, and mechanical properties, lowering the CTE and raising the  $T_g$  by altering the polymer backbone slightly would make it a potential candidate for the microelectronics application. Additionally, no outgassing would be expected as seen in the polyimides with SAPPD in the backbone.

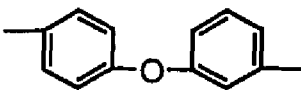

Figure 6.35 shows the characterization of ODPA + 3,4'-ODA:*p*-PDA copolymers. Inherent viscosities ranged from 0.70 to 1.34 dL/g.  $T_g$ s by TMA ranged from 237 to 350°C. Temperatures at which 10% weight loss occurred ranged from 511 to 533°C. CTEs ranged from 26.0 to 39.5 ppm/°C.

Several trends were noted. Generally, as the amount of 3,4'-ODA increased, the viscosity increased.  $T_g$ s increased as the amount of *p*-PDA increased due to the rigidity of the *p*-PDA versus a more flexible 3,4'-ODA. Weight loss temperatures increased and CTE decreased as the amount of *p*-PDA increased. This was due to the thermal stability and rigidity that *p*-PDA imparted in the polymer backbones.

Mechanical properties of ODPA + 3,4'-ODA:*p*-PDA are illustrated in Figure 6.36. Tensile strengths ranged from 16.9 to 30.0 ksi. Moduli ranged from 421.5 to 832.3 ksi. Elongations ranged between 6.5 and 47.8%.



Ar

		$\eta_{inh}^1$ , dL/g	$T_g^2$ , °C	$T_g^3$ , °C
0	100	0.88	ND <sup>4</sup>	350
50	50	1.08	265	301
60	40	1.28	251	255
75	25	1.32	248	245
90	10	0.70	248	243
100	0	1.34	238	237

		10% wt. loss <sup>5</sup> , °C	CTE <sup>6</sup> , ppm/°C
0	100	533	26.0
50	50	514	28.7
60	40	527	33.0
75	25	516	37.3
90	10	528	37.9
100	0	511	39.5

<sup>1</sup>Determined on 0.5% (w/v) DMAc solutions at 25°C

<sup>2</sup>Determined by DSC at a heating rate of 20°C/min on film samples

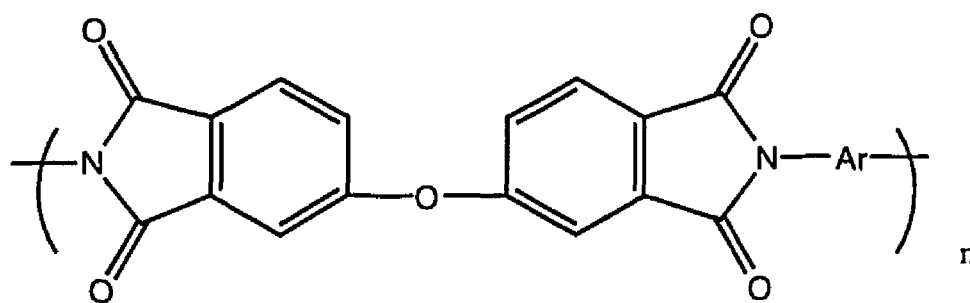
<sup>3</sup>Determined by TMA at a heating rate of 5°C/min on film samples

<sup>4</sup>ND = not detected due to decomposition or outgassing of the polymer sample

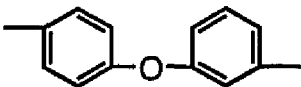

<sup>5</sup>Determined by TGA at a heating rate of 2.5°C/min in flowing air

<sup>6</sup>Determined by TMA at a heating rate of 2°C/min

**Figure 6.35 Characterization Of ODPA + 3,4'-ODA:p-PDA Copolymers**



Ar

		Tensile strength, ksi	Tensile Modulus, ksi	Elong., %
				
0	100	30.0	832.3	14.7
50	50	21.5	534.4	6.5
60	40	21.1	505.6	27.6
75	25	18.9	371.9	47.8
90	10	17.9	363.9	33.1
100	0	16.9	421.5	28.1

**Figure 6.36 Mechanical Properties Of ODPA + 3,4'-ODA:*p*-PDA Copolymers**

Several trends were noted. Tensile strengths and moduli increased with increasing amounts of *p*-PDA due to the rigidity of *p*-PDA. Elongation, however, did not follow a general trend. It was expected that as the *p*-PDA increased, the elongation would decrease; however, this was not the case. Elongation is strongly dependent on film quality and this could have altered the expected trend.

The best candidate from the ODPA + 3,4'-ODA:*p*-PDA series was the 60:40 copolymer. The  $T_g$  was 255°C; the 10% weight loss temperature was



527°C; the CTE was 33.0 ppm/°C; the tensile strength was greater than 20 ksi; the modulus was greater than 500 ksi; the elongation was 27%.

Figure 6.37 shows the moisture uptake and free volume data for the 75:25 polyimide and its homopolymers. Data were evaluated prior to the synthesis of the 60:40 copolymer which resulted in a better application candidate. The data should be similar for the 60:40 copolymer. The w/o was excellent for 75:25 copolymer and the two homopolymers and ranged from 0.96 to 1.22. The v/o ranged from 1.32 to 1.75. The size of the free volume was relatively small (2.4%) for the 75:25 copolymer and its inhibition factor was moderate.

Polyimide	Moisture	Moisture	Cell Size Å <sup>3</sup>	Free	Inhibition Factor
	Uptake (w/o)	Uptake (v/o)		Volume Fraction, f(%)	
ODPA/3,4'-ODA	0.96	1.32	16	3.5	0.35
75:25	1.05	1.44	4	2.4	0.60
ODPA/ <i>p</i> -PDA	1.22	1.75	3	2.0	0.85

**Figure 6.37 Moisture Uptake For The ODPA + 3,4'-ODA:*p*-ODA Copolymers**

#### **Copolymers of BTDA + 4,4'-ODA:*p*-PDA**

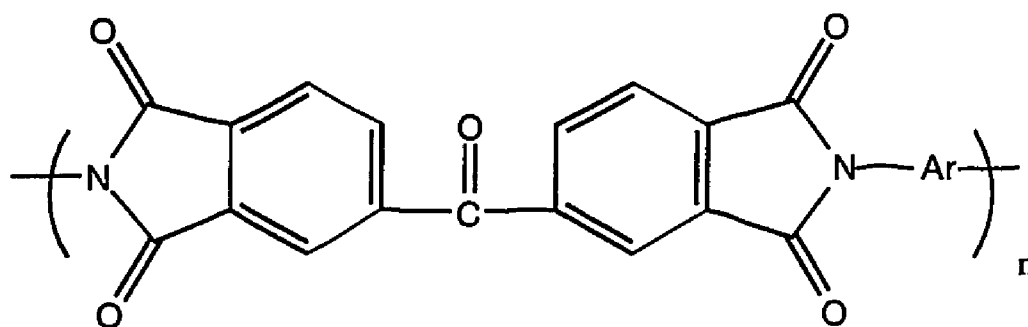
Copolymers were synthesized combining BTDA and 4,4'-ODA:*p*-PDA. Characterization data are shown in Figure 6.38. Inherent viscosities ranged from 1.21 to 1.49 dL/g.  $T_g$ s by TMA ranged from 271 to 357°C. Weight loss of

10% occurred between 501 and 527°C. CTEs ranged from 16.6 to 35.4 ppm/°C.

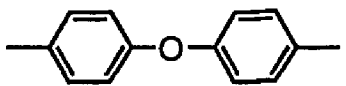

Several trends were observed. The inherent viscosities of the two homopolymers BTDA/*p*-PDA and BTDA/4,4'-ODA were approximately the same. The highest viscosity resulted from the 50:50 combination.  $T_g$ s did not follow a trend. Similar  $T_g$ s by TMA were observed for the 50:50 and 75:25 copolymers. Weight loss temperatures did not differ significantly in the series. CTEs ranged from 16.6 to 35.5 ppm/°C. As the amount of *p*-PDA increased, the CTE decreased. *p*-PDA imparted more dimensional stability than the 4,4'-ODA since it is more rigid.

Mechanical properties of the BTDA + 4,4'-ODA:*p*-PDA copolymers are shown in Figure 6.39. Tensile strengths ranged from 21.1 to 32.2 ksi. Moduli ranged from 426.6 to 786.4 ksi. Elongations ranged from 17.6 to 49.5%. Tensile strengths and moduli generally increased as the amount of *p*-PDA increased. Elongations, however, decreased as would be expected as a result of the stiffer *p*-PDA versus the flexible ether-containing 4,4'-ODA.

Based on the material requirements, the best candidate from the BTDA + 4,4'-ODA:*p*-PDA series was the 90:10 copolymer. Its inherent viscosity was high (1.21 dL/g). The  $T_g$  was 276°C. A weight loss of 10% occurred at 519°C. The CTE was 32.9 ppm/°C. Tensile strength, modulus, and elongation were 22.3 ksi, 426.6 ksi, and 49.5% respectively.



Ar

Ar		$\eta_{inh}^1$ , dL/g	$T_g^2$ , °C	$T_g^3$ , °C
				
0	100	1.21	ND <sup>4</sup>	341
50	50	1.49	ND <sup>4</sup>	357
60	40	1.28	251	255
75	25	1.38	292	355
90	10	1.21	277	276
100	0	1.22	273	271
		10% wt. loss <sup>5</sup> , °C	CTE <sup>6</sup> , ppm/°C	
0	100	516	16.6	
50	50	501	24.8	
60	40	527	33.0	
75	25	512	31.9	
90	10	519	32.9	
100	0	516	35.4	

<sup>1</sup>Determined on 0.5% (w/v) DMAc solutions at 25°C

<sup>2</sup>Determined by DSC at a heating rate of 20°C/min on film samples

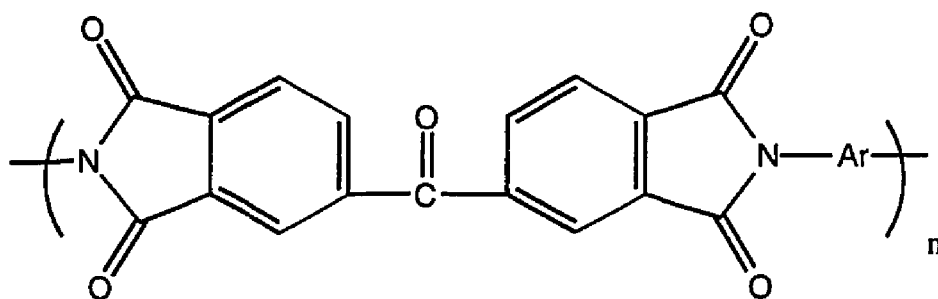
<sup>3</sup>Determined by TMA at a heating rate of 5°C/min on film samples

<sup>4</sup>ND = not detected due to decomposition or outgassing of the polymer sample

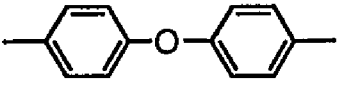

<sup>5</sup>Determined by TGA at a heating rate of 2.5°C/min in flowing air

<sup>6</sup>Determined by TMA at a heating rate of 2°C/min

**Figure 6.38 Characterization Of BTDA + 4,4'-ODA:*p*-PDA Copolymers**



Ar

Ar		Tensile strength, ksi	Tensile modulus, ksi	Elong., %
				
0	100	32.2	786.4	27.0
50	50	25.4	588.5	17.6
60	40	21.1	505.6	27.6
75	25	23.6	509.3	33.6
90	10	21.3	468.1	24.0
100	0	22.3	426.6	49.5

**Figure 6.39 Tensile Properties Of BTDA + 4,4'-ODA:*p*-PDA Copolymers**

Moisture uptake and free volume data are shown in Figure 6.40.

Polymer	Moisture Uptake (w/o)	Moisture Uptake (v/o)	Cell Size $\text{\AA}^3$	Free volume Fraction, f(%)	Inhibition Factor
BTDA/4,4'-ODA	1.34	1.82	6	3.0	0.58
90:10	1.38	1.88	18	3.8	0.42
BTDA/ <i>p</i> -PDA	2.12	2.97	6	2.9	1.00

**Figure 6.40 Moisture Uptake For BTDA + 4,4'-ODA:*p*-PDA Copolymers**

Lower moisture uptake by weight was observed for the BTDA/4,4'-ODA and 90:10 copolymers with values of 1.34 and 1.38, respectively, while the homopolymer BTDA/*p*-PDA exhibited a moisture uptake of 2.12%. Moisture uptake by volume ranged from 1.82 to 2.97. The cell size was quite large for the 90:10 copolymer which indicated that there was free volume available for occupancy by water molecules; however, their penetration was inhibited by some chemical or structural factor as indicated by the low moisture absorption value and low inhibition factor. The inhibition factors ranged from 0.42 to 1.00. The homopolymer BTDA/*p*-PDA exhibited an inhibition factor of 1.00, which indicated nearly all of the free volume was occupied by water molecules.

### 6.3. Polyimides For Harsh Environments

#### 6.3.1 Hydrolytically Stable Polyimides

The following polymers were evaluated for hydrolytic stability for potential aircraft cable and wire insulation applications. Most of the polymers in this study were ether-containing polyimides (greater than 70%). Commercially available, non-ether-containing polyimides were included for comparison, as well as non-ether-containing polymers required for a more comparative evaluation and broad database.

Table 6.1 lists the inherent viscosities of the various poly (amide acid)s,  $T_g$ s of the imidized films by DSC, and the dielectric constants. Inherent viscosities for the poly (amide acid) solutions ranged from 0.48 to 1.79 dL/g. Films of the polyimides varied in color from nearly colorless to light orange-brown after heating to 350°C, where all films should be fully imidized. All films were clear except LaRC™-CPI, which was translucent and exhibited crystallinity. Most of the polyimides were amorphous with  $T_g$ s from 222 to greater than 500°C. LaRC™-CPI and ODPA/*p*-PDA were semi-crystalline as evidenced by x-ray diffraction.

Polyimides are used widely in electronic applications because they have low dielectric constants. Variations in the backbone structure, such as the introduction of fluorine atoms, tend to afford better insulative properties, substantially improve thermo-oxidative stability, minimize moisture pick-up, and lower chain-chain interactions[35]. The dielectric constant of the state-of-the-art polyimide presently used for advanced electronics applications generally

Polyimide Film	Poly (amic acid) Inherent Viscosity, dL/g	T <sub>g</sub> , °C	Dielectric Constant
LaRC™-ITPI (IDPA/ <i>m</i> -PDA)	0.51, 0.47	259	3.29*
LaRC™-CPI (BTDA/1,3-BABB)	1.38, 1.57	222 (T <sub>m</sub> = 350)	3.10
LaRC™-TPI (comm.)	—	250	3.30
6F/3,5-DABTF	0.58, 0.48	297	2.58
BPDA/3,5-DABTF	0.96, 0.77	329	3.02
HQDEA/4-BDAF	0.68, 0.57	227	2.56
ODPA/3,4'-ODA (LaRC™-IA)	1.60, 1.79	245	3.06
PMDA/3,4'-ODA	0.70	>325	3.18
ODPA/ <i>p</i> -PDA	0.81	none (crystalline)	—
PMDA/4,4'-ODA	0.86	297	—
KAPTON®	—	(400)	3.20
APICAL®	—	(400)	3.00
UPILEX® R	—	285	3.50
UPILEX® S	—	>500	3.50

\* Calculated value of dielectric constant provided by J. R. Pratt, Amoco, Atlanta, GA.

Table 6.1 Physical Properties of Polyimides

Polyimide Film	T <sub>g</sub> , °C <sup>a</sup>	T <sub>g</sub> , °C <sup>b</sup>	TGA, °C <sup>c</sup>
LaRC™-ITPI (IDPA/ <i>m</i> -PDA)	259	274	481
LaRC™-CPI (BTDA/1,3-BABB)	222 (T <sub>m</sub> = 350)	ND <sup>d</sup>	487
LaRC™-TPI (comm.)	250	256	532
6F / 3,5-DABTF	297	299	480
BPDA / 3,5-DABTF	329	373	513
HQDEA / 4-BDAF	227	231	490
ODPA / 3,4'-ODA (LaRC™-IA)	245	252	497
PMDA / 3,4'-ODA	>325	ND <sup>d</sup>	503
ODPA / <i>p</i> -PDA	ND <sup>d</sup>	ND <sup>d</sup>	515
PMDA / 4,4'-ODA	297	251	495
KAPTON®	ND <sup>d</sup>	ND <sup>d</sup>	528
APICAL®	ND <sup>d</sup>	ND <sup>d</sup>	528
UPILEX® R	285	ND <sup>d</sup>	544
UPILEX® S	ND <sup>d</sup>	ND <sup>d</sup>	583

<sup>a</sup> By DSC. <sup>c</sup> 5% weight loss.  
<sup>b</sup> By TMA. <sup>d</sup> ND = not detected.

Table 6.2 Thermal Analysis Data of Polyimide Films

ranges from 3.2 to 4.0 depending on measurement frequency and moisture content of the polyimide. Two systems that exhibited dielectric constants below 2.6 were 6F/3,5-DABTF and HQDEA/4-BDAF[36-37].

Table 6.2 compares the  $T_g$ s by DSC and TMA.  $T_g$ s by TMA were slightly higher and ranged from 231 to 373°C. A  $T_g$  by TMA was not detected for 50% of the polyimides. TGA data determined 5% weight loss temperatures ranging from 480 to 583°C, which are excellent values for wire and cable insulators.

Several systems that showed low moisture regain of approximately 1% or less included LaRC™-CPI, LaRC™-TPI, UPILEX® R, 6F/3,5-DABTF, and HQDEA/4-BDAF as shown in Figure 6.41. Crystallinity or contiguity may contribute to low moisture absorption in LaRC™-CPI and UPILEX® R while the 6F/3,5-DABTF and HQDEA/4-BDAF systems contained fluorine atoms in the backbone which tend to impart low moisture pick-up. The tendency for polyimides to absorb moisture impacts their electrical performance and processability[38]. Many PMDA/ODA polyimides including KAPTON® and APICAL® exhibited high moisture absorption.



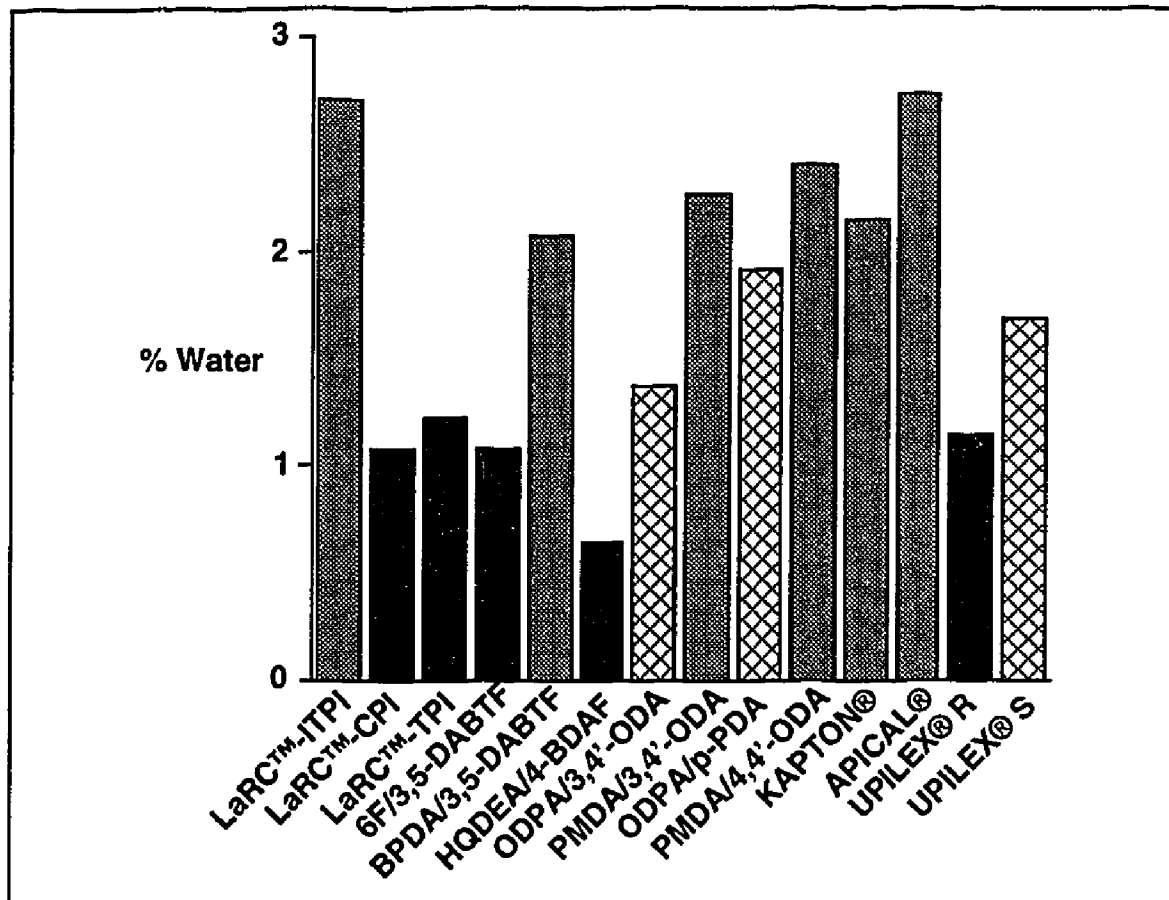


Figure 6.41 Moisture Absorption of Polyimides

The polyimides in this evaluation were subjected to basic solutions (pH 11-14) and their retention of mechanical properties (tensile strength, tensile modulus, and elongation at break) were determined. The chemical structure of the diamine and dianhydride, strength of the imide links, incomplete imidization after curing, morphology, and water absorption are several factors that can affect hydrolysis[39]. Figure 6.42 shows the hydrolysis mechanism of the imide ring.

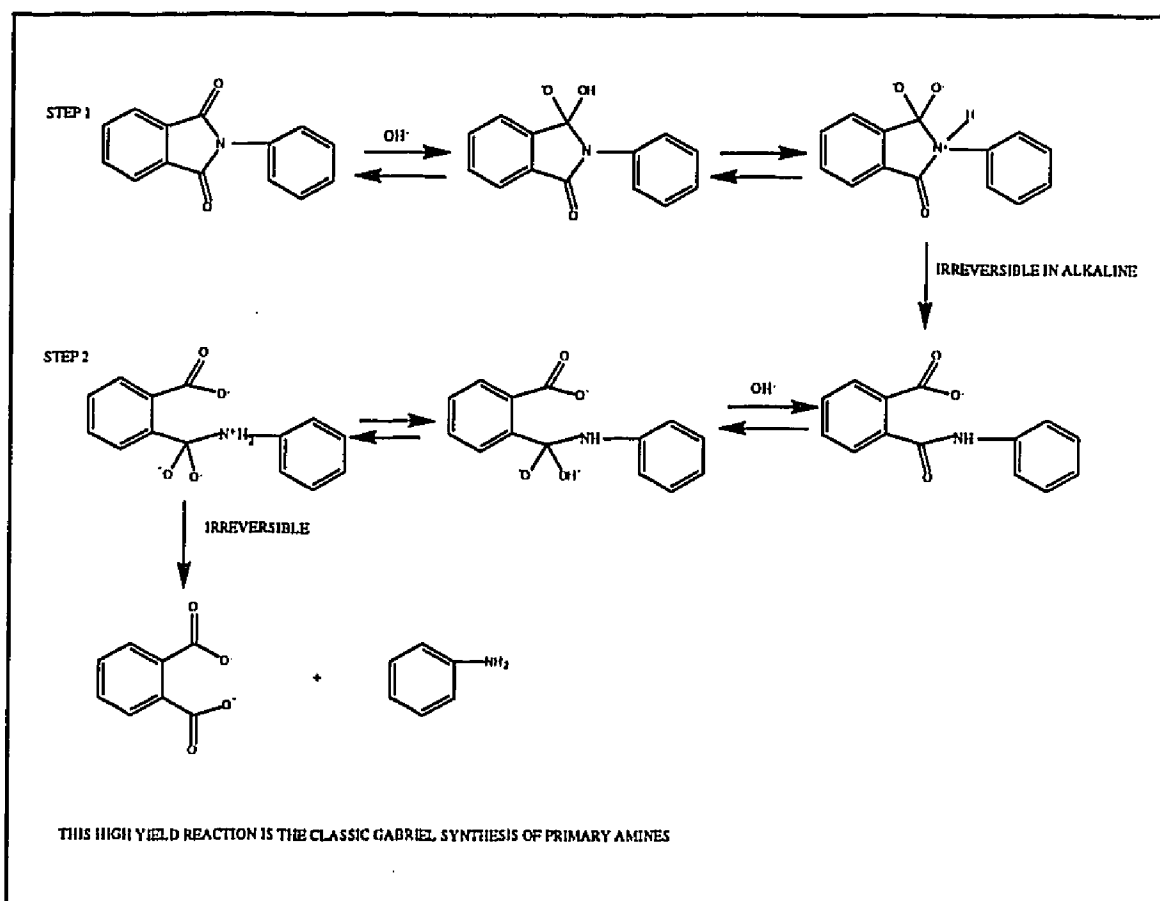


Figure 6.42 Hydrolysis of the Imide Moiety

Nominal changes in thickness before and after exposure to aqueous base were recorded to identify those polyimides that swelled during exposure. The PMDA/4,4'-ODA and ODPA/*p*-PDA systems swelled as much as 56% and 40% respectively in sodium hydroxide with smaller increases in the less basic solutions. It was not expected that the ODPA/*p*-PDA polyimide would swell because the film was semi-crystalline as evidenced by x-ray diffraction. The crystalline regions usually inhibit penetration of solvents. The other polyimide systems showed only a small increase in thickness after exposure to the basic solutions.

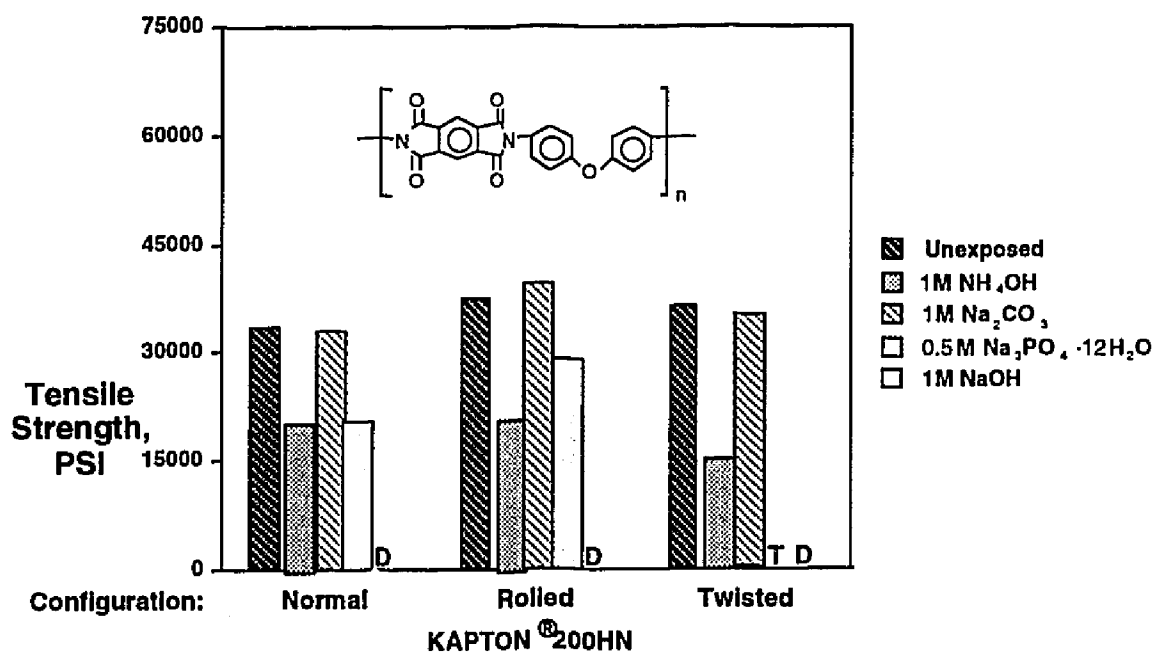
Caustic solutions were selected because they accelerate hydrolysis and are found in cleaning solutions used in aircraft maintenance. Three configurations were chosen to simulate unstressed and stressed conditions for the film specimens. The normal configuration was unstressed, and was used as a baseline to evaluate any effects induced by the other conditions. The rolled configuration induced a maximum stress of approximately 4 ksi, using a nominal 500 ksi modulus and a specimen size of 0.200 in wide and 0.002 in thick in the approximation. The twisted configuration stress was calculated using torque and maximum stress approximations for the same sample dimensions and four twists per unit length. The stress induced was approximately 2.3 ksi. These calculations are found in the Appendix. These configurations were chosen to simulate stresses the film may experience during a wire wrapping process or installation in the aircraft.

The following figures compare the tensile strengths for the normal (unstressed), rolled, and twisted configurations for the polyimides evaluated for wire and cable insulation. The scale is the same for all figures. The chemical structures and a legend for the basic pH 11-14 solutions is provided with each figure. Films were exposed to the basic solutions for 48 hr at RT. Generally,

moduli and elongations were not affected so these graphs will not be provided. Mention is made as to the retention of modulus and elongation for each polyimide.

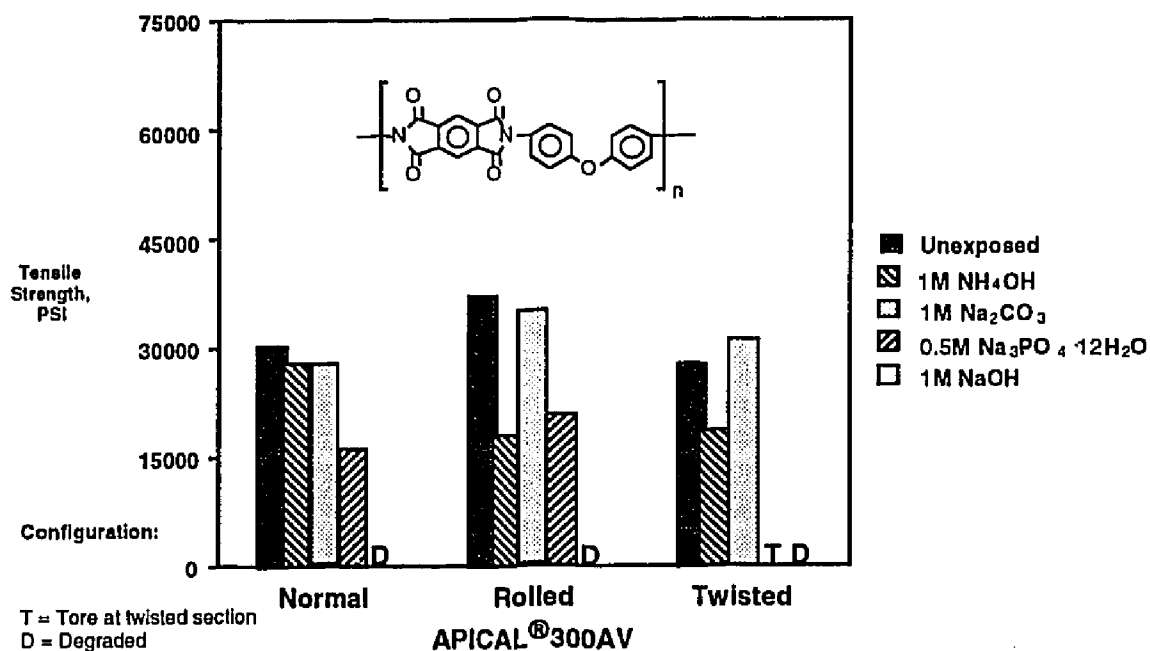
Figure 6.43 and 6.44 compare the tensile strengths of KAPTON® 200HN and APICAL® 300AV films for the three configurations. APICAL® is believed to be the same chemical structure as DuPont's KAPTON®. Both systems exhibited similar degradation in the ammonium hydroxide and sodium hydroxide solutions. Specimens tore from the stress induced by the twisting in the trisodium phosphate exposure and mechanical data could not be determined. Moduli and elongations of KAPTON® and APICAL® were essentially unaffected by the exposure in the basic solutions. KAPTON® and APICAL® retained approximately 100% of moduli except in cases of complete degradation. Modulus is dependent on the intermolecular forces whereas tensile strength depends strongly on molecular weight and would be affected when chain length was reduced.

Degradation is connected with the hydrolysis of the imide moiety. Resistance to hydrolysis seemed to depend strongly on the chemical nature of the dianhydride component of the polymer. PMDA based polyimides appeared to be the least resistant to hydrolysis of the polyimides studied[40].



T = Tore at twisted section  
D = Degraded

**Figure 6.43 Effect Of Chemical Exposure On Tensile Strength of Kapton®**

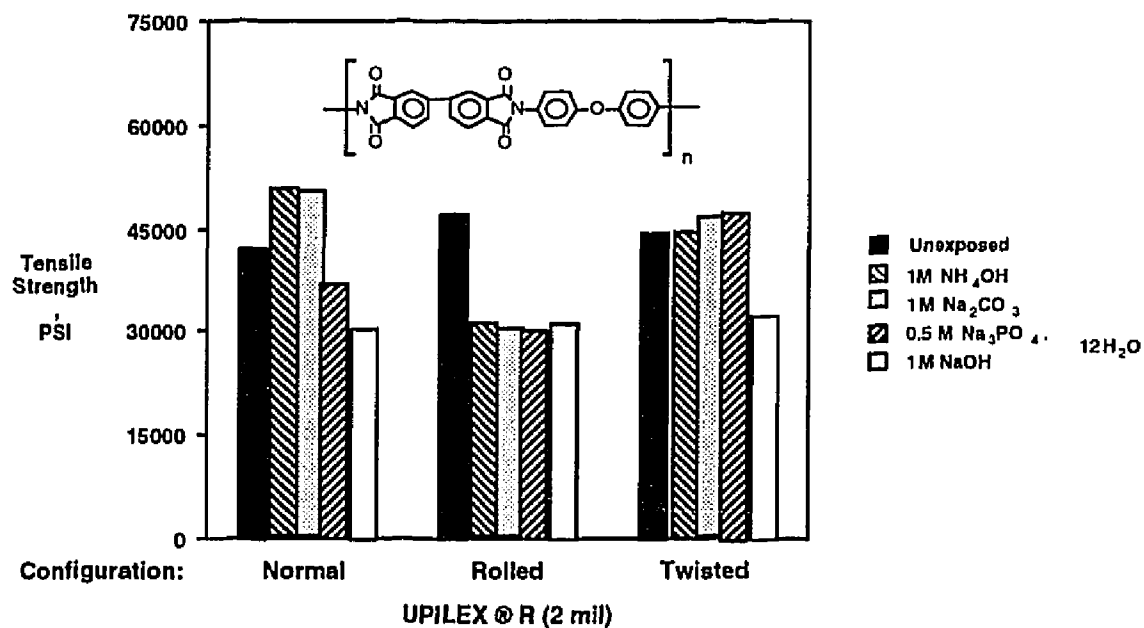


T = Tore at twisted section  
D = Degraded

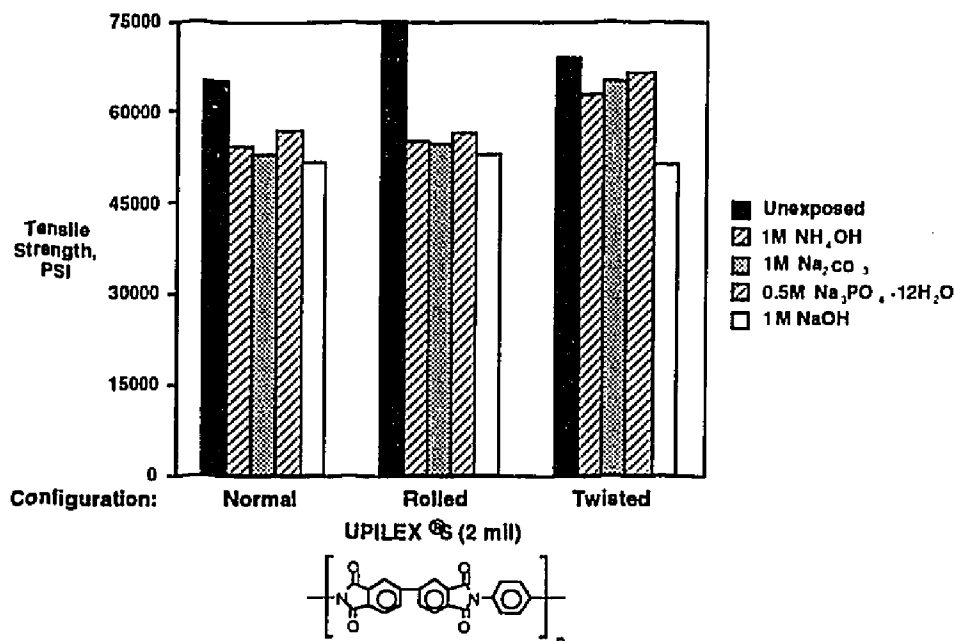
**Figure 6.44 Effect Of Chemical Exposure On Tensile Strength Of Apical®**

Figure 6.45 shows the tensile strength of UPILEX® R. In the rolled configuration, there was a significant drop in tensile strength during exposure with only 65% retention. Since UPILEX® R is a commercially available film, it is possible that the surface of the film differs from the interior portions. In the rolled configuration, the stress is greater on the surface and the surface becomes more susceptible to attack and degradation. Moduli and elongations of UPILEX® R were not greatly affected by exposure to the basic solutions.

It can be seen from Figure 6.46 that UPILEX® S exhibited behavior similar to that of UPILEX® R, having a reduction in tensile strength of 30% in the rolled configuration but being unaffected in the twisted configuration except in the sodium hydroxide solution. In all solution exposures, moduli and elongations were not greatly affected.



**Figure 6.45 Effect Of Chemical Exposure On Tensile Strength Of Upilex® R**

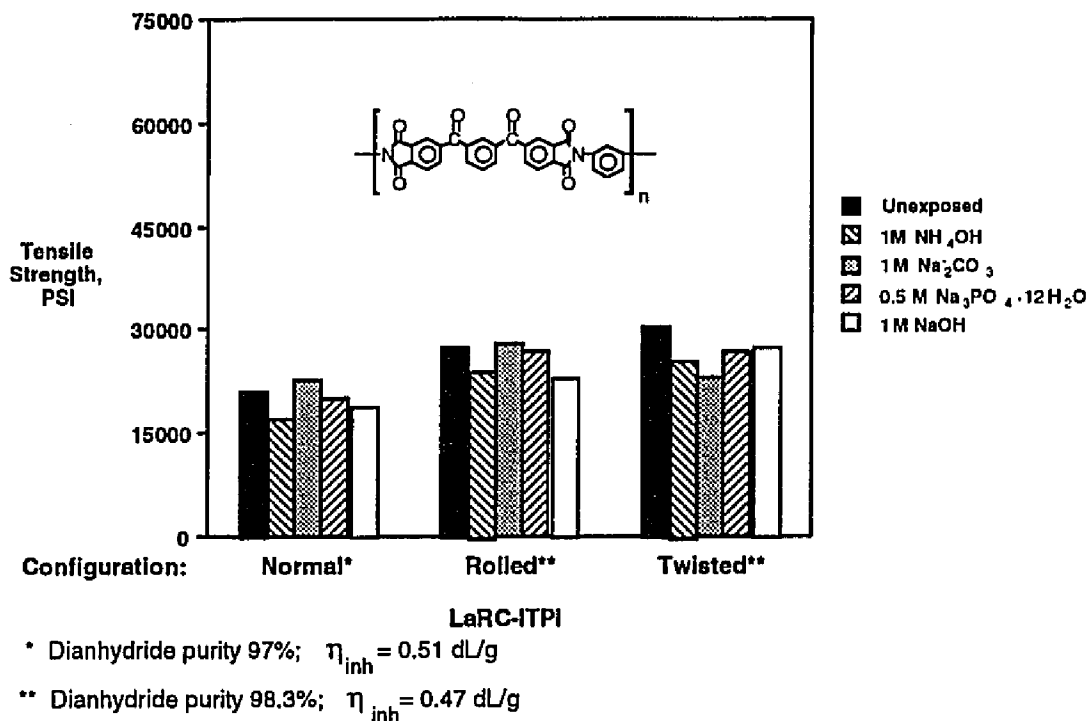


**Figure 6.46 Effect Of Chemical Exposure On Tensile Strength of UPILEX® S**

Figure 6.47 compares the tensile strengths of LaRC™-TPI in the test conditions, showing no drastic reduction induced by solvent or stress. LaRC™-CPI (unoriented) maintained excellent retention of tensile strength in all cases (Figure 6.48). Moduli and elongations of LaRC™-CPI samples were not affected by the stress or hydrolysis. LaRC™-ITPI exhibited good retention of tensile strength as shown in Figure 6.49. The increase in tensile strength in the rolled and twisted configurations was attributed to better monomer purity in the synthesis of the polymer. Good retention of modulus and elongation were maintained.



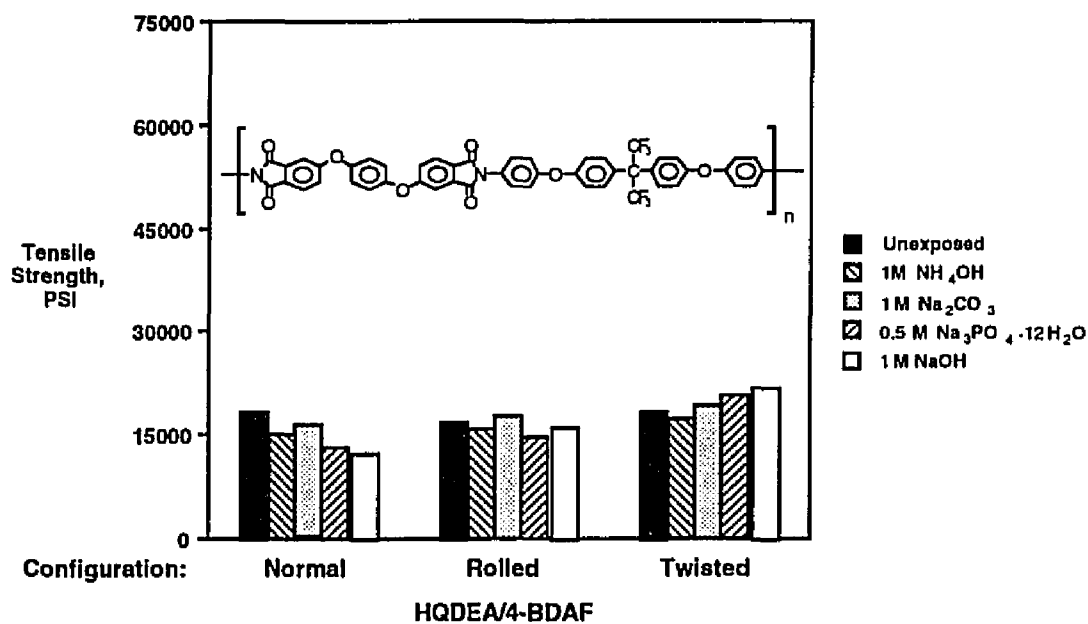




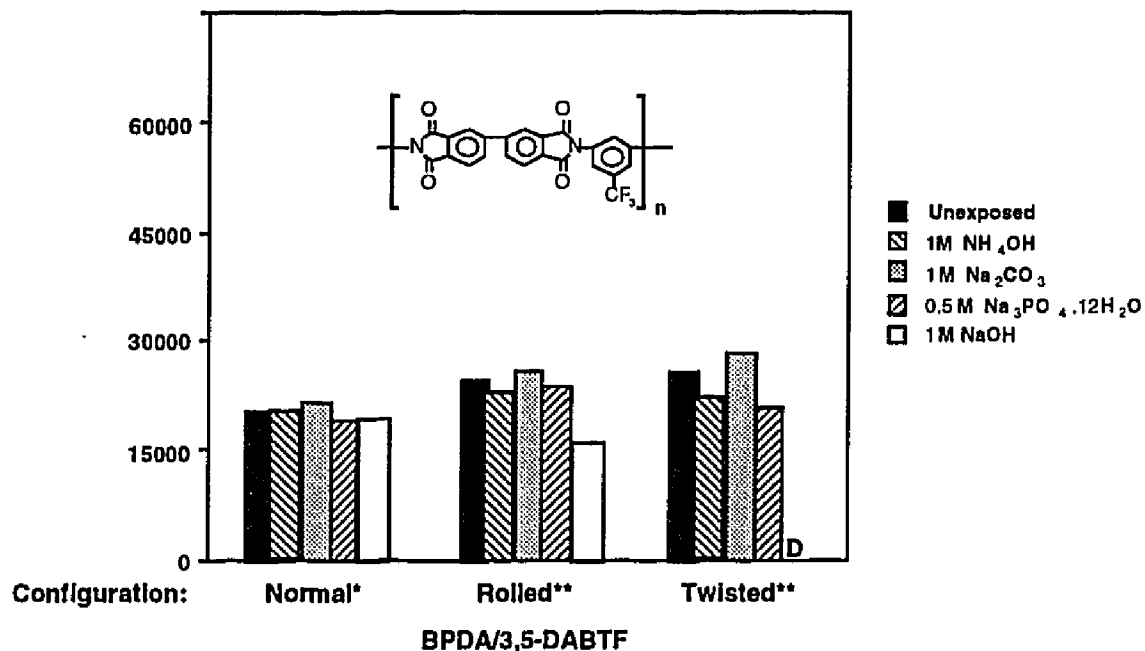
**Figure 6.49 Effect Of Chemical Exposure On Tensile Strength Of LaRC™. ITPI**

Figure 6.50 compares tensile strengths of HQDEA/4-BDAF. HQDEA/4-BDAF exhibited excellent retention of tensile strength as well as modulus and elongation in all cases. Another fluorinated polymer evaluated is shown in Figure 6.51. The BPDA/3,5-DABTF performed well except in the most caustic solution under stress. The twisted specimens in the sodium hydroxide test were deformed from curling and mechanical data could not be obtained. Retention of moduli of the BPDA/3,5-DABTF samples was excellent for all configurations. Elongations were affected in the ammonium hydroxide and sodium hydroxide solutions. However, since the elongation is strongly dependent on film quality and edge effects, it was difficult to draw a direct correlation to the exposure conditions. Figure 6.52 shows excellent retention of tensile strength in the

normal and rolled configurations of the 6F/3,5-DABTF system. However, the twisted configuration showed that the film specimens broke at the twisted sections during the exposure in ammonium hydroxide, trisodium phosphate, and sodium hydroxide. The film was brittle and therefore would be



**Figure 6.50 Effect Of Chemical Exposure On Tensile Strength Of HQDEA/4-BDAF**

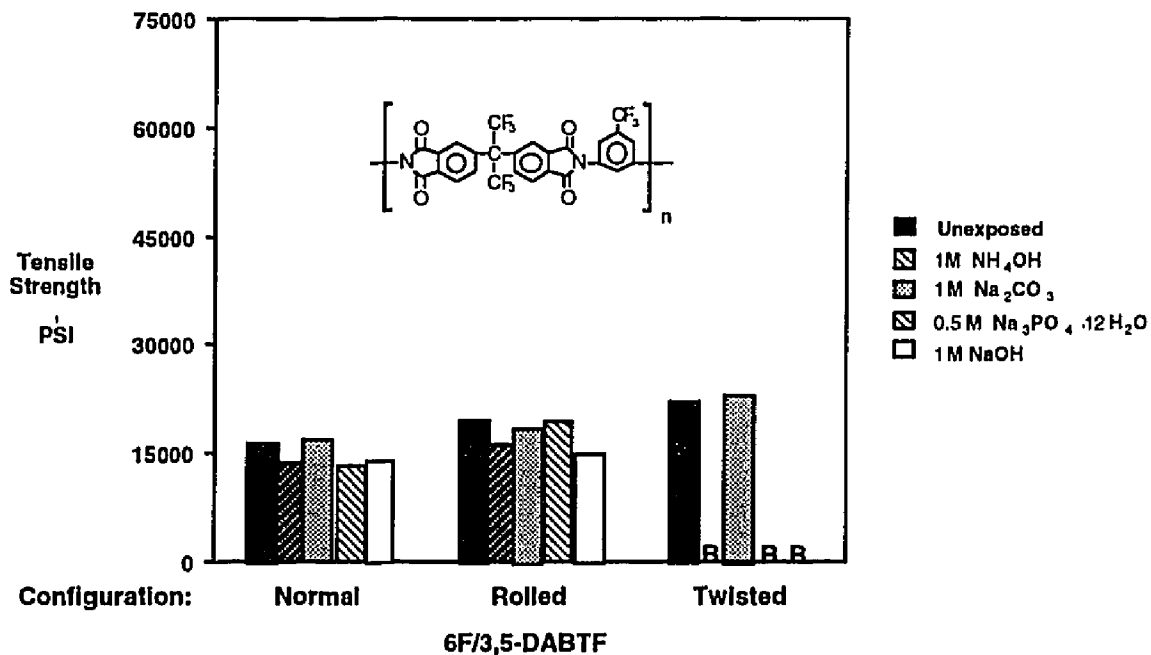


\* 3,5-DABTF prepared in-house

\*\* 3,5-DABTF provided by OXYCHEM

D = Specimens deformed

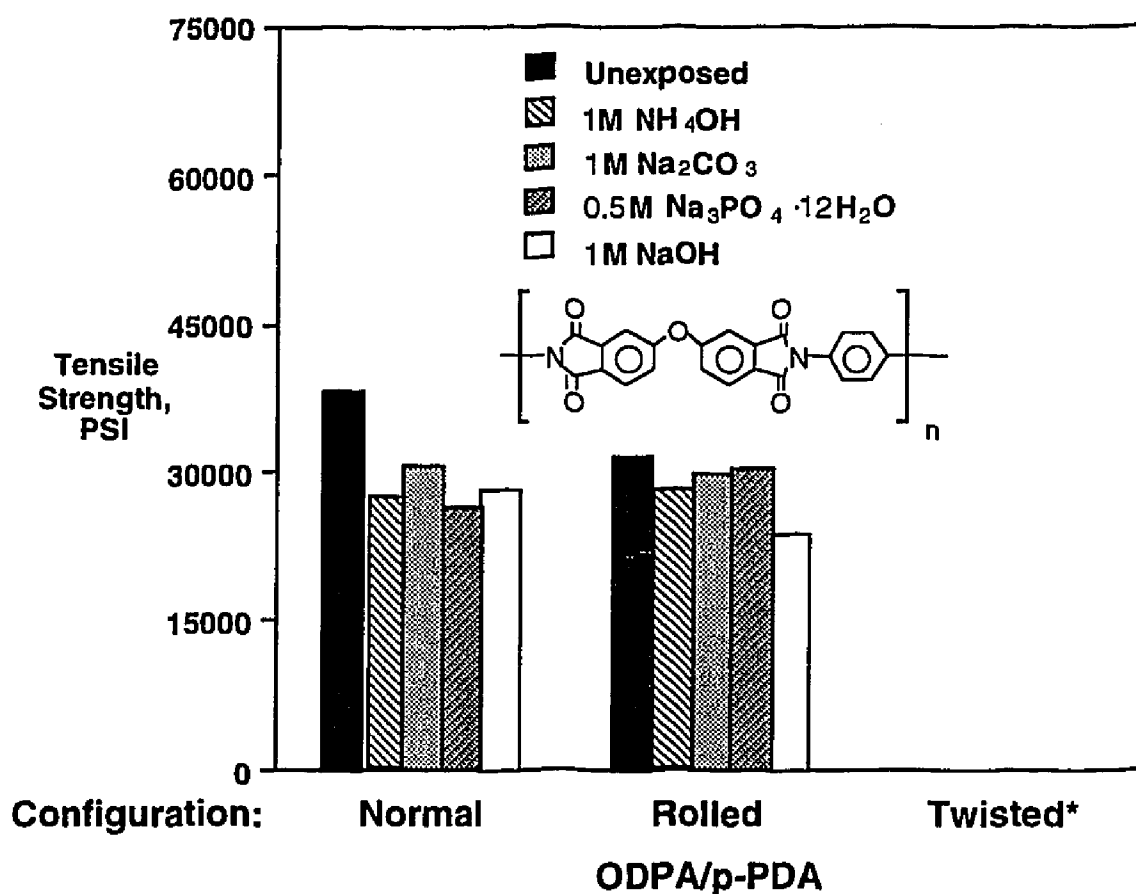
**Figure 6.51 Effect Of Chemical Exposure On Tensile Strength Of BPDA/3,5-DABTF**



**Figure 6.52 Effect Of Chemical Exposure On Tensile Strength Of 6F/3,5-DABTF**

most affected by the stress induced from twisting. These stress sites would be more susceptible to attack from the more caustic solutions. Modulus and elongation retention were good.

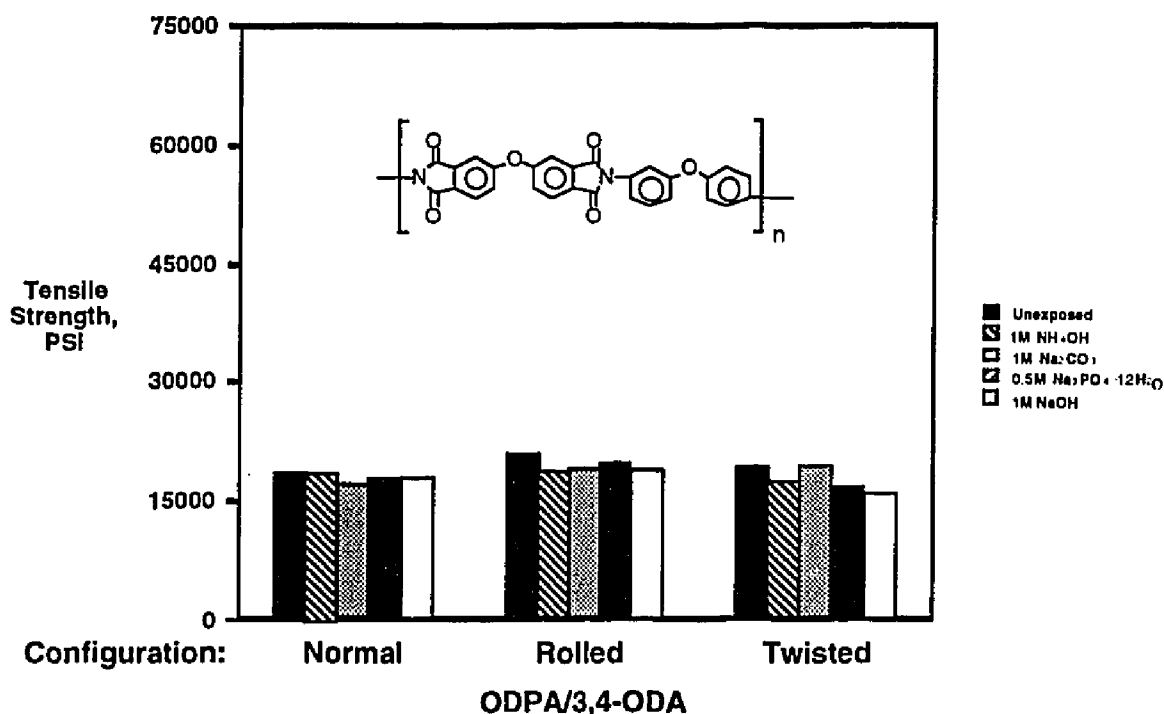
Figure 6.53 showed that ODPA/*p*-PDA exhibited good retention of tensile strength for the normal and rolled configurations but specimens broke from the twisting stress prior to exposure in the basic solutions. Moduli and elongation retention were good.



\* Specimens broke during twisting

Figure 6.53 Effect Of Chemical Exposure On Tensile Strength Of ODPA/*p*-PDA

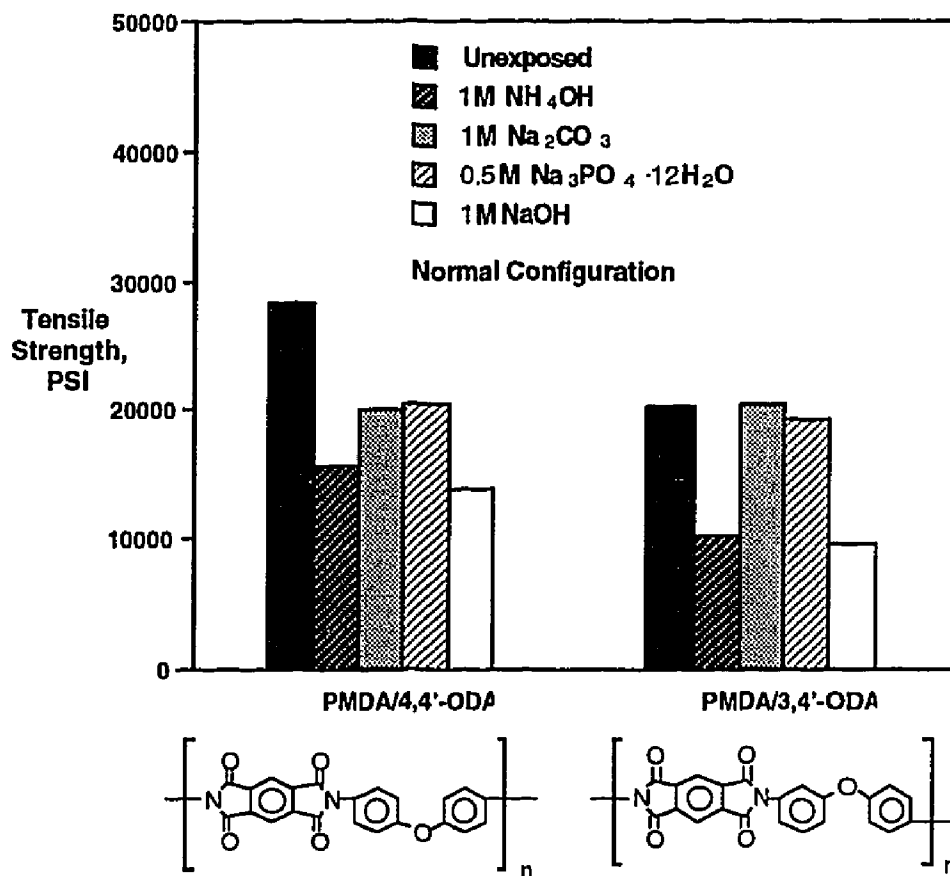
Figure 6.54 compares the tensile strength of the ODPA/3,4'-ODA (LaRC™-IA) system. ODPA/3,4'-ODA exhibited excellent retention of tensile strength as well as modulus and elongation. Figure 6.55 compares two PMDA based systems for the normal configurations only. PMDA/3,4'-ODA did not perform well in the exposure and was not evaluated in the stressed configurations. The laboratory version of Kapton® (PMDA/4,4'-ODA) was only evaluated in the normal configuration. ODPA based polyimides were more resistant to base hydrolysis than similar PMDA polymers.



**Figure 6.54 Effect Of Chemical Exposure On The Tensile Strength Of ODPA/3,4'-ODA**

Several polyimides were selected for evaluation for resistance to degradation to various aqueous solutions[41-42]. Commercially available PMDA based films appeared to be least resistant to hydrolysis of the

polyimides evaluated. LaRC™-CPI, LaRC™-IA (ODPA/3,4'-ODA), and HQDEA/4-BDAF exhibited excellent resistance to hydrolysis while under stress.



**Figure 6.55 Effect Of Chemical Exposure On Tensile Strength Of PMDA Polyimides**

### 6.3.2 Radiation Resistant Polyimides

NASA's increased commitment to the exploration of outer space and the use of orbital instrumentation to monitor the Earth has focused attention on the organic polymeric materials for a variety of applications in space. Certain high performance polymers offer attractive features such as low density, high strength, optical transparency, and low dielectric constant. Polymeric matrix composites also offer weight savings, high strength, stiffness, and dimensional stability. Certain polymeric materials have exhibited short-term (3-5 yr) space environmental durability; however, future spacecraft are being designed with lifetimes projected to be 10-30 years. This gives rise to concern that material property change brought about during operation may result in unpredicted spacecraft performance[43]. Of particular concern is the electron radiation component of the geosynchronous orbit (GEO) environment that will deposit an appreciable in-depth radiation dose ( $10^9$ - $10^{10}$  rads) during a typical 30 year exposure[44].

Depending on the altitude and inclination, a spacecraft in orbit around the Earth can be subjected to the simultaneous effects of thermal cycling, atomic oxygen, ultraviolet radiation (UV), charged particles (electrons, protons, etc.), and high vacuum. To develop space durable polymeric materials, the mechanisms of environmentally induced degradation should be understood. This poses a difficult problem as no ground based simulation facility exists which can accurately reproduce all aspects of a particular space environment. Available facilities use either combined exposures (e.g., electrons and UV) or sequential exposures, in an attempt to simulate a specific orbital environment. However, the use of sequential exposures may be misleading because of the absence of synergistic effects such as those

believed to occur when copolyperfluoroethylene propylene (FEP) is exposed to atomic oxygen and UV simultaneously[45]. In addition, simulation of 30 years of exposure in a reasonable amount of time requires high dose rates.

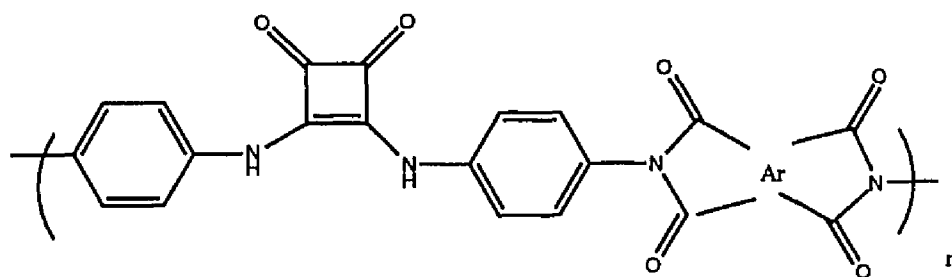
In an effort to develop electron radiation-resistant materials, polyimides containing squaric acid derivatives were synthesized, characterized, and evaluated for potential space applications. The polyimide films were then exposed to 1 MeV electrons using a Radiation Dynamics, Inc., Dynamitron Model 1000/10 accelerator. Total dosages were  $5 \times 10^7$  rads and  $1 \times 10^9$  rads electron radiation without interruption at  $2 \times 10^{-7}$  torr pressure. These dosages simulated short-term exposure (5-10 yr) and long-term exposure (25-30 yr) in GEO, respectively. Exposure to electrons can cause chain scission as well as crosslinking; often these two effects are in competition. Crosslinking may increase the tensile strength, modulus, and  $T_g$ , but decrease elongation. Chain scission would decrease all of these parameters. The retentions of mechanical properties at RT, 177°C, and 232°C after electron radiation exposures were then determined.

The preliminary study evaluated polyimides containing the squaric acid diamine (SAPPD) with the following dianhydrides: BTDA, ODP, PMDA, and BPDA. SAPPD was prepared by stirring 1,4-diaminobenzene dissolved in methanol with a solution of the diethylester of squaric acid in methanol at room temperature under a nitrogen atmosphere. The stirring was stopped after three days, and the SAPPD precipitated as a crystalline material when the reaction mixture was allowed to stand for several hours. The SAPPD was collected by filtration, washed with methanol, and dried under vacuum. The SAPPD that was used for this work was obtained free of charge from Kwoya Hakko Kogyo Co., Ltd., Japan. Different cure cycles were examined to determine the cure



temperature which would afford the best quality film for examination. No electron exposures or mechanical properties were performed for this series.

Figure 6.56 illustrates the weight loss characteristics of squaric acid polyimides with cure temperatures of 200, 300, and 400°C. Temperatures at which 5%, 25%, and 50% weight loss occurred were reported. Also included was the physical character of the films defined by color and flexibility.



Weight loss  
Temperature, °C

Ar	$\eta$ , dL/g	Cure , °C	5%	25%	50%	Physical character
BTDA	1.19	200	283	490	531	Orange/brown; flexible
ODPA	0.77	200	259	458	516	Yellow/Brown; Brittle
PMDA	64	200	206	453	516	Orange/brown; brittle
BPDA	0.64	200	317	491	529	Light brown; brittle
BTDA	1.19	300	329	500	532	Red/brown; Flexible
ODPA	0.77	300	317	494	527	Yellow/brown flexible
PMDA	1.64	300	309	462	514	brown/orange; flexible
BPDA	0.64	300	319	507	540	Light brown; brittle
BTDA	1.19	400	337	491	526	Red/brown; flexible

Figure 6.56 LaRC™ Squaric Acid Polyimides

Inherent viscosities ranged from 0.64 to 1.64 dL/g. Temperatures were reported for weight losses of 5, 25, and 50%. The lowest weight loss temperatures were observed with the 200°C cure cycle. This was expected since the polyimide film was not fully cured and residual solvent could remain in the sample. The BTDA/SAPPD system was the only flexible film for the 200°C series. All films were translucent but not transparent after the 200°C cure, which indicated crystallinity; however, no melting was noted on the DSC thermogram.

The films cured at 300°C showed an increase for the 5% weight loss temperatures, except for the BPDA/SAPPD polyimide which had approximately the same 5% weight loss temperature after curing at 200°C and 300°C. Thermo-oxidative stabilities at 300°C (where the polyimides should be fully imidized) were very similar. The electron deficiencies for BTDA, PMDA, ODPDA, and BPDA are similar and the same diamine was used for each polymer, so similar thermo-oxidative stabilities were postulated. Translucency persisted after the 300°C cure. The ODPDA/SAPPD film was flexible when cured at 300°C. The BTDA/SAPPD polymer was flexible after the 300 and 400°C cures.

Due to the brittleness of the polyimides synthesized from PMDA and BPDA with the SAPPD diamine, these polymers were not included in the electron radiation-resistant study. Instead, polyimides synthesized from IPAN and Si(CH<sub>3</sub>)<sub>2</sub>DA were utilized along with the flexible polyimide films from the preliminary work.

Table 6.3 shows the inherent viscosities and thermal analysis of the four polyimides evaluated for radiation resistance. Structures and acronyms are illustrated in Table 4.4 in Chapter 4: Experimental Section.

POLYIMIDE	$\eta^1$ , dL/g	Tg <sup>2</sup> , °C	Tg <sup>3</sup> , °C	Tg <sup>4</sup> , °C	ITGA <sup>5</sup> , %
BTDA/SAPPD	1.60	320	>400	>400	60.3
ODPA/SAPPD	1.21	300	382	362	47.5
IPAN/SAPPD	1.12	324	340	335	39.0
Si(CH <sub>3</sub> ) <sub>2</sub> DA/SAPPD	1.28	333	338	334	68.1
	TGA <sup>6</sup> , °C	TGA <sup>7</sup> , °C	TGA <sup>8</sup> , °C		
BTDA/SAPPD	338	352	345		
ODPA/SAPPD	387	359	352		
IPAN/SAPPD	348	333	348		
Si(CH <sub>3</sub> ) <sub>2</sub> DA/SAPPD	361	355	337		

<sup>1</sup>Determined on 0.5% poly(amide acid) solutions (DMAc, 25°C)

<sup>2</sup>Tgs of thin films after curing 1 hr each at 100, 200, and 300°C by TMA at 3°C/min.

<sup>3</sup>Tgs of thin films by TMA after exposure to  $5 \times 10^7$  rads electron radiation.

<sup>4</sup>Tgs of thin films by TMA after exposure to  $1 \times 10^9$  rads electron radiation.

<sup>5</sup>% weight retention of film after 100 hr at 350°C.

<sup>6</sup>Temperature of 5% weight loss by thermogravimetric analysis in air at a heating rate of 2.5°C/min.

<sup>7</sup>Temperature of 5% weight loss of thin films after exposure to  $5 \times 10^7$  rads electron radiation.

<sup>8</sup>Temperature of 5% weight loss of thin films after exposure to  $1 \times 10^9$  rads electron radiation.

**Table 6.3 Thermal Analysis of LaRCT<sup>TM</sup> Squaric Acid Polyimides**

Inherent viscosities for all polyimides were high. Higher inherent viscosities for the ODPA and BTDA polymers compared to the preliminary

evaluation values were attributed to the SAPPD monomer purity. A new batch of SAPPD diamine was obtained from Kwoya Hakko Kogyo, Ltd., Japan, and was vacuum-dried prior to use. Higher inherent viscosities of the poly (amic acid)s resulted. Films were very difficult to remove from the plate glass after curing. The  $\text{Si}(\text{CH}_3)_2\text{DA}/\text{SAPPD}$  polyimide was cast onto plate glass covered with Frekote® treated aluminum foil because it could not be removed from the glass plate. This indicated the possible adhesive applications for these systems.

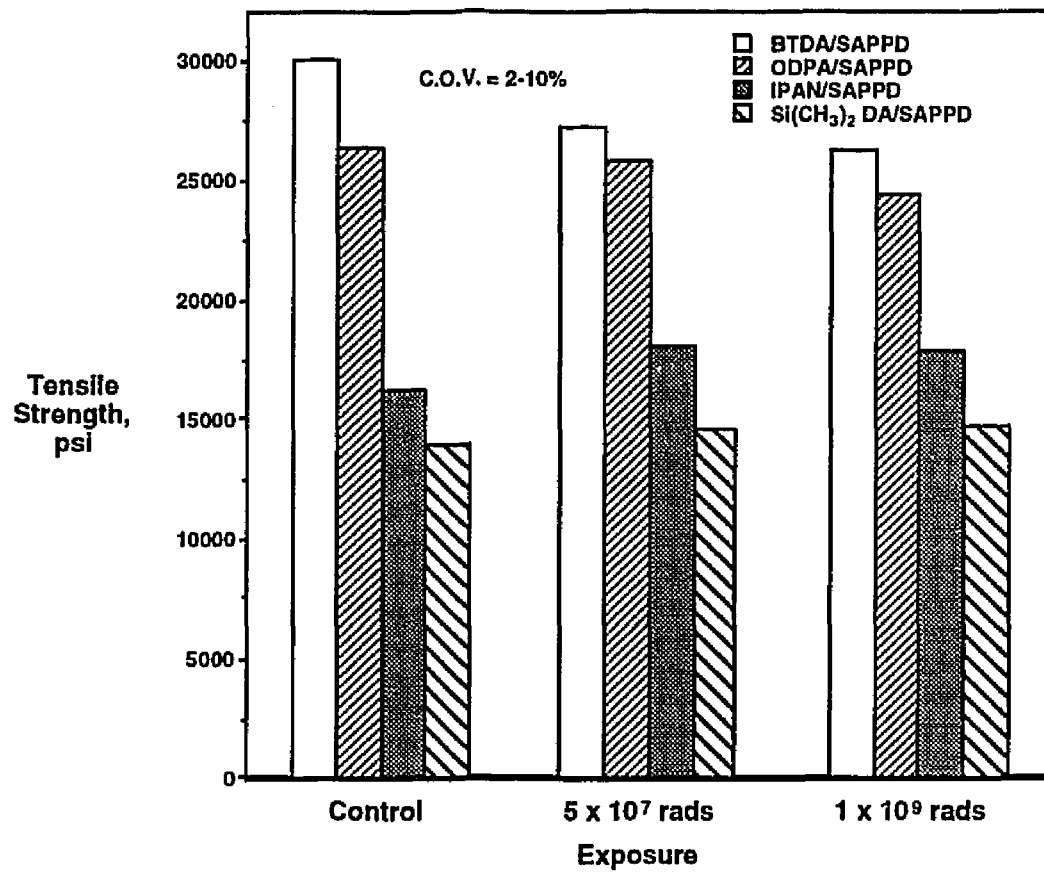
The  $T_g$ s by TMA did not differ significantly and all were greater than  $300^\circ\text{C}$  for the control film samples. The  $T_g$  by TMA for the BTDA/SAPPD increased from  $320^\circ\text{C}$  to  $> 400^\circ\text{C}$  for exposures of  $5 \times 10^7$  rads and  $1 \times 10^9$  rads. The  $T_g$  by TMA increased to  $382^\circ\text{C}$  after exposure to  $5 \times 10^7$  rads for the ODPa/SAPPD polyimide and increased to  $362^\circ\text{C}$  after exposure to  $1 \times 10^9$  rads. Increases in the  $T_g$ s after electron exposure may be the result of crosslinking. There was only a slight increase in  $T_g$ s observed for the IPAN/SAPPD and  $\text{Si}(\text{CH}_3)_2\text{DA}/\text{SAPPD}$  polyimides after both exposures.

Weight loss retention after an isothermal hold at  $350^\circ\text{C}$  for 100 hr ranged from 39.0 to 68.1% with the following thermal stability order: IPAN < ODPa < BTDA <  $\text{Si}(\text{CH}_3)_2\text{DA}$ . Weight loss of 5% was measured for the control film and the films exposed to  $5 \times 10^7$  rads and  $1 \times 10^9$  rads electron radiation. The temperature at which 5% weight loss occurred for BTDA/SAPPD increased slightly after exposure. The ODPa/SAPPD polyimide 5% weight loss temperature decreased slightly after exposure. There was little change in thermo-oxidative stability for the IPAN/SAPPD and  $\text{Si}(\text{CH}_3)_2\text{DA}/\text{SAPPD}$  polyimides after exposure.

There were several notable observations. All films adhered well to the glass plates and further investigation may indicate the usefulness of these

squaric acid polyimides as adhesives. There was a significant increase in the  $T_g$ s of the BTDA/SAPPD and ODPA/SAPPD polyimides after exposure to electron radiation, possibly due to crosslinking. This was not observed in the IPAN/SAPPD and  $\text{Si}(\text{CH}_3)_2\text{DA/SAPPD}$  polyimides. The highest weight retention was observed for the BTDA/SAPPD and  $\text{Si}(\text{CH}_3)_2\text{DA/SAPPD}$  polyimides for an isothermal hold at 350°C for 100 hr. Five percent weight loss temperatures did not change significantly after exposure to either  $5 \times 10^7$  rads or  $1 \times 10^9$  rads compared to the control films.

Tensile properties at RT, 177°C, and 232°C were measured for the control films and films of the two different electron radiation exposures. Room temperature (RT) tensile strengths, moduli, and elongations are shown in Figures 6.57-6.59. Tensile strengths for the control group ranged from 13.1 to 28.1 ksi. Tensile strength retentions for film specimens exposed to  $5 \times 10^7$  rads were greater than 90%; tensile strength retentions for film specimens exposed to  $1 \times 10^9$  rads were greater than 88%. The % coefficient of variance (%COV) is a measure of the experimental error and is shown in each figure. Moduli for the control group ranged from 496.3 to 961.6 ksi. Moduli retention at RT were greater than 93% for the exposed specimens compared to the control films. Elongations for the control group ranged from 3.7 to 9.5% with a %COV of 19 to 32%. Elongation was film quality dependent and, as expected, larger changes were reported than with tensile strengths and moduli. Elongations may decrease after exposure to electron radiation due to crosslinking.



**Figure 6.57 RT Tensile Strength Of Squaric Acid Polyimides After Exposure To Electron Radiation**

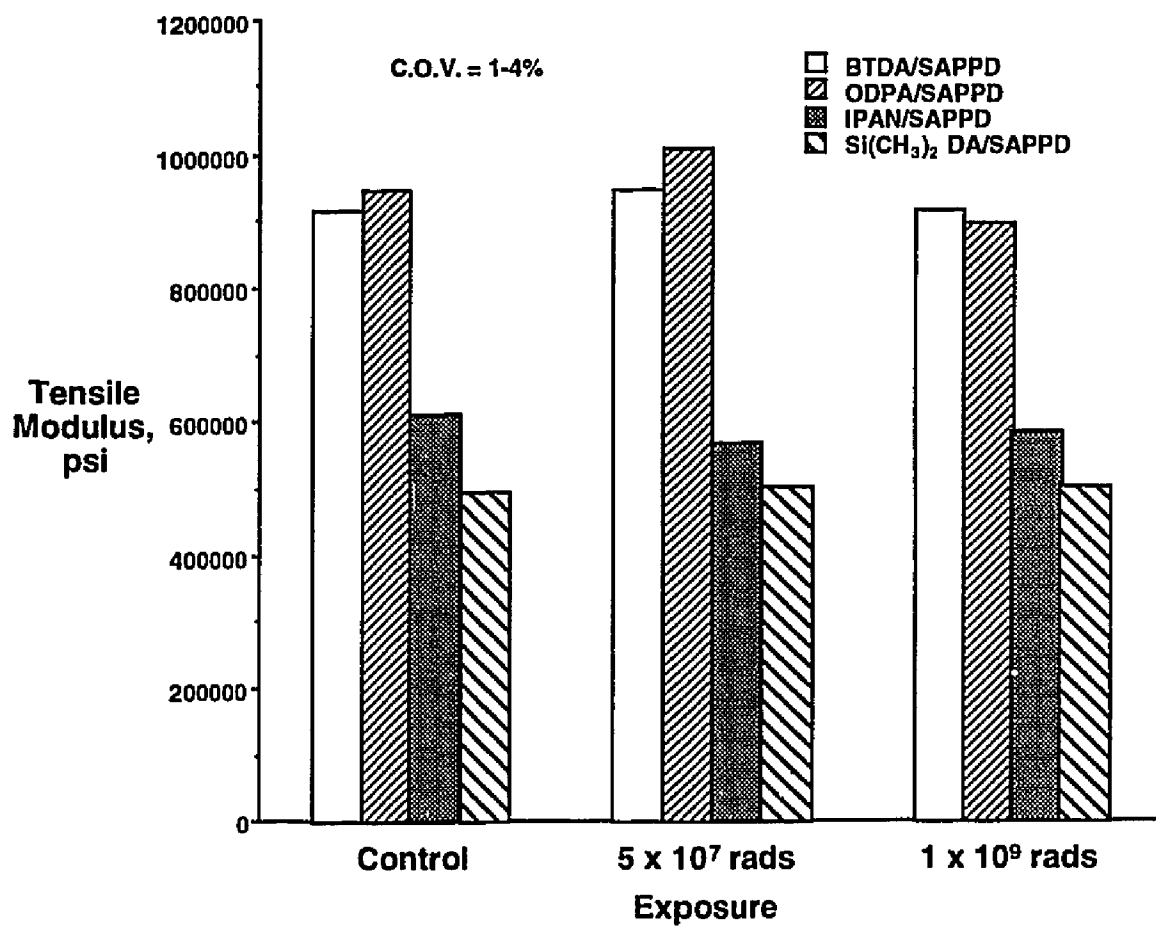
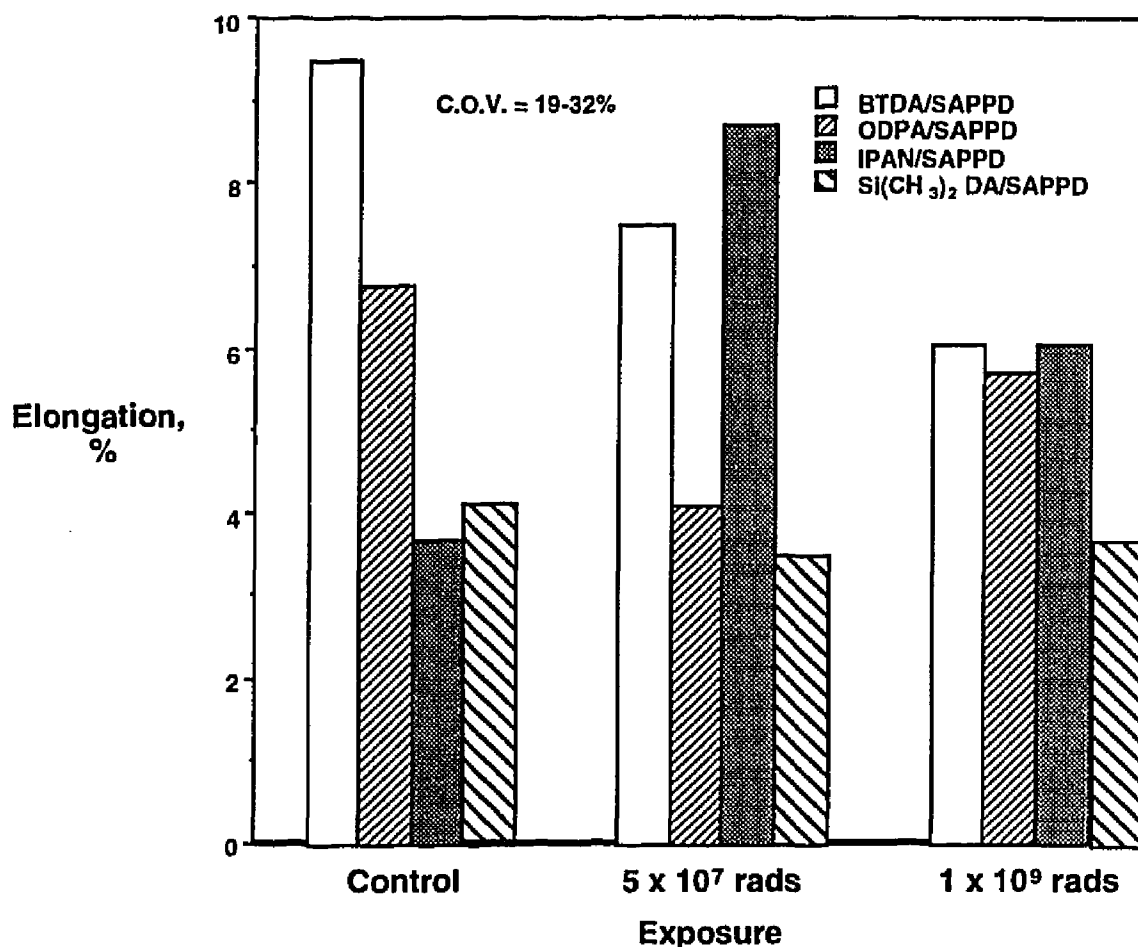


Figure 6.58 RT Moduli Of Squaric Acid Polyimides After Electron Radiation Exposure

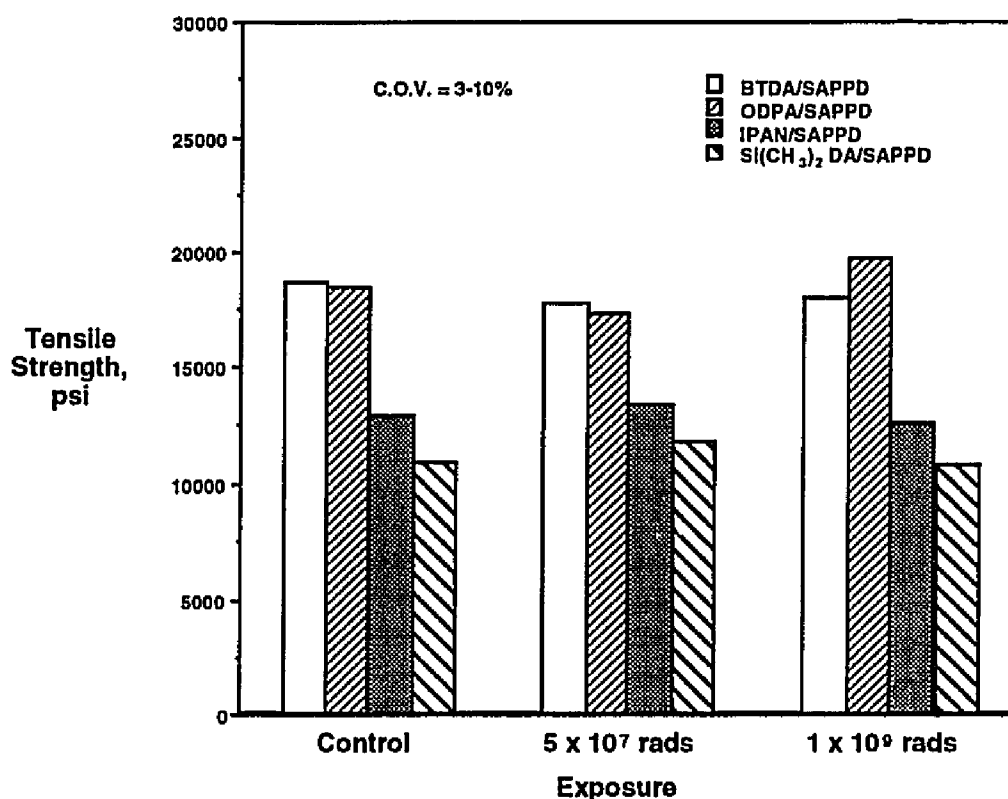




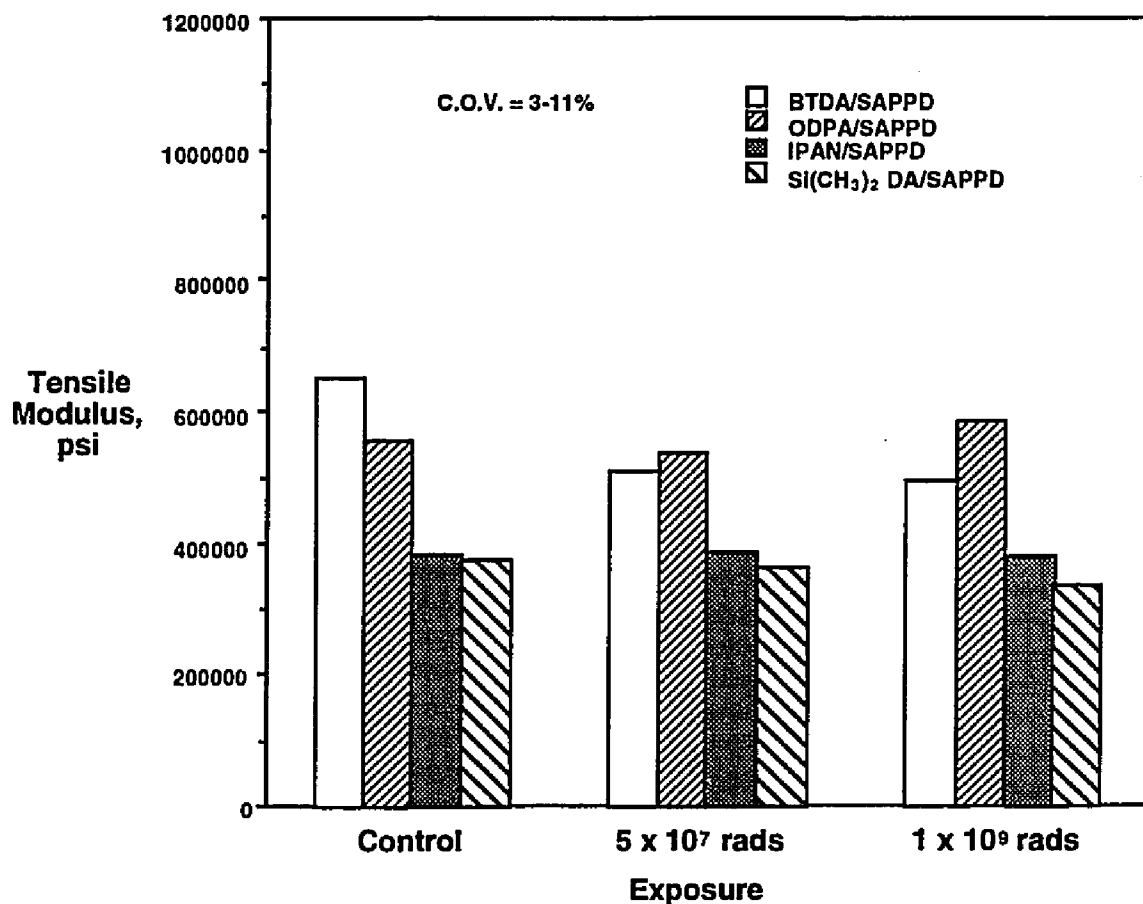
**Figure 6.59 RT Elongation Of Squaric Acid Polyimides After Exposure To Electron Radiation**

Film properties at 177°C are shown in Figures 6.60-6.62. Tensile strength retention of the control specimens at 177°C versus RT ranged from 67 to 86%. Higher retentions at 177°C were observed for the IPAN/SAPPD and Si(CH<sub>3</sub>)<sub>2</sub>DA/SAPPD compared to the BTDA/SAPPD and ODPA/SAPPD polyimides. Moduli retention at 177°C of the control specimens ranged from 58 to 78% with higher retentions observed for the IPAN/SAPPD and Si(CH<sub>3</sub>)<sub>2</sub>DA/SAPPD. Although the 177°C tensile strengths and moduli of the

control specimens decreased from their RT values, values did not change significantly for specimens exposed to electron radiation and tested at 177°C. Film specimens exposed to  $5 \times 10^7$  rads and tested at 177°C retained 67 to 91% of their tensile strength. Higher retentions were observed for the IPAN/SAPPD and  $\text{Si}(\text{CH}_3)_2\text{DA/SAPPD}$  compared to the BTDA/SAPPD and ODPDA/SAPPD polyimides. Moduli retention for specimens exposed to  $5 \times 10^7$  rads and tested at 177°C was 54 to 74%. Higher retentions were observed with the IPAN/SAPPD and  $\text{Si}(\text{CH}_3)_2\text{DA/SAPPD}$  polyimides.

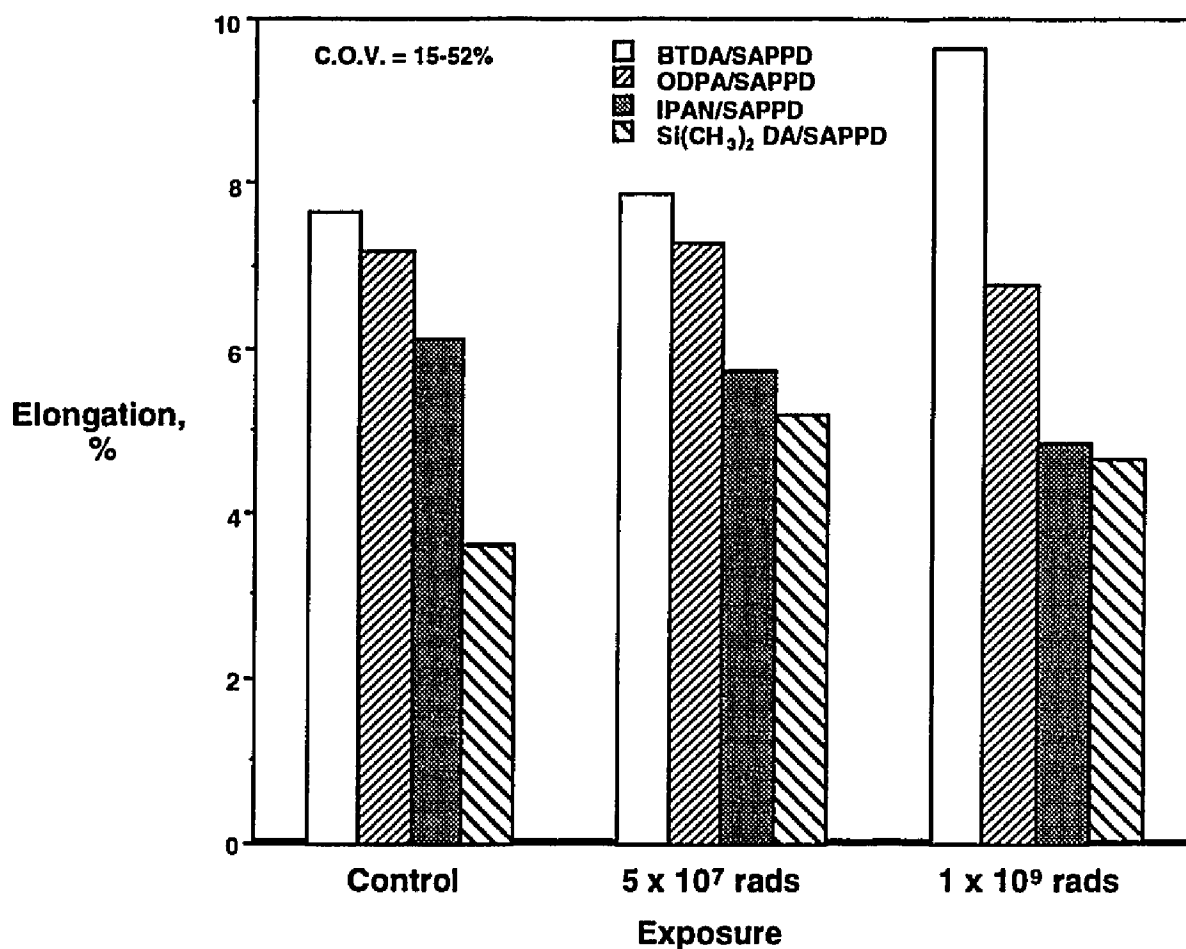


**Figure 6.60 177°C Tensile Strength Of Squaric Acid Polyimides After Exposure To Electron Radiation**



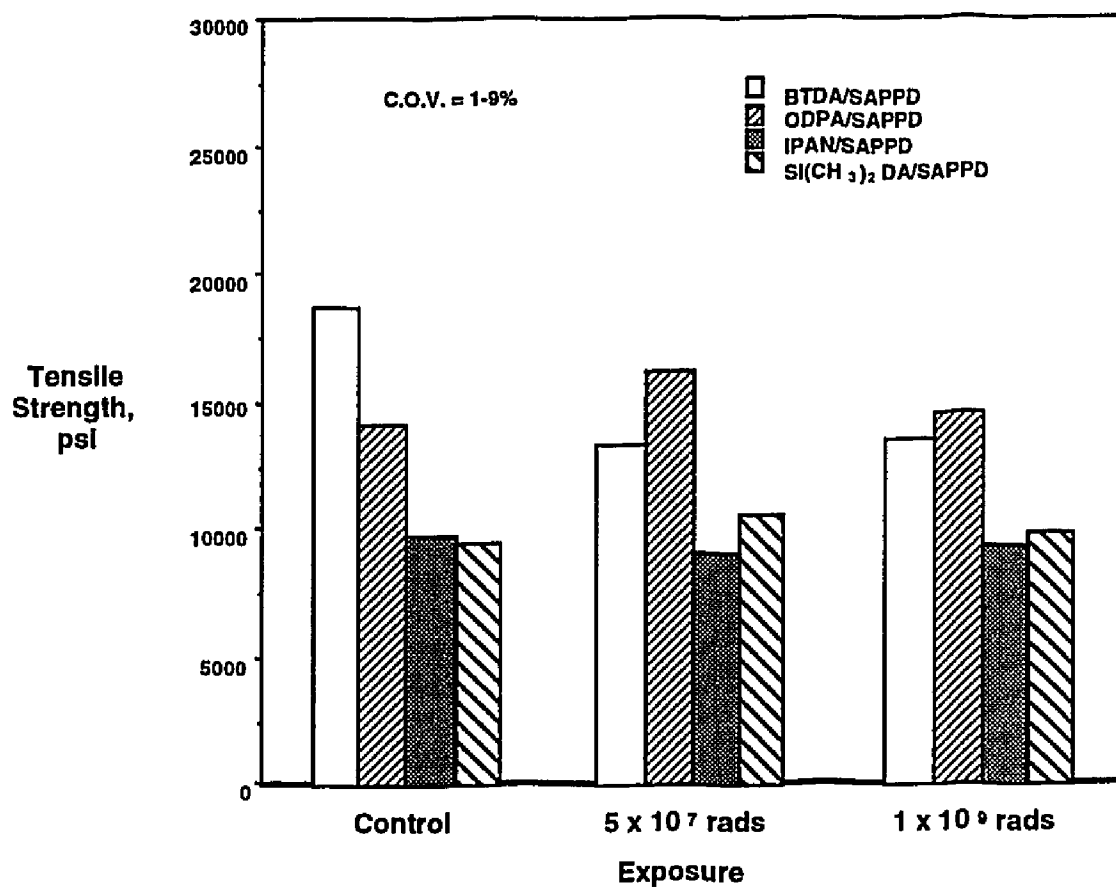
**Figure 6.61 177°C Moduli Of Squaric Acid Polyimides After Exposure To Electron Radiation**

Elongations did not change significantly after exposure to the two different electron radiation dosages. However, the %COV was very high (15-52%), which indicated the data were not reproducible.



**Figure 6.62 177°C Elongation Of Squaric Acid Polyimides After Exposure To Electron Radiation**

Mechanical properties at 232°C for the control films and radiation exposure films are shown in Figure 6.63-6.65. Retentions of tensile strength at 232°C for the control group ranged between 58 to 70%. These were excellent retentions considering the extreme temperature. Tensile strength retentions at 232°C of films exposed to 5 x 10<sup>7</sup> rads was 43 to 72%. Tensile strength retentions of films exposed to 1 x 10<sup>9</sup> rads ranged from 55 to 65%.



**Figure 6.63 232°C Tensile Strength Of Squaric Acid Polyimides After Exposure To Electron Radiation**

Moduli retention at 232°C for the control group ranged between 42 to 47%. Moduli retention ranged from 46 to 67% for films exposed to  $5 \times 10^7$  rads. Moduli retention of films exposed to  $1 \times 10^9$  rads was 42 to 47%.

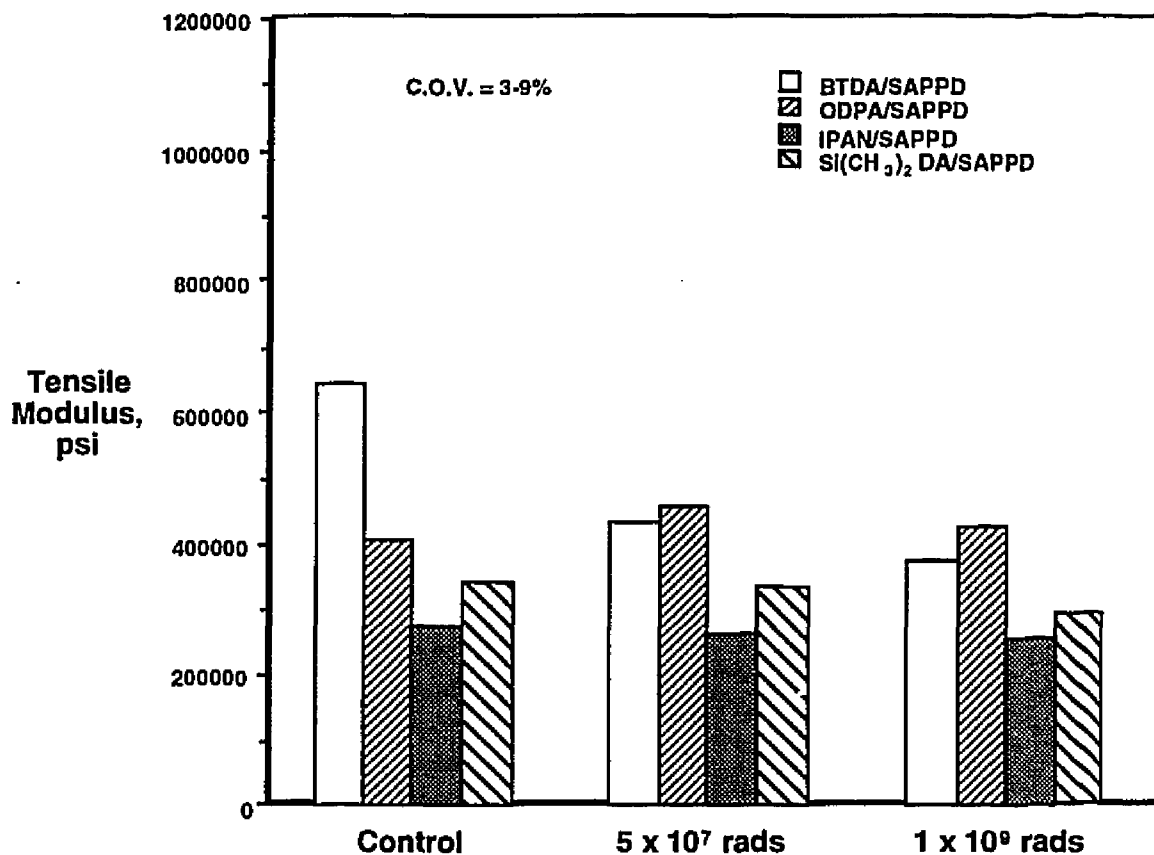
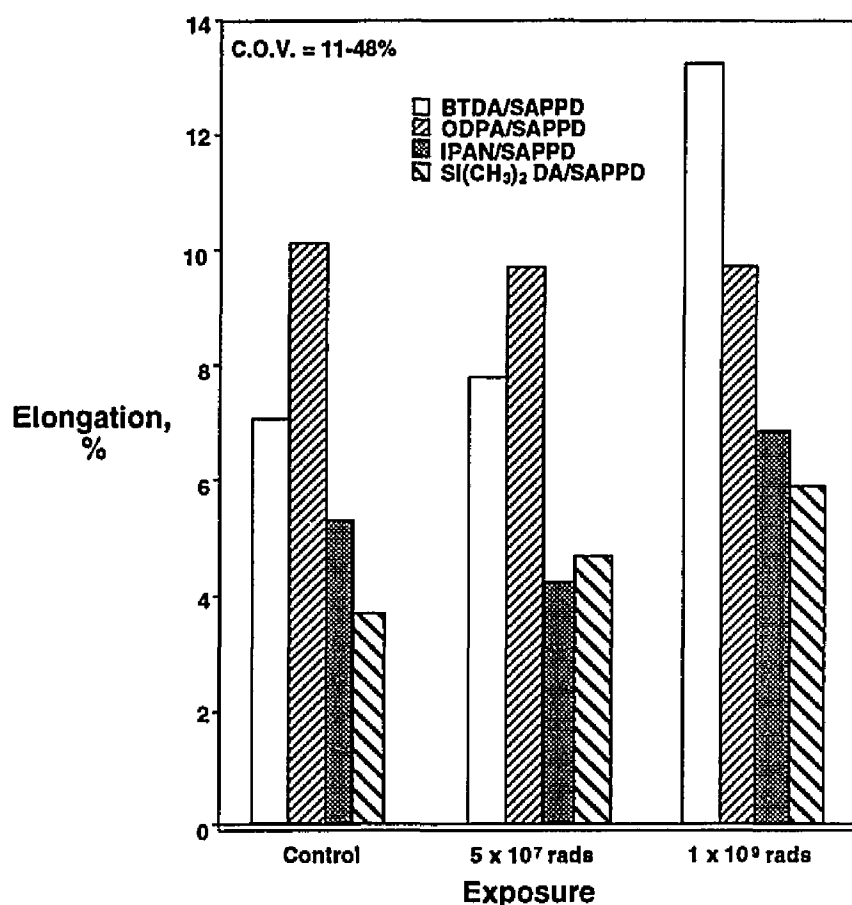


Figure 6.64 232°C Tensile Modulus Of Squaric Acid Polyimides After Exposure To Electron Radiation



**Figure 6.65 232°C Elongation Of Squaric Acid Polyimides After Exposure To Electron Radiation**

Some general trends were noted. The BTDA/SAPPD and ODPAs/SAPPD polyimides had higher tensile strengths and moduli than the IPAN/SAPPD and Si(CH<sub>3</sub>)<sub>2</sub>DA/SAPPD polyimides. However, higher retentions of tensile strength and moduli at elevated temperatures were observed for the IPAN/SAPPD and Si(CH<sub>3</sub>)<sub>2</sub>DA/SAPPD polyimides. The decrease in properties was attributed to the elevated temperatures and not the electron radiation exposures since there was not much change for a given temperature. The squaric acid polyimides showed good resistance to electron radiation even at elevated temperatures

and would be potentially useful in space applications in GEO as coatings, encapsulants, or adhesives.

Linear aromatic polyimides containing SAPPD exhibited high thermal and thermo-oxidative stabilities, which make them useful in structural components exposed to hot and/or oxidative environments, as in jet engines and on the outer surfaces of supersonic aircraft. The SAPPD polyimides demonstrated excellent retention of mechanical properties when exposed to high-energy radiation. In addition, electrons in the SAPPD moieties are known to be readily excited to states of higher energy upon exposure to ultraviolet light[46], giving rise to electronic properties with potential utility in photovoltaic, photoconductive, and/or photoemissive devices, for example.



## 6.4 REFERENCES

1. Paolo La Mantia, F., *Thermotropic Liquid Crystal Polymer Blends*, Technomic: Lancaster, PA, 1993.
2. Evans, D.; Morgan, J. T. *Cryogenics* **1991**, *31*, 220-222.
3. Collyer, A. A. *Materials Science and Technology* **April 1989**, *5*, 309-322.
4. *High Modulus Polymers: Approaches to Design and Development*, Zachariades, A. E.; Porter, R. S. , Eds.; Marcel Dekker: New York, 1988.
5. *Liquid Crystallinity in Polymers: Principles and Fundamental Properties*; Ciferri, A. , Ed.; VCH Publishers: New York, 1991.
6. *Polymeric Liquid Crystals*; Blumstein, A., Ed.; Plenum: New York, 1983.
7. Hergenrother, P. M.; Jensen, B. J.; Havens, S. J. *Polymer* **Feb. 1988**, *Vol. 29*, 358-369.
8. March, J. *Advanced Organic Chemistry, Third Edition*; John Wiley and Sons: NY, 1985.
9. Staniland, P. A.; Wilde, C. J.; Bottino, F. A.; Di Pollicino, G.; Recca, A. *Polymer* **1992**, *Vol. 33, No. 9*, 1976-1981.
10. Schwartz, Jr., W. T. *High Performance Polymers* **1990**, *Vol. 2, No. 2*, 189-196.
11. Schwartz, Jr., W. T. U. S. Patent 4 868 316, September 1989.
12. Clark, J. H.; Owen, N. D. S. *Tetrahedron Letters* **1987**, *28(31)*, 3627-3630.
13. Aranuma, T.; Oikawa, H.; Ookawa, Y.; Yamaguchi, A. *Polym. Prepr.* **1993**, *34 (2)*, 827.
14. Yamaguchi, K.; Urakami, U.; Tanabe, Y.; Yamazaki, M.; Tamai, S.; Yamaya, N.; Ohta, M.; Yamaguchi, A. Eur. Pat Appl. EP 425 265, May 2, 1991; *Chem. Abstr.* **1992**, *115*, 93782n.
15. Fay, C. C.; Smith, Jr., J. G.; St. Clair, T. L. *Polymer Preprints* **1994**, *35(1)*, 541-542.

16. Smith, Jr., Joseph G., NASA Langley Research Center, Composites and Polymers Branch, Polymer Scientist, unpublished results, 1993-94.
17. Tai, H.; Phillips, D. H., NASA Technical Memorandum 101674, June, 1990; p 1-97.
18. Hinkley, J. A., NASA Langley Research Center, Composites and Polymers Branch, Polymer Scientist, unpublished results.
19. Takahashi, N.; Yoon, D. Y.; Parrish, W. *Macromolecules* **1984**, *17*, 2583-2588.
20. Ronca, G.; Yoon, D. Y. *J. Chem. Physics* **1984**, *80*, 930.
21. Fay, C. C.; Smith, Jr., J. G.; St. Clair, T. L. Presented at the Gordon Research Polymer Conference, Wolfeboro, NH, July 3-8, 1994.
22. Noel, C.; Laupretre, F.; Freidrich, C.; Fayolle, B.; Bosio, L. *Polymer* **1984**, *25*, 808.
23. Meurisse, P.; Noel, C.; Monnerie, L.; Fayolle, B. *Brit. Polym. J.* **1981**, *13*, 55.
24. Krigbaum, W. R.; Watanabe, J. *Polymer* **1983**, *Vol. 24*, 1299.
25. Senturia, S. D. *Proc. of the ACS Div. of Polym. Mat.: Sci. and Eng.* **1986**, *55*, 1986, 385.
26. Stoakley, D. M.; St. Clair, A. K.; Baucom, R. M. Presented at the SAMPE Electronic Conference, Los Angeles, CA, June 19-22, 1989.
27. St. Clair, A. K.; Slemp, W. S. *SAMPE Journal* **1985**, *Vol. 21 (4)*, 1985, 28-33.
28. Research Triangle Institute, NASA Langley's Colorless and Low Dielectric Polyimide Thin Film Technologies, May, 1994.
29. St. Clair, A. K.; St. Clair, T. L.; Winfree, W. P. Presented at the National Meeting of the American Chemical Society, Los Angeles, CA, Sept. 25-30, 1988; *Proceeding of the Division of Polymeric Materials: Science and Engineering* **1988**, *Vol. 59*, 28.

30. Jones, R. J.; O'Rell, M. K. US Patent 4 196 277, 1980.
31. Stoakley, D. M.; St. Clair, A. K.; Croall, C. I. *Journal of Applied Polymer Science* **1994**, Vol. 51, 1479-1483.
32. St. Clair, T. L. In *Polyimides*; Wilson, D.; Stenzenberger, H. D.; Hergenrother, P. M., Eds.; Chapman & Hall: NY, 1990; p 58-70.
33. Eftekhari, A.; St. Clair, A. K.; Stoakley, D. M.; Sprinkle, D. R.; Singh, J. J. In *Polymers For Microelectronics, Resists And Dielectrics* **1994**, Chapter 38, 535-545.
34. Progar, D. J.; St. Clair, T. L. *Journal of Adhesion Science and Technology* **1990**, Vol. 4, No. 7, 527-549; U S Patent 5 147 966, September, 1992.
35. St. Clair, A. K.; St. Clair, T. L.; Winfree, W. P. *Polymeric Materials: Science and Engineering* **1988**, 59, 28-32.
36. St. Clair, A. K.; St. Clair, T. L.; Winfree, W. P. U.S. Patent Application Serial No. 071073542, 1987.
37. Gerber, M. K.; Pratt, J. R.; St. Clair, A. K.; St. Clair, T. L. *Polymer Preprints* **1990**, 31, 340.
38. Goff, D. L.; Yuan, E. L. *Polymeric Materials: Science and Engineering* **1988**, 59, 186-189.
39. Kreuz, J. A., E. I. DuPont de Nemours and Company, Electronics Department, Circleville, Ohio, unpublished results.
40. Bessonov, M. I.; Koton, M. M.; Kudryavtsev, V. V.; Lains, L. A. *Polyimides, Thermally Stable Polymers*, 1987; p 151-157.
41. Croall, C. I.; St. Clair, T. L., NASA Technical Memorandum 104202, January, 1992.
42. Croall, C. I.; St. Clair, T. L. *Journal of Plastic Films and Sheeting* **July 1992**, Vol. 8, No. 3, 172-190.

43. Connell, J. W.; Siochi, E. J.; Croall, C. I. *High Performance Polymers* **1993**, *5*, 1-14.
44. Funk, J. G.; Sykes, Jr., G. F. *SAMPE Quarterly* **1988**, *Vol. 19, No. 3*, 19-26.
45. Stiegman, A. E.; Brinza, D. E.; Anderson, M. S.; Minton, T. K.; Laue, F. G.; Liang, R. H., Jet Propulsion Laboratory Publication 90-10, 1991.
46. Scott, Gary W., "Development of Organic Thin Film Solar Cells for Space Applications", CalSpace Proposal CS-11-92, April 1992; p 3-9.

## Chapter 7: Applications

### 7.1 Potential Liquid Crystalline Polyimides

Liquid crystalline polymers (LCP)s have combined properties exhibited by conventional amorphous polymers and conventional crystalline polymers, making them good replacement candidates where metals, thermosets, ceramics, and other high performance thermoplastics were previously used[1]. The performance requirements for printed circuit boards (mechanical strength and toughness, good processability and molding to tight tolerances, dimensional stability, chemical resistance, and low CTE) are met with LCPs but their high cost is a barrier despite their excellent properties.

#### 7.1.1 Repairable Adhesives

Zymet, Inc., East Hanover, New Jersey, was looking for a polymer system for utilization as a "repairable" adhesive. The company wanted an adhesive to attach electronics packages to substrates. If the microelectronics package needed repair, the adhesive must give way or liquefy below 200°C so that the package can be removed without additional heat or pressure. It should give way (liquefy) very easily at 170-200°C, yet have excellent mechanical properties at 150°C and below. Low CTE, good processability, and low moisture absorption were also required. Zymet, Inc. was sent two novel polyimide films and five blends of extruded ribbon. One copolymer designation

was 1,3-BAPDBB/0.75 BTDA/0.25 BPDA with 3% PA endcapper. The stoichiometric offset was 1.5%. Also evaluated was BMDEDA/*p*-PDA polymer. Both films were excellent adhesives but did not give way below 200°C. Although the  $T_g$ s were below 200°C, the softening of the polyimide film was not enough to remove the electronic package from the substrate. Use of higher temperatures was being attempted at Zymet, Inc. but the preferred melting temperature range was 200°C or below. The five blends sent to Zymet, Inc. were comprised of LaRC™-IA (Improved Adhesive) and a liquid crystalline polyimide powder from Mitsui Toatsu (LC-PI). Weight loadings of the LC-PI ranged between 5 and 25%. The melt transition temperatures exceeded the desired range (>250°C). Zymet, Inc. is presently evaluating an experimental material from Hoescht but it does not have good processability. Zymet, Inc. would be interested in samples for evaluation should any liquid crystalline or crystalline materials be developed that have low melt temperatures.

## **7.2 Polyimides For Microelectronic Applications**

From the early 1950's, polymers have played a key role in the growth of the semiconductor industry. The polymer industry has furnished a variety of materials, ranging from radiation sensitive resists used to pattern the circuitry on chips and boards, to polymers used as insulators on chip carriers, and encapsulants, for protecting the electronic integrated circuit (IC) devices from an adverse environment and as well as increasing their long term reliability.

### **7.2.1 Stress Relief Layers, Dielectrics, And Encapsulants**

NASA's Langley Research Center and a private microelectronics company are in the process of executing a memorandum of agreement in order to explore the synthesis, development, and evaluation of aromatic polyimides and other polymers as second generation microelectronic materials. The recommended uses of these proposed materials included semiconductor stress relief layers, interlayer dielectrics, and encapsulants. The primary application for the polyimides in this study was as encapsulants to protect the electronic device package.

Encapsulants are used in IC devices to protect them from an adverse environment and increase their long term reliability. Moisture, contaminants, mobile ions, hostile environmental conditions, and ultra-violet , visible, and alpha-particle radiation can cause degradation and ultimately affect the performance or lifetime of the IC[2-5]. Other hostile environments are encountered during normal operating conditions of integrated circuits, including extreme cycling temperatures, high relative humidity, shock, and vibration.

Encapsulants must provide a protective barrier for transport of chemical species that could attack the underlying device. They must adhere well to the substrate. Encapsulants must have sufficient mechanical, electrical, and physical properties to be effective in IC devices. They must possess a low dielectric constant to reduce the device propagation delay, and excellent thermal conductivity to dissipate heat produced by IC and high density packages. The encapsulant must be ultrapure since ion contaminants can destroy the device. From a processing standpoint, the encapsulant must be easy to apply over the package and repair in production and service.

In the design and development of these polyimides, the guidelines used included glass transition temperatures ranging from 250 and 300°C; cure temperatures between 250 and 325°C; resistance to hydrolysis; resistance to adhesion loss after a water boil test at 120°C and 2 ATM; high toughness; electronically pure materials; inherent viscosities between 0.9 and 1.2 dL/g or higher if there were no obvious gels; good mechanical properties; insoluble polymers after curing; insoluble partially imidized poly(amide acid)s in strip solvents (i.e. ketones, butyl acetate); and a low coefficient of thermal expansion (30 and 35 ppm/°C)[6].

Twenty-four polymers have been synthesized and characterized. After review of the data, three polymers were selected for scale-up, and have been supplied to the microelectronics company for further evaluation.

### **7.2.2 Pacemakers**

The human heart is a four-chamber pump consisting of muscles, valves, and a specialized conduction system[7]. Blood is collected from a small chamber called the atrium and pumped to a larger chamber called the ventricle. The ventricle then contracts and delivers blood to either the lungs to receive oxygen, or to other organs, depending on whether it is the right or left side of the heart. Normal hearts are synchronized by "pacemaker cells", a unique cluster of tissues that fire spontaneously at a particular rate determined by the concentration of particular chemicals. Timing of the chamber contractions is set by the time it takes these electrical impulses to travel to tissue which trigger muscle contraction, as well as the time these muscles are in refractory after contraction. In a diseased heart, damage to either the pacemaker cells or to



the conduction system prevent proper operation of the pump. An implantable electronic pacemaker seeks to replace the action of both of these.

The first successful, self-containing coronary pacing device was implanted in the United States in 1960. By 1984, over 100,000 patients had received permanent pacemakers. In 1994 alone, Medtronic, Inc., a leading manufacturer of pacemakers, sold 100,000 in the United States and over 200,000 worldwide[8].

Each pacemaker unit consists of a pulse operator, a power source, a lead connecting the pulse generator to the heart, and the accompanying electronic circuit package[9]. Presently, the polymeric insulator between the ceramic interconnect and the titanium shield in the electronic package is Kapton®, manufactured by DuPont. Due to the potential liability associated with biomedical applications, DuPont has informed biomedical companies that it will no longer sell Kapton® for biomedical applications after January 1, 1996. As a result, a new insulating material in the electronic package in pacemakers will be necessary[10]. Due to the number of polyimides developed and synthesized for potential liquid crystalline and microelectronic applications, there were several candidates that would potentially be suitable as the interlayer dielectric in pacemakers.

Fourteen polyimide films were sent to Medtronic, Inc. for evaluation as the interlayer dielectric in pacemakers. A new compatible adhesive was also required for the pacemaker application. No data from Medtronic, Inc. have been released to date on the evaluation of these materials.

## 7.3 Polyimides For Harsh Environments

### 7.3.1 Hydrolytically Stable Polyimides

Wiring failures linked to insulation damage had drawn much attention in the aerospace industry and concerns had developed regarding the stability and safety of polyimide insulated electrical wire. Several polyimides were selected for evaluation for resistance to degradation by various aqueous alkaline solutions. The polyimides under evaluation included commercially available films such as KAPTON<sup>®</sup>, APICAL<sup>®</sup>, LaRC<sup>™</sup>-TPI (Thermoplastic Polyimide), and UPILEX<sup>®</sup> R and S, as well as a number of experimental films prepared at NASA's Langley Research Center, including LaRC<sup>™</sup>-ITPI (Isomeric Thermoplastic Polyimide), LaRC<sup>™</sup>-IA (Improved Adhesive), and LaRC<sup>™</sup>-CPI (Crystalline Polyimide). Thermally imidized films were studied for their retention of mechanical properties after exposure to high pH solutions under stressed conditions.

Polyimide insulated wire is routinely exposed to high humidity, alkaline cleaners, and paint removers while under mechanical stresses due to the nature of the wiring and its installation in aircraft. Electrical insulating materials are known to deteriorate by a number of chemical and physical mechanisms which can be related to the polymer structure and the intensity of the various service stresses acting upon it. The predominant mechanism of deterioration is believed to be hydrolysis, a chemical reaction of water or aqueous fluids with the polymer chain. Hydrolytic chain-scission reduces the average chain length resulting in loss of strength and other properties. The rate of hydrolysis has been shown to be dependent upon the mechanical stresses from bending and stretching[11-12].

The polyimide films that showed excellent retention of mechanical properties after exposure to high pH solutions would be good candidates for applications where hydrolytic stability was required. As a result of this study, film candidates LaRC™-IA and HQDEA/4-BDAF have been evaluated further for wire insulation and capacitance humidity sensor applications.

### **7.3.2 LaRC™-IA Wire Insulation**

LaRC™-IAX is synthesized with 10% *p*-PDA in the backbone of the LaRC™-IA polymer. LaRC™-IAX has been successfully extruded onto 20 gauge stranded aircraft conductor-ASTM B 33 (tin coated copper wire), resulting in a commercial quality wire configuration meeting the requirements of MIL-W-22759[13]. Imitec, Inc., in cooperation with Barcel Wire and Cable manufactured aircraft wire from LaRC™-IAX. Abrasion resistance, dielectric strength, low weight, dimensions, non-burning, non-blocking, solvent resistant, low temperature capability, low shrinkage, and 200 and 230°C properties were all excellent.

LaRC™-IAX was selected based on its toughness and chemical resistance. The wire tested in the contract represented some of the most significant properties desired in military and commercial aircraft specifications and control documents.

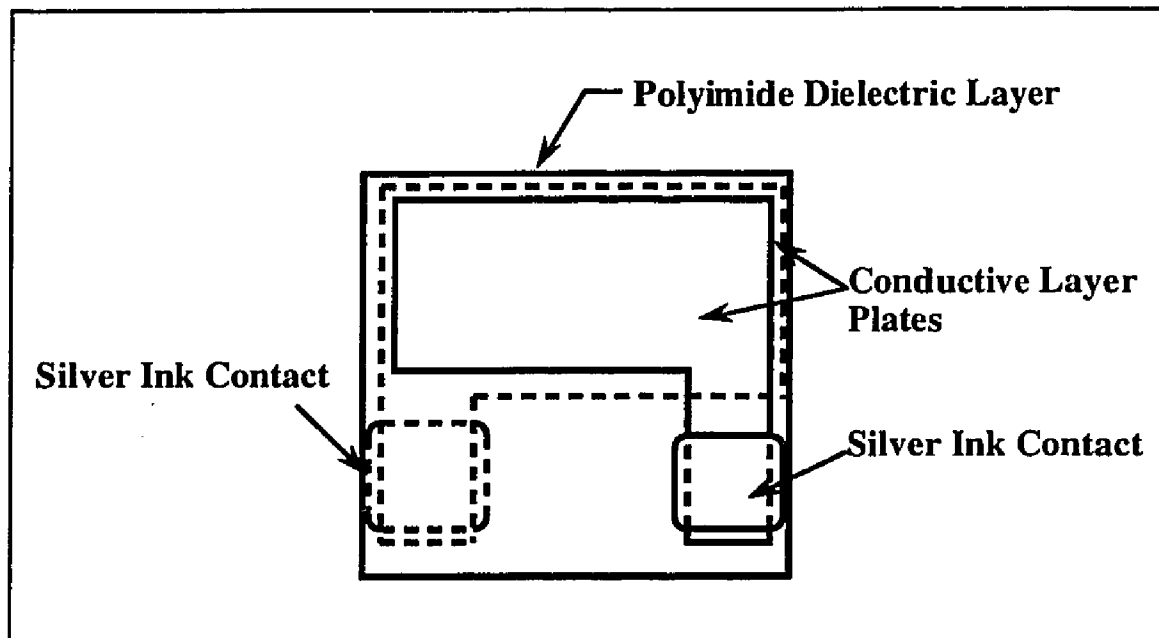
### **7.3.3 Capacitance Humidity Sensor**

As a result of the study evaluating the hydrolytic stability of polyimides for aircraft wire insulation, Johnson Controls, Inc., Milwaukee, Wisconsin, requested film samples for evaluation in their humidity sensor study. The three

best candidates from the hydrolytic stability study, LaRC™-CPI, HQDEA/4-BDAF, and LaRC™-IA, along with PMDA/4,4'-ODA, were synthesized and sent to Johnson Control, Inc. Film thicknesses ranged between 0.0005 and 0.001 in. These films were very thin but successful fabrication showed Johnson Controls, Inc. that these polymers could be made in an experimental laboratory without any expensive specialized equipment.

The film application was the capacitance humidity sensor shown in Figure 7.1[14]. The capacitance humidity sensor has a film core which is in contact with a pair of conductive layers bonded to opposite faces of the core. The core is made up of a polyimide having a dielectric constant which varies substantially linearly with humidity. To determine the application potential of the polyimide in the humidity sensor, capacitance was measured as a function of relative humidity for up to 28 days. Figure 7.2 depicts Kapton® HN film. Hysteresis, drift, and nonlinearities were the result of the hydrolytic instability of Kapton® in the humid environment[14]. Kapton® would not be a suitable dielectric layer because the sensor would drift. Upilex® R was a vast improvement over Kapton®. The hydrolytic stability was improved as shown by Figure 7.3[14]. Upilex® R was being used as the Johnson Control, Inc. relative humidity sensor material. Figure 7.4 showed the HQDEA/4-BDAF polymer results from the humidity sensor study[14]. There was little change after aging to 28 day. The curve was almost perfectly linear. Johnson Control, Inc. stated that this polymer was more hydrolytically stable than any other polymer evaluated in the humidity sensor study. Johnson Control has issued a patent application for use of HQDEA/4-BDAF in a capacitance humidity sensor[15]. Patents for composition of matter[16] and application of HQDEA/4-BDAF[17] as a dielectric are held by NASA's Langley Research Center.

Another major producer of humidity sensors recently purchased enough LaRC™-IA film to produce 250,000 sensor units. Their earlier experimental work showed the HQDEA/4-BDAF to be the best material, however, LaRC™-IA was significantly better than Kapton® or Upilex® and it was available in melt-extruded film form. These sensors will be fabricated by January, 1996.



**Figure 7.1** Capacitance Humidity Sensor

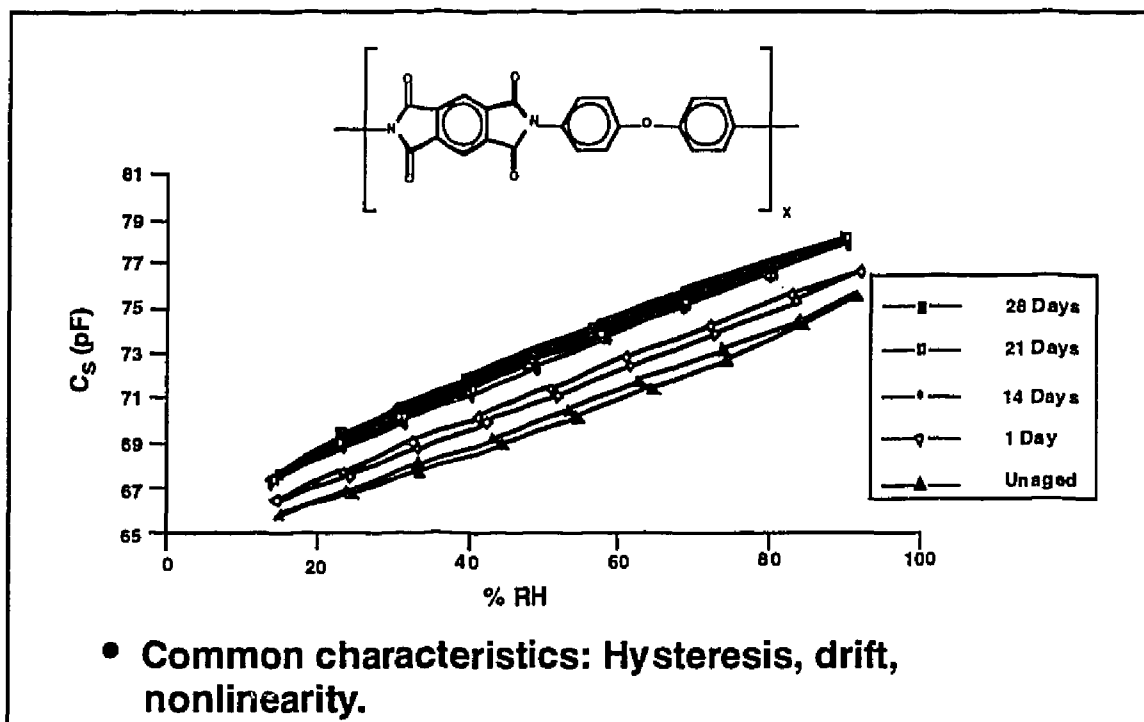


Figure 7.2 Capacitance As A Function Of Relative Humidity For Kapton® HN Film

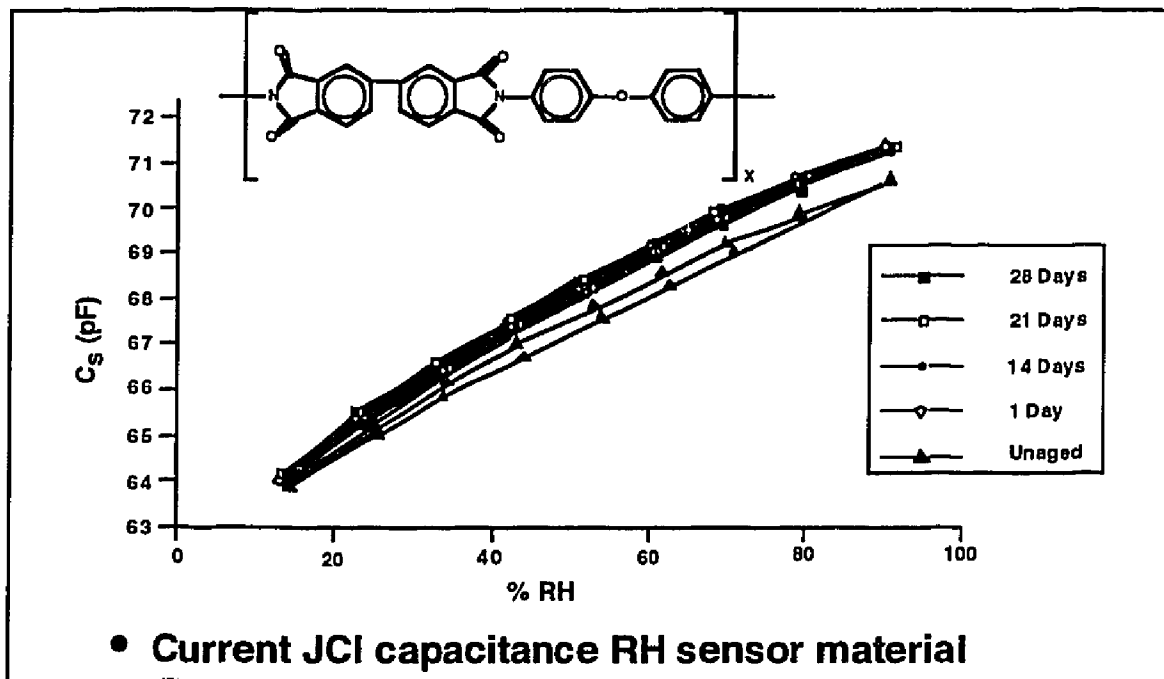


Figure 7.3 Capacitance As A Function Of Relative Humidity For Upilex® R Film

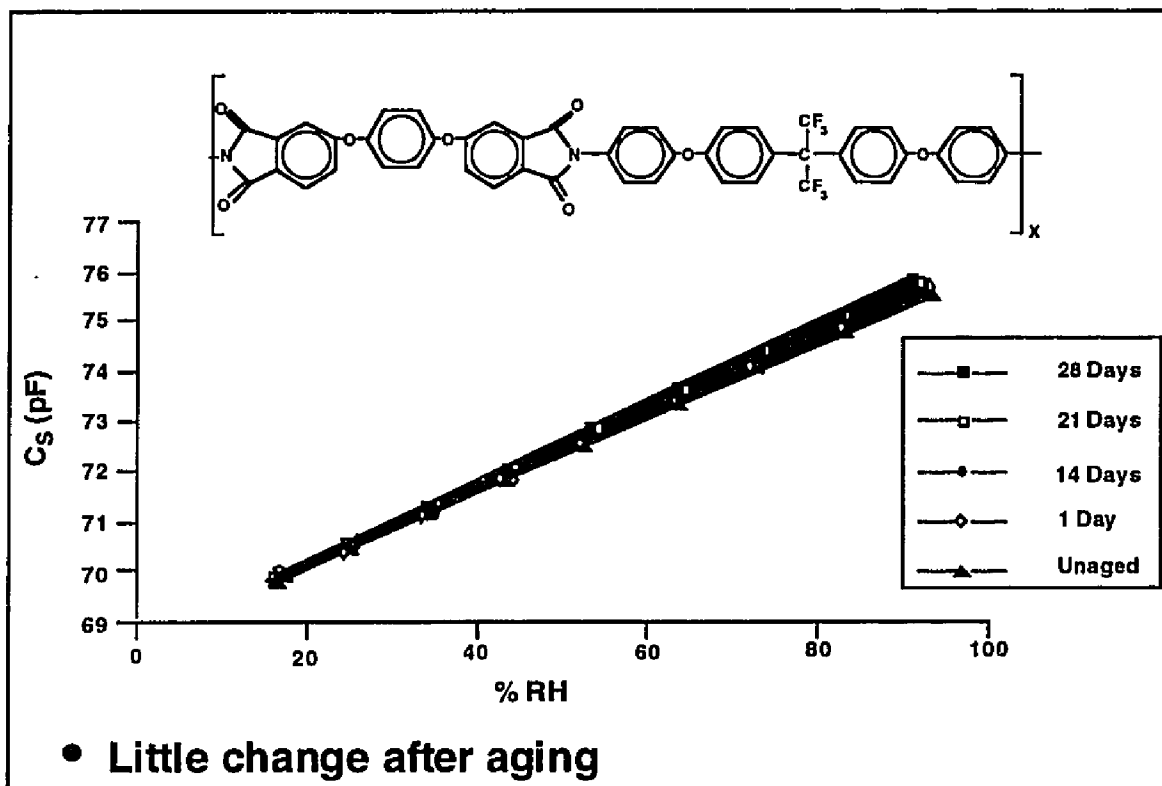


Figure 7.4 Capacitance As A Function Of Relative Humidity For HQDEA/4-BDAF Film

#### 7.4 Radiation Resistant Polymers

Space exploration has often been limited by the lifetime of the power source. In order to extend the missions, development of methods to provide long-term power sources was necessary. Within the last decade, a new class of materials (squarylium dyes) has been shown to have much higher photovoltaic quantum efficiencies.

This research developed polyimides containing squaric acid derivatives for application as power sources in space, and as radiation-resistant polymers. Additionally, photoconductive properties were investigated.



Polymer solutions were sent to DuPont Central Research and Development, Experimental Station, for investigation of photoconductive properties. Samples were spin-coated onto ITD glass to provide a conductive groundplane. The photoconductivity of the films was studied using the standard technique of xerographic discharge[18]. Positive surface charge was deposited on the film with a high tension corona wire. Irradiation was carried out with CW white light at  $5 \times 10^{-2} \text{ W/cm}^2$  directly through the electrostatic voltmeter. Film response was measured via surface charge dissipated as a function of time.

The polymers contained electron hole pairs which migrate in the presence of the applied electric field to neutralize the surface charge. The sensitivity of the films was not very high. The slope of the decay curve was quite shallow. This indicated either a low quantum yield of charge carriers or poor mobility of the carriers in the matrix. There were no striking features of the SAPPD systems evaluated to indicate a need for further study[19].

## 7.5 REFERENCES

1. La Mantia, F. P. *Thermotropic Liquid Crystalline Polymer Blends*; Technomic: Lancaster, PA, 1993; Chapters 1-6.
2. Wong, C. P., "Recent Advances in IC Passivation and Encapsulation," In *Polymers for Electronic and Photonic Applications*; Wong, C. P., Ed.; Academic Press, Inc: 1993; p 167-220.
3. *Encyclopedia of Polymer Science and Engineering*, John Wiley and Sons: Vol. 5, 1987; p 638-641.
4. Kinjo, N.; Ogat, M.; Nishi, K.; Kaneda, A., "Epoxy Molding Compounds as Encapsulation Materials for Microelectronic Devices" In *Specialty Polymers/Polymer Physics*; Springer-Verlag: New York, 1989; p 1-83.
5. Wong, C. P., "Application of Polymer in Encapsulation of Electronic Parts" In *Electronic Applications*; Springer-Verlag: 1988; p 63-83.
6. Personal communication with microelectronics company, name withheld.
7. Stotts, L. J.; Infinger, K. R.; Babka, J.; Genzer, D. *IEEE Journal of Solid State Circuits* **April 1989**, Vol. 24, 292-300.
8. Medtronic, Inc., Technical Services Department, Minneapolis, Minnesota, 1-800-328-2518 (EXT. 8575).
9. *IEEE Spectrum* **Oct. 1985**, Vol. 22, 20.
10. Rausch, A., Medtronic, Inc., verbal and written communication.
11. Campbell, F. J., "Temperature Dependence of Hydrolysis of Polyimide Wire Insulation", *IEEE Transactions on Electrical Insulation* **1985**, Vol. EI-20, 111-116.

12. Campbell, F. J., "Hydrolytic Deterioration of Polyimide Insulation on Naval Aircraft Wiring", *Proceedings, IEEE Conference on Electrical Insulation and Dielectric Phenomena* **1988**, 180-188.
13. Keating, J., NASA Contractor Report 195048, "Development of LaRC™-IA Thermoplastic Polyimide Coated Aerospace Wiring", Imitec, Inc.; December 1994.
14. Data provided by Johnson Control, Inc., Milwaukee, WI.
15. Thoma, Paul *et. al.* U S patent 5 408 381, April, 1995.
16. St. Clair, A. K.; St. Clair, T. L. U S Patent 5 428 102, 1995.
17. St. Clair, A. K.; St. Clair, T. L.; Winfree, W. P. U S Patent 5 338 826, August, 1994.
18. *Polymer and Plastics Technology and Engineering* **1981**, Vol. 17, 139-191.
19. Freilich, Steven C., DuPont Central Research and Development, Experimental Station, Wilmington, DE, personal communication.

## Chapter 8: Conclusions

Ether-containing polyimides were synthesized, characterized, and evaluated for three applications: thermotropic liquid crystalline polyimides as processing aids, polyimides for microelectronics, and polyimides for harsh environments.

### 8.1 Potential Thermotropic Liquid Crystalline Polyimides As Processing Aids

Very few thermotropic liquid crystalline polyimides free of ester or carbonate groups have been developed to date. These thermotropic liquid crystalline polyimides have been synthesized using flexible diamines and rigid dianhydrides. Novel dianhydrides were synthesized that contained flexible units (ethers), flexible spacers, rigid units, and/or bulky groups. These flexible dianhydrides were combined with rigid diamines to afford alternating rigid/flexible backbones, thus creating some of the favorable components for liquid crystallinity.

Twenty-five different polymers were synthesized from these novel dianhydrides. The majority of the polymers were crystalline, had  $T_g$ s below 200°C, possessed low color, and had other good qualities of polyimides. The synthesis of novel polyimides and their precursors was accomplished and has provided a new structure-property database. Inconclusive data were obtained regarding the potential liquid crystalline characteristics.

The most promising polymer appeared to be the polymer that was analogous to the Mitsui Toatsu liquid crystalline polyimide. The elemental compositions were identical for the BMDEDA/*p*-PDA polymer and the Mitsui Toatsu Chemicals PMDA/1,3-BAPDBB (LC-PI) polymer. The LC-PI exhibited liquid crystalline characteristics by thermal analysis, optical microscopy, and melt viscosity measurements. The most promising results were obtained from a BMDEDA/*p*-PDA polymer system synthesized in GBL with a 6% molar offset and endcapped with phthalic anhydride. It exhibited a double melting peak. After this polymer powder was extruded, the extrudate was ground and a melt viscosity measurement was performed. The melt viscosity was 1530 poise at 307°C. The extrudate no longer exhibited a second melting transition. The low melt viscosity could be attributed to low MW. No colors or textures were seen under the crossed polarizers of an optical microscope.

One of the BMDEDA/*p*-PDA polymer films exhibited a double melting peak on the first DSC scan. The melting peaks were not recovered on the second DSC scan. The TMA data supports the possibility that there were two different liquid crystalline forms at the melting temperatures shown on the DSC scan. It may be that it takes a long time for the system to reorganize into a liquid crystal phase after it has been heated to the probable isotropic phase above 290°C. After the first heat with the DSC up to greater than 300°C, the isotropic phase is locked in upon quenching and the original melting transitions cannot be found because the sample hasn't had enough time for the liquid crystal ordering to reform. However, optical microscopy to 300°C did not show any colors or textures under crossed polarizers. Other films of BMDEDA/*p*-PDA did not show multiple melting peaks.

Molecular modeling was used to investigate structural differences in the polymer backbone that may explain this phenomena. The aspect ratios only

differed by 9%; however, the number of virtual bond lengths was five for the LC-PI while the BMDEDA/*p*-PDA polymer was comprised of seven for the same fully extended chain length. There was two additional kinks in the BMDEDA/*p*-PDA polymer, and therefore it was not as rigid as the LC-PI. Neither polymer exhibited the critical mean axial ratio  $L_K/D$  of the Kuhn for freely jointed chains. This suggested that Yoon's[1-2] theory needs additional evaluation for predicting liquid crystallinity in polymers.

Other combinations using BMDEDA were semicrystalline but did not exhibit liquid crystalline characteristics. Although these polymers did not exhibit classical liquid crystalline behavior, additional studies using optical microscopy, birefringence measurements, molecular orientation, and thermal annealing may provide additional information and confirmation as to the crystalline/liquid crystalline characteristics of these polymers.

## **8.2 Polyimides For Microelectronics Applications**

Four series of polyimide copolymers were synthesized. The general trends observed were that the addition of the SAPPD diamine to the polymer backbone decreased the CTEs and increased the strengths and moduli. SAPPD was also observed to decrease the thermal oxidative stabilities and caused outgassing, depending on the amount in the backbone. The best candidates for polyimides as interlayer dielectrics and encapsulants are shown in Table 8.1. These five candidates exhibited the best combination of properties based on the outlined material requirements. Three of these polymers have been synthesized in larger quantities and shipped to a microelectronics company for further evaluation.

<b>Polyimide Designation</b>	<b><math>\eta_{inh}</math>, dL/g</b>	<b><math>T_g</math> by DSC, °C</b>	<b><math>T_g</math> by TMA, °C</b>	<b>TGA, 10% wt loss, °C</b>
HQDEA + 75 4,4'-ODA:25SAPPD	1.42	266	256	503
HQDEA +60 4,4'-ODA:40SAPPD	1.45	254	274	474
ODPA + 80 3,4'-ODA:20SAPPD	1.23	252	254	505
ODPA + 60 3,4'-ODA:40p-PDA	1.28	251	255	527
BTDA + 90 4,4'- ODA:10p-PDA	1.21	277	276	519
	<b>CTE, ppm/°C</b>	<b>Tensile strength, ksi</b>	<b>Tensile modulus, ksi</b>	<b>Elong., %</b>
HQDEA + 75 4,4'- ODA:25SAPPD	38.9	17.8	387.6	42.7
HQDEA +60 4,4'-ODA:40SAPPD	37.0	17.2	387.2	11.1
ODPA + 80 3,4'-ODA:20SAPPD	36.0	20.7	463.2	10.6
ODPA + 60 3,4'-ODA:40p-PDA	33.0	21.1	505.6	27.6
BTDA + 90 4,4'- ODA:10p-PDA	32.9	21.3	468.1	24.0

**Table 8.1 Best Candidates For Application As Interlayer Dielectrics And Encapsulants**

### 8.3 Polyimides For Harsh Environments

Several polyimides were selected for evaluation for resistance to degradation to various aqueous solutions to determine their hydrolytic stability. Commercially available PMDA based films appeared to be the least resistant to hydrolysis of the polyimides evaluated. UPILEX<sup>®</sup> films showed good retention of properties except in the rolled configuration, where they showed a significant loss in tensile strength. LaRC<sup>™</sup>-TPI exhibited good retentions of properties also. Of the experimental films synthesized, LaRC<sup>™</sup>-CPI, ODPA/3,4'-ODA (LaRC<sup>™</sup>-IA), and HQDEA/4-BDAF exhibited excellent resistance to base hydrolysis while under stress. Moduli and elongations were generally not greatly affected by the exposure to the basic solutions.

#### Radiation-resistant Polyimides

In an effort to develop electron radiation-resistant materials, polyimides containing squaric acid derivatives were synthesized, characterized, and evaluated for potential space applications. Polyimides were exposed to 1 MeV electrons to simulate a short-term exposure (5-10 yr) and long-term exposure (25-30 yr) in geosynchronous orbit (GEO).

The BTDA/SAPPD and ODPA/SAPPD polyimides had higher tensile strengths and moduli than the IPAN/SAPPD and Si(CH<sub>3</sub>)<sub>2</sub>DA/SAPPD polyimides. However, higher retentions of tensile strength and moduli at elevated temperatures were observed for the IPAN/SAPPD and Si(CH<sub>3</sub>)<sub>2</sub>DA/SAPPD polyimides. The decrease in properties was attributed to the elevated temperatures and not the electron radiation exposures since there was not much change for a given temperature.



Linear aromatic polyimides containing SAPPD exhibited high thermal and thermo-oxidative stabilities, which make them useful in structural components exposed to hot and/or oxidative environments, as in jet engines and on the outer surfaces of supersonic aircraft. The SAPPD polyimides demonstrated excellent retention of mechanical properties when exposed to high-energy radiation. In addition, electrons in the SAPPD moieties are known to be readily excited to states of higher energy upon exposure to ultraviolet light, giving rise to electronic properties with potential utility in photovoltaic, photoconductive, and/or photoemissive devices, for example[3].

#### **8.4 Papers And Presentations**

Some of the work contained in this research has been published and/or presented to the scientific community at technical conferences. A list follows with the presenter underlined, and a brief statement as to the subject matter:

**Paper and Presentation:** Catharine I. Croall and Terry L. St. Clair in *Advances in Polyimide Science and Technology: Proceedings of the Fourth International Conference on Polyimides*, Oct. 30-Nov. 1, 1991, Ellenville, NY, p 618-635; "The Mechanical Properties of Polyimide Films After Exposure to High pH" evaluated the hydrolytic stability of polyimides and their potential application as wire and cable insulators.

**Journal Article:** Catharine I. Croall and Terry L. St. Clair, *Journal of Plastic Film and Sheeting* 1992, Vol. 8, 172-190; "The Mechanical Properties of Polyimide Films After Exposure to High pH."

**Paper and Presentation:** James F. Dezern and Catharine I. Croall in *Advances in Polyimide Science and Technology: Proceedings of the Fourth International Conference on Polyimides*, Oct. 30-Nov 1, 1991, Ellenville, NY, p 468-481; "Structure-Property Study of Keto-Ether Polyimides" investigated the effect of structural changes in the backbone of keto-ether linear polyimides on their mechanical and thermal properties.

**Presentation:** Catharine I. Croall and Terry L. St. Clair, "Polyimides Containing Squaric Acid Derivatives" presented at the Fourth Interdisciplinary Symposium on Recent Advances in Polyimides and Other High Performance Polymers, Reno/Sparks, Nevada, Jan. 18-21, 1993, evaluated the effect of high-energy radiation on the physical and mechanical properties of squaric acid polyimides.

**Presentation:** Terry L. St. Clair, James F. Dezern, and Catharine I. Croall, "Polyimide Chemical Structure/Property Relationships: Recent Work" presented at the Fourth Interdisciplinary Symposium on Recent Advances in Polyimides and Other High Performance Polymers, Reno/Sparks, Nevada, Jan. 18-21, 1993.

**Journal Article:** John W. Connell, Emilie J. Siochi, and Catharine I. Croall, *High Performance Polymers* 1993, Vol. 5, 1-14. "The Effect of High-energy Radiation on Poly (arylene ether)s" investigated the effect of 1 MeV electrons while under high vacuum on the polymer's physical and mechanical properties.

**Paper and Presentation:** Diane M. Stoakley, Anne K. St. Clair, and Catharine I. Croall, *Polymer Preprints* 1993, Vol. 34(1); "Low Dielectric, Fluorinated Polyimide

Copolymers" developed copolymers of fluorinated polyimides and BPDA as films and composite laminates for aircraft matrix resins.

**Journal Article:** Diane M. Stoakley, Anne K. St. Clair, and Catharine I. Croall, *Journal Of Applied Polymer Science* **1994**, Vol. 51, 1479-1483; "Low Dielectric, Fluorinated Polyimide Copolymers."

**Paper and Presentation:** Terry L. St. Clair, James F. Dezern, and Catharine I. Croall in *Proceedings of the 51st ANTEC, SPE*, May 9-13, 1993, New Orleans, LA, p 650-658; "Mechanical Property-Structure Relationships of Linear Aromatic Polyimide Films."

**Paper and Presentation:** Catharine C. Fay, Joseph G. Smith, Jr., and Terry L. St. Clair, "Potential Liquid Crystalline Polyimides," *Polymer Preprints* **1994**, Vol. 35, No. 1, 541-542, developed potential liquid crystalline polymers utilizing the Bisphenol M derivative.

**Presentation:** Catharine C. Fay, Joseph G. Smith, Jr., and Terry L. St. Clair, "Potential Liquid Crystalline Polymers, Copolymers, and Blends," presented at the Gordon Research Conference on Polymers, July 3-8, 1994, Wolfeboro, New Hampshire, developed potential liquid crystalline copolymers using Bisphenol M derivatives.

**Paper and Presentation:** Catharine C. Fay and Anne K. St. Clair, "Dimensionally Stable Polyimide Copolymers for Microelectronic Applications" to be presented orally at the National Meeting of the American Chemical Society, Polymer-based Electronic Packaging and Interconnects Symposium,

New Orleans, LA, March 24-29, 1996, and published in *Polymer Preprints*, developed polyimide copolymers as encapsulants and interlayer dielectrics.

## 8.5 REFERENCES

1. Takahashi, N.; Yoon, D. Y.; Parrish, W. *Macromolecules* **1984**, *17*, 2583-2588.
2. Ronca, G.; Yoon, D. Y. *J. Chem. Physics* **1984**, *80*, 930.
3. Scott, Gary W., "Development of Organic Thin Film Solar Cells for Space Applications", CalSpace Proposal CS-11-92, April 1992; p 3-9.

## APPENDIX

### Film Stretching Of Potential Liquid Crystalline Polyimides

In order to install and calibrate the T. M. Long Film Stretcher, several preliminary activities were performed. The film stretcher was attached to an I-beam to ensure stability in raising the cover, and was subsequently load tested. The electrical system (heaters, ground, etc.) was certified by an electrician and repairs were made as necessary. An air source was installed in order to lift the cover. A hydraulic pump was installed to hold the film in place prior to inserting it in the actuators, and quenching and removing it after stretching. After these preliminary items were completed, the operation of the film stretcher was examined.

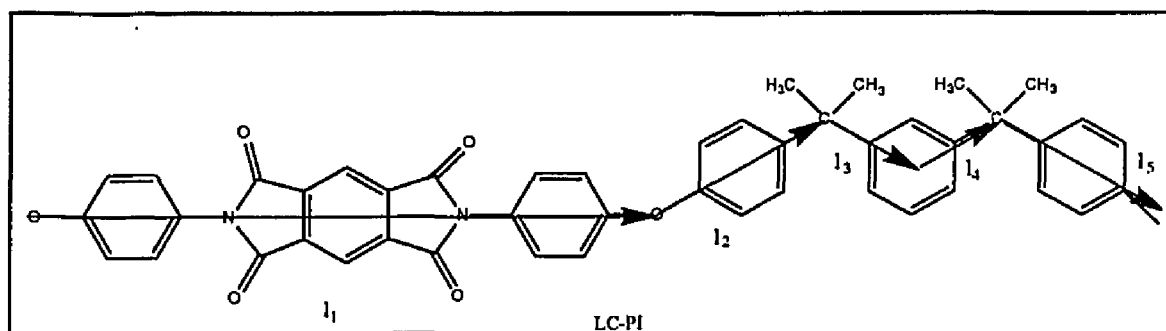
Several parts were broken or missing. The ceramic stand-offs for the heaters were damaged and replaced. Shims were ordered and installed because the level of the stretcher was critical for uniform stretching. The 52 actuators that hold the film during stretching did not operate properly. Some actuators did not close fully when pressure was applied. The o-ring for each actuator, and some of the hairpin tubes, were replaced.

Mylar® was used as a test film because of its availability, low glass transition temperature (80-90°C), and low melting point (254°C). Many attempts were made to stretch the Mylar®. Temperatures up to 200°C and pressures up to 500 psi were used but the film continually pulled out of the clips on one or two sides of the film specimen. The rate of stretching and the force applied were adjusted to allow smoother movement of the stretching mechanism. The hydraulic system was bled to remove any air that may have caused the

stretching process to be discontinuous. Efforts are still being made to bring the T. M. Long Stretcher into full operation.

### Molecular Modeling Of Potential Liquid Crystalline Polyimides Containing The Bisphenol M Derivative

The molecular diagram indicating the virtual bond lengths,  $l_1$ - $l_5$ , is shown for the LC-PI:



The calculations for the LC-PI were as follows:

$$L = l_1 + l_2 + l_3 + l_4 + l_5 = 18.14 \text{ \AA} + 2 (5.71 \text{ \AA}) + 2 (2.92 \text{ \AA}) = 35.4 \text{ \AA}$$

$$D = (MW / \rho N_A L) = \frac{710.786 \text{ g/mole}}{(1.255 \text{ g / cm}^3) (6.02 \times 10^{23} \text{ molecules/mole}) (35.4 \text{ \AA})}$$

$$D = 5.16 \text{ \AA}$$

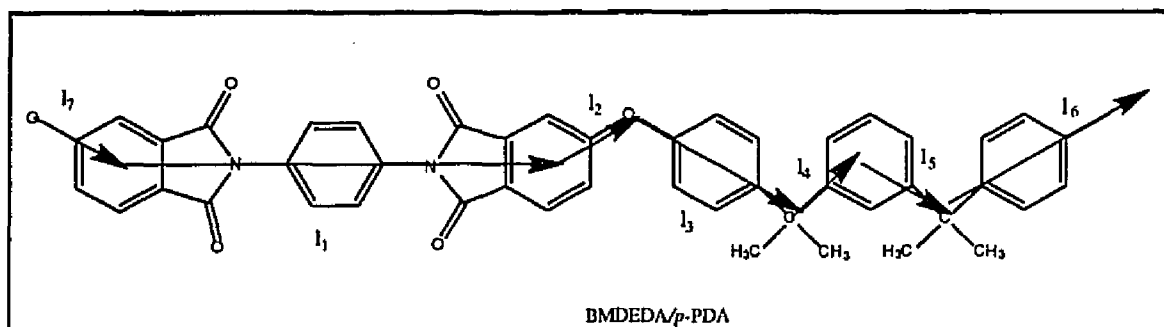
$$r^2/n = 154.19 \text{ \AA}^2/\text{bond}$$

$$(154.19 \text{ \AA}^2) 5 = 770.95 \text{ \AA}^2/\text{repeat unit}$$

$$r^2/L = 21.83 \text{ \AA} = L_c$$

$$L_c/D = 21.83/5.16 = 4.23$$

The molecular diagram indicating the virtual bond lengths,  $l_1$ - $l_7$ , is shown for the BMDEDA/*p*-PDA polymer:



The calculations for the BMDEDA/*p*-PDA polymer using the same method described above were as follows:

$$L = 2.79 \text{ \AA} + 12.47 \text{ \AA} + 2.79 \text{ \AA} + 5.71 \text{ \AA} + 2.92 \text{ \AA} + 2.92 \text{ \AA} + 5.71 \text{ \AA} = 35.31 \text{ \AA}$$

$$D = (710.786 \text{ g/mole}) / (1.242 \text{ g/cm}^3) (6.02 \times 10^{23} \text{ molecules/mole}) (35.31 \text{ \AA})$$

$$D = 5.19 \text{ \AA}$$

$$r^2/n = 101.00 \text{ \AA}^2 = 707 \text{ \AA}^2/\text{repeat unit}$$



$$L_c = 707 \text{ \AA}^2 / 35.31 \text{ \AA} = 20.02 \text{ \AA}$$

$$L_c/D = 20.02 \text{ \AA} / 5.19 \text{ \AA} = 3.8$$

### Calculation of Stress Induced by Rolled and Twisted Configurations

In the *Polyimides for Harsh Environments* Section, Wire and Cable Insulation, two stresses were induced in the specimens exposed to high pH solutions. Calculations for the approximated stresses induced in the twisted and rolled configurations for the high pH solutions are shown below.

#### Outer Fiber Strain (Rolled Configuration)

$$\epsilon_{xx} = (y - y_o)/R$$

where  $y - y_o$  = distance from the neutral axis, length of specimen = 5 in, specimen width = 0.2 in, specimen thickness = 0.002 in, and the diameter = 0.125 in.

$$\epsilon_{xx} = 0.001 \text{ in} / 0.125 \text{ in} = 0.008$$

$$\text{Tensile stress} = E (\epsilon_{xx})$$

$$\text{Tensile stress} = 500 \text{ ksi} (0.008) = 4 \text{ ksi}$$

#### Twisted Configuration Stress

$$\text{torque: } T = ab^3\mu G\theta/L$$

where  $\theta$  = twist in radians,  $L$  = length,  $G$  = modulus,  $2a$  = long side of rectangle, and  $2b$  = short side of rectangle [Trayer, G. NACA Report 334, 1929].

$$\text{maximum stress: } q = \gamma T / \mu a b^2$$

$$G = E / (1 + \mu)^2 = 430 \text{ ksi} / (1.35)^2 = 159 \text{ ksi}$$

$$\theta / L = 4.2\pi \text{ rad} / 3.5 \text{ in} = 7.18$$

$$T = (0.1 \text{ in}) (0.001 \text{ in})^3 (5.300) (7.18) 159 \text{ ksi}$$

$$T = 6.05 \times 10^{-4} \text{ in}\cdot\text{lb}$$

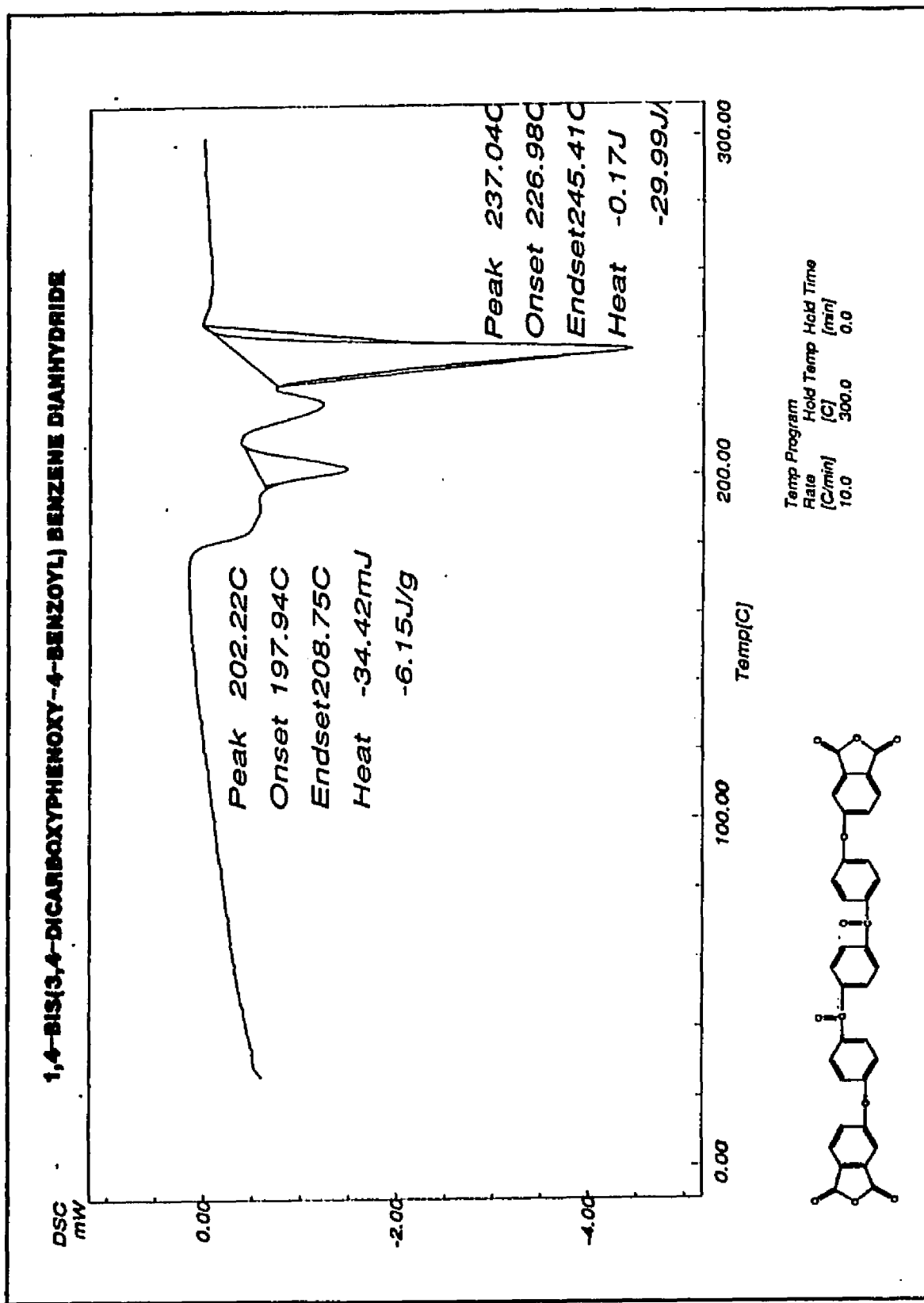
$$q = (\gamma a b^3 \mu G \theta / L) / \mu a b^2$$

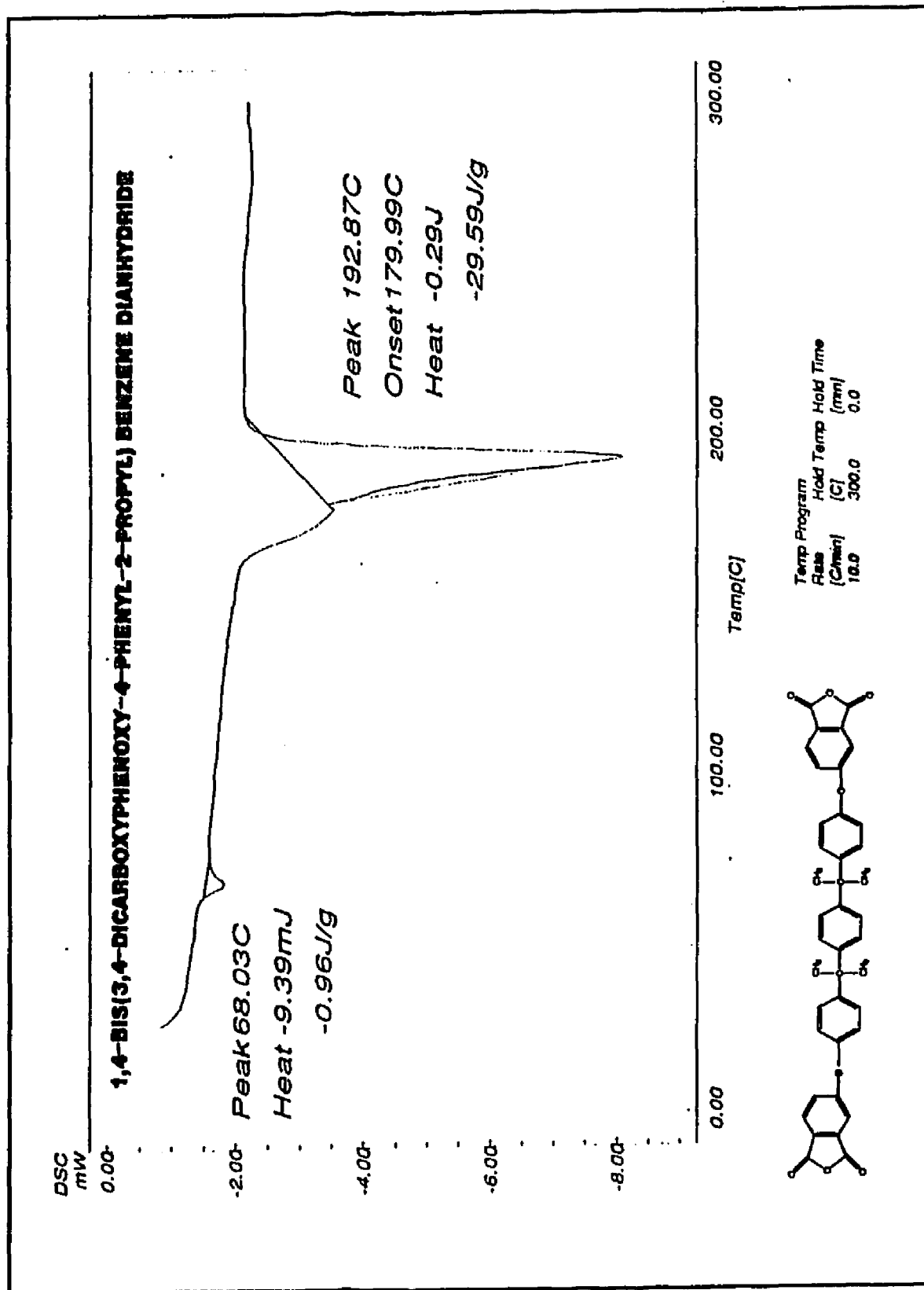
$$q = \gamma b G \theta / L$$

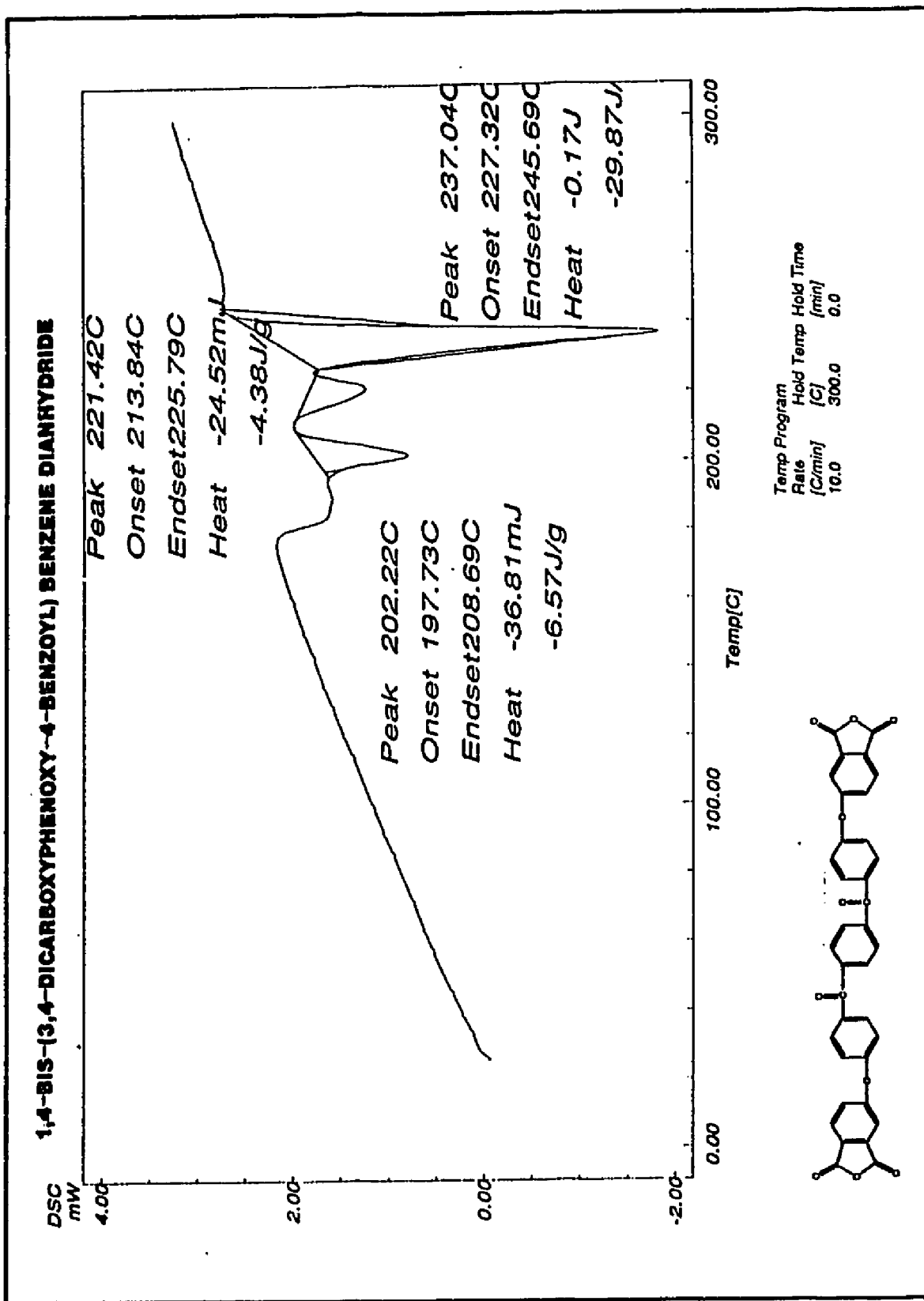
$$q = (2.00) (0.001) (159 \text{ ksi}) (7.18)$$

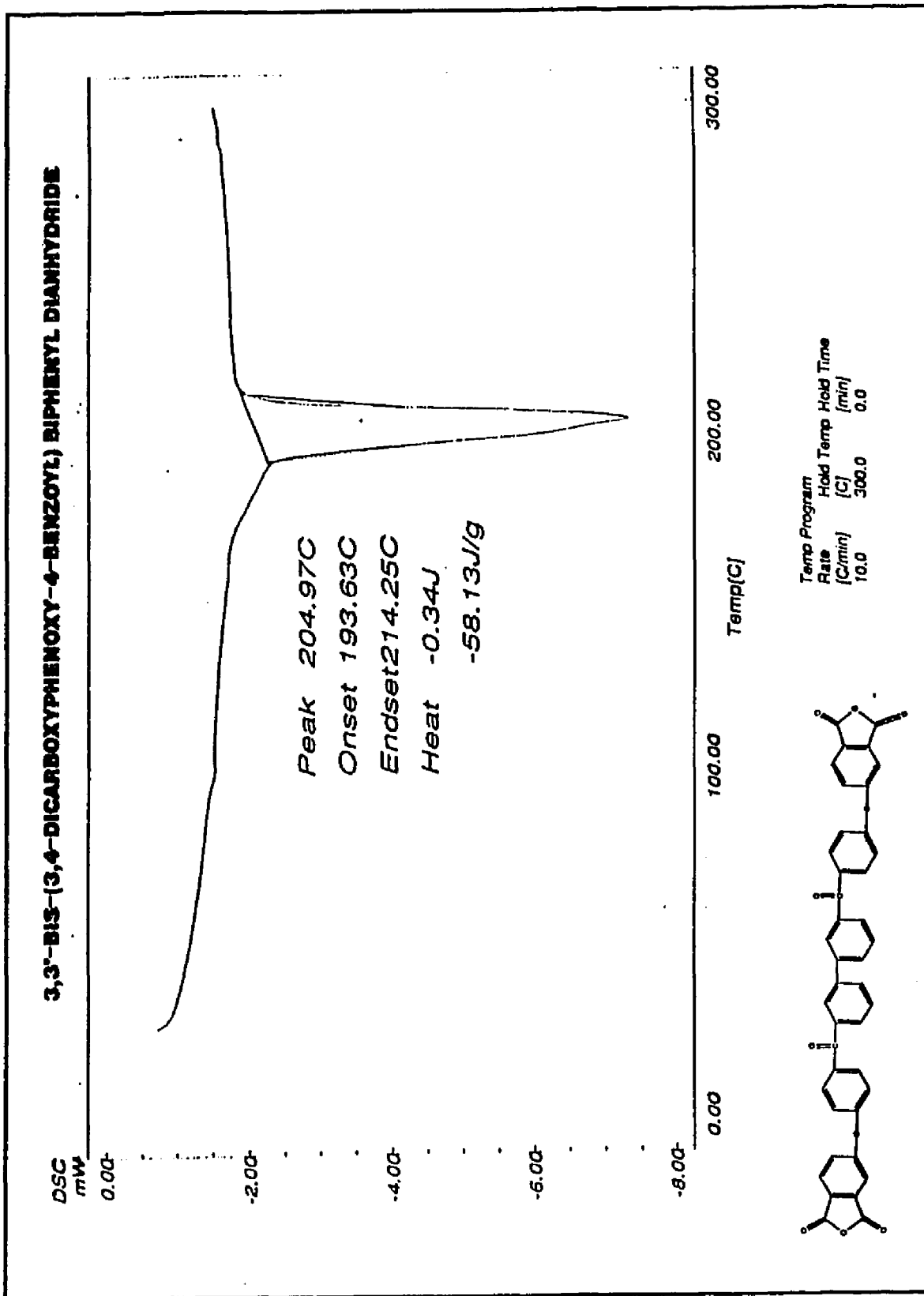
$$q = 2.3 \text{ ksi}$$

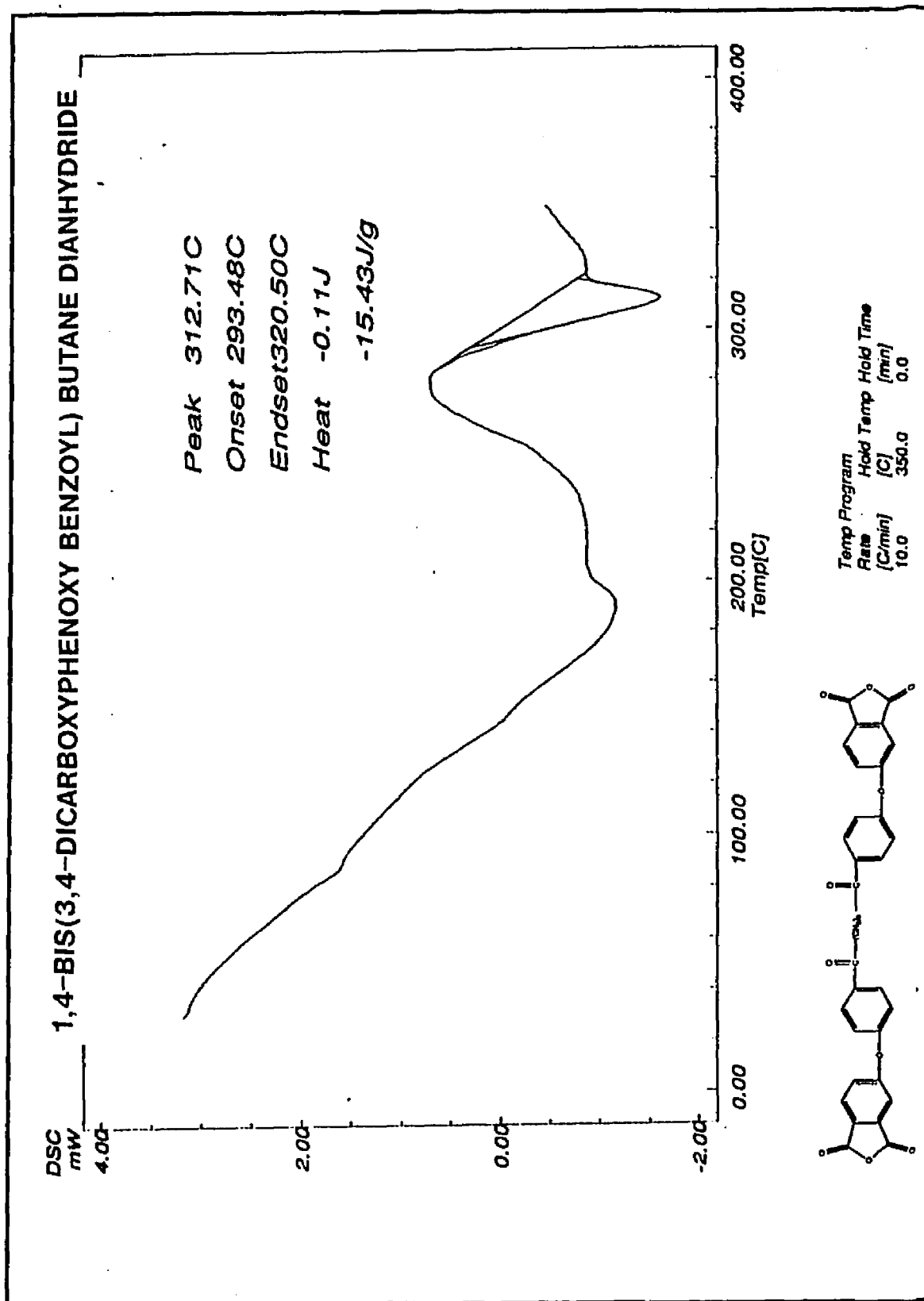
## MELTING POINTS



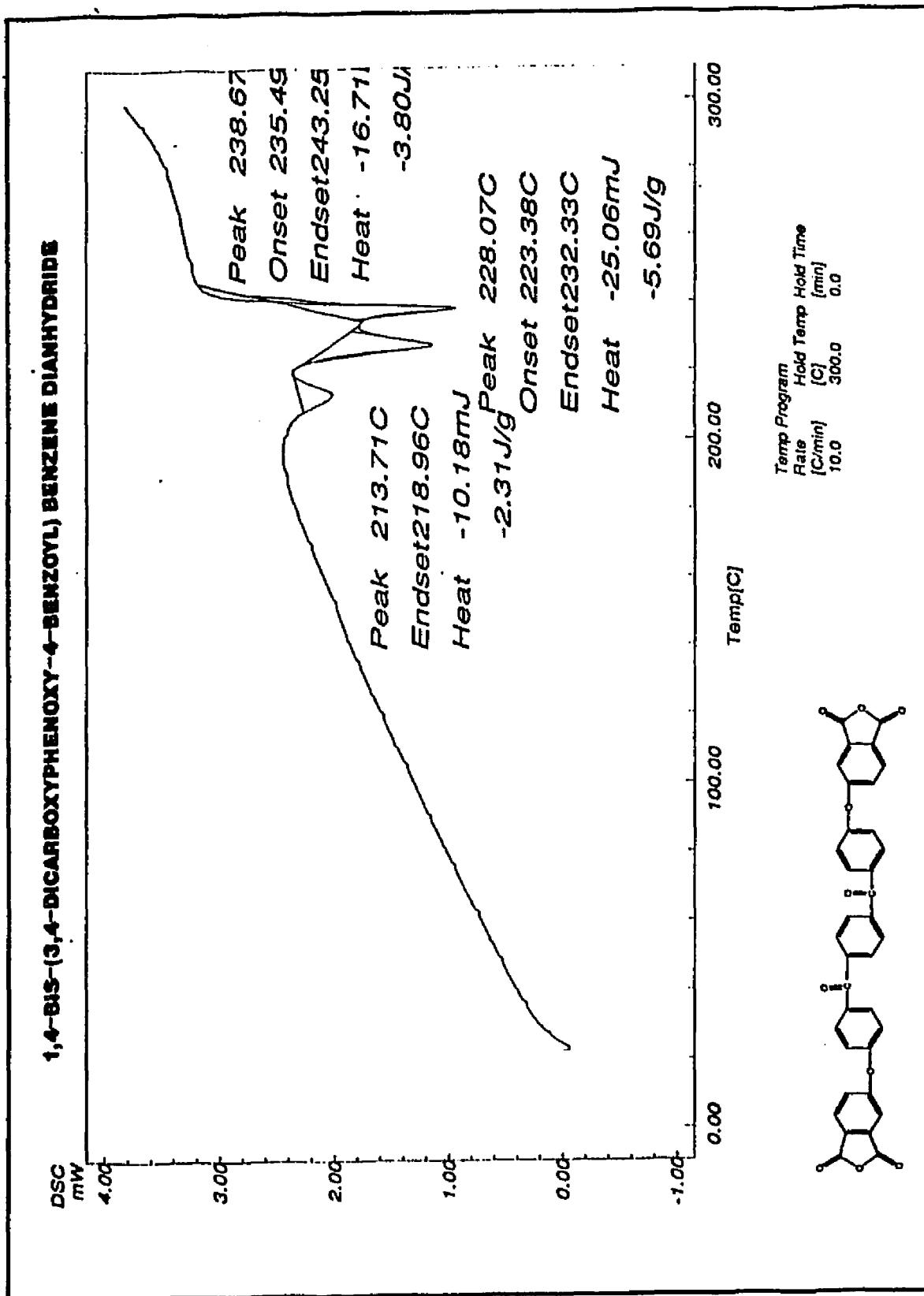


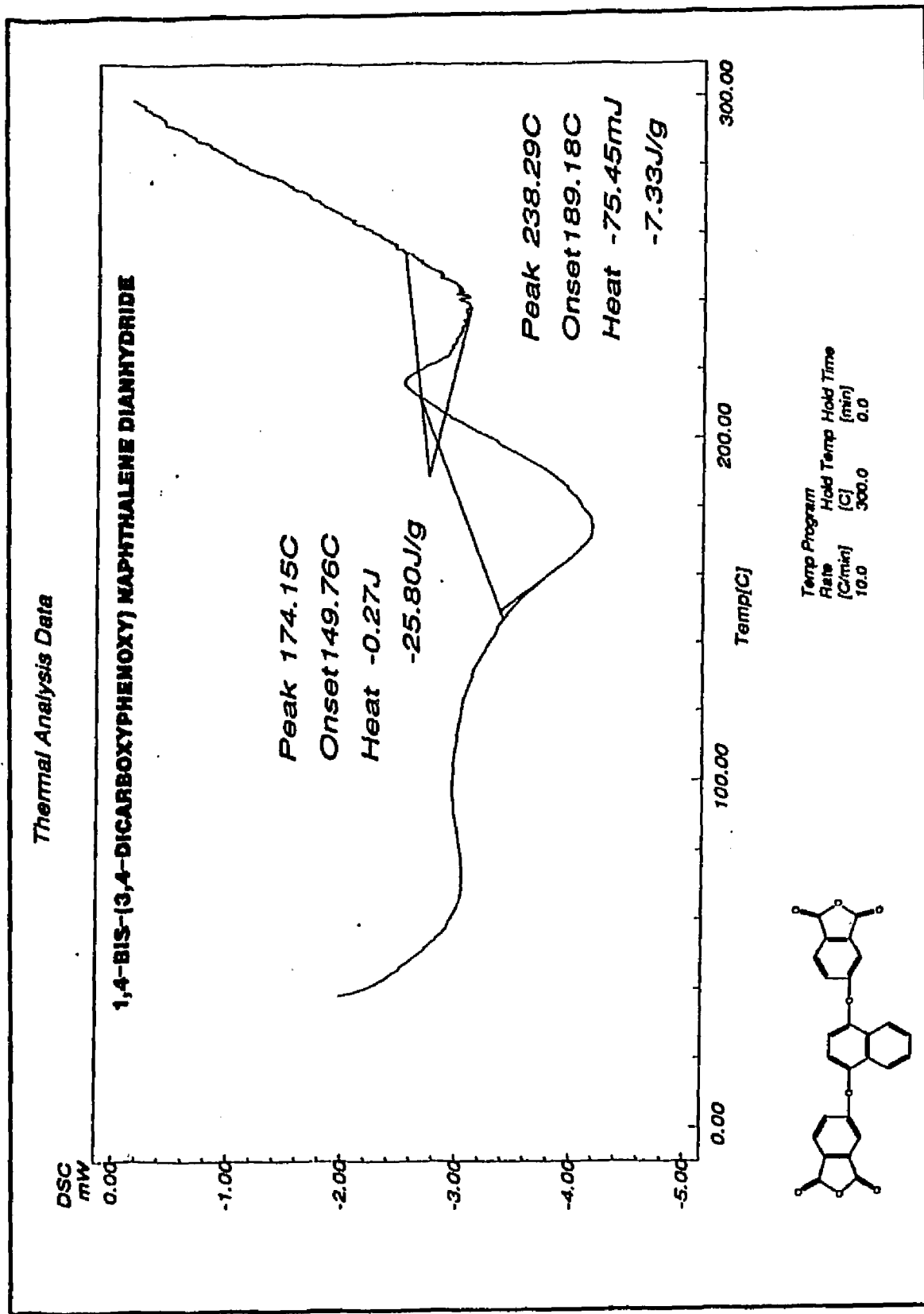


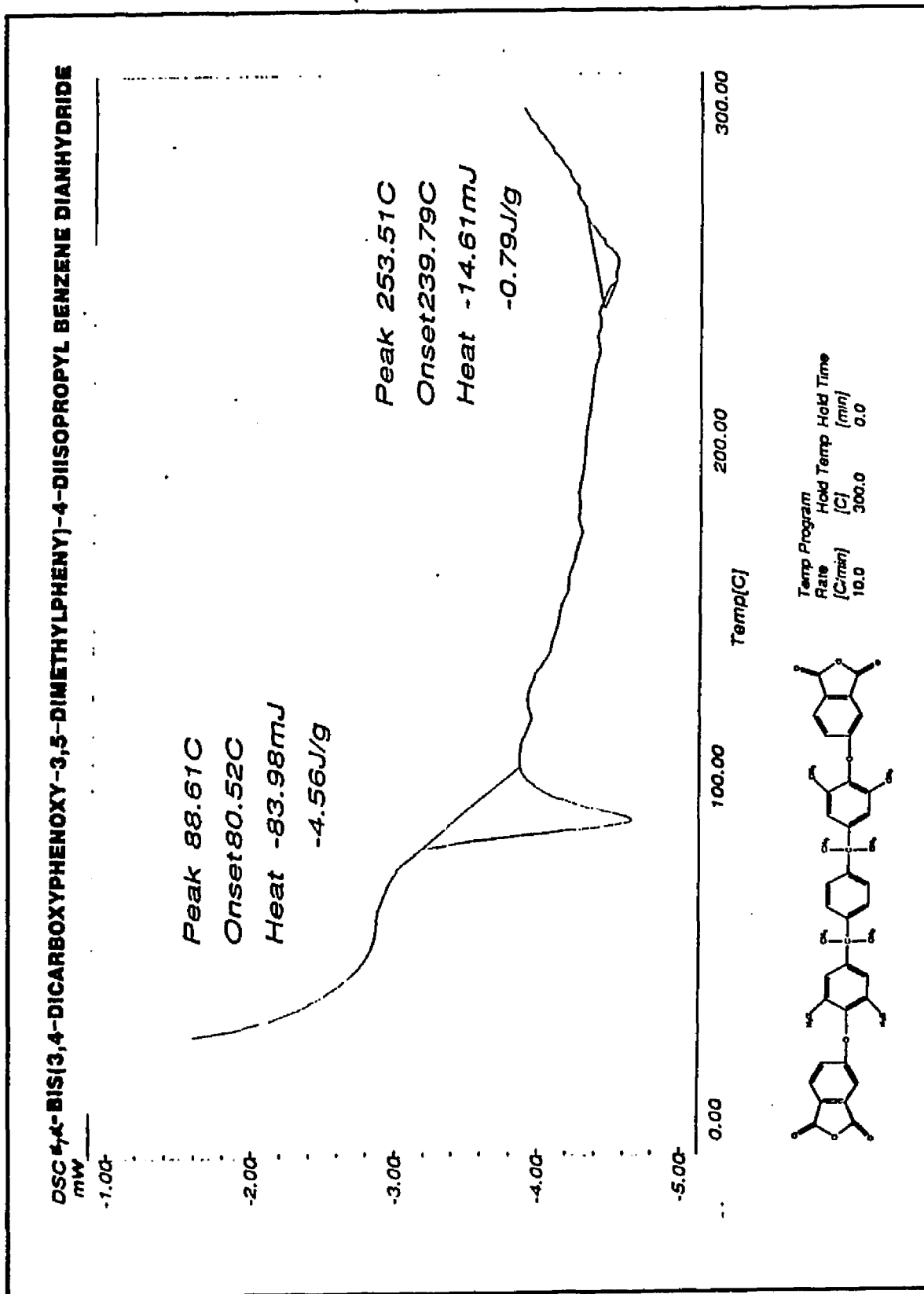


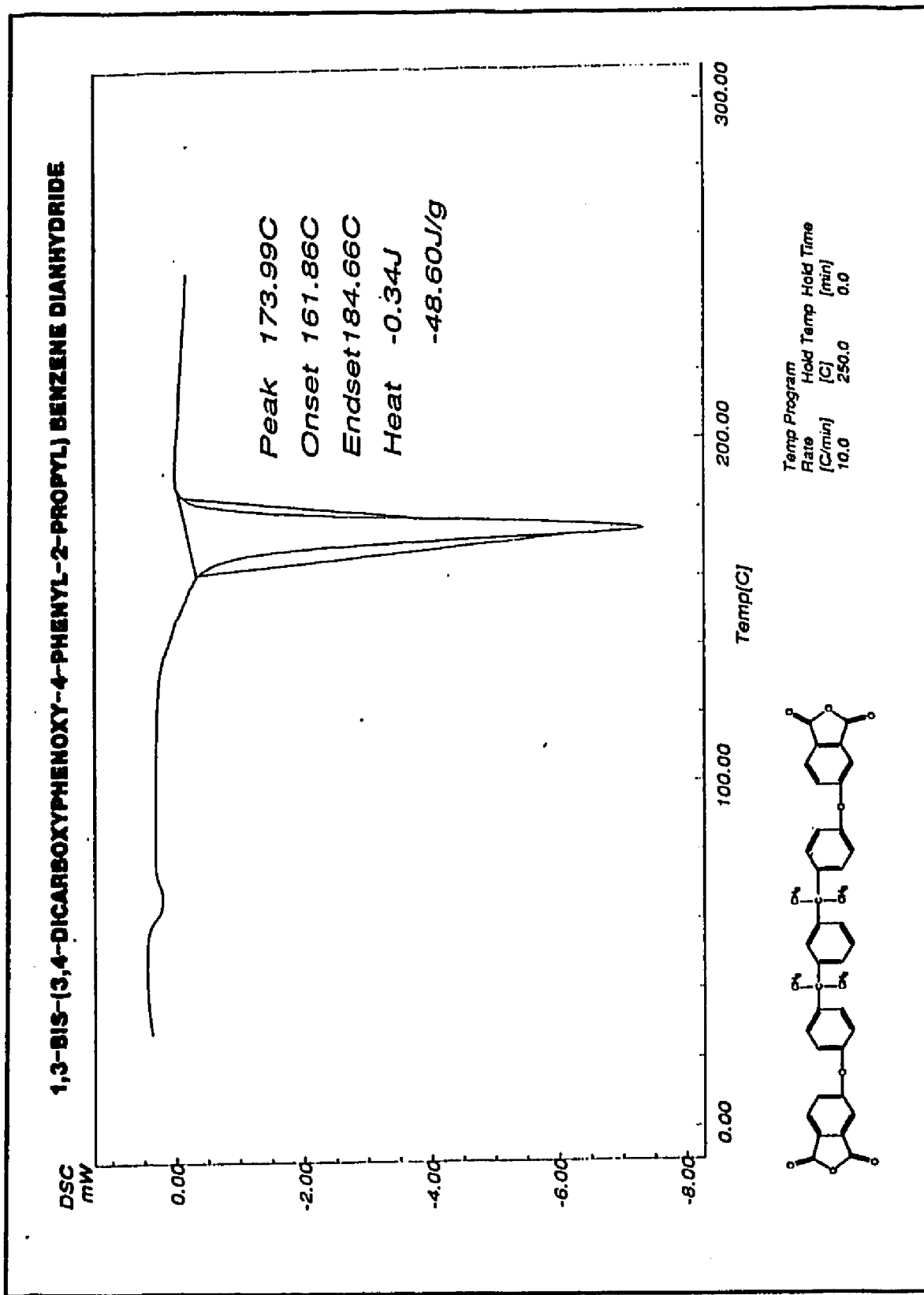


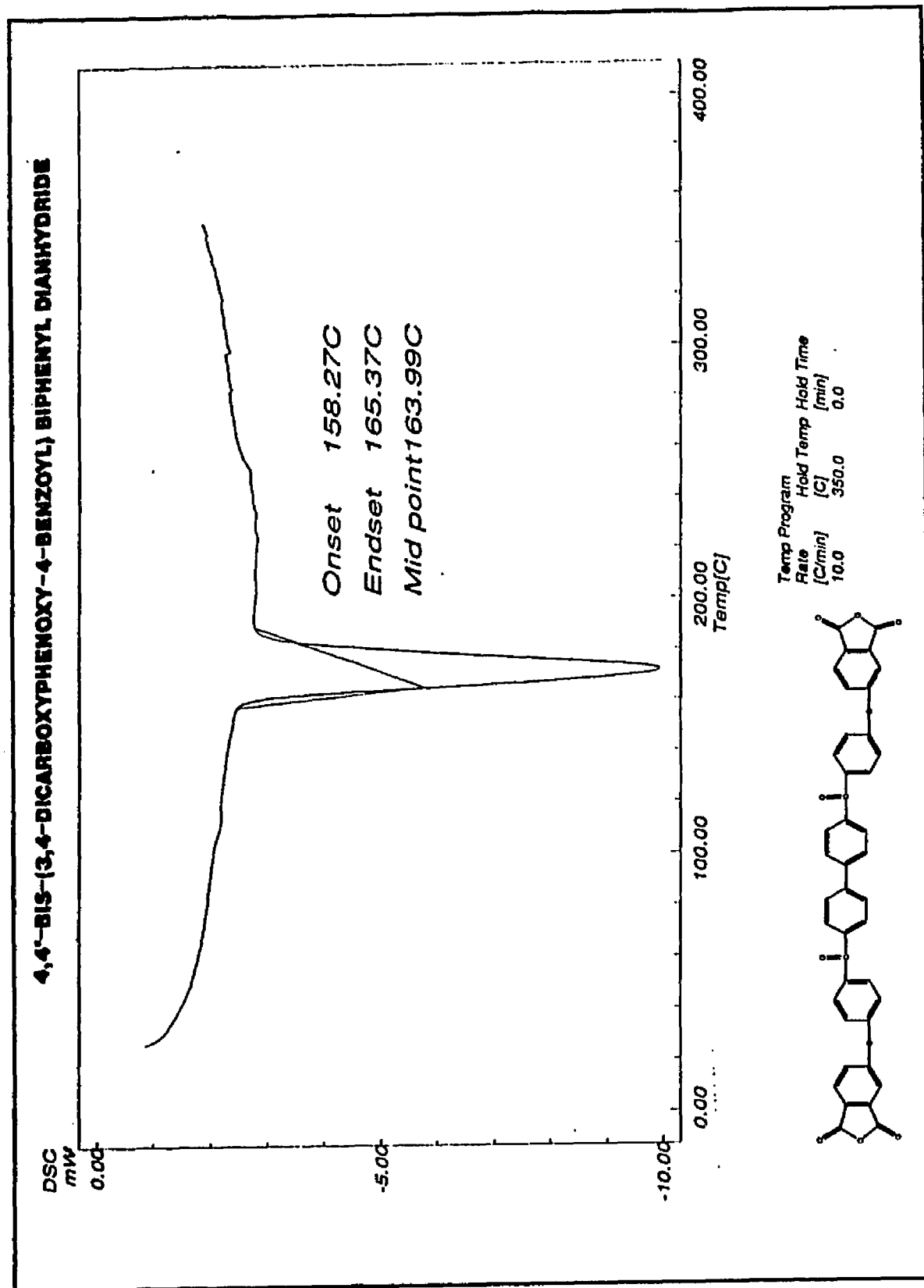




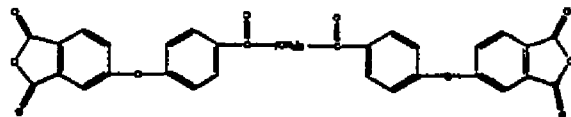
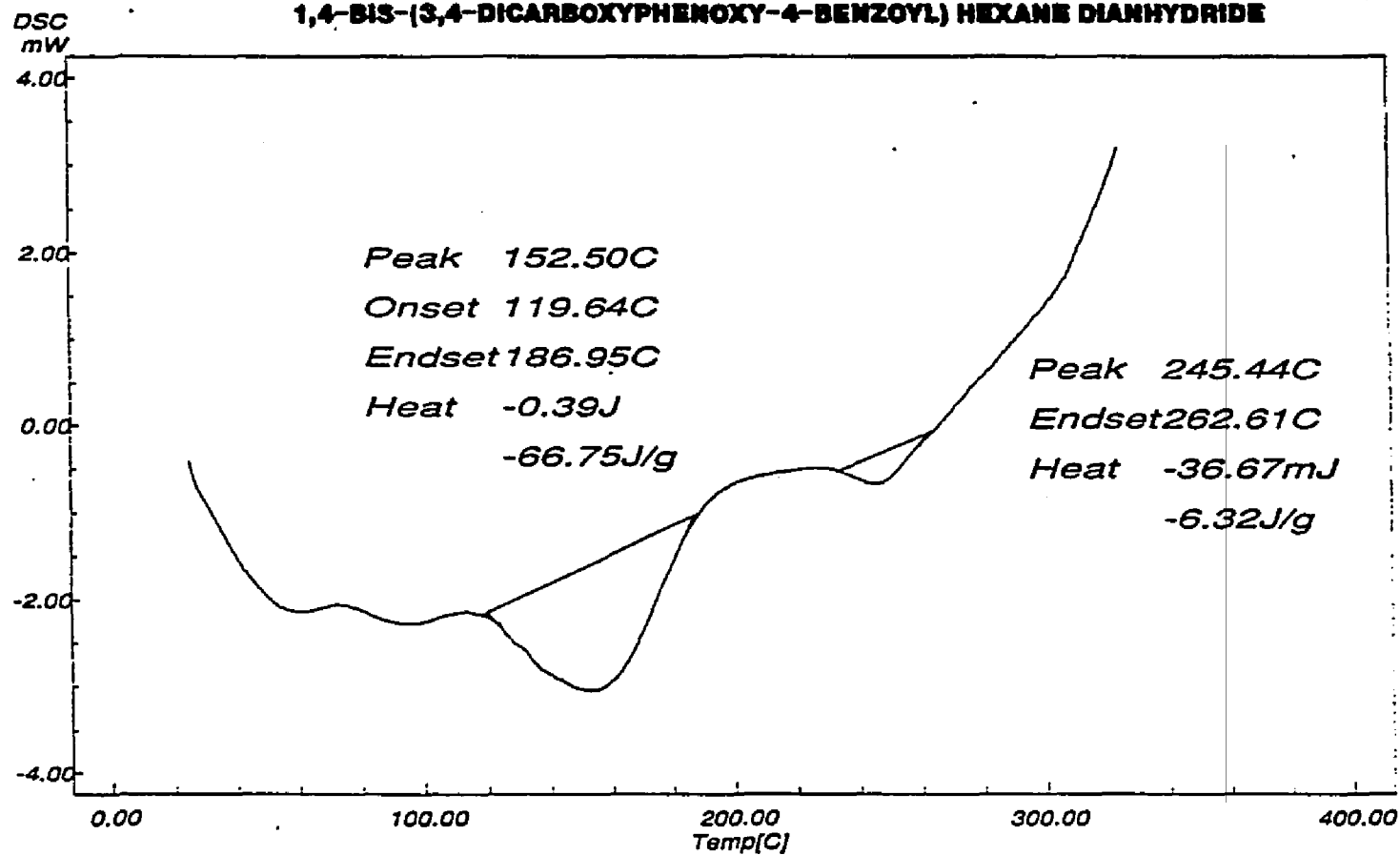




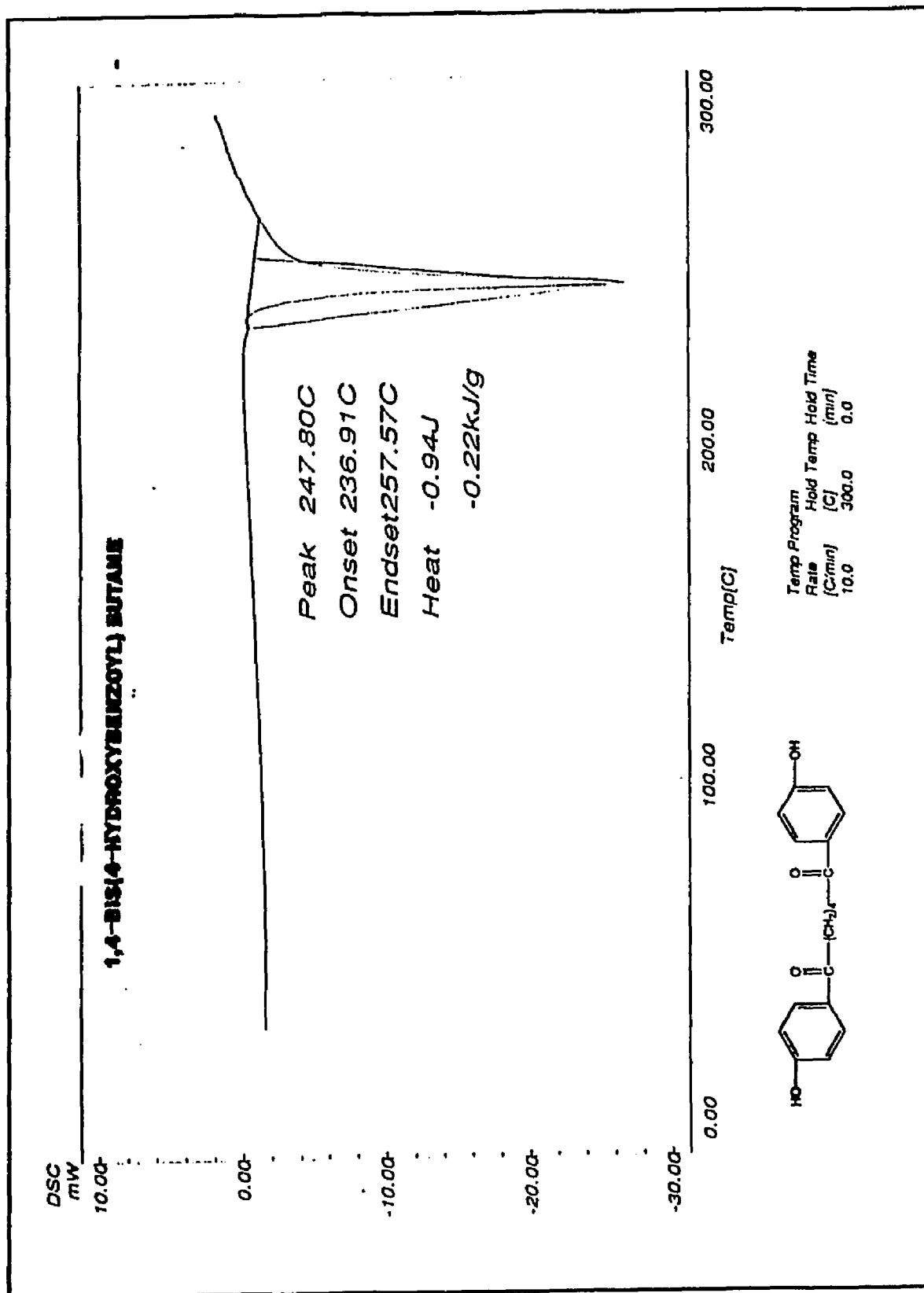


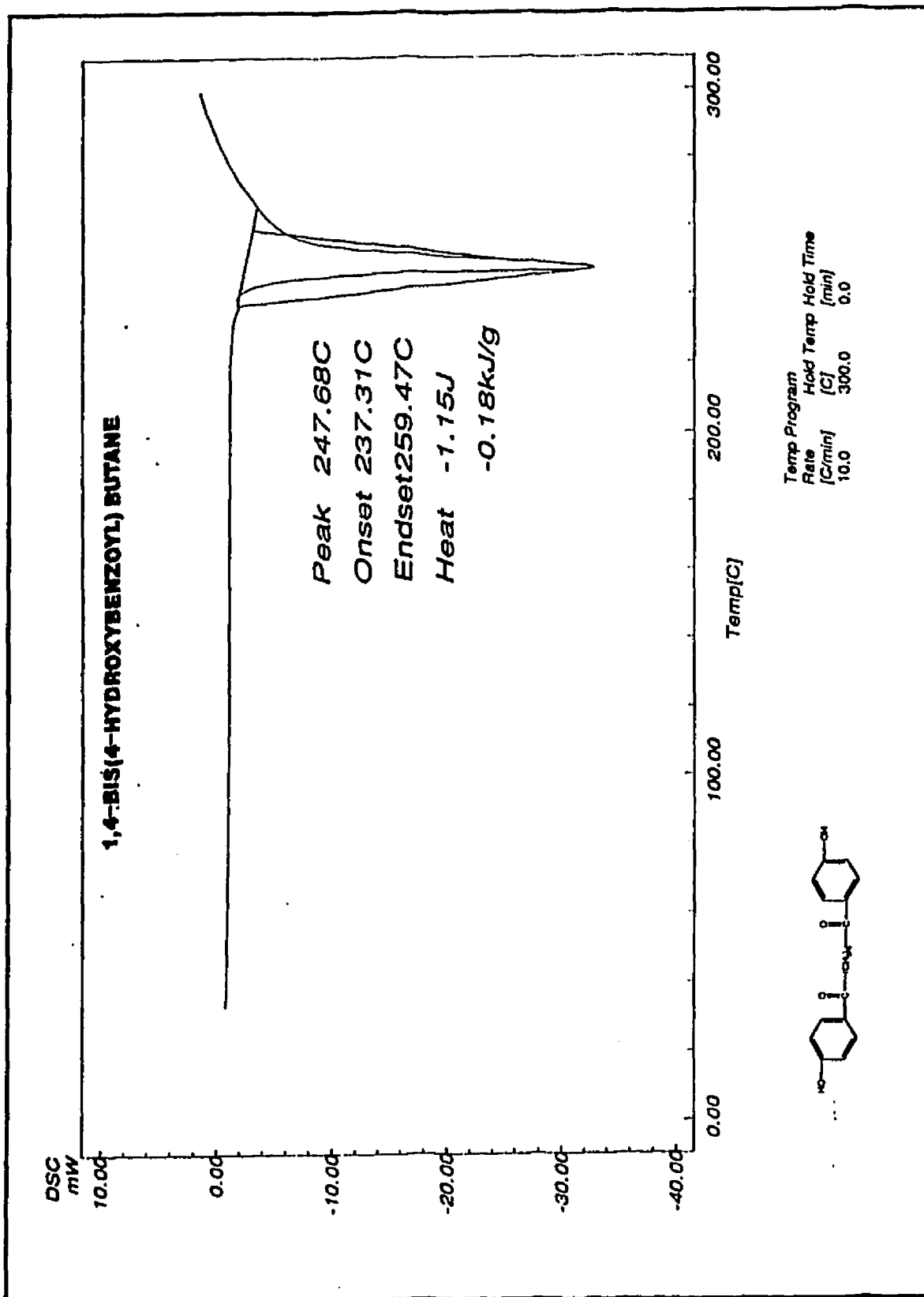


**1,4-BIS-(3,4-DICARBOXYPHENOXY-4-BENZOYL) HEXANE DIANHYDRIDE**



Temp Program		
Rate	Hold Temp	Hold Time
[C/min]	[C]	[min]
10.0	325.0	0.0







**1,3-BIS(3,4-DICARBOXYPHENOXY-4-BENZOYL) BENZENE DIANHYDRIDE**

DSC  
mW

2.00

0.00

-2.00

-4.00

-6.00

Peak 142.00C

Onset 129.62C

Endset 153.04C

Heat -0.41J

-34.13J/g

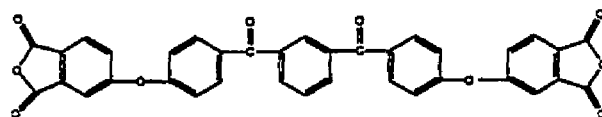
0.00

100.00

Temp[C]

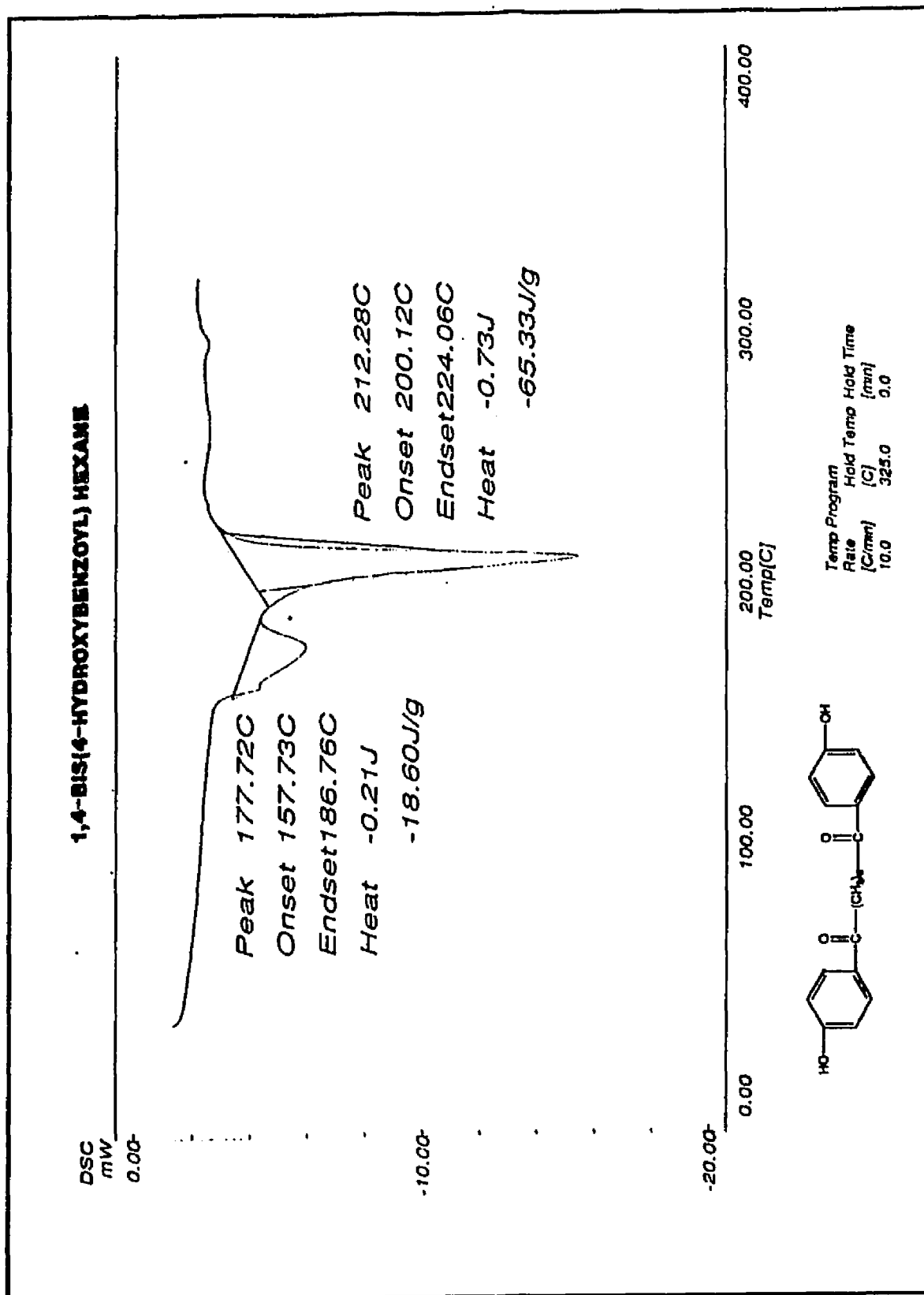
200.00

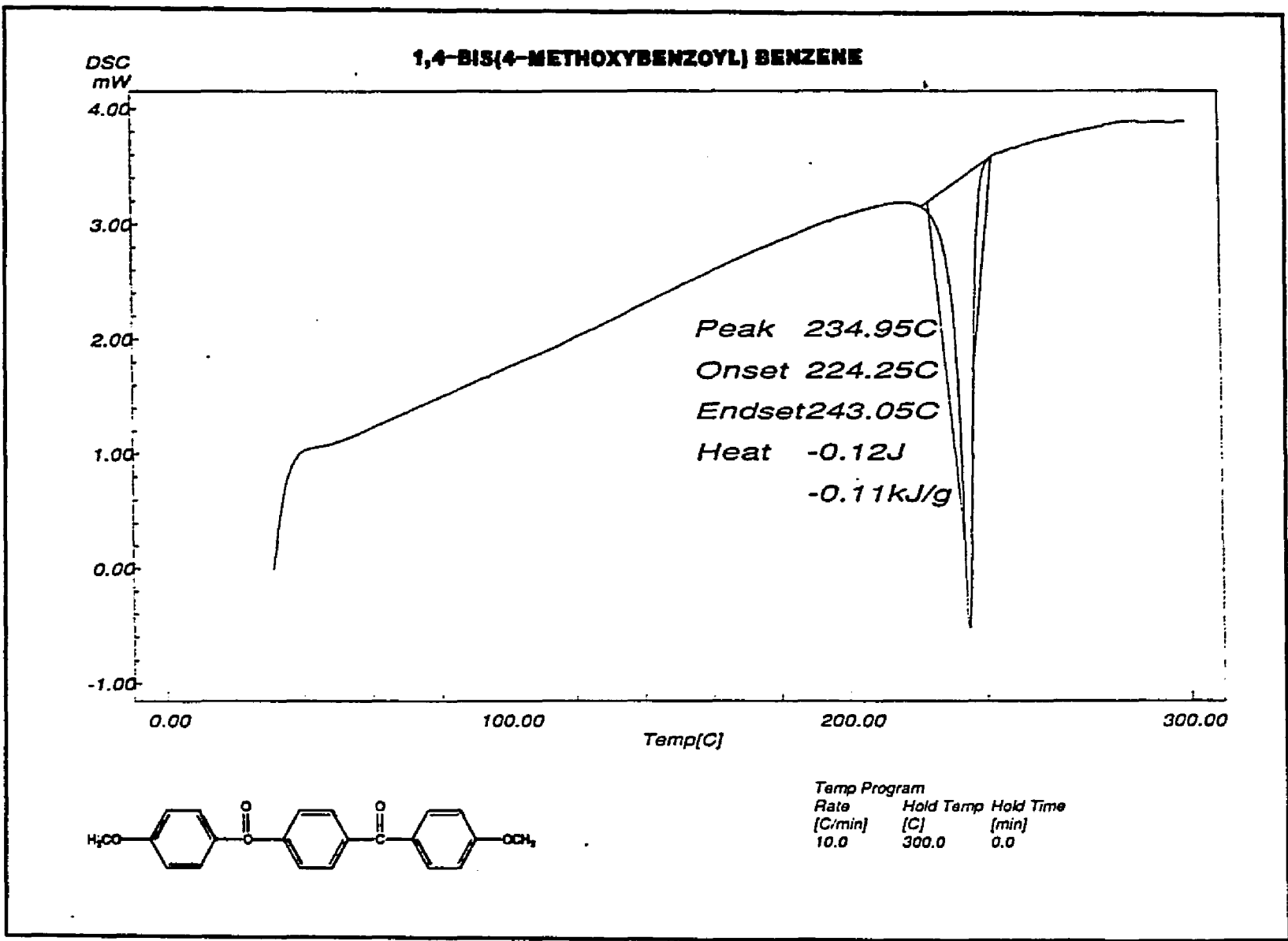
300.00

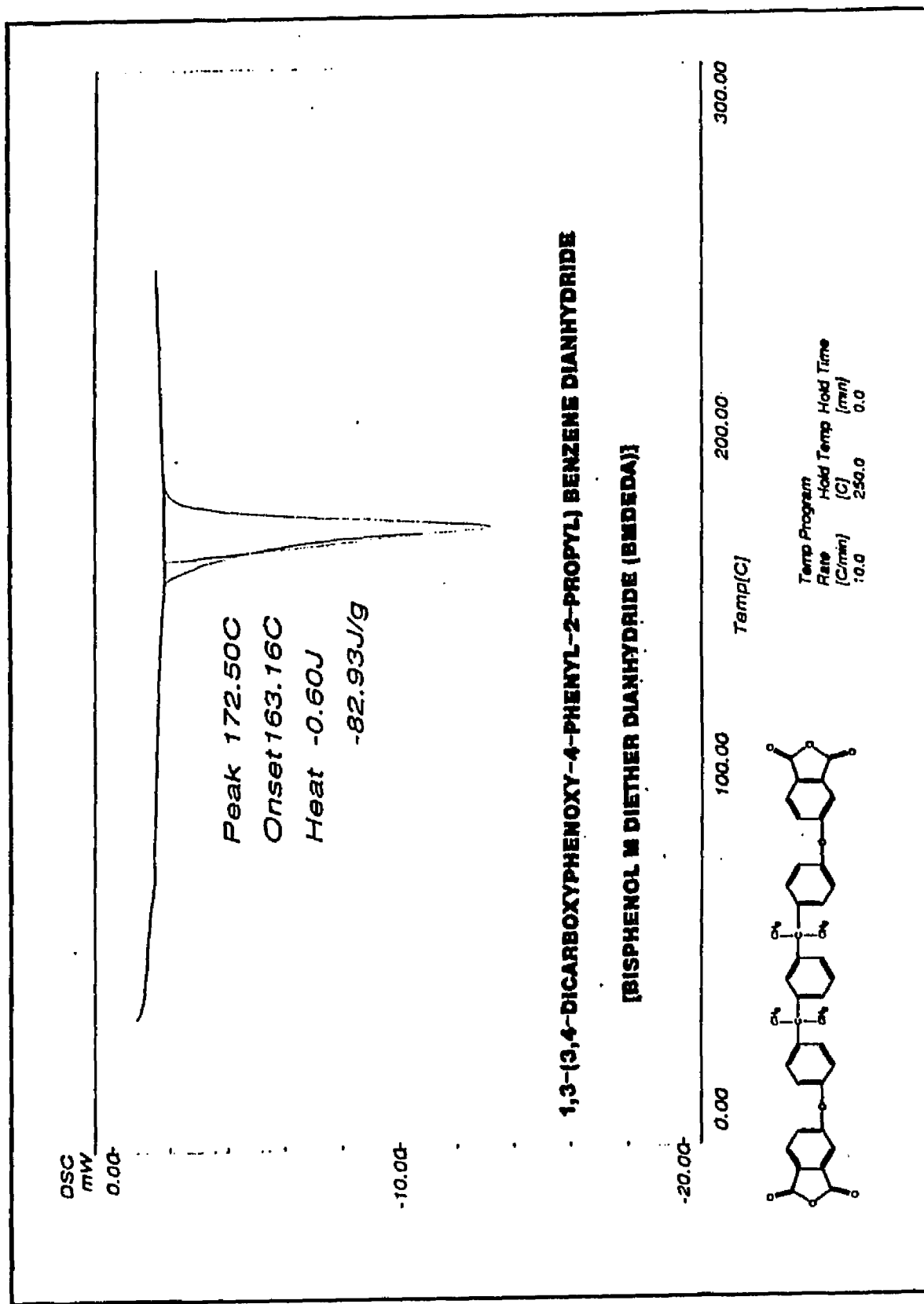


Temp Program

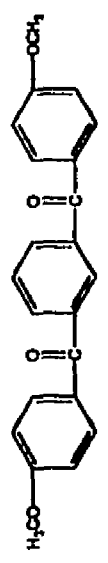
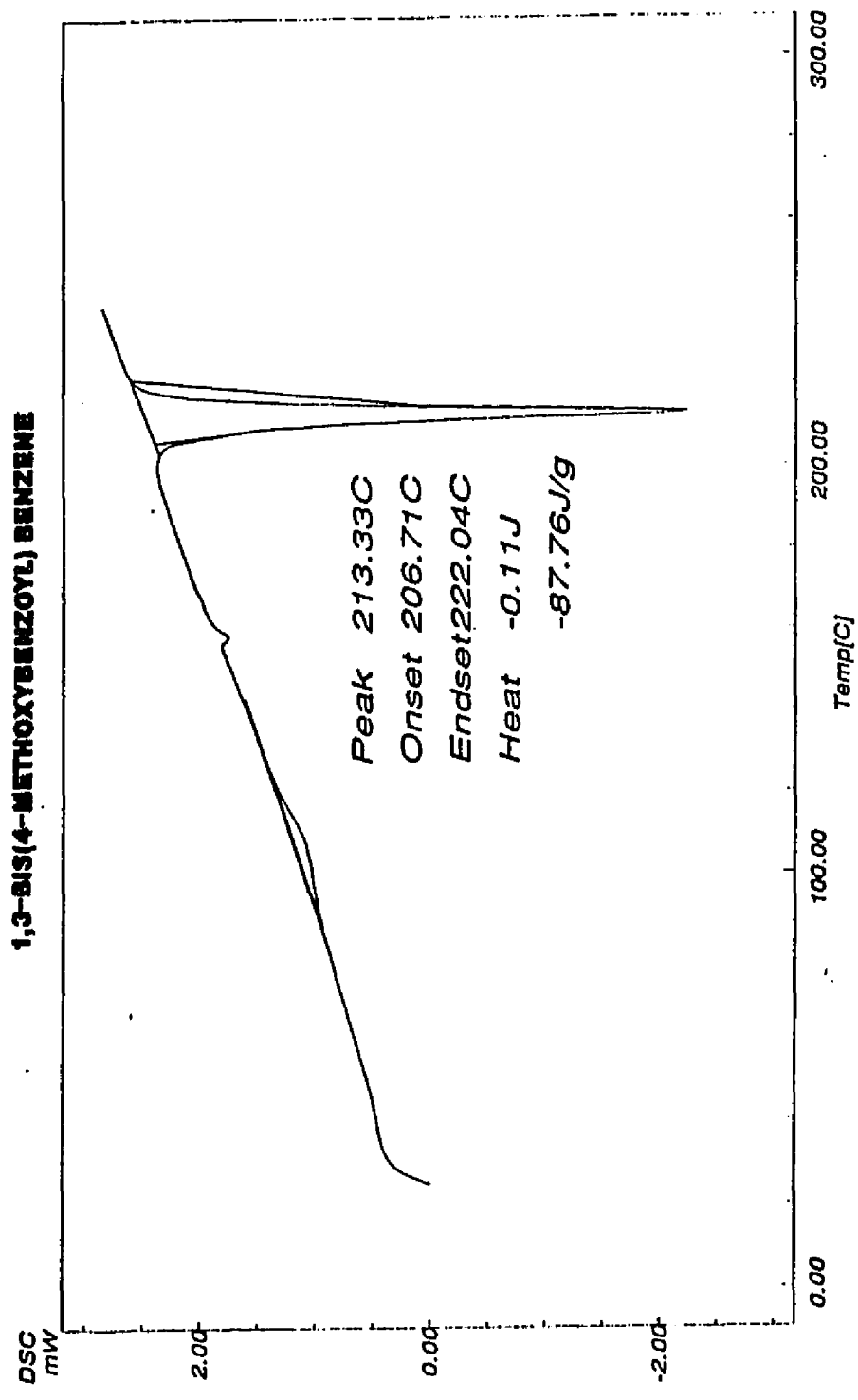
Rate [C/min]	Hold Temp [C]	Hold Time [min]
10.0	250.0	0.0



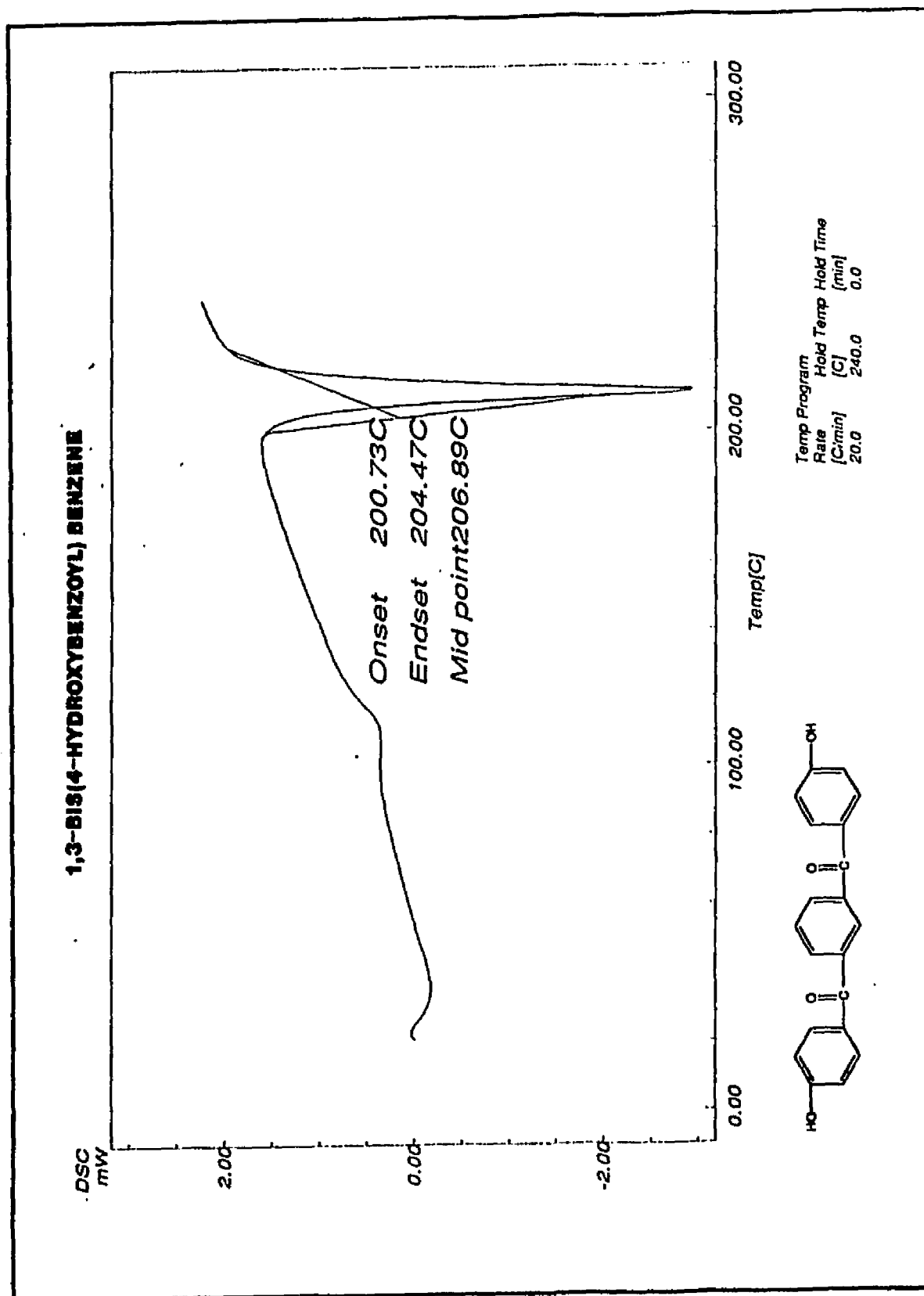


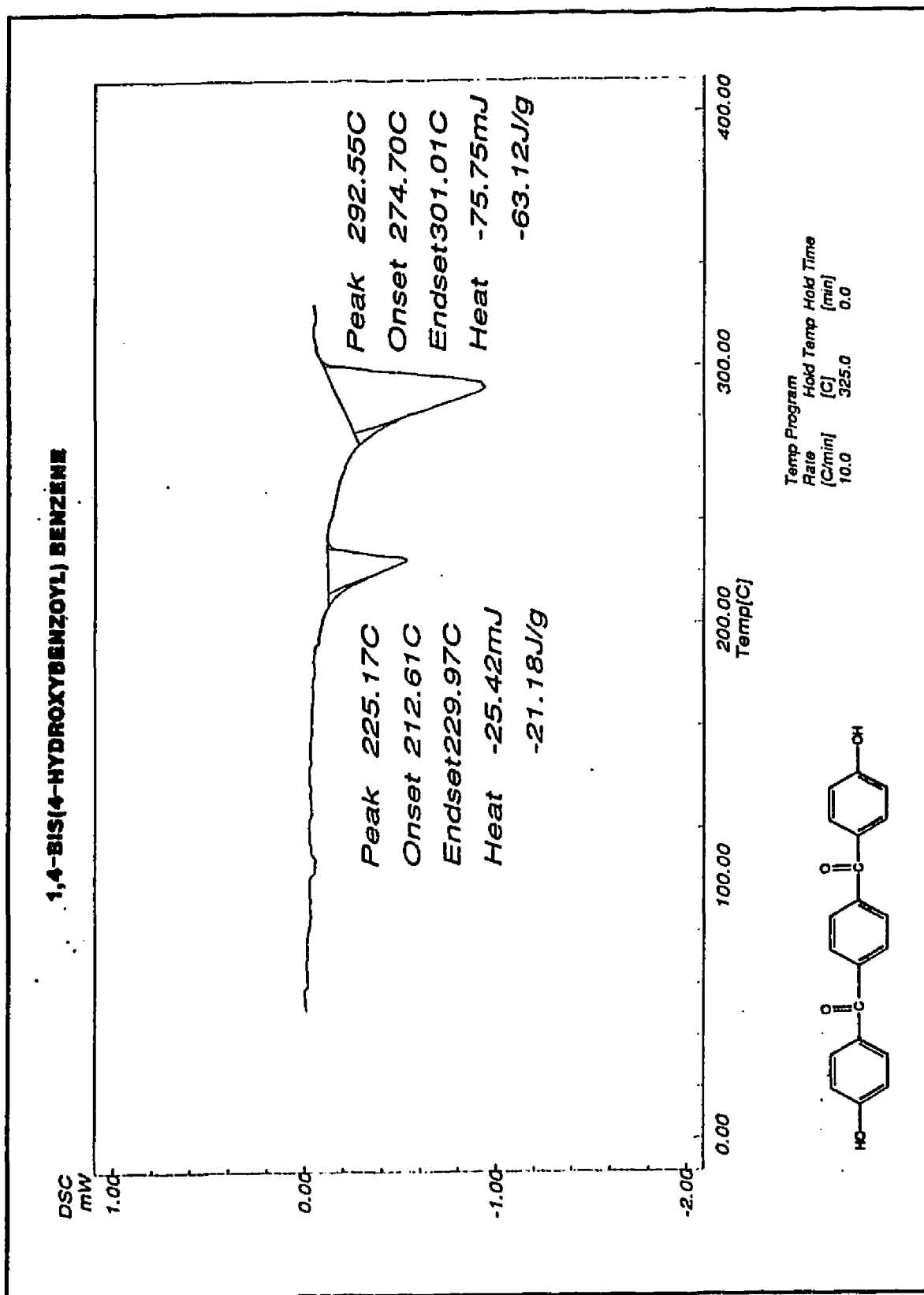


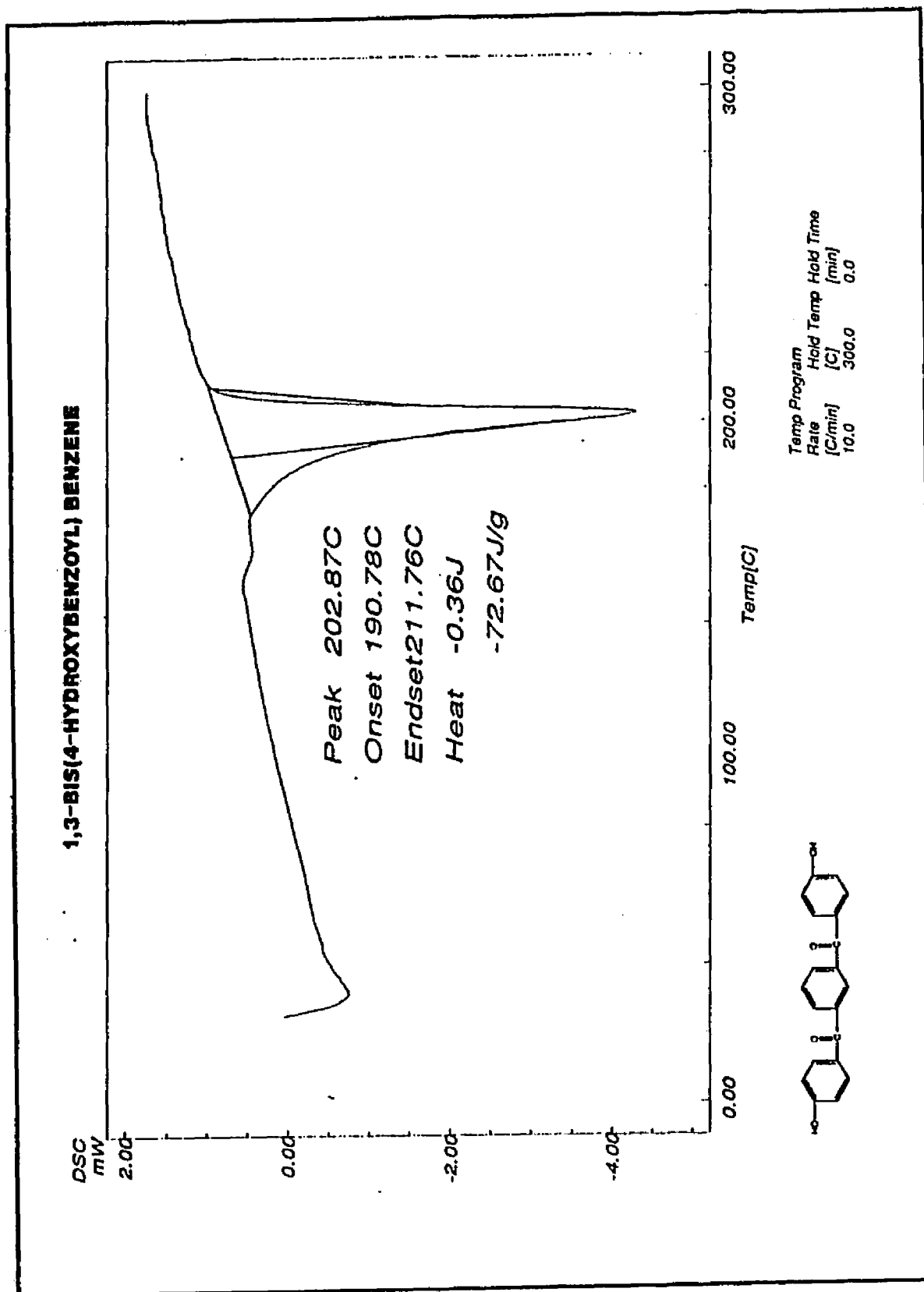
**1,3-BIS(4-METHOXYBENZOYL) BENZENE**



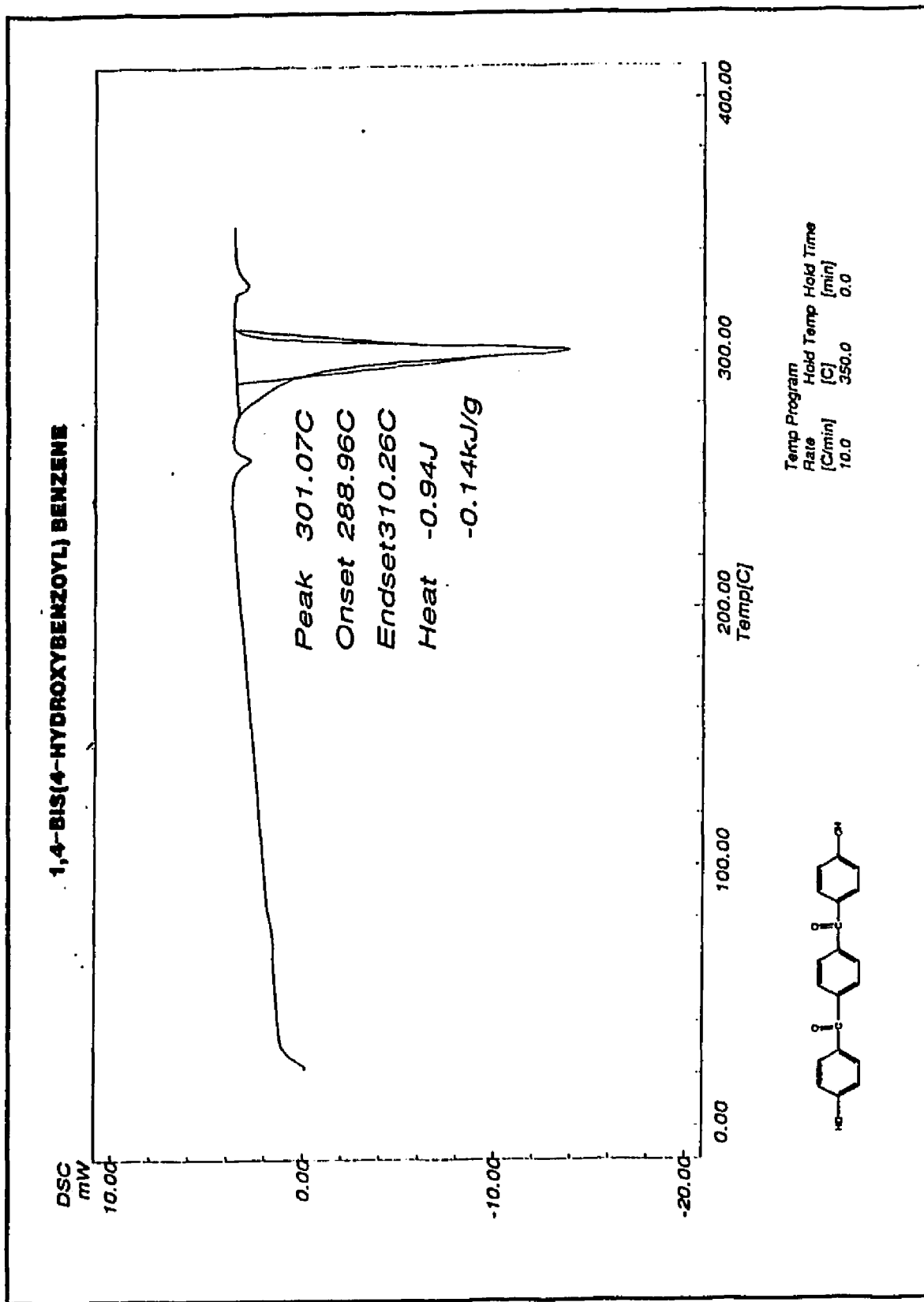
Temp Program  
Rate (C/min) 10.0  
Hold Temp (C) 240.0  
Hold Time (min) 0.0

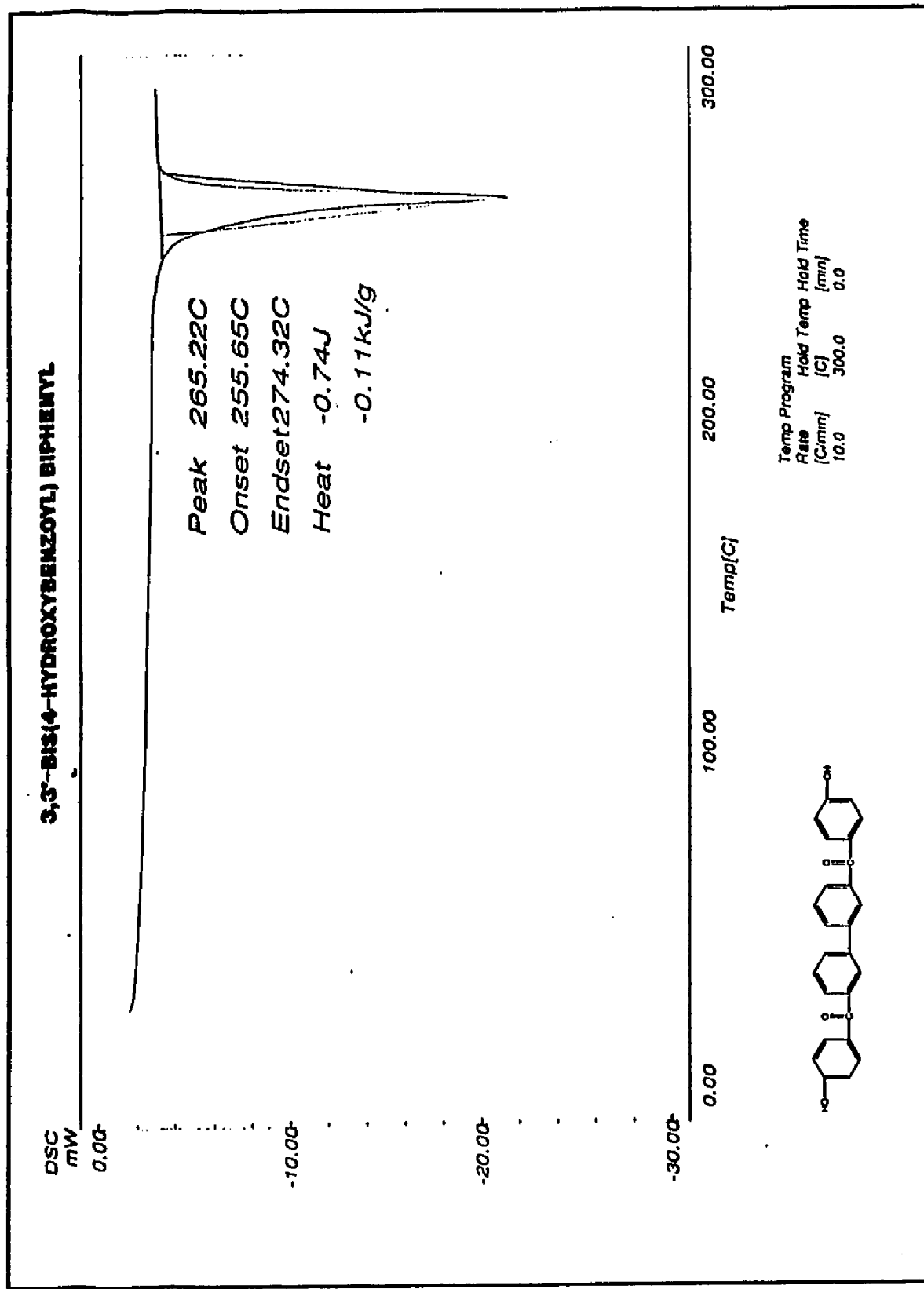




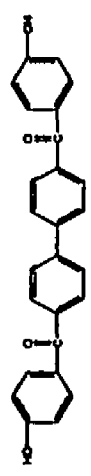
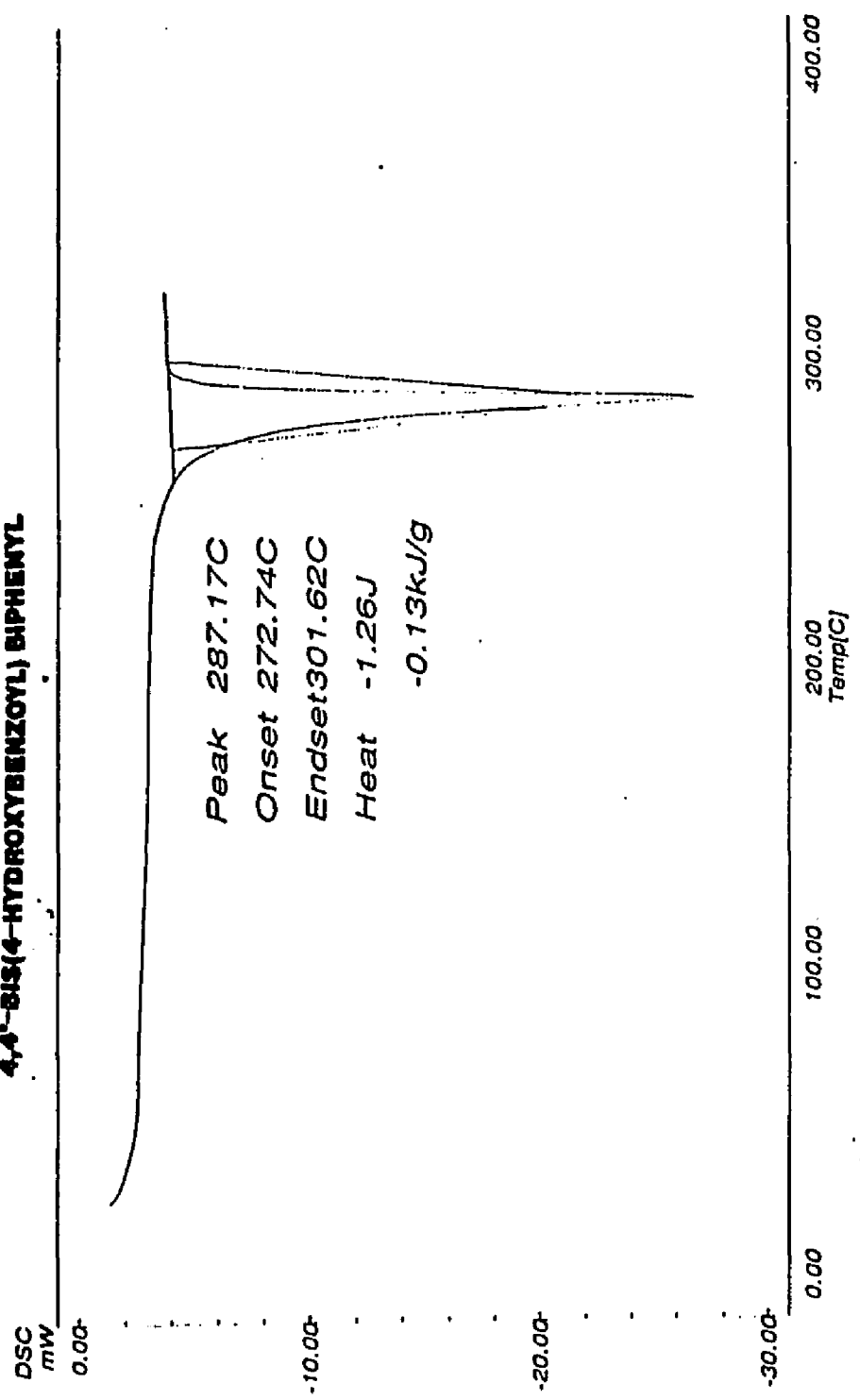




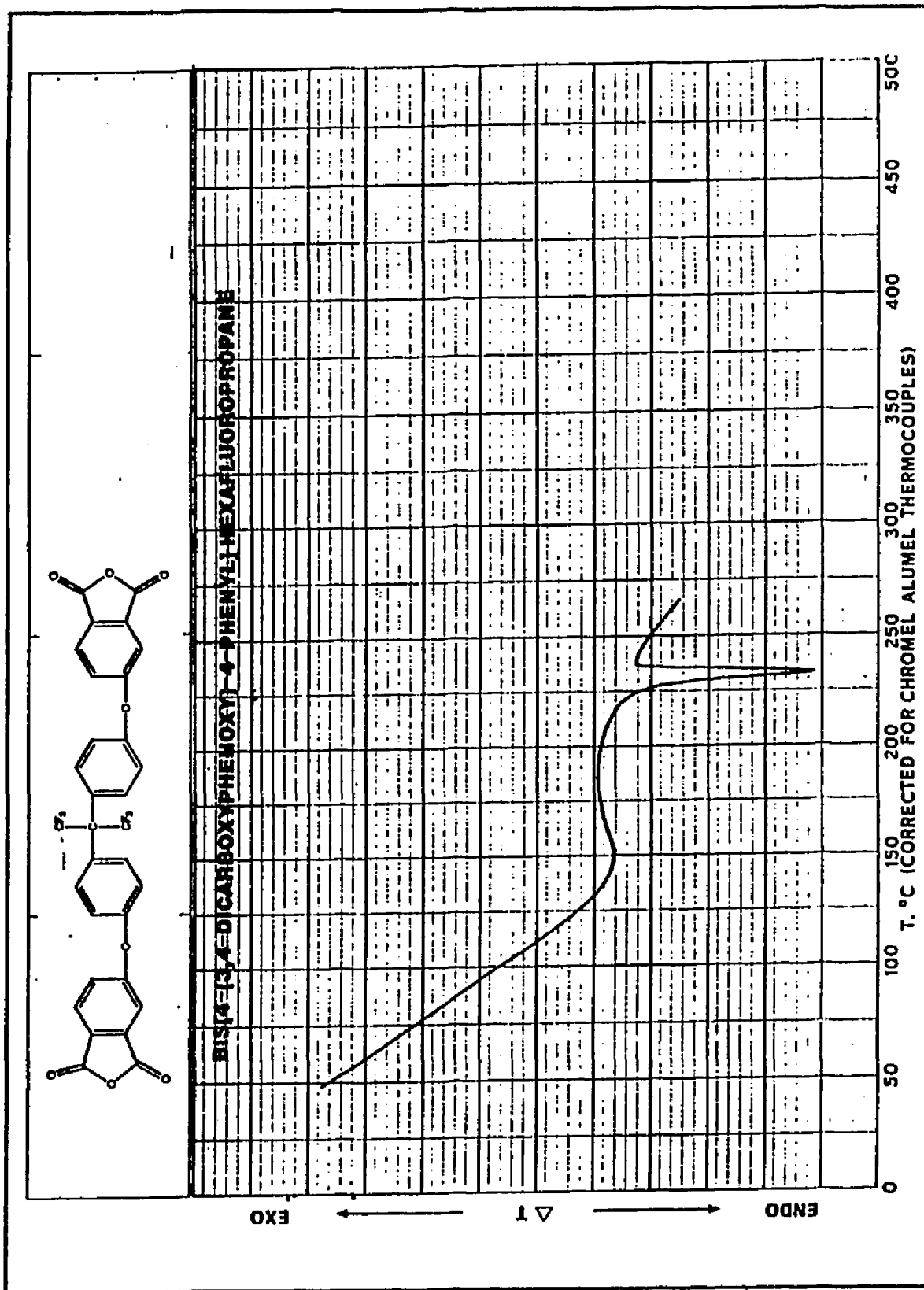


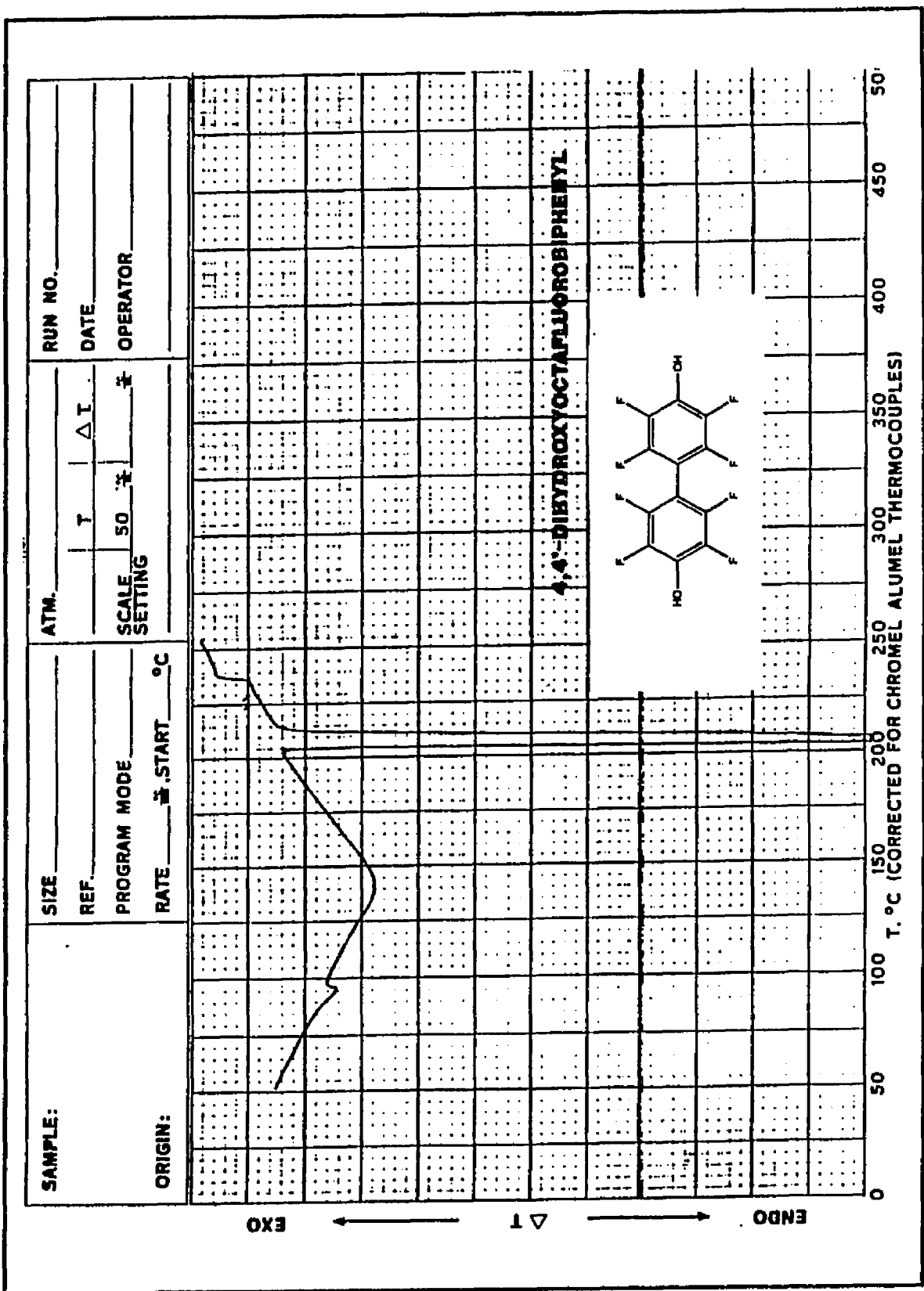


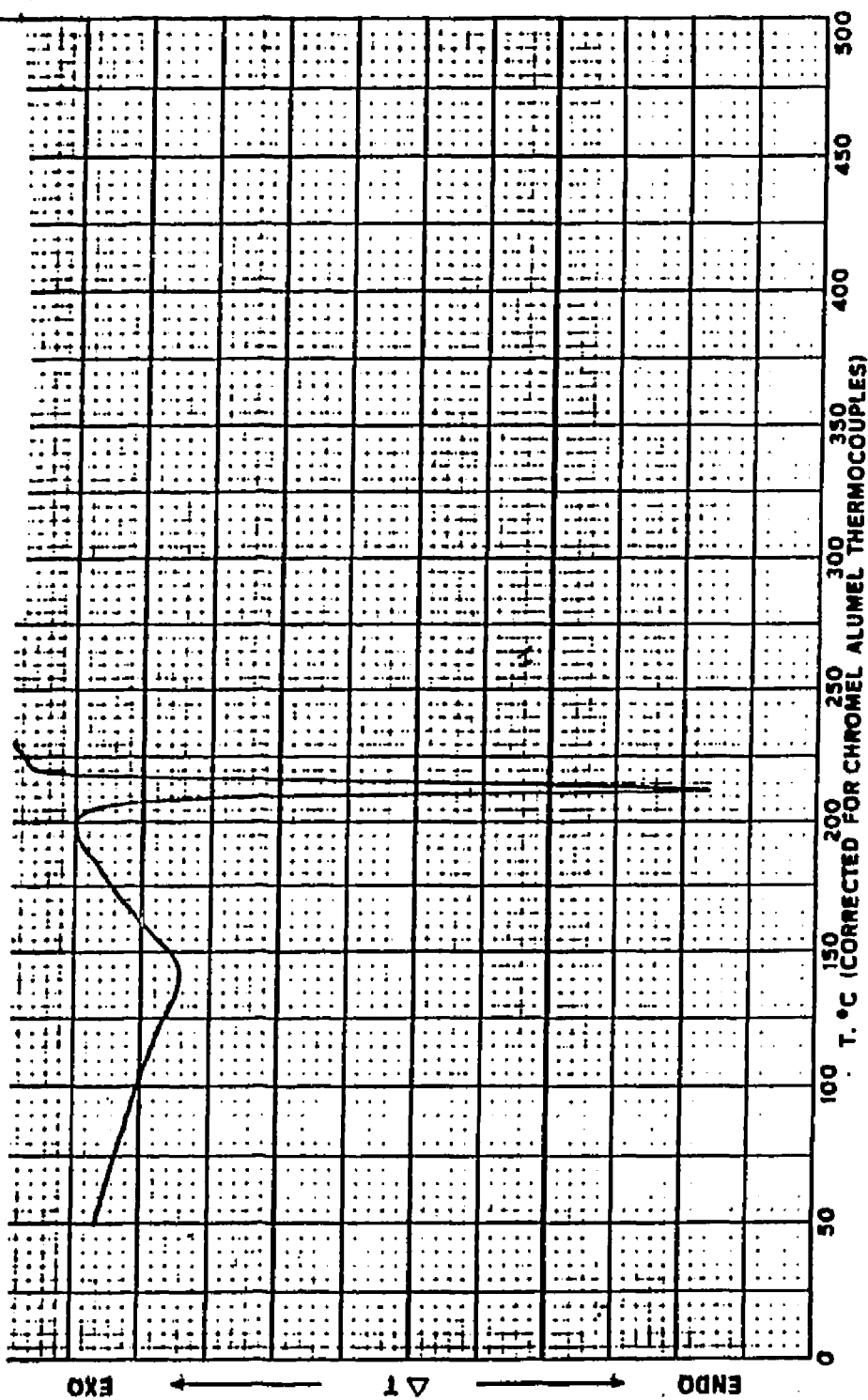
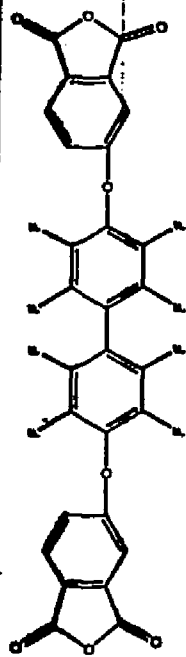
**4,4'-BIS(4-HYDROXYBENZOYL) BIPHENYL**



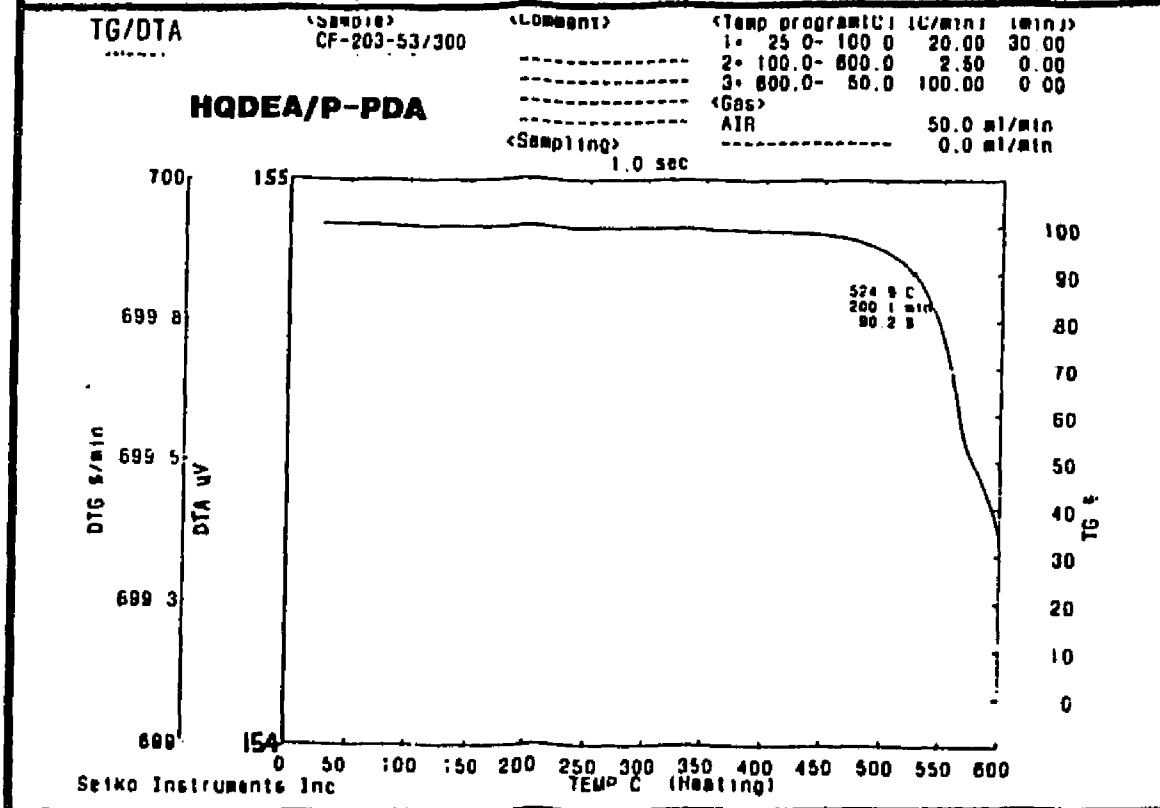
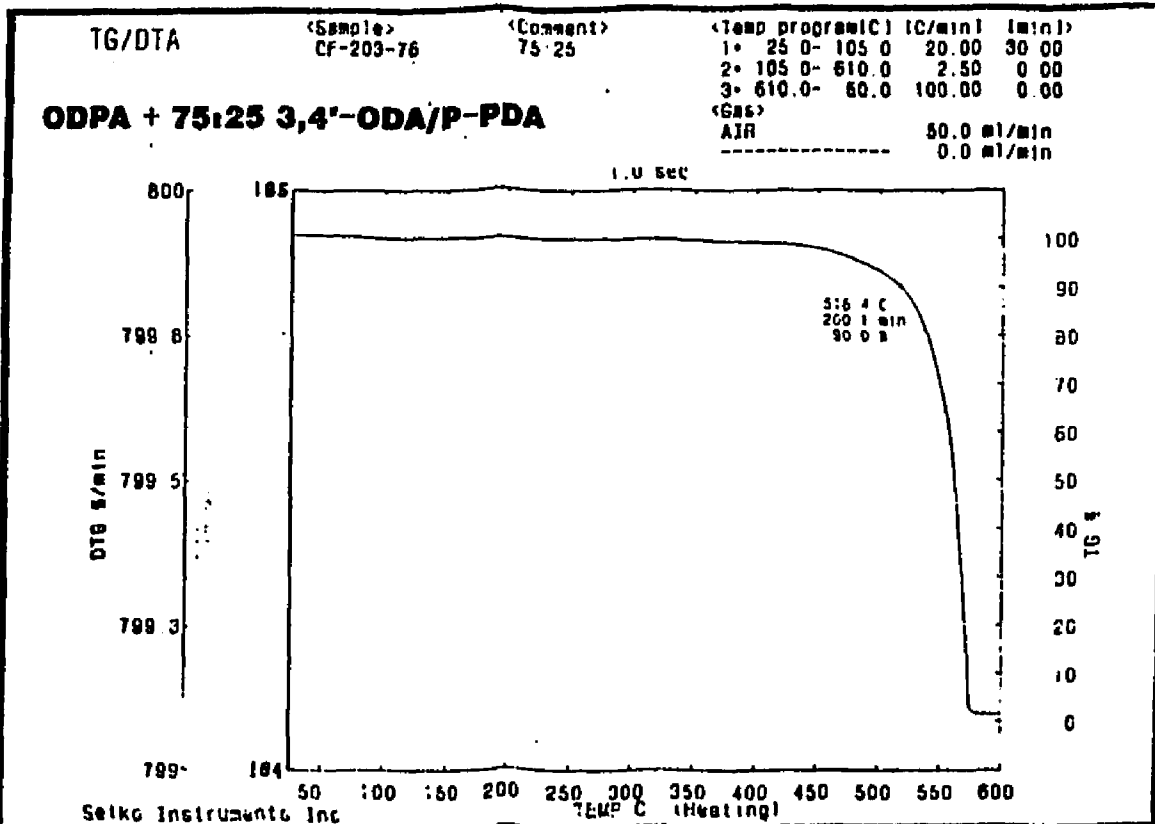
Temp Program  
Rate (C/min) 10.0  
Hold Temp (C) 325.0  
Hold Time (min) 9.0



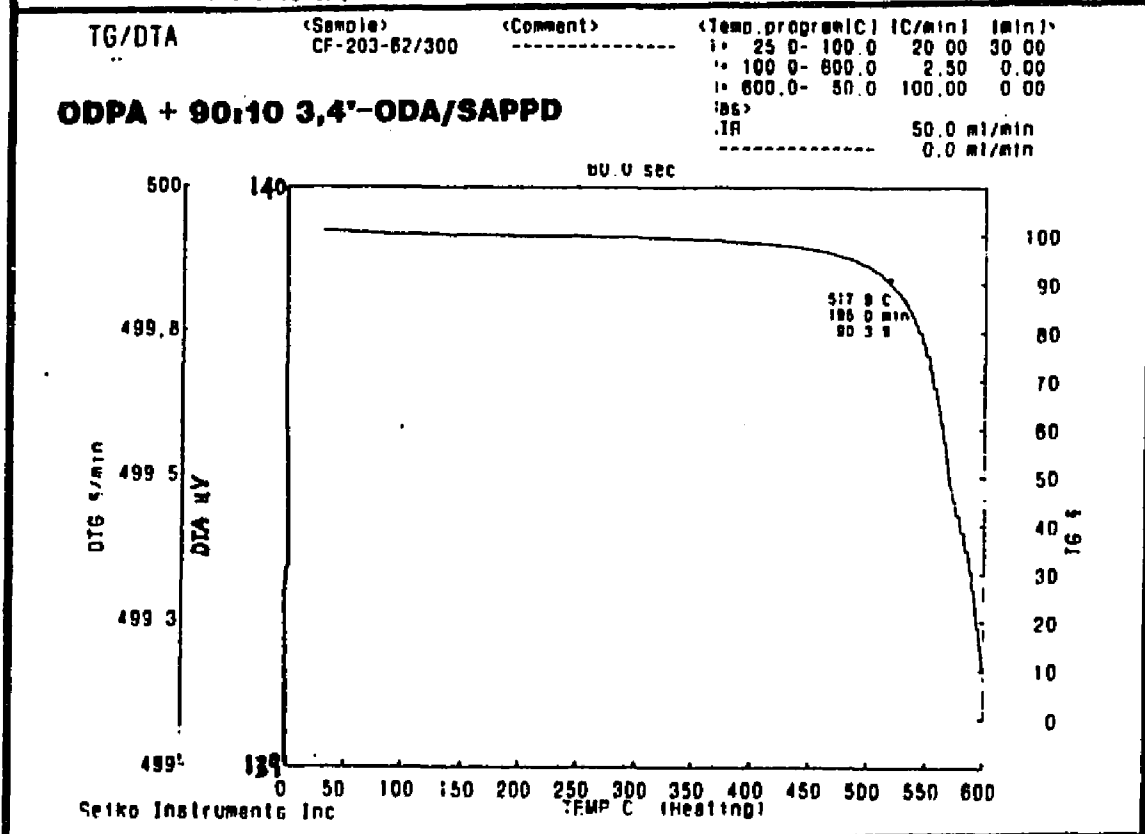
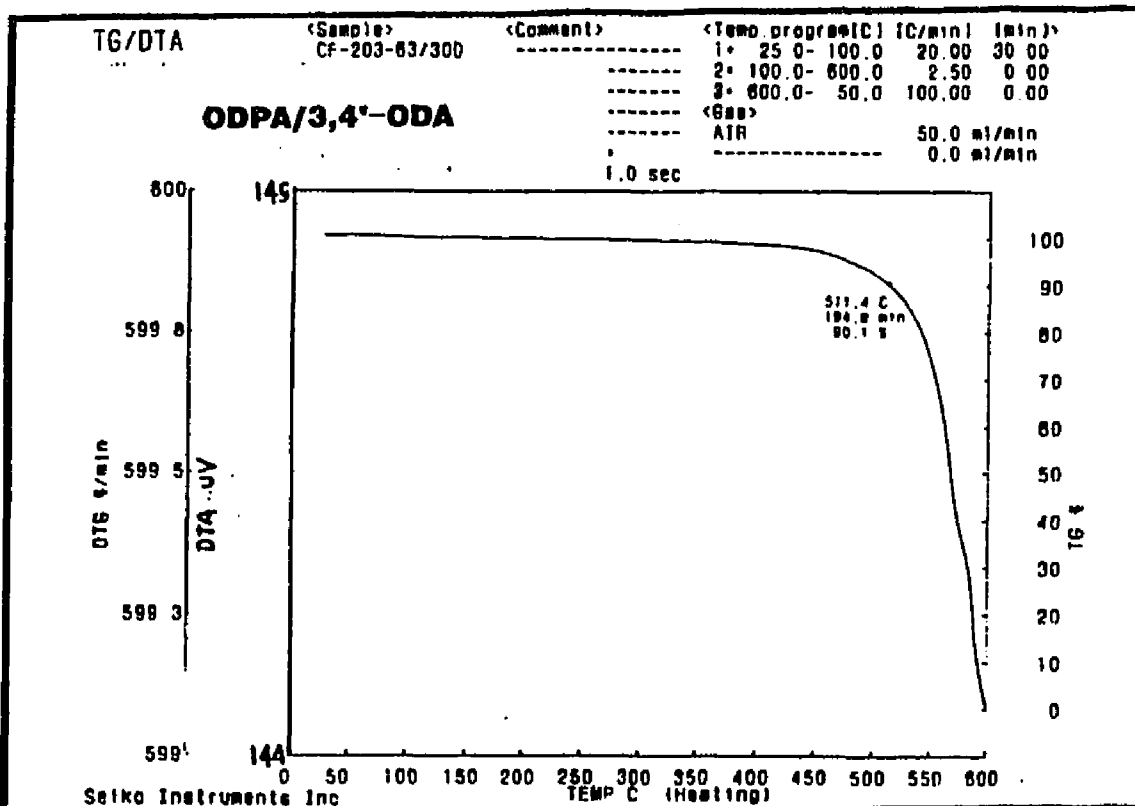


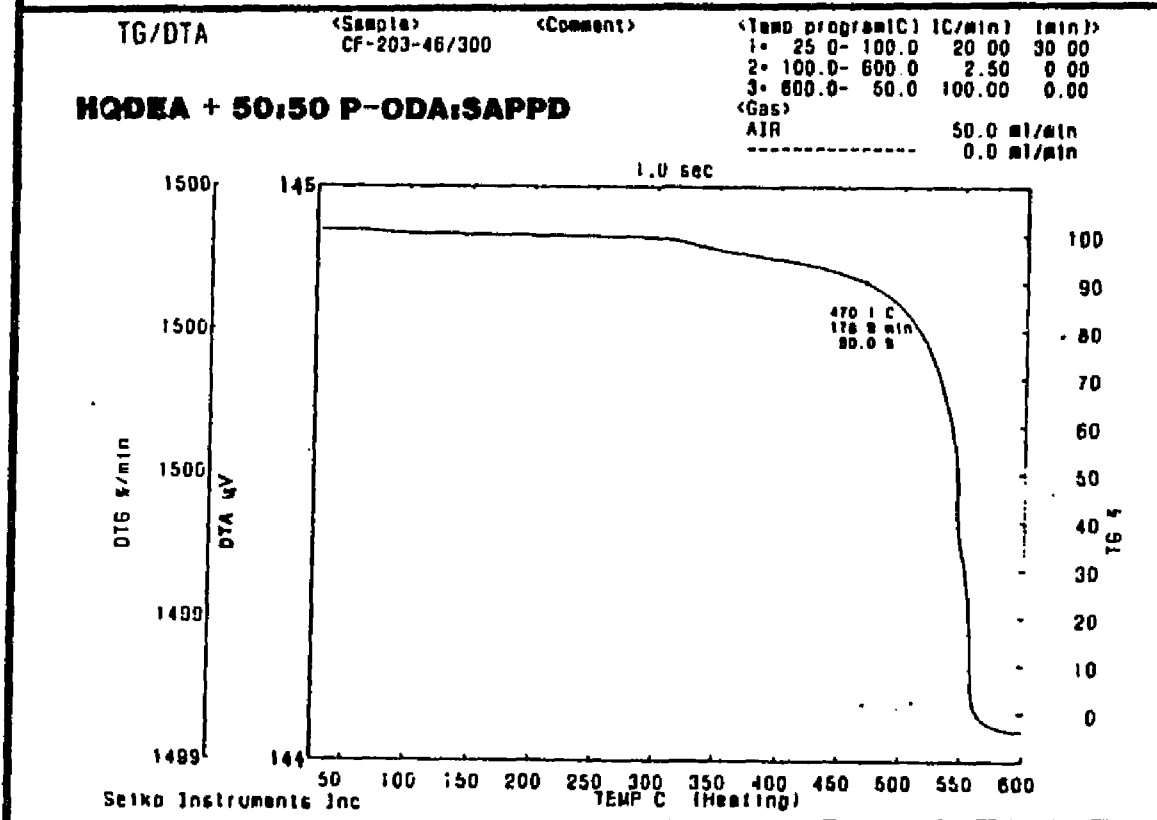
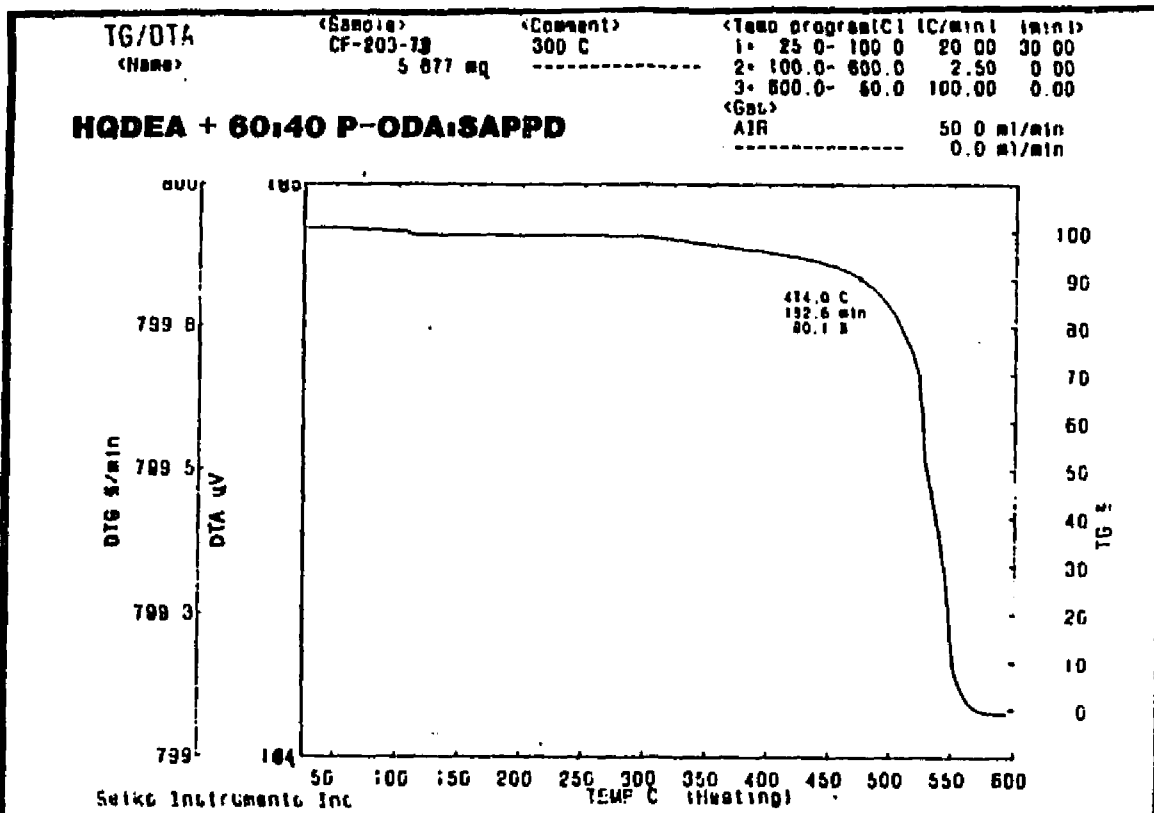
**4,4'-DIBIP-2,6-DICARBOXYPHENONYL****OCTAFLUOROBIPHENYL DIANHYDRIDE**

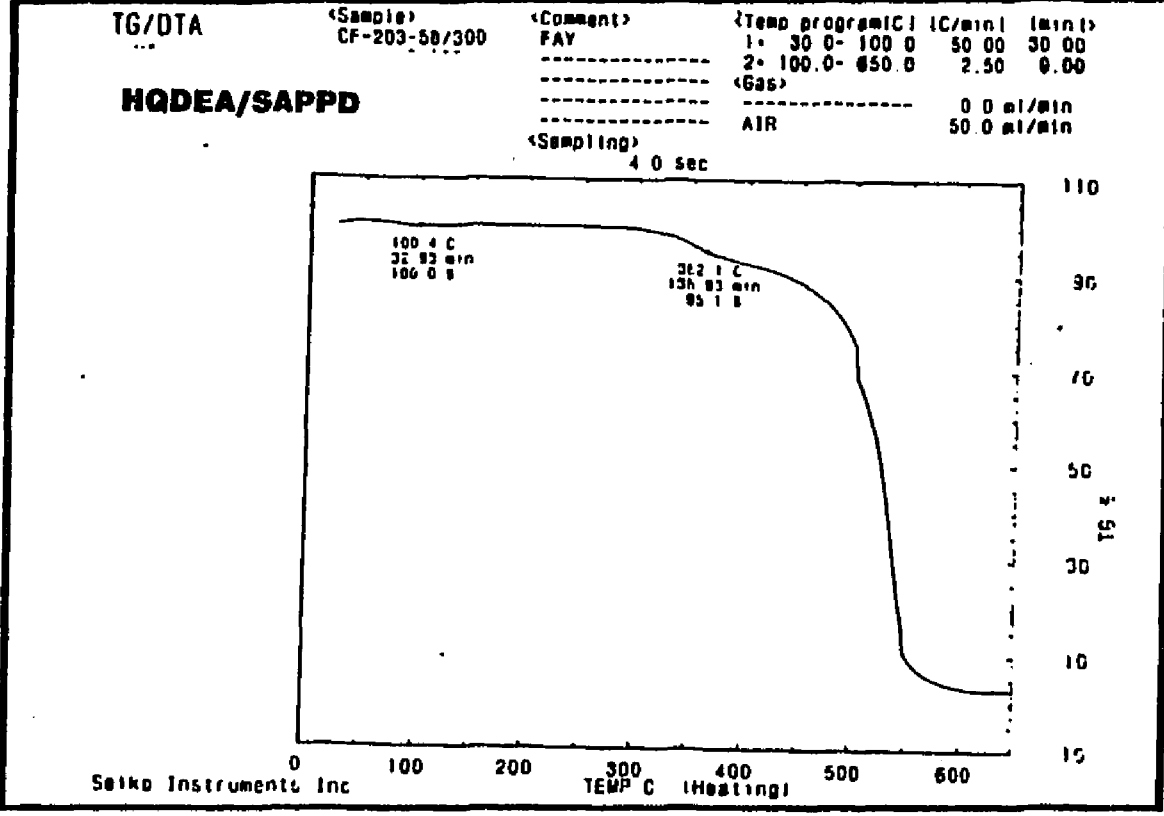
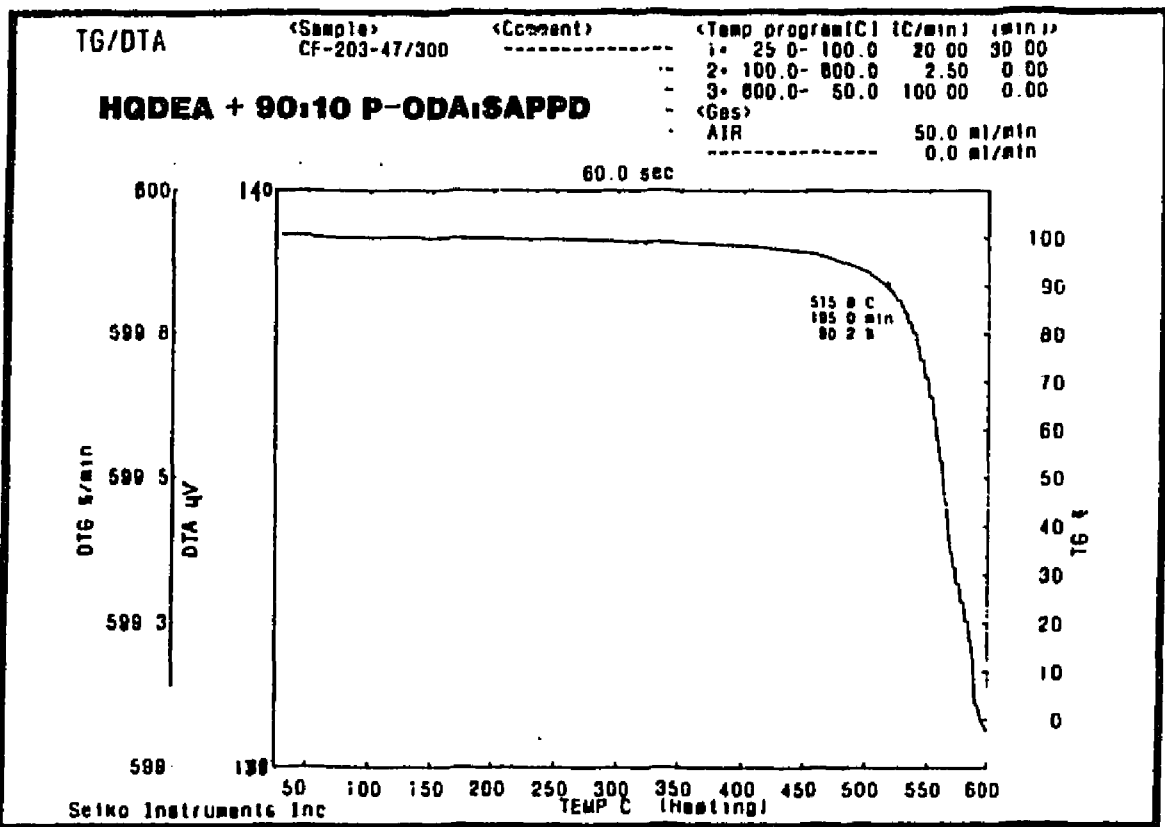
## THERMAL ANALYSIS: TGA, DSC, TMA, AND CTE







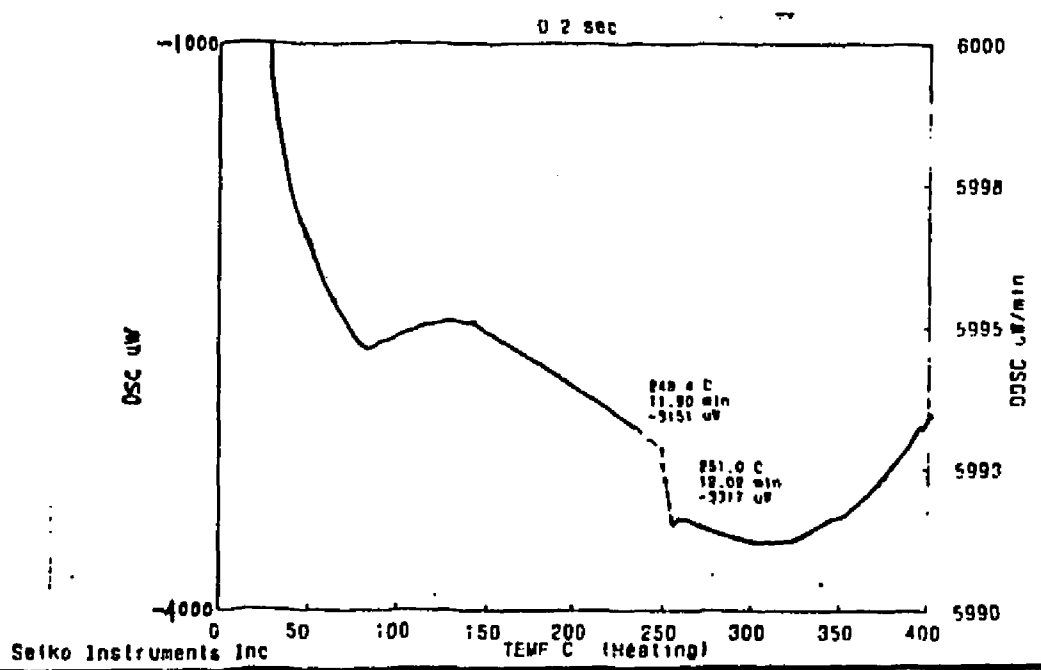




DSC

<Sample> CF-203-47/300  
<Comment> -----  
<Temp Program(C) (C/min) (min)>  
1: 25 0- 550 0 20 00 0 00  
2: -----  
----- 0.0 ml/min  
----- 0.0 ml/min

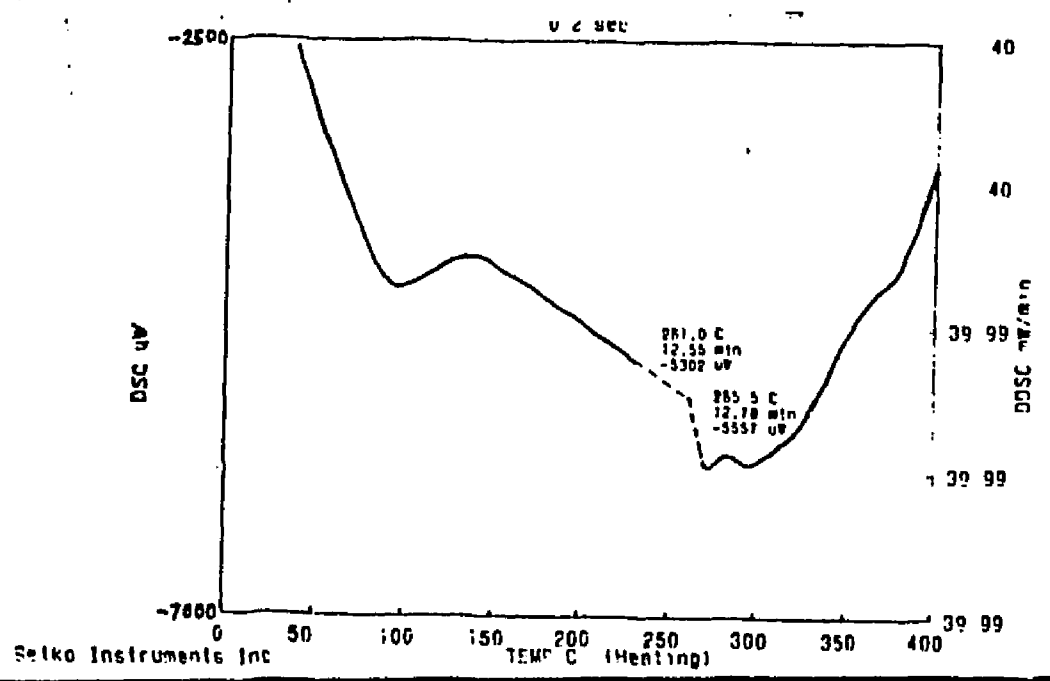
**HQDEA + 90:10 4,4'-ODA/SAPPD**

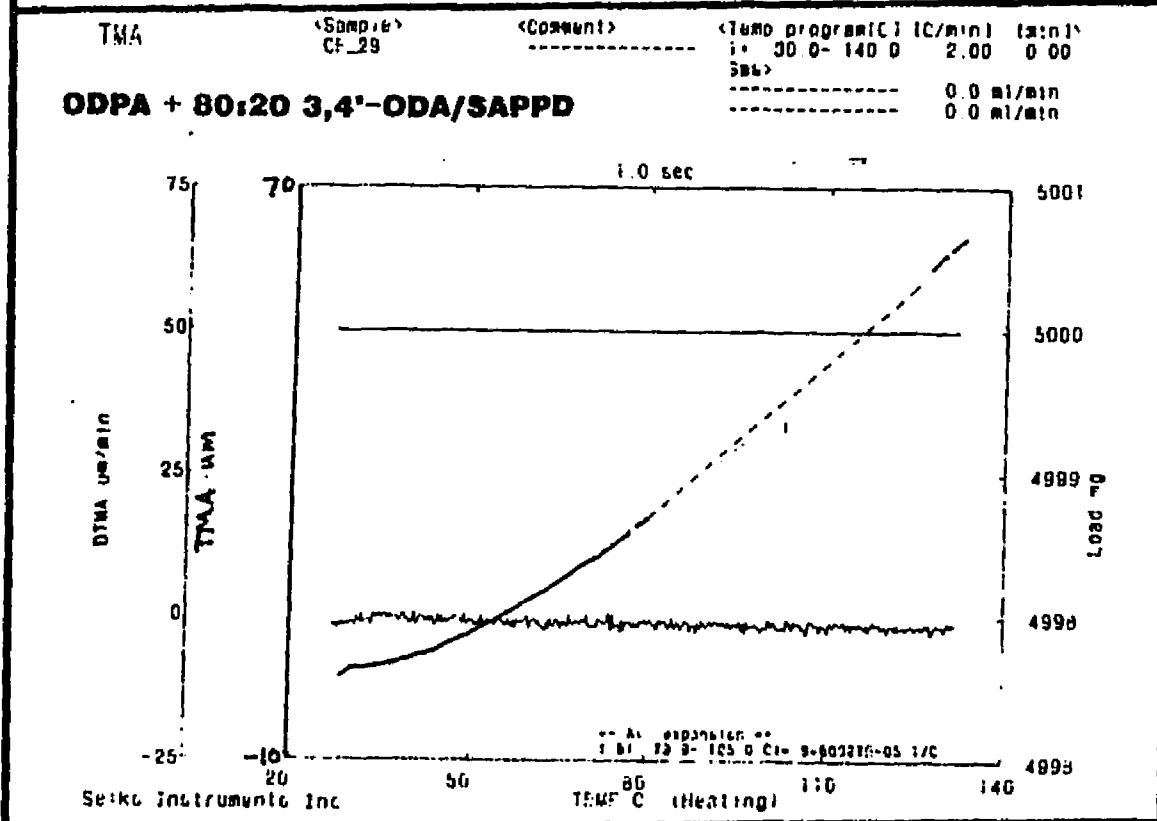
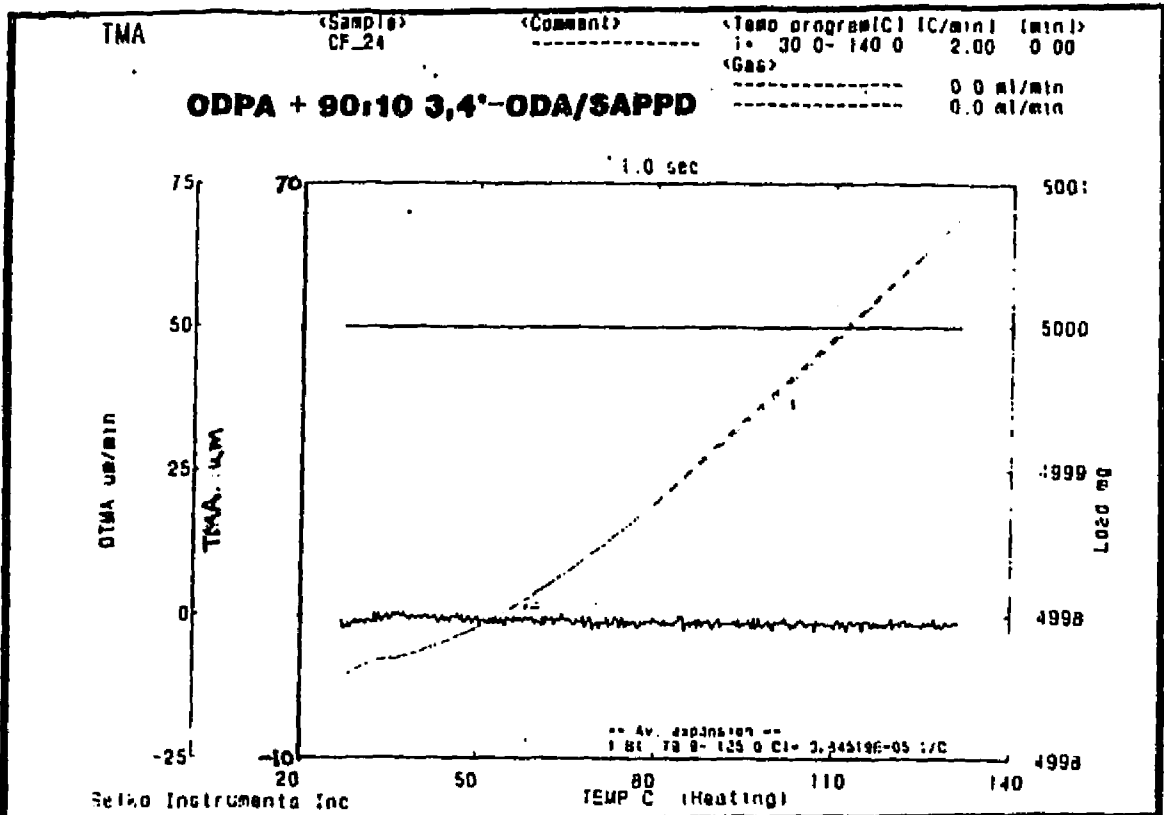


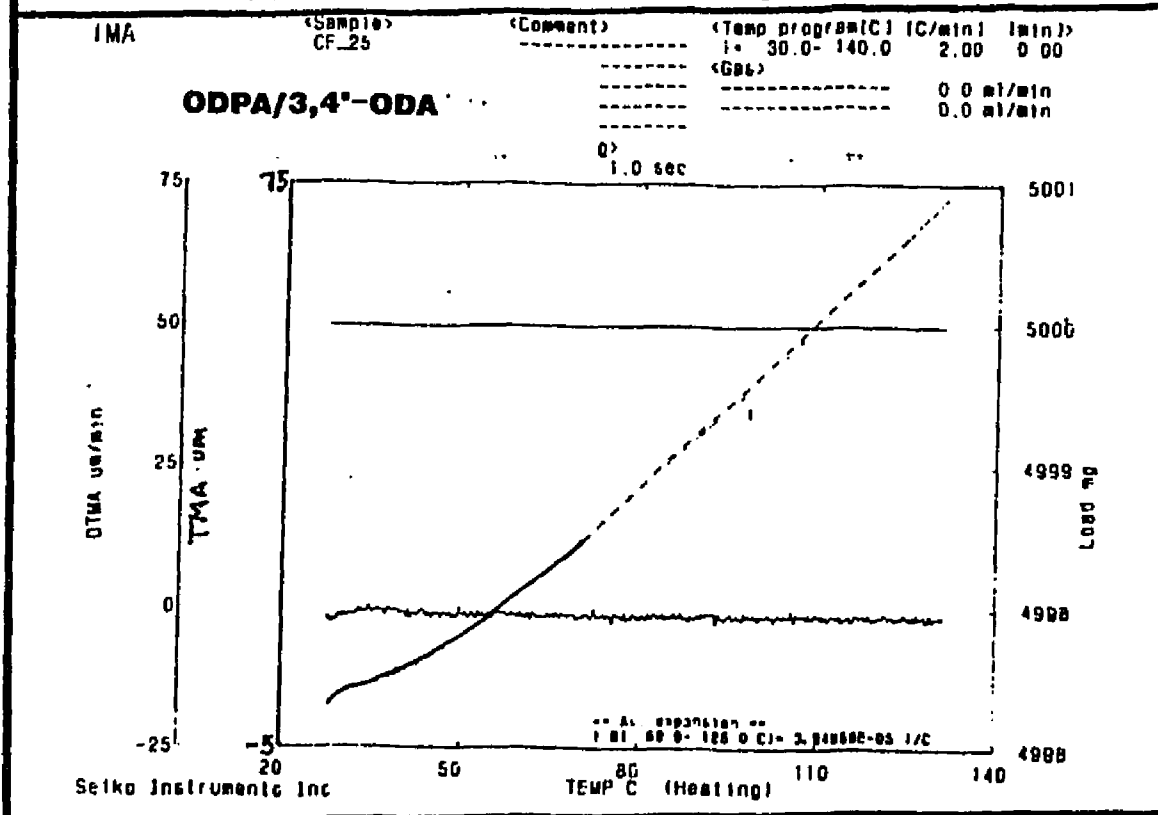
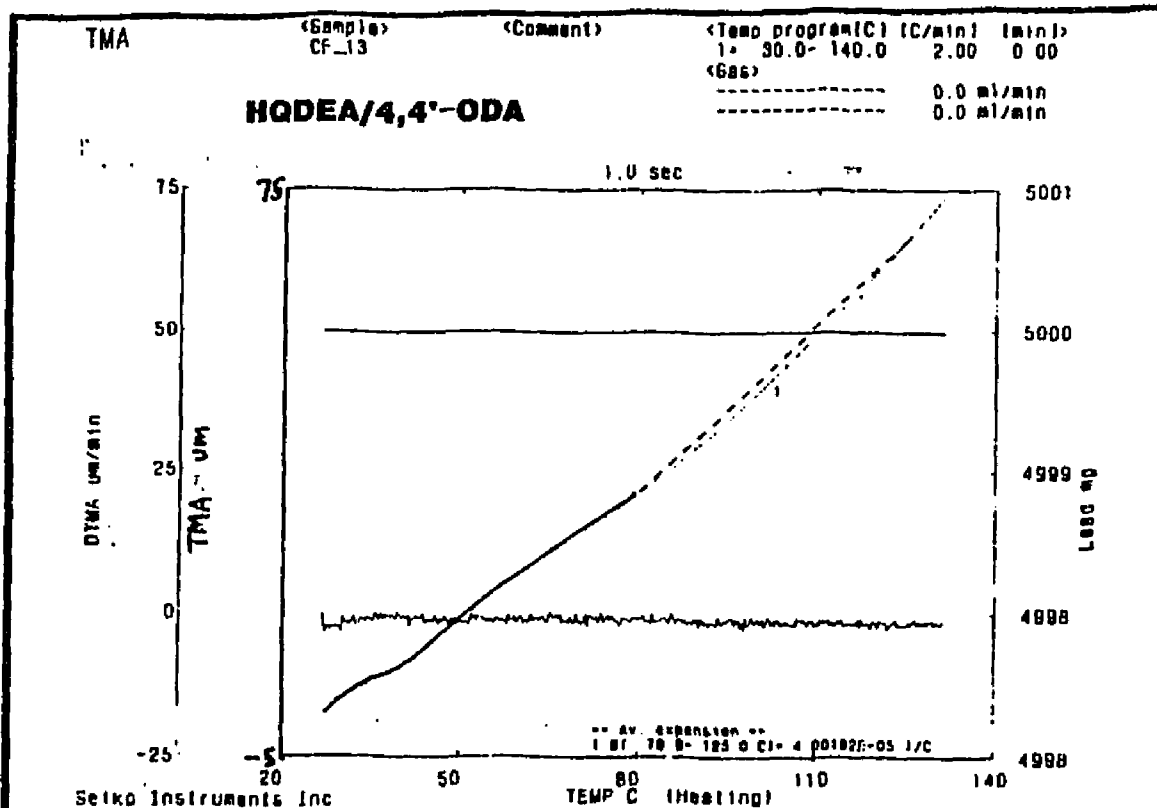
DSC

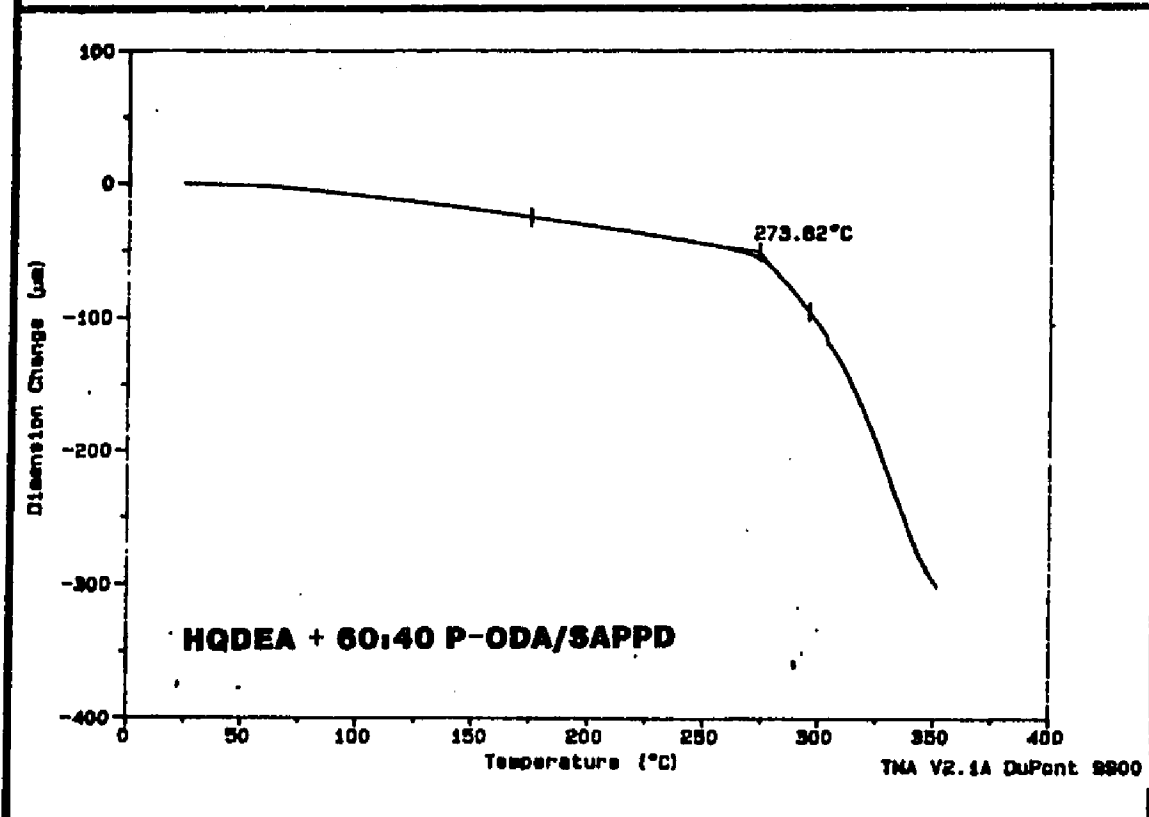
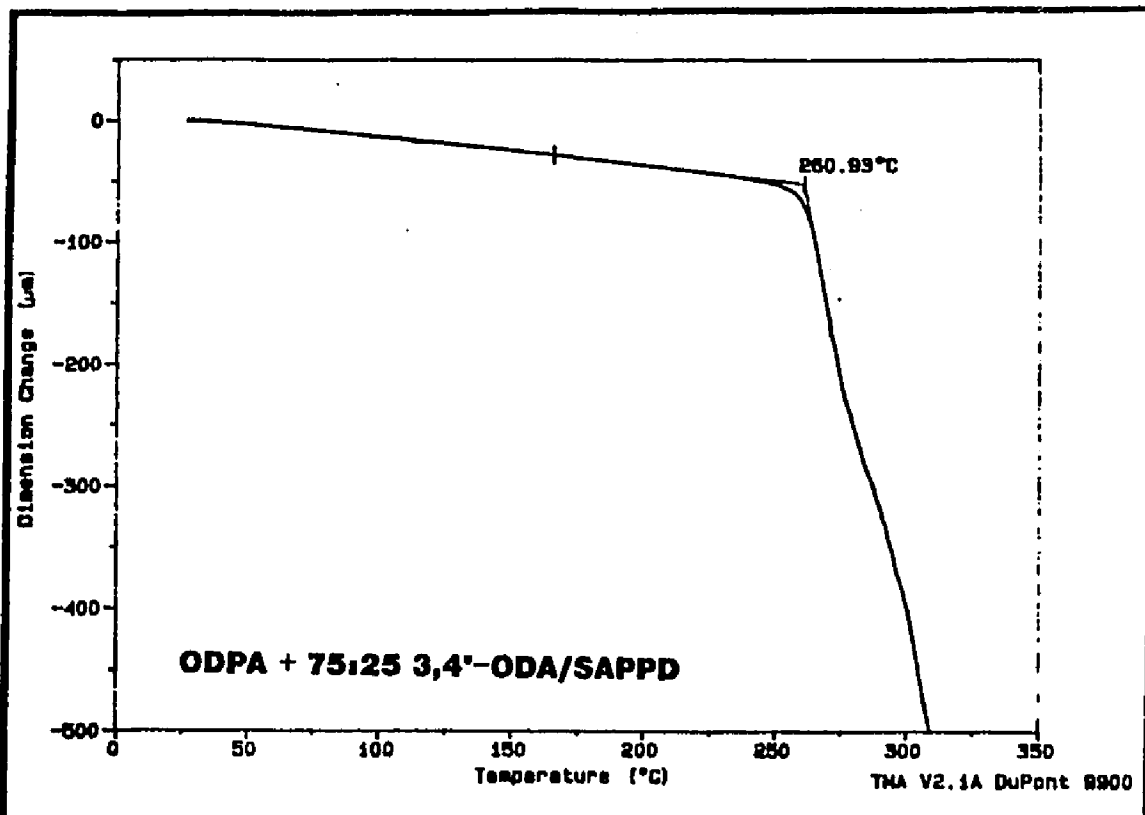
<Sample> CF-203-45/300  
<Comment> 1ST RUN  
<Temp Program(C) (C/min) (min)>  
1: 25 0- 550 0 20 00 0 00  
2: -----  
----- 0.0 ml/min  
----- 0.0 ml/min

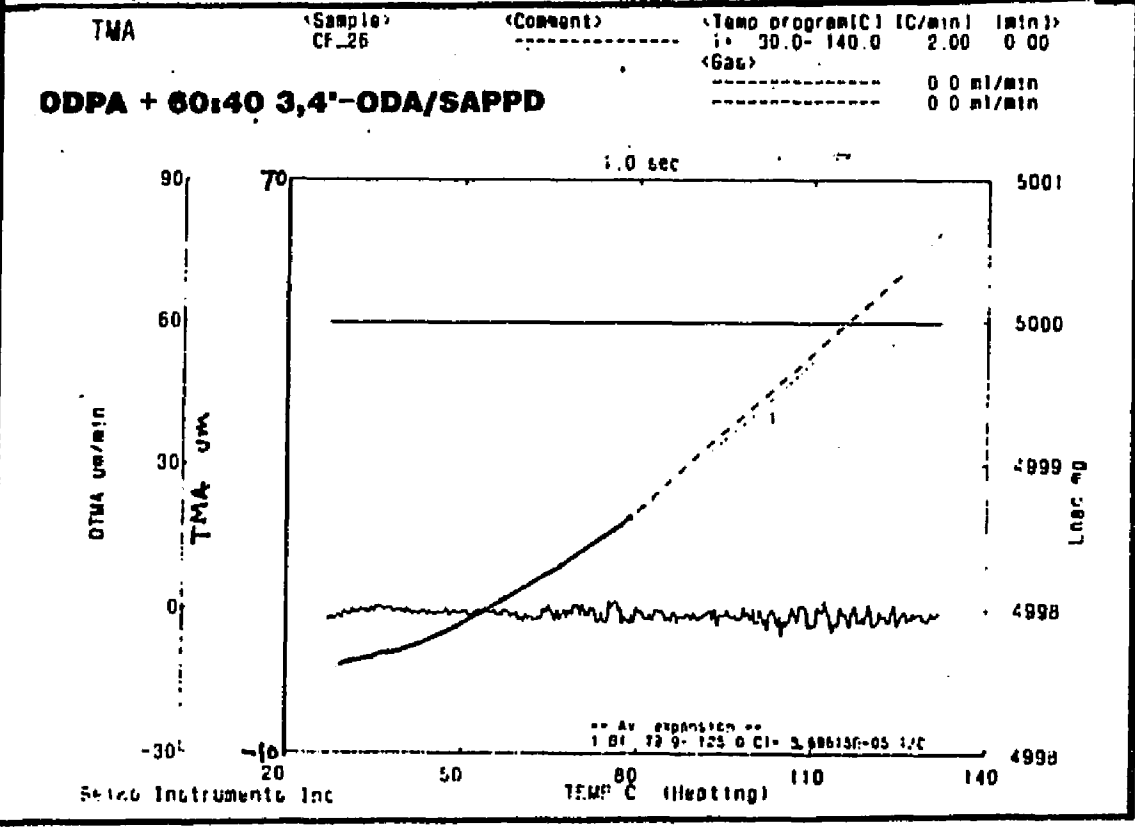
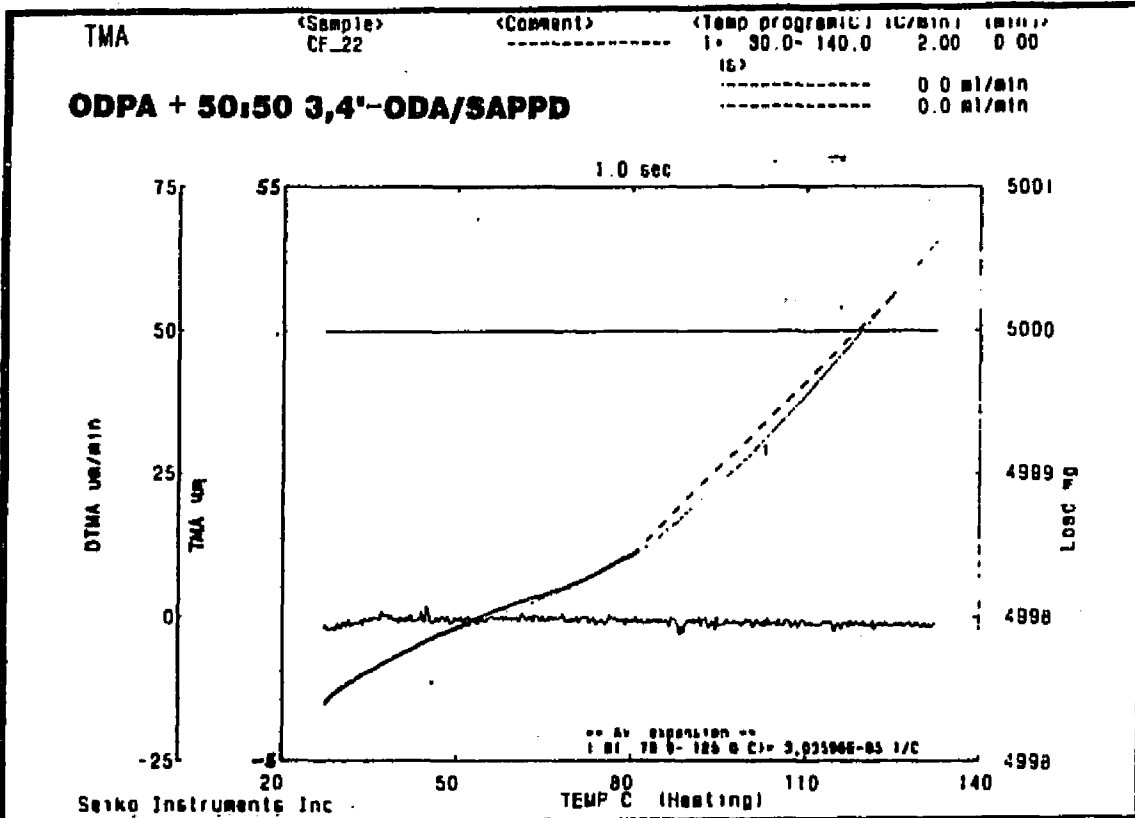
**HQDEA + 75:25 4,4'-ODA/SAPPD**



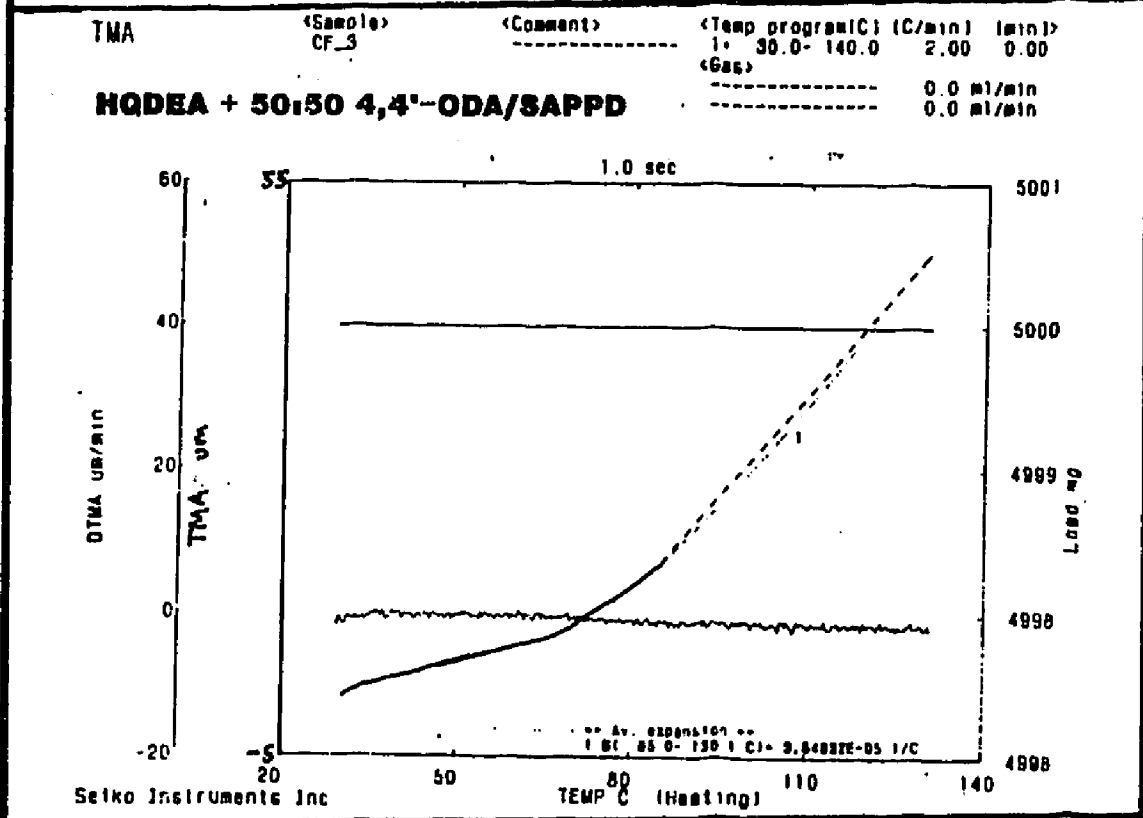
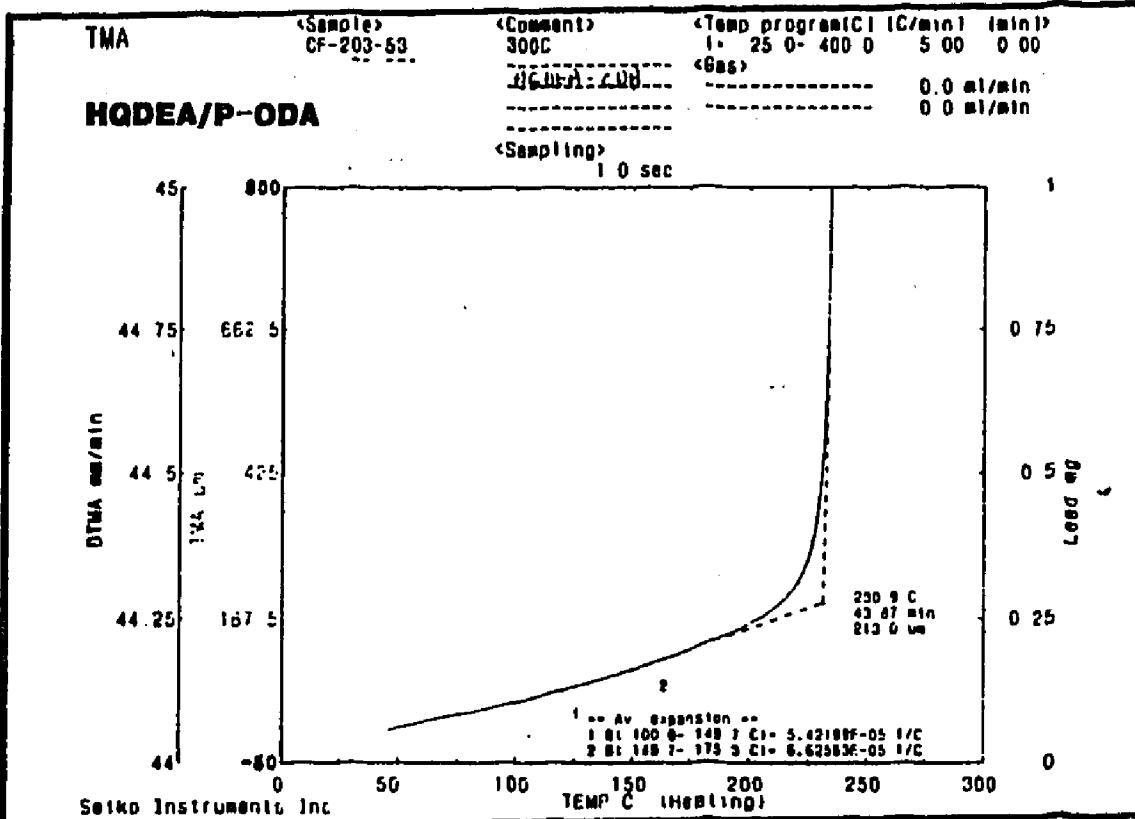


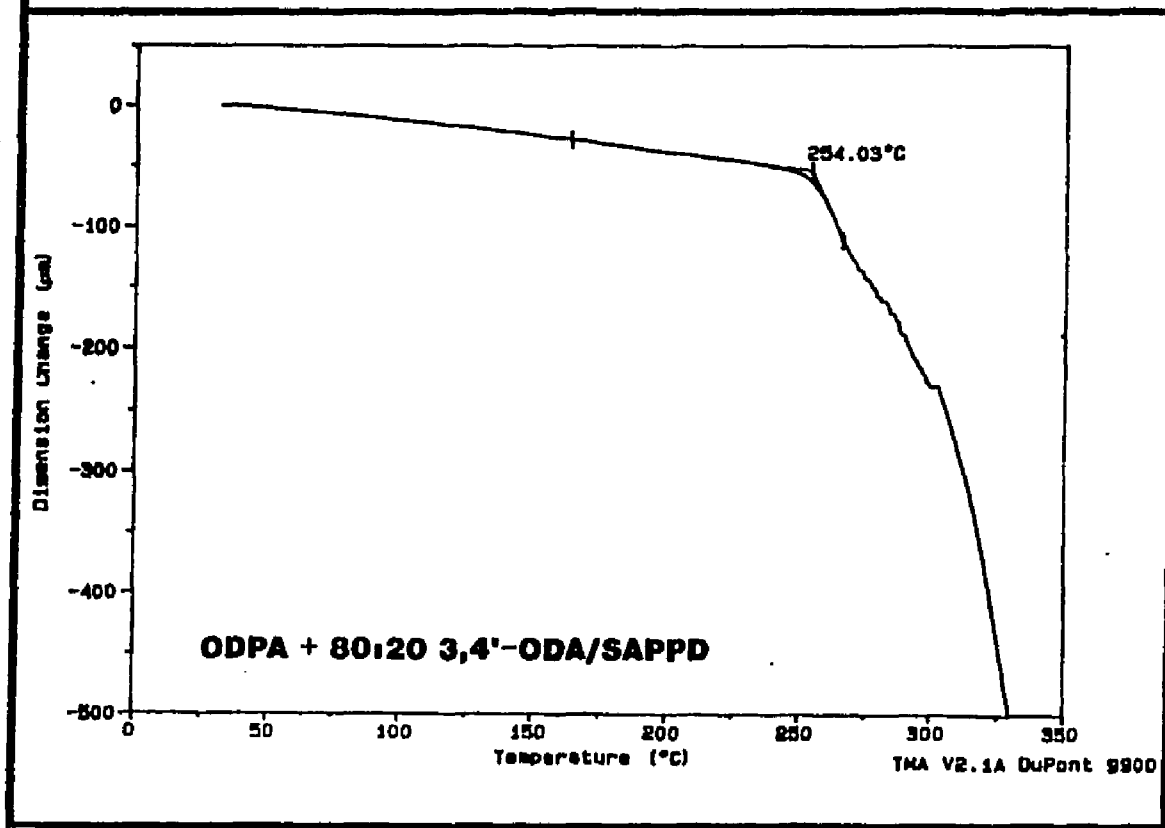
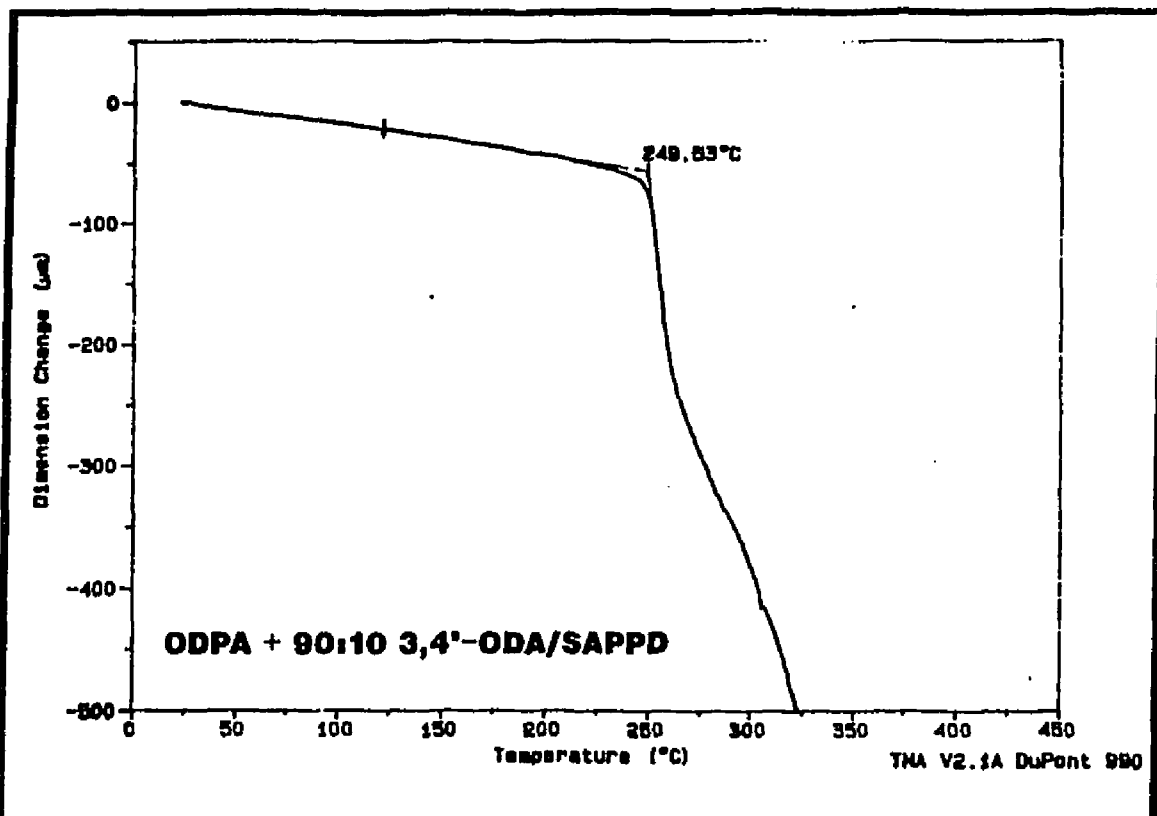








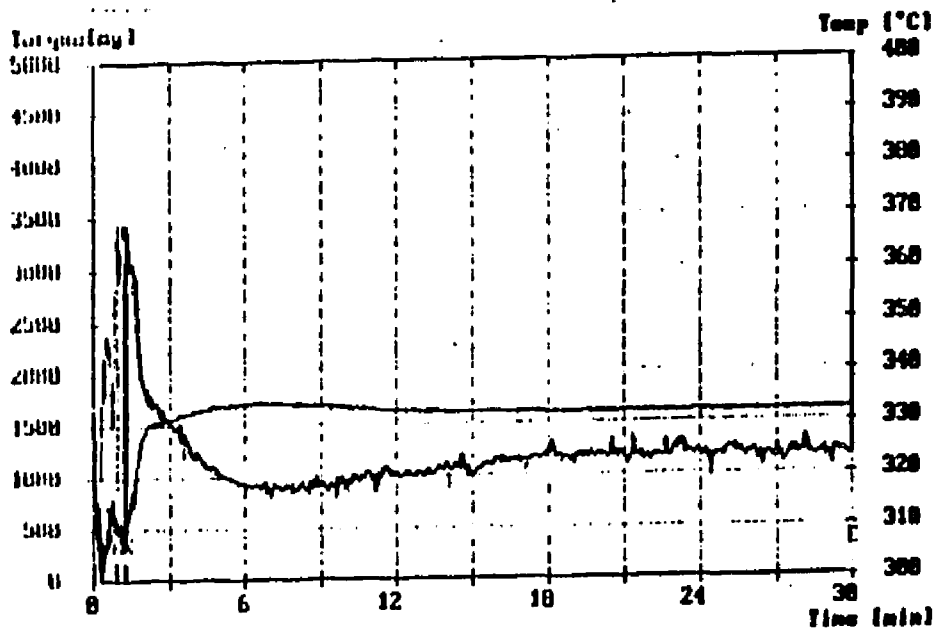




## MELT VISCOSITY AND COMPLEX VISCOSITY

**BRABENDER** 2.9  
**Date-Processing PLANTI-CORDER PL2000 and Mixer Measuring Head**  
**Fusion Behaviour**

<b>Test Conditions</b>			
Order	: NABA-Langley	Mixer Temp.	: 330 °C
Operator	: DC. WORKING	Speed	: 20 rpm
Test Date	: 16. Jun 94	Peak Range	: 10000 mg
PC Type	: 2000-G	Zero Suppr.	: 0
Mixer Type	: Half Size Elect HLD	Damping	: 3
Load Chute	: Manual 4.5 kg	Test Time	: 30.0 min
Sample	: LARC-1A 300FUEL	Sample Weight	: 26.70 g
Additive	: 15% JAP LC-P1	Code Number	:
		Start Temp.	: 334 °C



Value		Time	Torque [mg]	Stacktemp. [°C]
Loading Peak	A	00:00:58	3192	336
Minimum	B	00:01:10	2835	333
Intersection Point	D	00:01:14	3030	333
Maximum	X	00:01:20	3155	333
End	E	00:30:00	3174	331

**Integration / Energy**

- Loading Peak to Minimum	A - B	: U1	=	77.7	[mg]
- Minimum to Maximum	B - X	: U2	=	4230.1	[mg]
- Maximum to End	X - E	: U3	=	134.4	[mg]
- Loading Peak to End	A - E	: U5	=	4374.8	[mg]
- Specific Energy (U5/Sample Weight)	(E - X)	: U6	=	163.8	[mg/g]
- Abscissa Area Above B	(B - X)	: U7	=	7.0	[mg]

**Results**

- Fusion Time	A - B	: L	=	00:00:12	(sec)
- Gelation Speed	A - B	: V	=	2582	(mg/min)

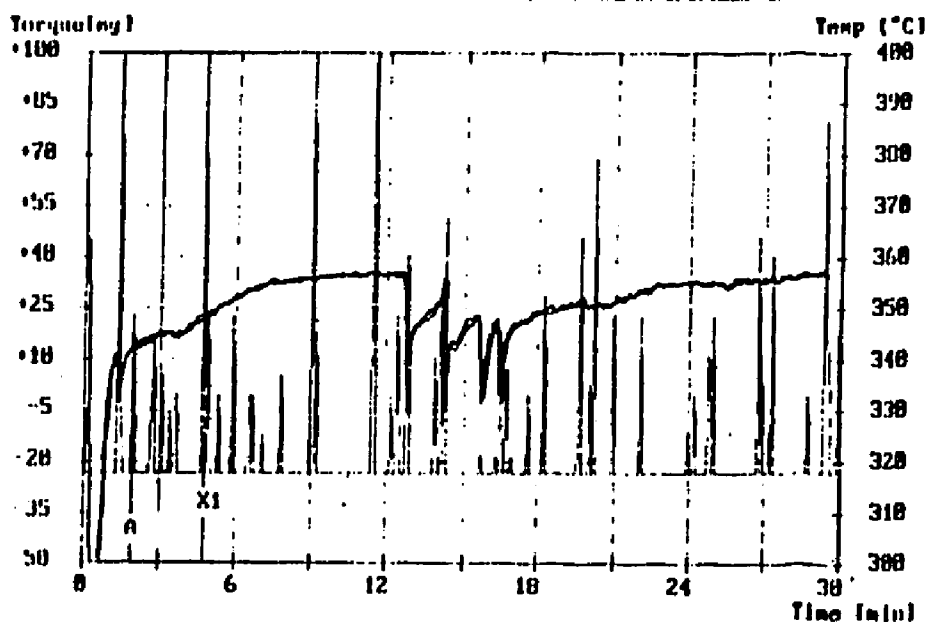
4000 P

**BRABENDER**

Data-Processing Plant | -Corder PL2000 and Mixer Measuring Head  
Semi-Automatic Universal Evaluation / 0.9.4

**Test-Conditions**

Operator	DC. WORKING	Mixer-Temp.	160 °C
Check-Date	10. Jun 91	Speed	20 rpm
Pl.-Type	1000-6	Meas. Range	10000 mg
Mixer-Type	HALF SIZE ELC HTD	Zero-Point	0 %
Load. Chute	MANUAL 2.5 kg	Damping	3
Sample	CC-176-G2 JXOFSET	Test-Time	21.0 min
Additive	BMDEA/p-PDA/PA	Sample-Weight	27.10 g
		Countdown	0
		Start-Temp.	16.1 °C



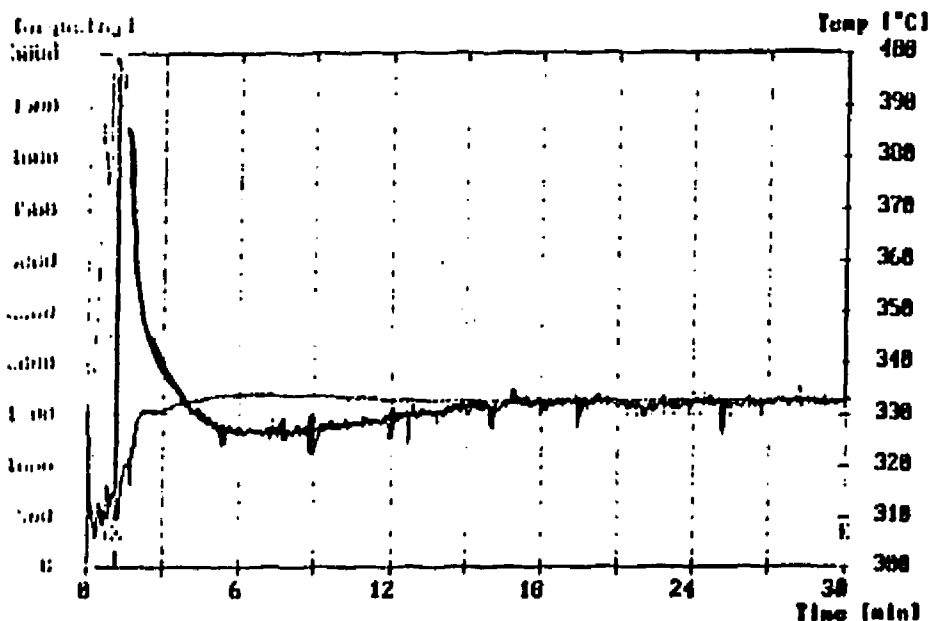
	Time [min] X to X	Time [min] 0 to X	Torque [mg] at X	Temp. [°C] at X	Energy [E] [mg] X to X	Energy [E] [mg] 0 to X
A	1.6	11.6	-21.1	313	-3.6	-3.6
X1	16.8	28.1	-33.1	319	-5.0	-8.6

**BRABENDER**

2.9

**Data-Processing PLANTI-CUMMINS PL2000 and Mixer Measuring Head  
Fusion Behaviour**

<b>Test Conditions</b>		Mixer Temp.	330 °C
Order	NASA-Langley	Speed	20 rpm
Operator	DC. WARKING	Max. Range	10000 mg
Test Date	17 Jun 94	Zero Suppr.	0 %
Pl. Type	2000-G	Dampng	3
Mixer Type	Half Size Elect Htd	Test Time	30.0 min
Load Chute	Nappa 4 kg	Sample Weight	27.30 g
Sample	LARC-1A STOFFER	Code Number	
Additive		Start Temp.	332 °C



Value	Time	Torque (mg)	Stactemp. (°C)
Loading Peak A	00:00:51	5191	312
Minimum B	00:01:02	4120	316
Inflection Point C	00:01:08	5106	318
Maximum X	00:01:12	5790	319
End E	00:30:00	1609	313

**Injection / Energy**

- Loading Peak to Minimum A - B : 178.4 [kg]
- Minimum to Maximum X - B : 5071.8 [kg]
- Maximum to End X - E : 6063.7 [kg]
- Loading Peak to End A - E : 222.7 [kg]
- Specific Energy (W/Sample Weight) (B - X) : 19.8 [kg]
- Gelation Area Above B (B - X) : 19.8 [kg]

**Results**

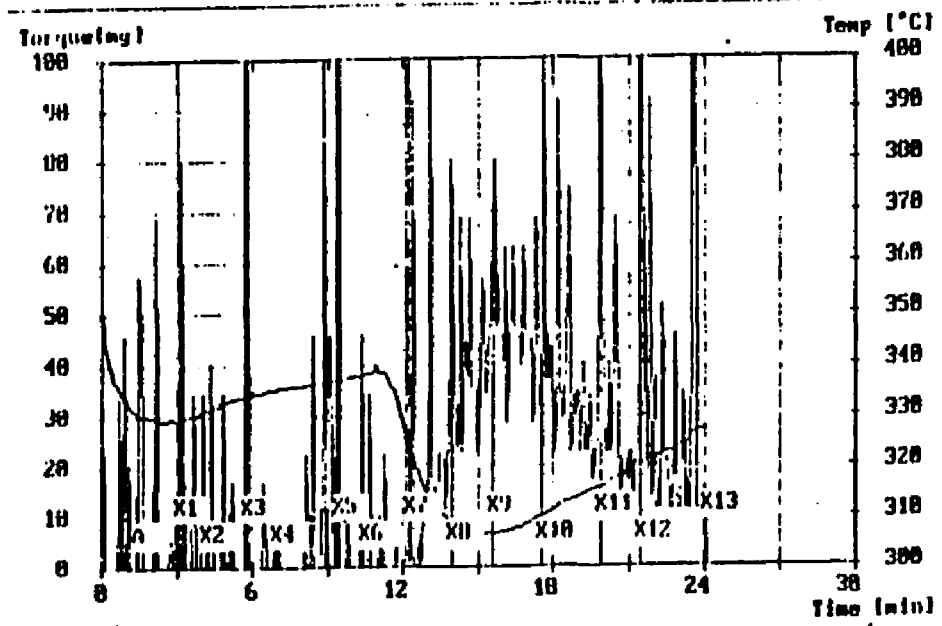
- Fusion Time A - X : 00:00:18
- Gelation Speed B ± 20% : 11978 [mg/min]

S-1700P

**BRABENDER**

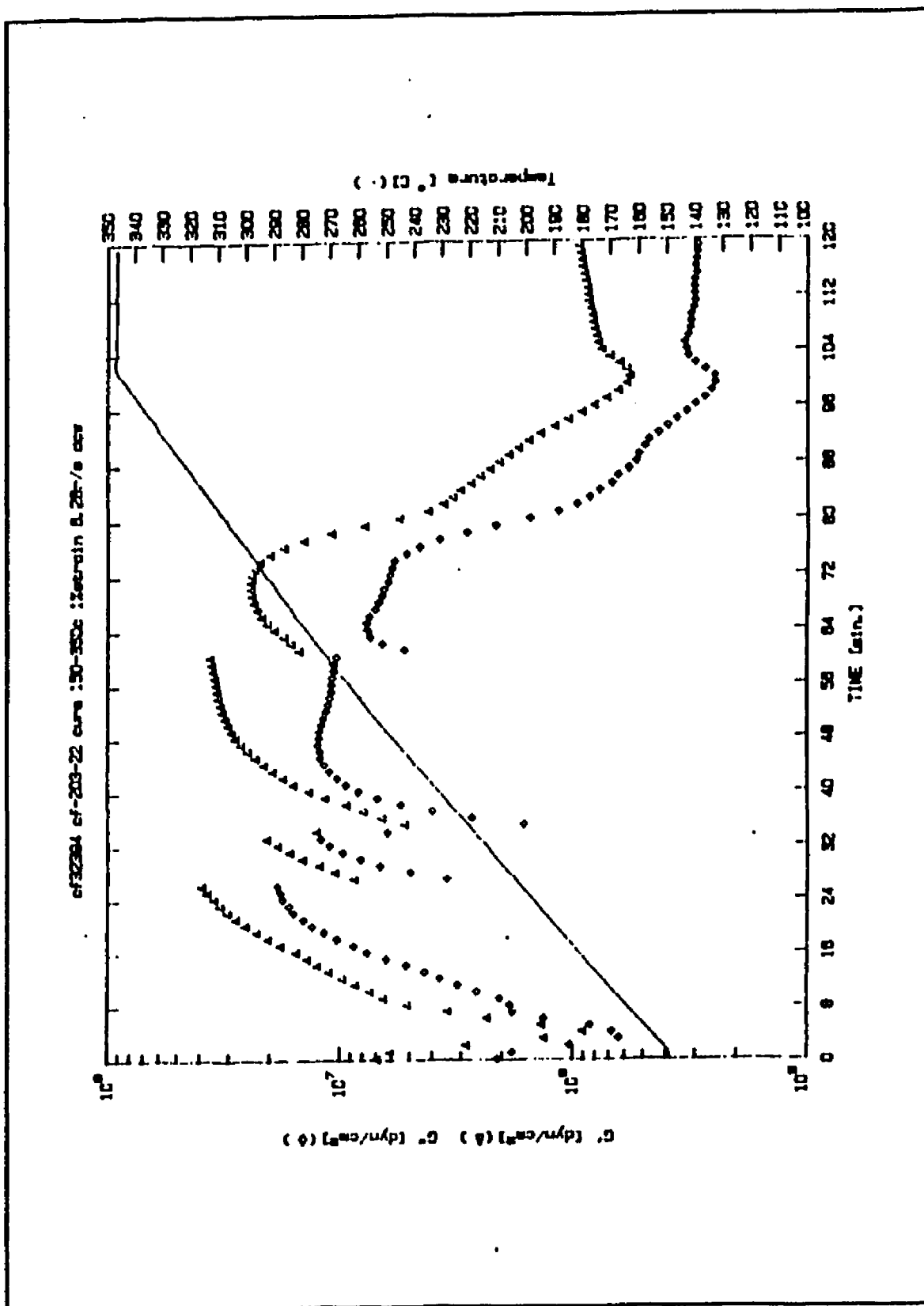
Data-Processing Plast-Corder PL2000 and Mixer Measuring Head  
Semi-Automatic Universal Evaluation / 0.9.4

<b>Test-Conditions</b>		Mixer-Temp. :	150 °C
Operator :	UC. WORKING	Speed :	20 rpm
Check-Date :	18. Jun 93	Meas. Range :	10000 mg
PL-Type :	2000-6	Zero-Point :	0 %
Mixer-Type :	HALF-SIZE P.L.C. HTD	Damping :	3.0
Load-Chart :	MANUAL 0.5 KG	Total-Time :	91.30 min
Sample :	CC-176-63 350 FORT	Sample-Weight :	27.10 g
Additive :	BMDEA/p-PDA/PA	Code-number :	
		Start-Temp. :	150 °C

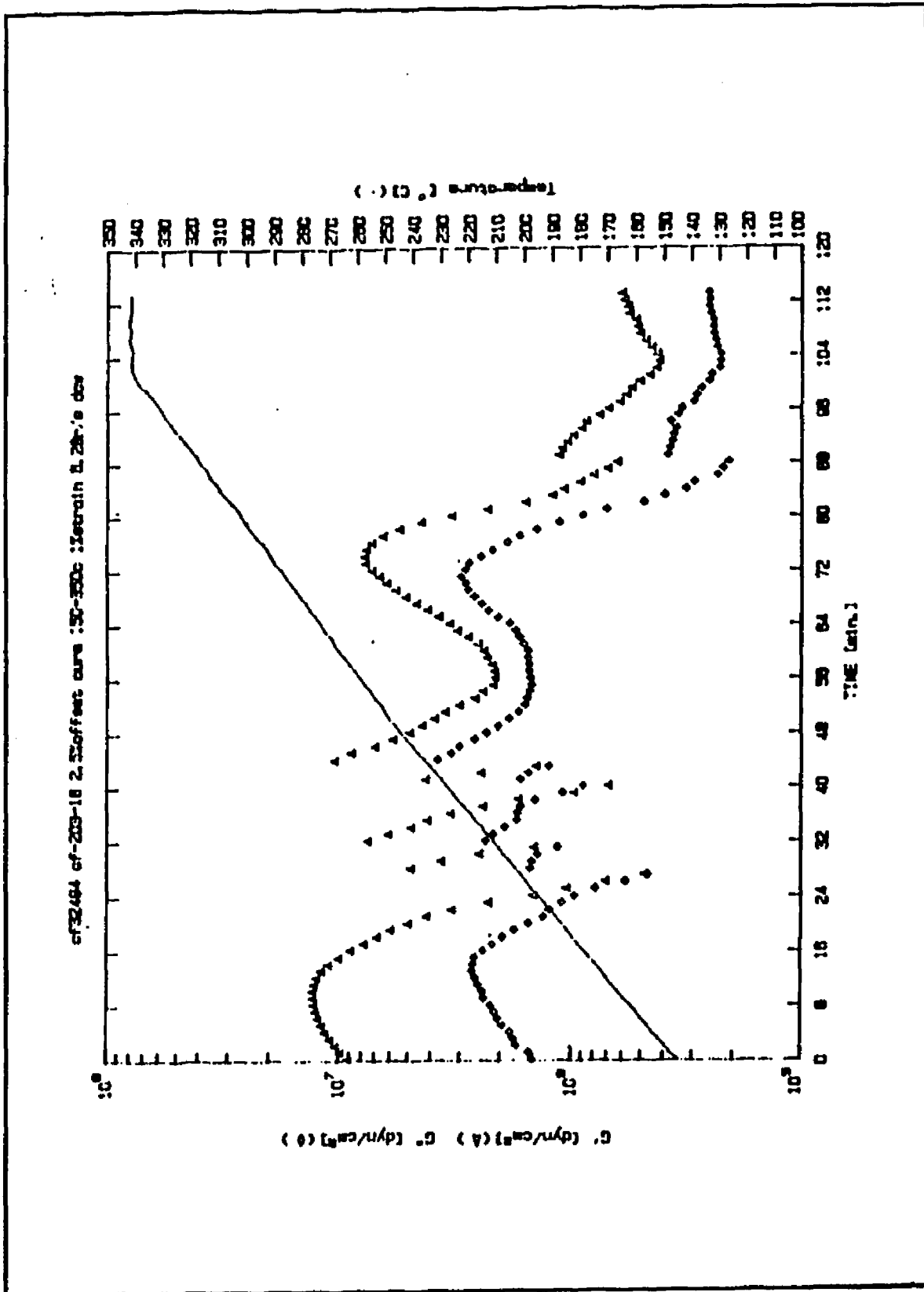


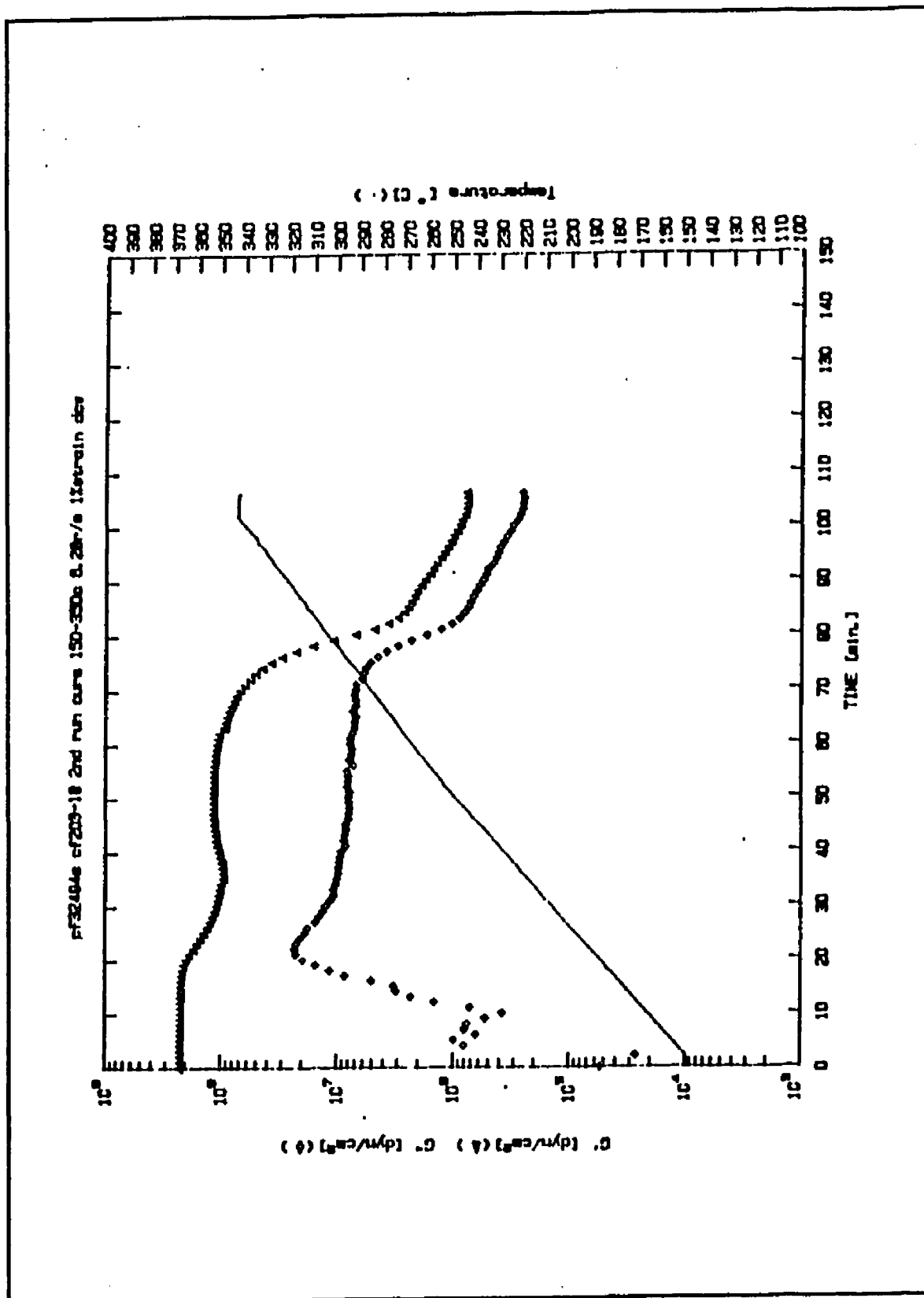
	Time (s) X to X	Time (s) 0 to X	Torque (mg) at X	Temp. (°C) at X	Energy (FJ mg) X to X	Energy (FJ mg) 0 to X
Operator UC. WORKING	89	89	57.5	311	1.5	1.5
	96	145	23.0	310	1.3	2.8
	97	146	28.0	311	1.6	4.4
	98	147	270.1	311	1.3	5.7
	99	148	0.0	315	0.7	6.4
	100	149	252.8	317	1.2	7.6
	101	150	0.0	310	0.5	8.1
	102	151	0.0	323	2.5	10.6
	103	152	57.5	309	5.6	16.2
	104	153	69.0	307	8.1	24.3
	105	154	73.0	310	2.0	26.3
	106	155	11.9	316	9.9	36.2
	107	156	70.1	321	7.0	43.2
108	157	11.5	328	9.8	53.0	

307°C TV = 1530/min

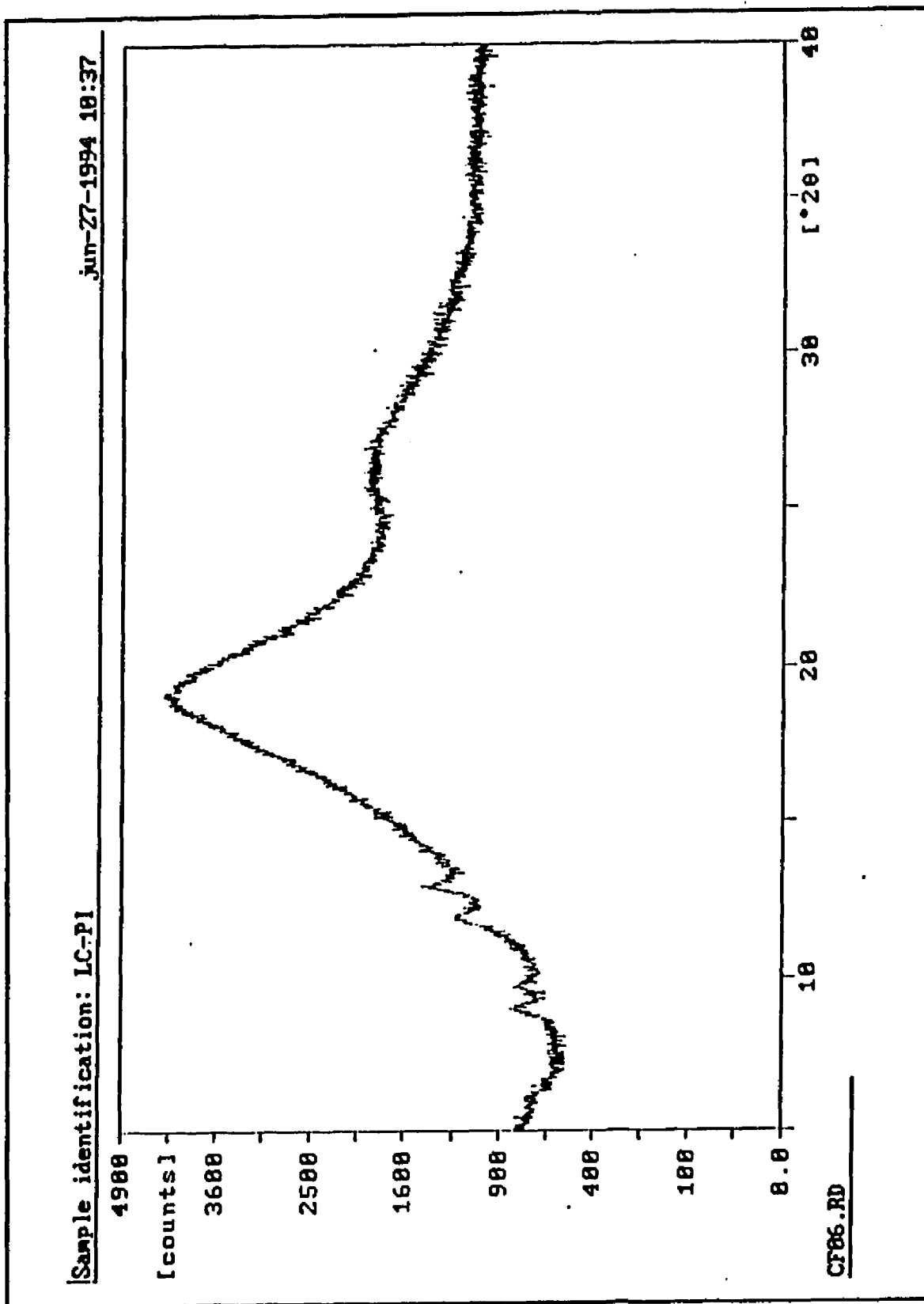


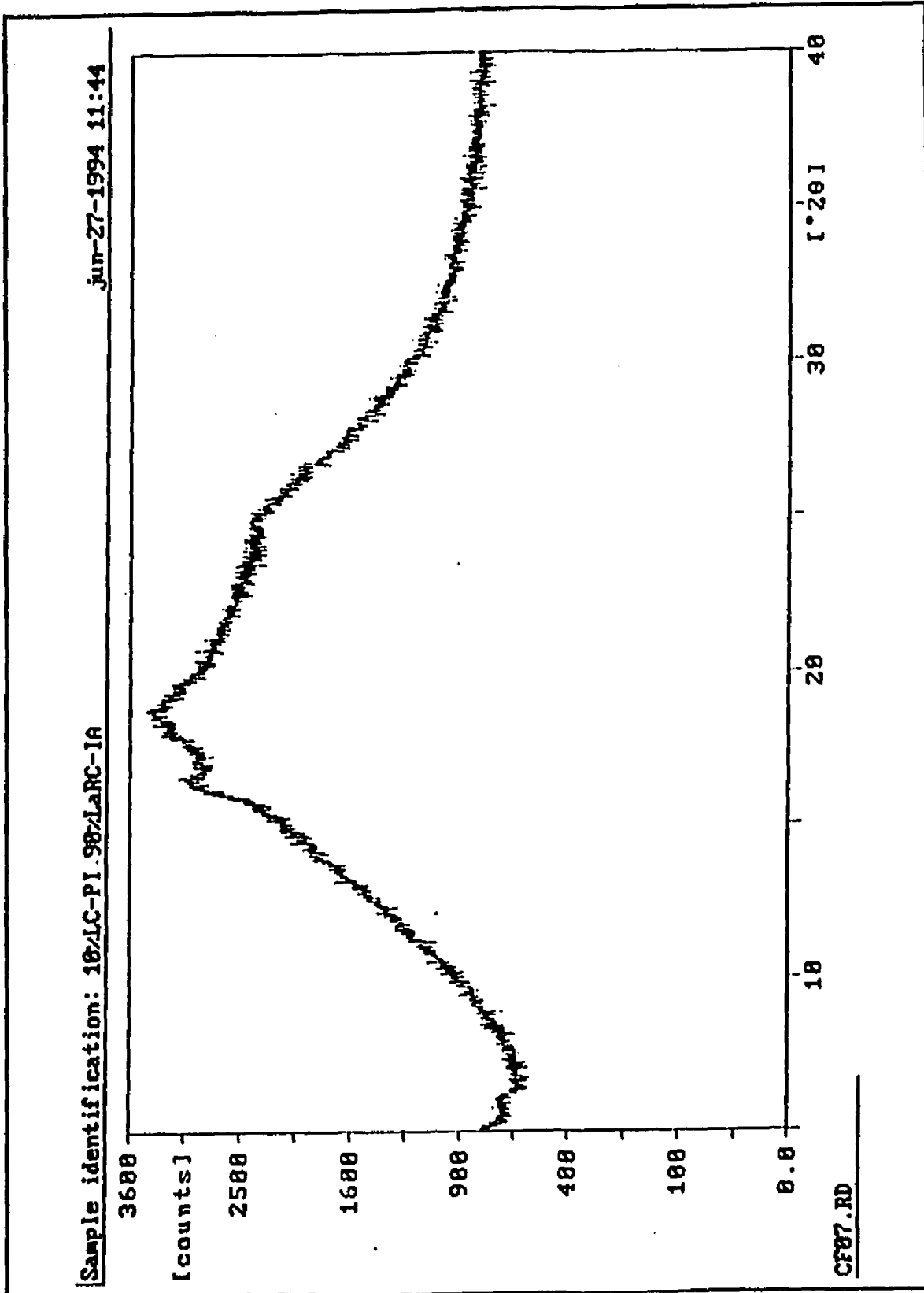


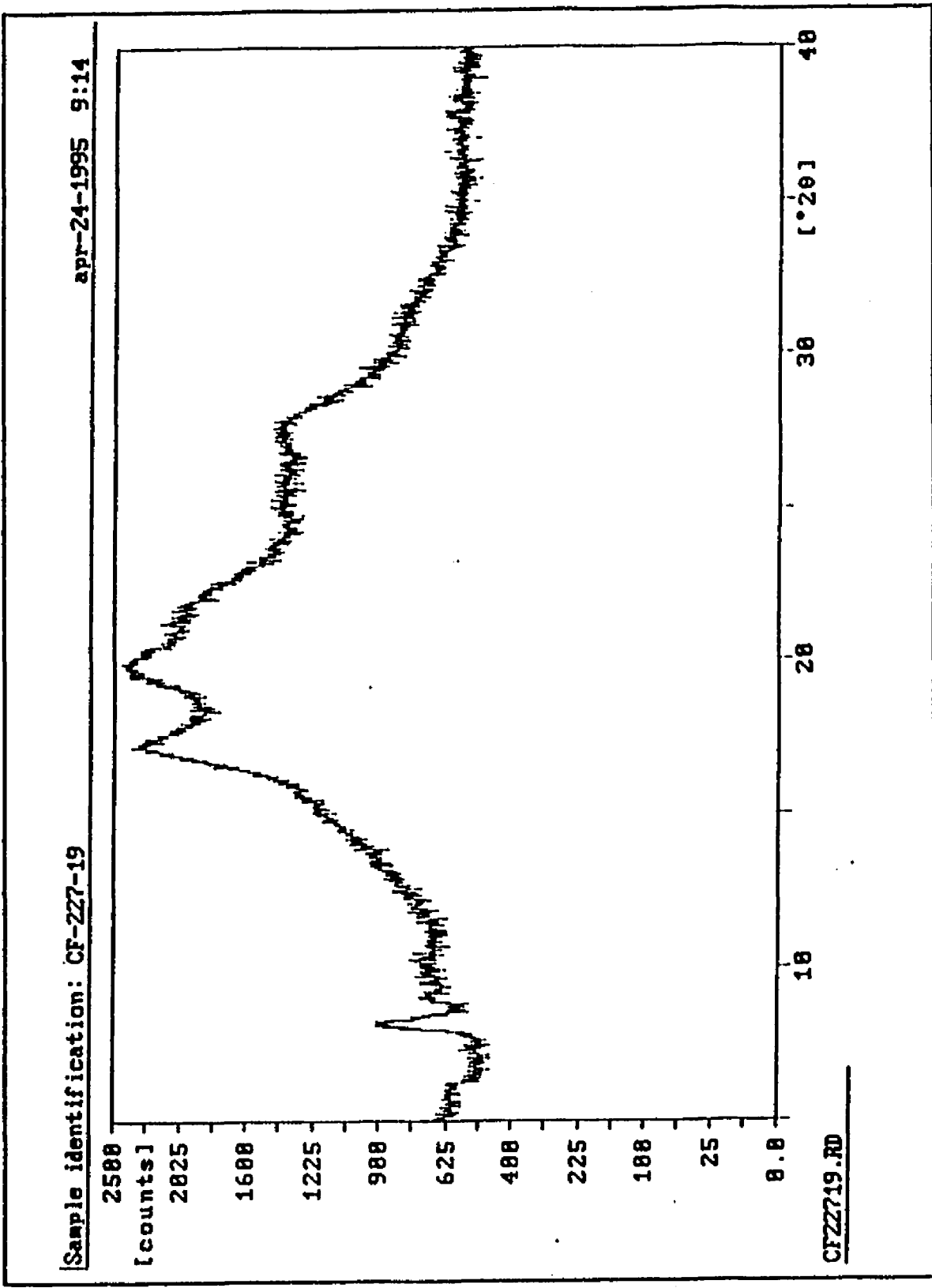


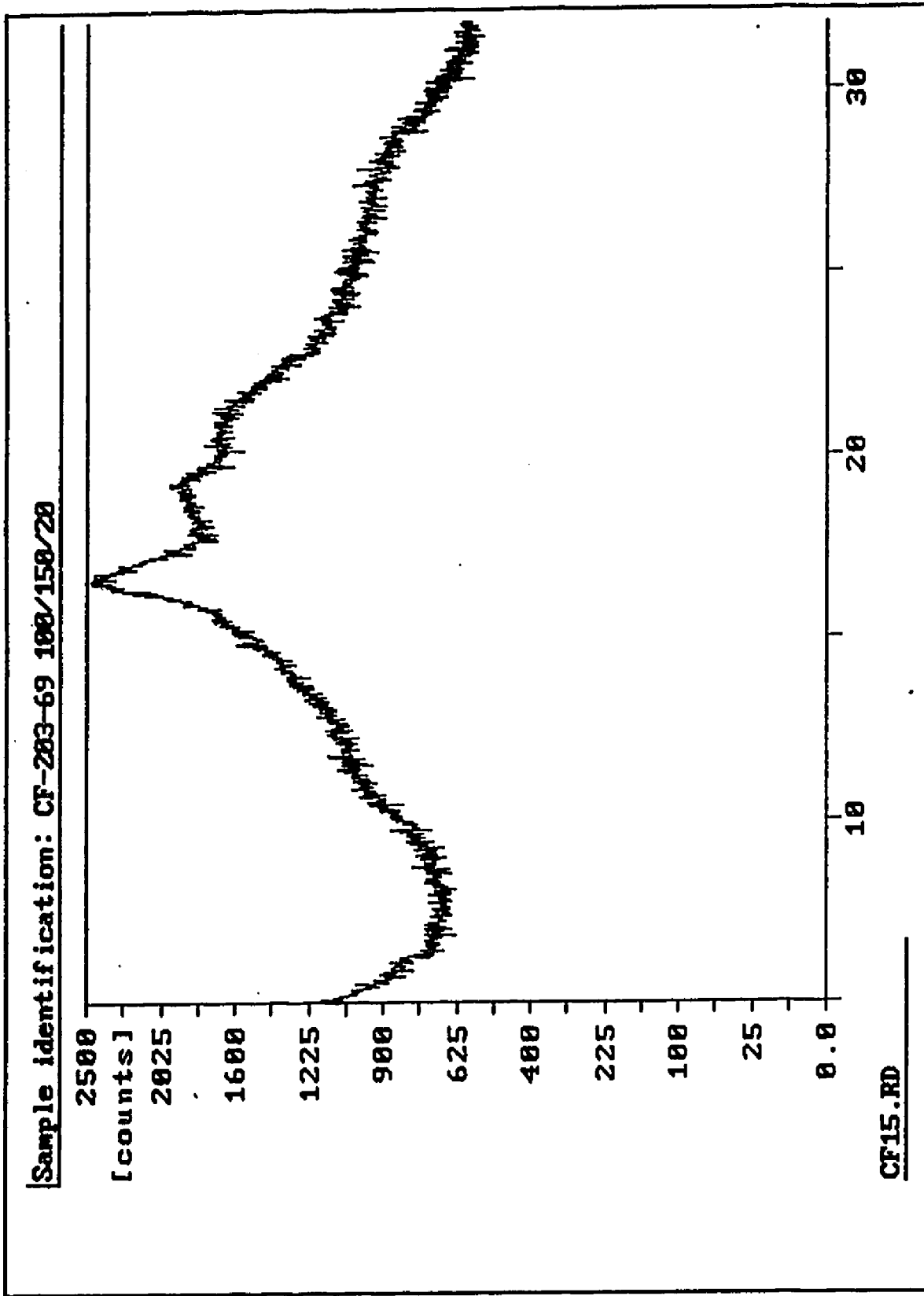


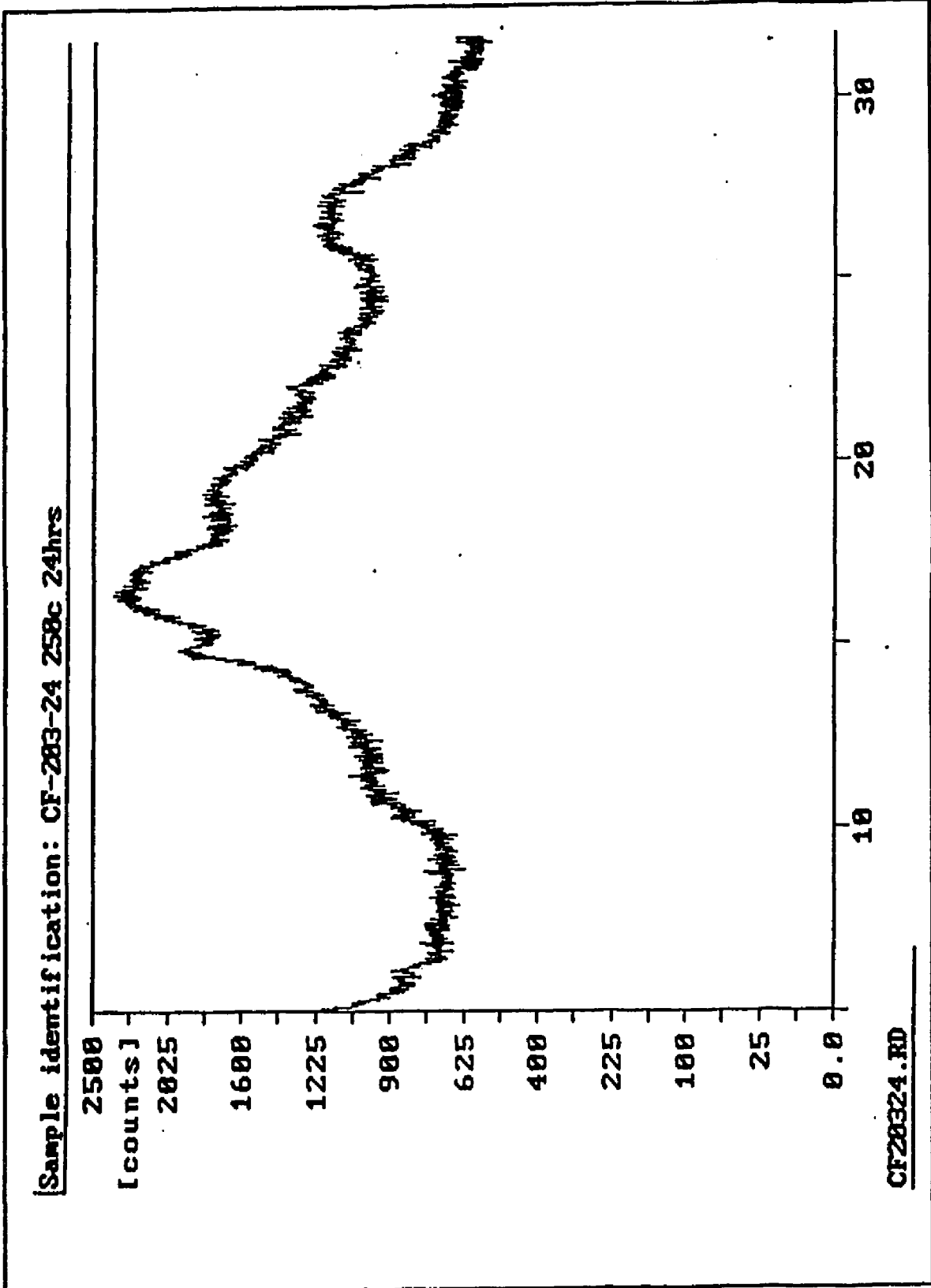
## X-RAY DIFFRACTION







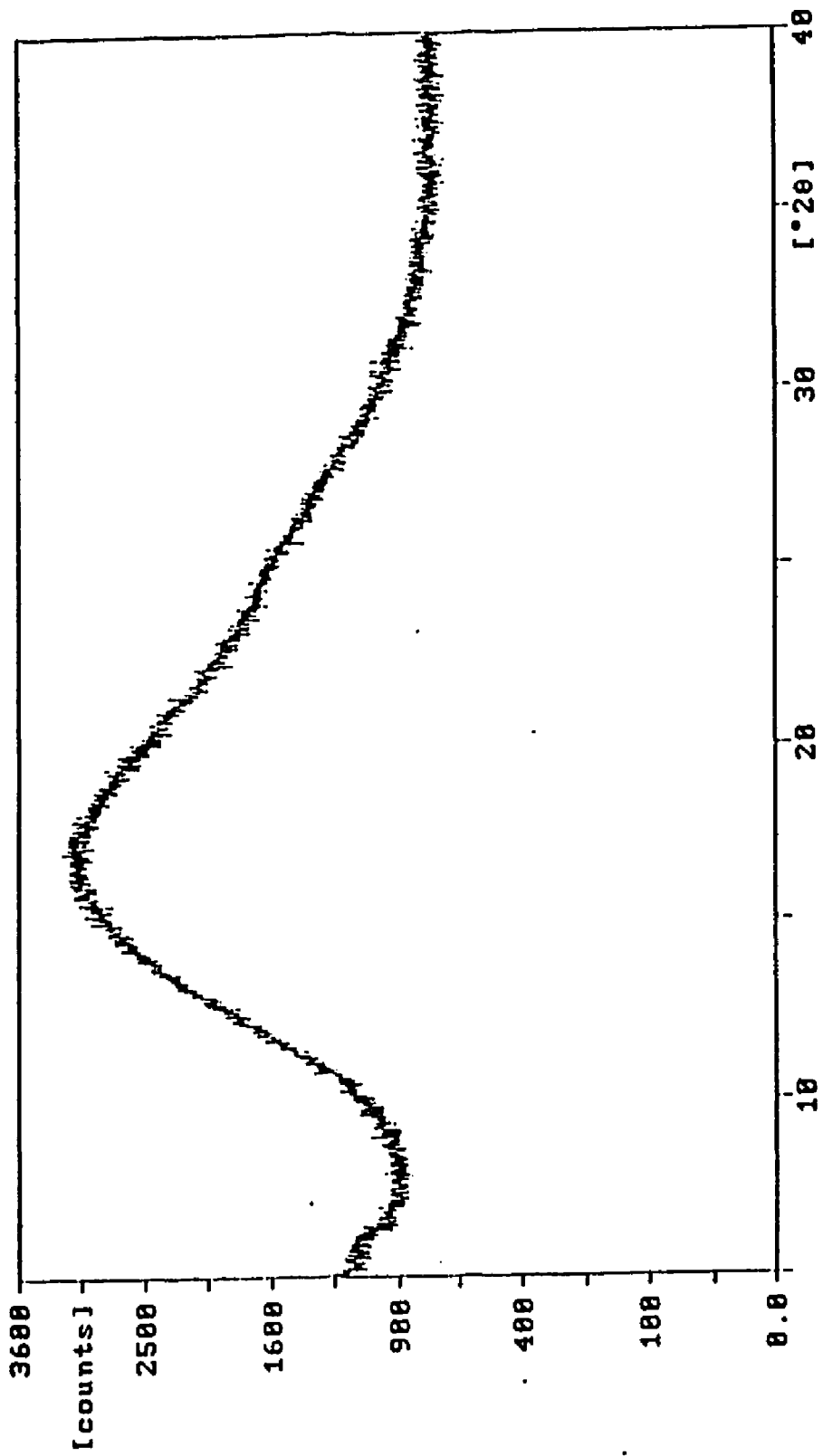




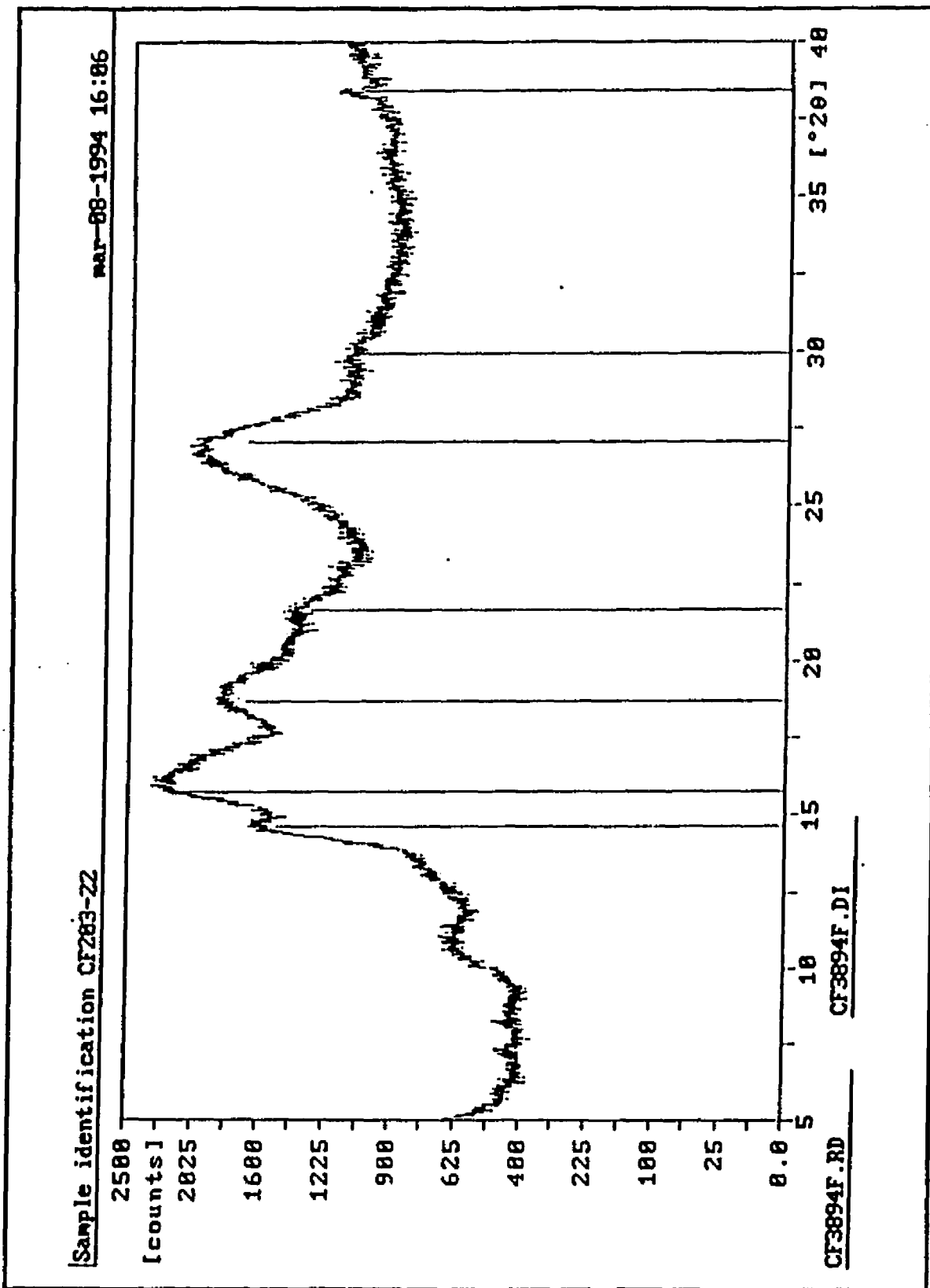


Sample identification: CF-283-33

may-26-1994 9:23



CF28333.RD



## TENSILE PROPERTIES

\*\*\*\*\* FILM TENSILE TEST \*\*\*\*\*

\*\*\*\*\* WIRE INSULATION STUDY \*\*\*\*\*

Method: 50 LB CELL WIRE INSULATION STUDY  
Sample ID: CC-176-79A150C

Test Date: Oct 26, 1975  
Operator: DR: Cally

Sample Information:

TEMP TESTED AT: 150C  
RESEARCHER: C.FAY  
FILM TYPE: BMDEA/P-FDA  
FILM WIDTH: 0.200 IN.

	Thickness in	Break Load lb	Break Load PBI	Elong @ Break in	Elong @ Break %	Energy @ Break In-Lb	Yield Load lb	Yield Load PBI	Elong @ Yield in	Elong @ Yield %	Modulus PBI
1	0.0019	3.32	8723.83	0.07	3.75	0.11	3.39	8918.85	3.39	345017.74	
2	0.0019	3.30	8471.82	0.06	2.90	0.11	3.30	8471.82	2.90	304787.51	
3	0.0020	3.25	8127.87	0.06	3.24	0.14	3.26	8131.77	3.19	407209.45	
4	0.0019	3.17	7926.71	0.06	3.15	0.12	3.01	7930.75	3.16	371579.89	
5	0.0019	3.30	9112.89	0.07	3.05	0.15	3.62	9316.90	3.29	343418.64	
Mean	0.0019	3.28	8332.67	0.07	3.28	0.14	3.37	8638.82	3.16	378043.26	
Min	0.0019	2.97	7926.71	0.06	2.90	0.11	3.01	7930.75	2.90	343418.64	
Max	0.0020	3.30	9112.89	0.07	3.75	0.16	3.62	9316.90	3.39	407209.45	
SD%	0.0000	0.21	618.85	0.01	0.33	0.02	0.22	630.30	0.31	35858.15	
SE%	2.3292	6.53	7.14	10.83	10.83	16.27	6.50	7.39	9.68	6.19	
Def	00000000	01000000	00000000	00000000	00000000	00000000	01000100	00000000	00000000	00000000	00000000

Sample Input(s):

Gage Length 2.00 in  
Brk % Drop 10 %  
Brk Drop Elong 0.00 in  
XStrain Point1 5.00 %

Test Input(s):

Crosshead Speed 0.20 In/Min  
Load Limit III 50.00 Lb  
Ext L.Limit III 20.0 In  
Brk Sensitivity 75 %

Comments:

1 : FILM BROKE AT THE TOP CLAMP

## Sample Report

\*\*\*\*\* FILM TENSILE TEST \*\*\*\*\*

\*\*\*\*\* WIRE INSULATION STUDY \*\*\*\*\*

Method: 50 LB CELL WIRE INSULATION STUDY  
Sample ID: CF-203-33:25CTest Date: Jun 16, 1974  
Operator ID: Gally

## Sample Information

TEMP. TESTED AT:	25C
RESEARCHER:	C. FAY
POLYMER TYPE:	EMUL/14/DA/DAM
FILM WIDTH:	100/50/50

	Thickness in	Break Load lb	Break Load PSI	Elong @ Break in	% Elong @ Break %	Energy @ Break I	Break Yield Load in-lb	Yield Load lb	Yield Load PSI	% Elong @ Yield %	Modulus PSI
1	0.0035	0.47	12716.50	0.13	6.63	0.07	0.09	12697.03	5.96	37490.22	
2	0.0033	0.37	12391.10	0.11	5.40	0.62	0.37	12601.39	5.45	38307.07	
3	0.0032	0.23	12092.32	0.11	5.29	0.35	0.76	12900.23	5.26	387200.78	
4	0.0033	0.40	12033.07	0.11	5.31	0.57	0.40	12033.07	5.31	386720.52	
5	0.0033	0.34	12629.02	0.12	5.79	0.63	0.41	12710.73	5.52	391369.06	
6	0.0030	7.70	12970.19	0.12	5.07	0.61	7.06	13093.63	5.62	386511.94	
Mean	0.0031	0.30	12710.13	0.11	5.75	0.64	0.30	12029.13	5.52	383606.93	
Min	0.0030	7.70	12310.90	0.11	5.29	0.35	7.06	12601.39	5.26	374900.22	
Max	0.0035	0.42	12970.19	0.13	6.63	0.02	0.09	13093.63	5.96	387200.78	
Stdv	0.0002	0.29	203.02	0.01	0.09	0.10	0.33	133.72	0.23	4010.32	
1/Dev	0.9990	3.43	1.93	0.39	0.39	15.17	3.99	1.71	6.62	1.17	
1/Dev		0.000000	0.000000	0.000000	0.000000	0.000000	0.000000	0.000000	0.000000	0.000000	

## Sample Input(s):

Gage Length	2.00	in
Brk % Drop	10	%
Brk Drop Elong	0.00	in
%Strain Point1	5.00	%

## Test Input(s):

Crosshead Speed	0.20	in/Min
Load Limit III	50.00	lb
Ext Limit III	20.0	in
Brk Sensitivity	75	%

## Comments:

1 : FILM BROKE AT BOTH CLAMPS

Method: SOUTH BELL WIRE INSURANCE STUDY  
 Sample ID: CF-203-31125C

Test Date: Jun 17, 1994  
 Operator: DR. GATIN

Sample Information:

TEMP TESTED AT: 75C  
 RESEARCHER: C. JAY  
 POLYMER TYPE: PHDLA/17/DA/NDA  
 FILM WIDTH: 100/50/50

	Thickness In	Break Load Lb	Break Load PSI	Elong @ Break In	% Elong @ Break	Energy @ Break J	Yield Load In-Lb	Yield Load Lb	Yield Load % PSI	Elong @ Yield In	Modulus PSI
1	0.0021	6.48	13030.00	0.11	5.56	0.43	6.48	13030.00	5.56	417497.33	
2	0.0022	6.09	13045.12	0.09	4.72	0.34	6.09	13045.12	4.72	386150.75	
3	0.0023	6.16	13045.37	0.11	5.31	0.42	6.16	13045.37	5.31	386150.61	
4	0.0021	6.42	13209.09	0.12	5.07	0.48	6.42	13209.09	5.07	413891.40	
5	0.0021	6.20	12940.54	0.12	5.76	0.46	6.20	12940.54	5.76	413045.79	
Mean	0.0022	6.35	12711.22	0.11	5.45	0.45	6.35	12711.22	5.45	406025.03	
Min	0.0021	6.09	13045.12	0.09	4.72	0.34	6.09	13045.12	4.72	386150.61	
Max	0.0023	6.16	13045.37	0.12	5.07	0.48	6.16	13045.37	5.07	413891.40	
SD	0.0001	0.16	725.73	0.01	0.46	0.04	0.16	725.73	0.43	13250.87	
TCor	4.1009	2.57	4.95	0.37	0.37	13.07	2.50	4.94	0.30	5.76	
Z Cor		00000000	00000000	00000000	00000000	00000000	00000000	00000000	00000000	00000000	

Sample Input(s):

Gage Length 2.00 In  
 Brk % Drop 10 %  
 Brk Drop Elong 0.40 In  
 %Strain Point1 5.00 %

Test Input(s):

Crosshead Speed 0.20 In/Min  
 Load Limit HI 50.00 lb  
 Fat Limit HI 20.0 In  
 Brk Sensitivity 75 %

Comments:

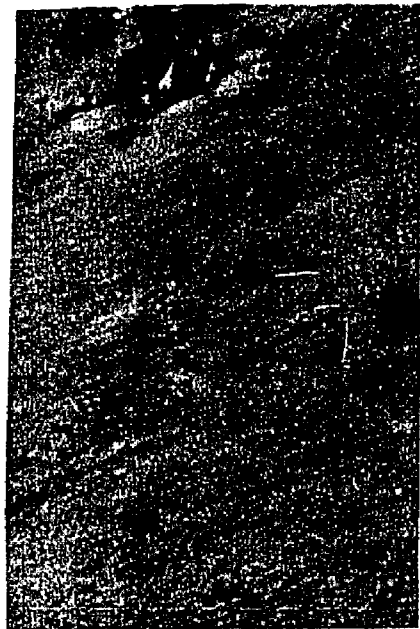
1 : FILM BROKE AT BOTH CLAMPS

Page No. 2

Comments:

2 : FILM BROKE AT TOP AND MIDDLE  
 3 : FILM BROKE AT BOTTOM AND MIDDLE  
 4 : FILM BROKE AT THE BOTTOM CLAMP  
 5 : FILM BROKE AT BOTH CLAMPS

## POLARIZING PHOTOMICROGRAPHS



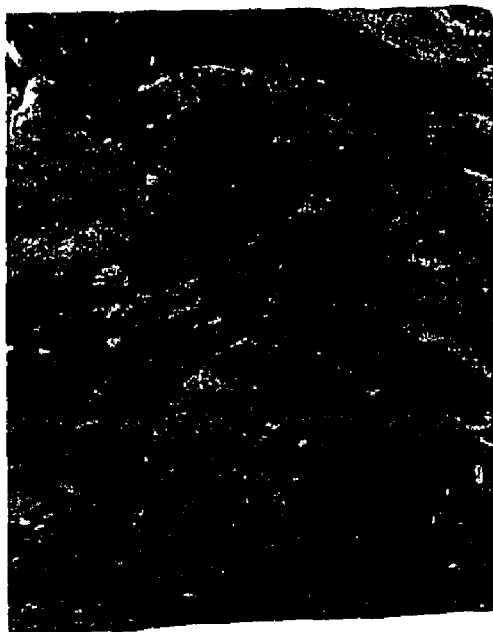
100X, 263°C →



100X, 260°C →



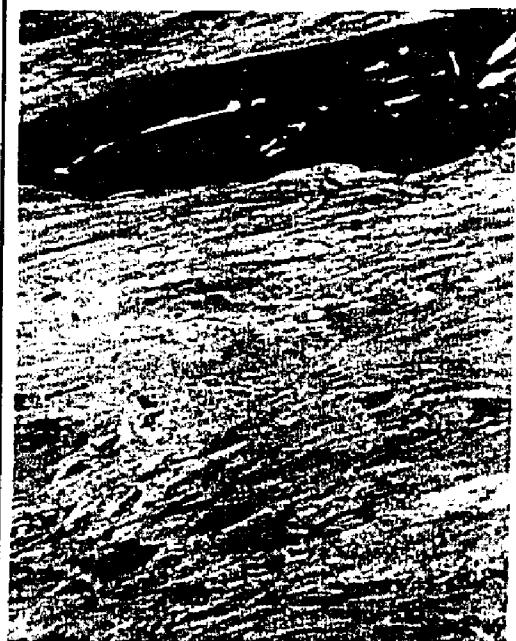
100X, 251°C



100X, 268°C

1,3-BAPDBB/0.75 PMDA/0.25 BPDA

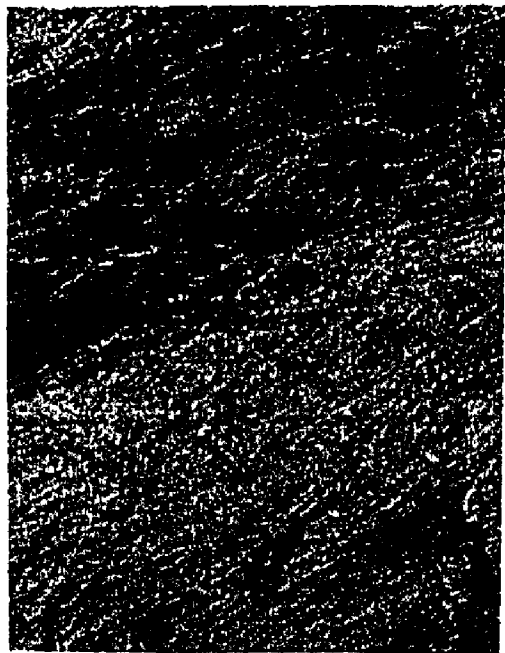




100X, 250°C ←



100X, 221°C ←

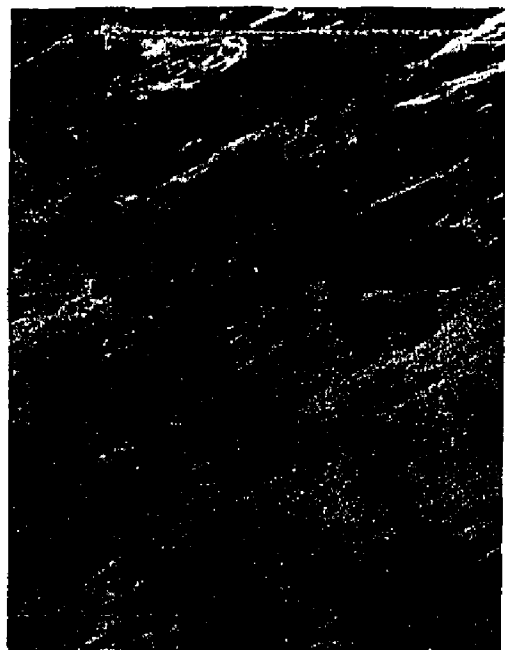


100X, 208°C



100X, 225°C ←

1.3-BAPDBB/0.50 PMDA/0.5 BTDA



100X, 250°C



100X, 23°C



100X, 237°C

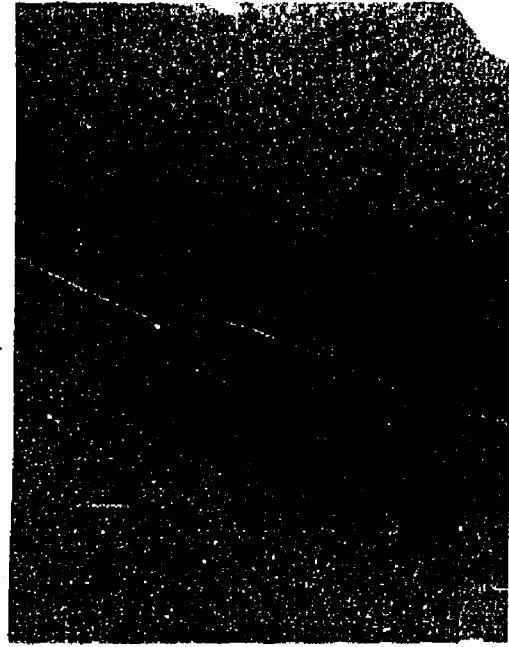


250X, 238°C

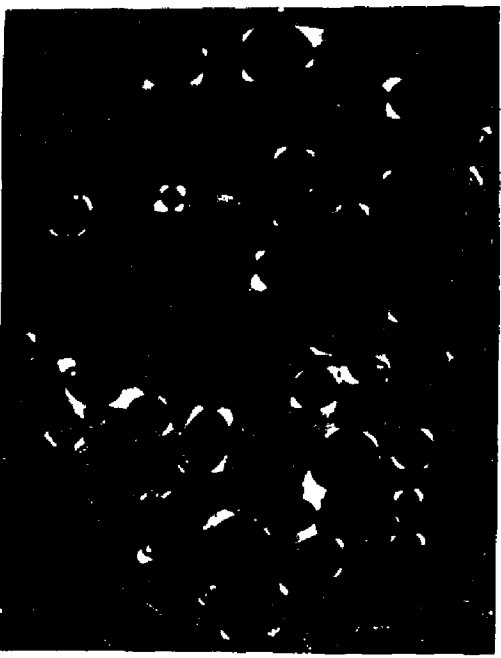
1.3-BAPDBB/0.25 PMDA/0.75 BPDA



100X, 237°C



250X, 23°C



100X, 213°C

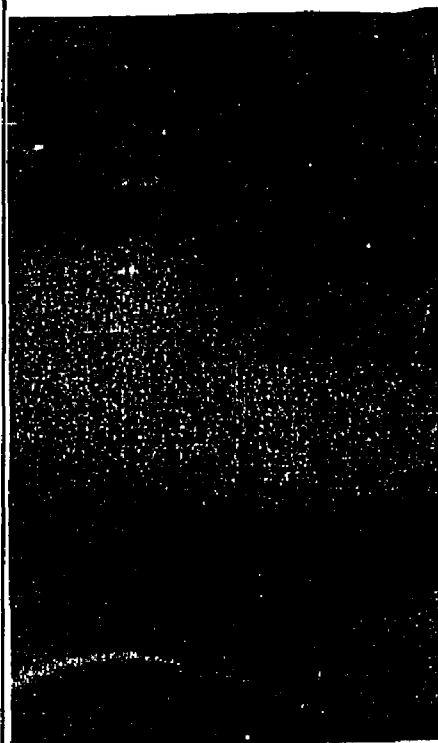


100X, 23°C

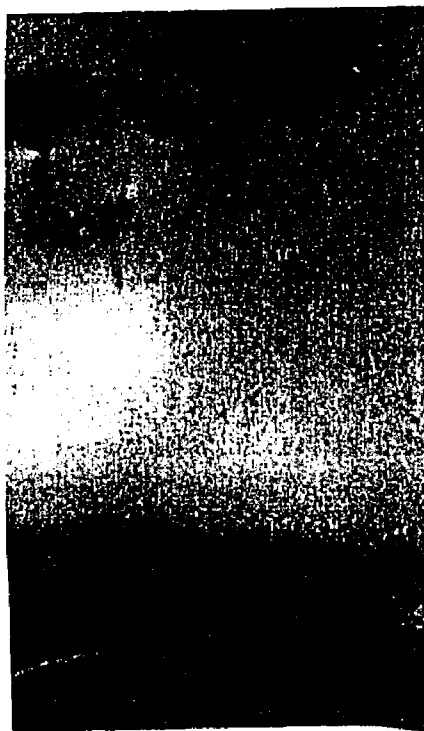
1.3-BAPDBB/0.25 PMDA/0.75 BPDA



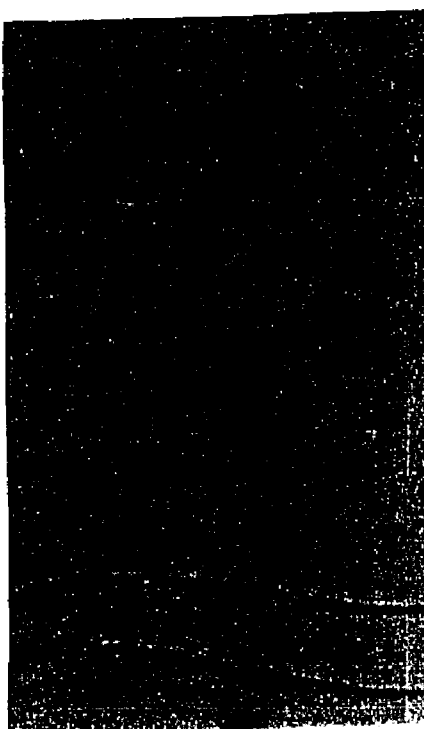
**Glass state ; 533 K**



**Initial liquid crystal phase ; 549 K**



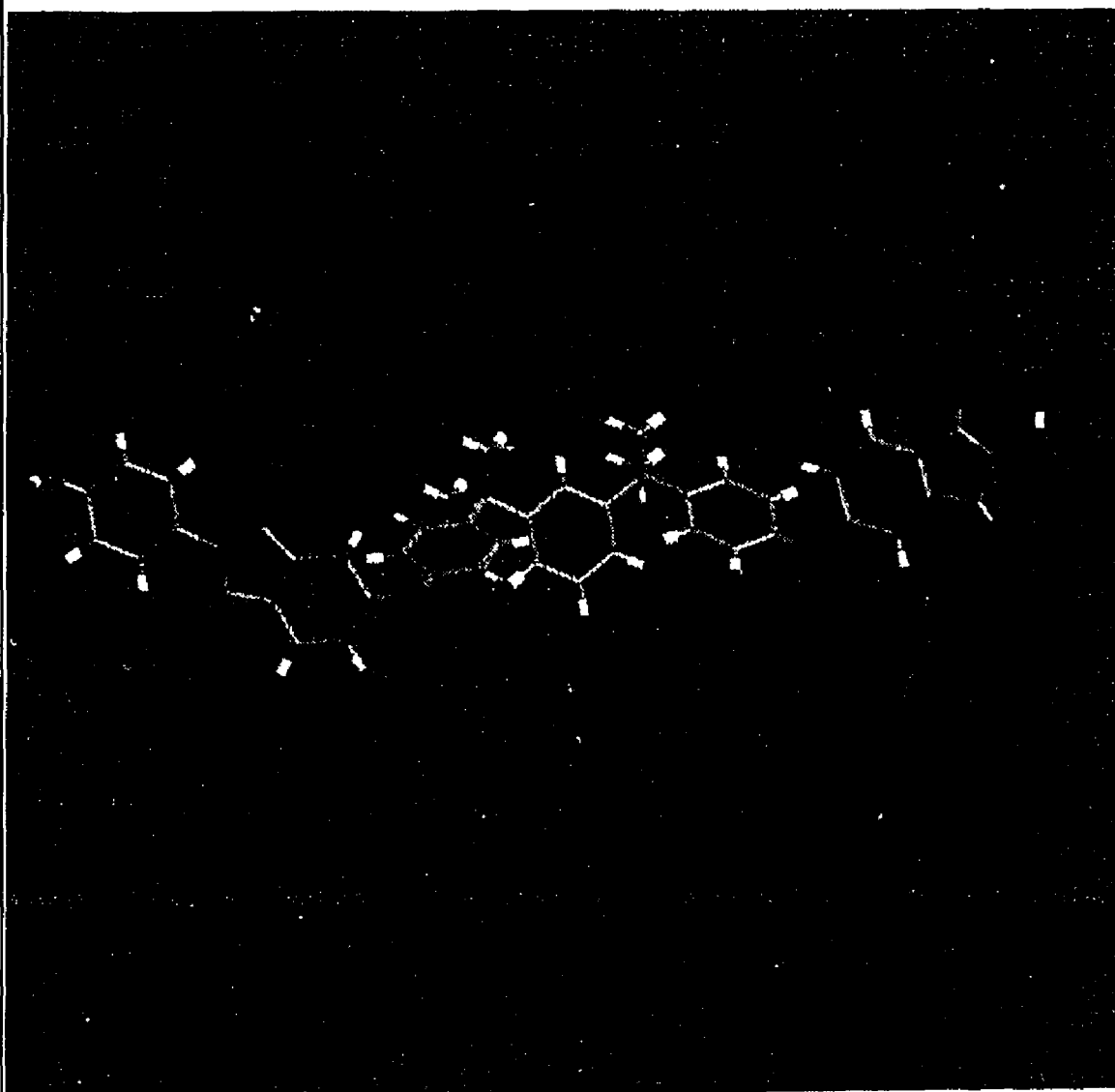
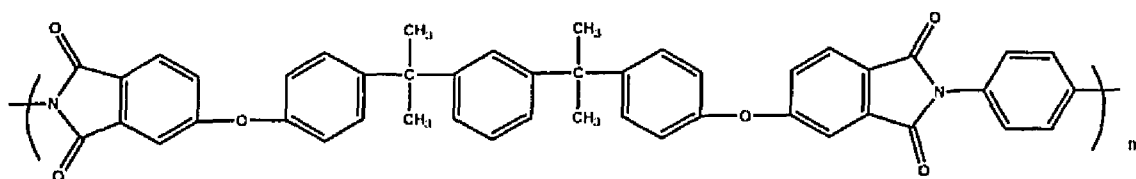
**Final liquid crystal phase ; 587 K**

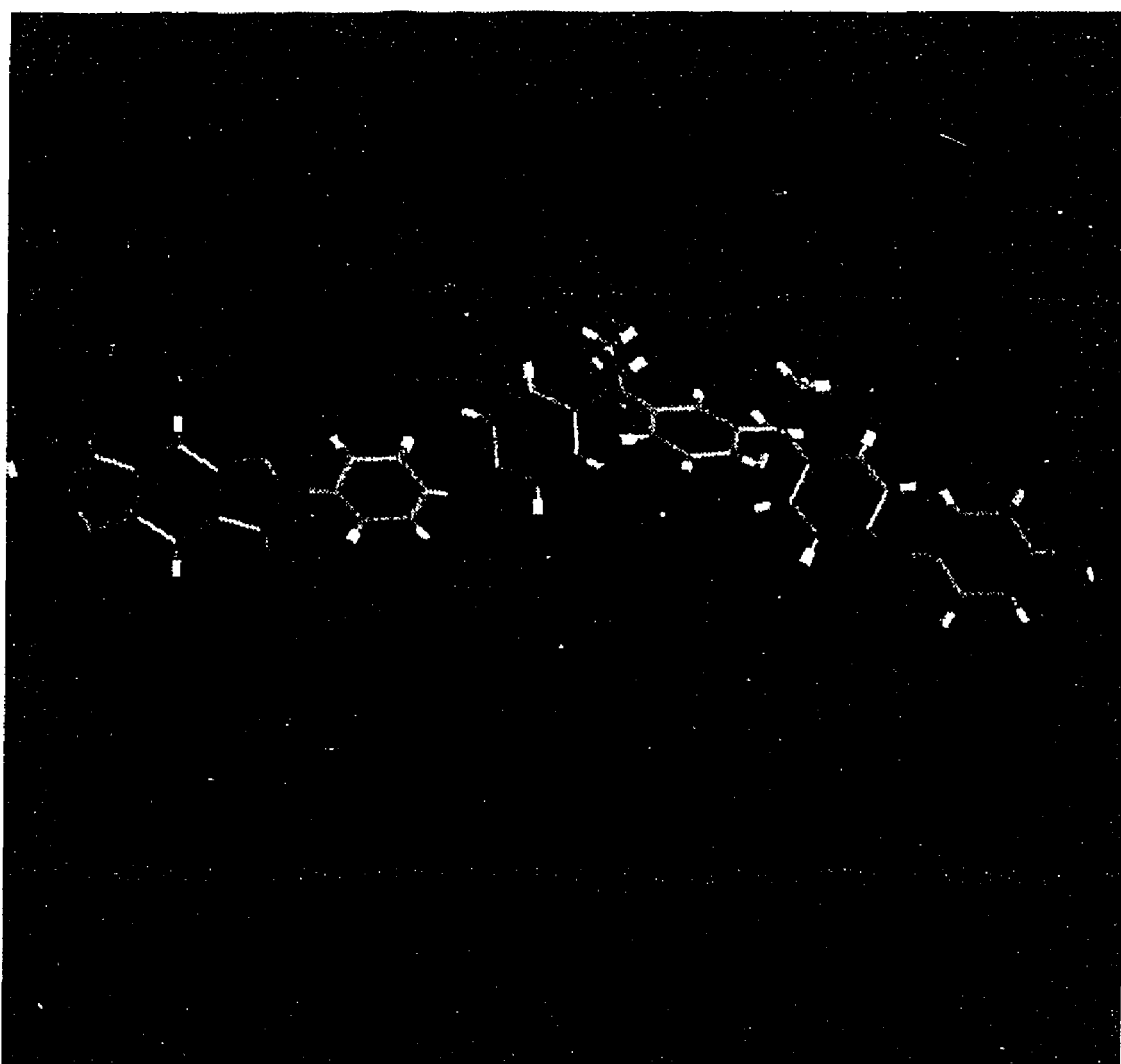
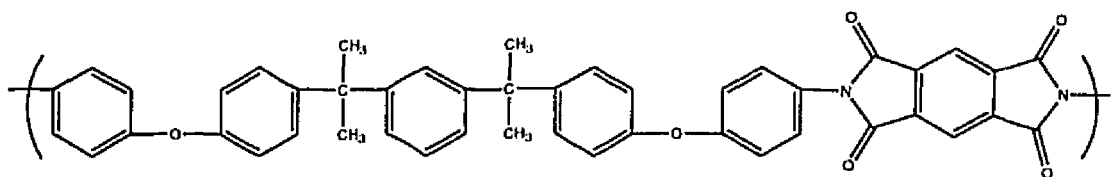


**Isotropic melting state ; 593 K**

POLARIZING MICROPHOTOGRAPHS OF LC-PI  
Provided by Mitsui Toatsu Chemicals, Inc.

# MOLECULAR MODELING





## Synthia Table File

**USER SPECIFIED VALUES**  
 Molecule Name: TEST

**PARAMETERS CORRESPONDING TO THE AVERAGE REPEAT UNIT**

Molecular Weight:	710.79 AMU
Length:(end to end distance)	22.22 Angstroms
Number of Atoms:	88
Number of Non-Hydrogen Atoms:	54
Van der Waals Volume:	381.59 cm <sup>3</sup> mole <sup>-1</sup>
Connectivity indices:	
OX:	37.5176
OXv:	30.0456
IX:	25.8951
IXv:	17.7362
Rotational Degrees of Freedom Parameter:	
Backbone:	10.00
Side Group:	4.00
Total:	14.00

**THERMOPHYSICAL PROPERTIES**

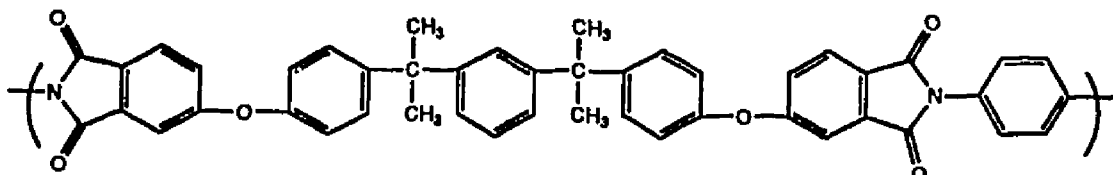
Tg:	463 K
Temp of Half Decomposition: (in inert atm)	816 K
Coefficient of Volumetric Thermal Expansion at 298 K:	213 ppm K <sup>-1</sup>
Molar Volume at 298 K:	579.93 cm <sup>3</sup> mole <sup>-1</sup>
Density at 298 K:	1.226 g cm <sup>-3</sup>
Molar Volume at 0 K:	543.06 cm <sup>3</sup> mole <sup>-1</sup>
Molar Heat Capacity At Constant Pressure (J/(mole*K)) at 298 K:	
Solid:	810.43
Liquid:	1109.91
Delta Cp(Tg):	136.36
Cohesive Energy (kJ mole <sup>-1</sup> ):	
Fedors-like:	284.60
van Krevelen-like:	295.14
Solubility Parameter (SQRT(J cm <sup>-3</sup> )) at 298 K:	
Fedors-like:	22.15
van Krevelen-like:	22.56
Surface Tension calculated using 3 methods at 298 K (dyn/cm):	
Molar Parachor:	47.87
Ecoh-Fedors:	46.66
Ecoh-van Krevelen:	47.81
Thermal Conductivity (J(Kms) <sup>-1</sup> ):	
(at 298 K)	0.19
(at Tg)	0.21

**ELECTRICAL, OPTICAL, AND MAGNETIC PROPERTIES**

Refractive Index: (at 298 K)	1.639
Molar Refraction (Lorentz and Lorenz):	208.59
Dielectric Constant: (at 298 K)	3.08
Volume Resistivity: (ohm*cm at 298 K)	6.87E+16
Diamagnetic Susceptibility: (mole <sup>-1</sup> )	425.11*10 <sup>-6</sup> cm <sup>3</sup>

**MECHANICAL PROPERTIES AT 298 K**

Bulk Modulus:	4904 MPa
Shear Modulus:	1205 MPa
Young's Modulus:	3342 MPa
Poisson's Ratio:	0.386
Shear Yield Stress:	93.57 MPa
Brittle Fracture Stress:	87.66 MPa

**MECHANICAL PROPERTIES AT 493 K (Inception of Rubbery Plateau)**


BMDBDA/p-PDA



## Synthia Table File for BMDEDA/p-PDA (Continued)

Molar Volume:	607.85 cm <sup>3</sup> mole <sup>-1</sup>
Density:	1.169 g cm <sup>-3</sup>
Bulk Modulus:	2213 MPa
Shear Modulus:	1.09 MPa
Young's Modulus:	3.26 MPa
Poisson's Ratio:	0.500
<b>CHAIN STIFFNESS AND ENTANGLEMENT PROPERTIES</b>	
Steric Hindrance Parameter:	1.31
Characteristic Ratio:	3.44
Molar Stiffness Function K (g <sup>0.25</sup> )*(cm <sup>1.5</sup> ) (mole <sup>-0.75</sup> ):	270.09
Entanglement MW:	4414 AMU
Critical MW:	8828 AMU
Entanglement Length:	137.96 Angstroms
<b>TRANSPORT PROPERTIES</b>	
Activation Energy For Viscous Flow (relevant for T > 1.2*Tg):	71.30 kJ mole <sup>-1</sup>
Permeability at 298 K (Dow Units - See documentation)	
O2: 146.4	N2: 37.4
	CO2: 665.2

## BIBLIOGRAPHY

1. Adrova, N. A., Israel program for Scientific Translation, Jerusalem, 1968.
2. Alam, S.; Kandpal, L.; Varna, I. K. *J. Macromol. Sci., Res. Macromol. Chem. Phys.* **1993**, *33*, 291.
3. Androva *et. al.*, *Vysokomol. Soedin* **1979**, *B17(5)*, 409.
4. Aranuma, T.; Oikawa, H.; Ookawa, Y.; Yamaguchi, A. *Polymer Preprint* **1993**, *34(2)*, 827.
5. Ardashnikov, A. Ya.; Kardash, I. Ye.; Pravednikov, A. N. *Polym. Sci. USSR* **1971**, *13(8)*, 2092.
6. Asanuma, T.; Oikawa, H.; Ookawa, Y.; Yamasita, W.; Matsuo, M. *J. Polymer Science Part A: Polymer Chemistry* **1994**, *Vol. 32*, 2111-2118.
7. Auman, B. C. *Polymer Preprints* **1993**, *34(1)*, 443-444.
8. Auman, B. C.; Higley, D. P.; Scherer, K. V. *Polymer Preprints* **1993**, *34(1)*, 389-90.
9. Auman, B. C.; Trofimenko, S. *Polym. Mater. Sci. Eng.* **1992**, *66*, 253-254.
10. Baise, A. I. *J. Appl. Polym. Sci.* **1986**, *32*, 4043.
11. Beaman, R. G. *J. Polym. Sci.* **1955**, *9(5)*, 470.
12. Beck & Co., French Patent 1 373 383, 1964.
13. Bell, V. L.; Gager, H. *J. Polym. Sci.: Polymer Chem. Ed.* **1976**, *Vol. 14*, 2275-2292.
14. Bessonov, M. I.; Koton, M. M.; Kudryavtsev, V. V.; Laius, L. A.; *Polyimides: Thermally Stable Polymers*, 2nd Ed.; Plenum: New York, 1987; p 1-95.
15. Billmeyer, Jr., F. W. *Textbook of Polymer Science*; John Wiley and Sons: NY; 1984.

16. Biosym Technologies, Inc., "Computational Techniques for Solving Polymer Problems"; 1994.
17. Blizzard, K.; Haghghat, R. R. *Polym. Eng. Sci.* **1993**, Vol. 33, No. 13, 799-808.
18. Bogert, T. M.; Renshaw, R. R. *J. Am. Chem. Soc.* **1908**, 30, 1140.
19. Bower, G. M.; Frost, L. J. *Polym. Sci.* **1963**, A1, 3135.
20. Brinegar, W. C.; Fleischer, D.; Kirsch, G. *Hoechst High Chem Magazine* **1992**, 6, 36-45.
21. Brown, G. H.; Crooker, P. P. *Chemical and Engineering News* **Jan. 31, 1983**, 24-37.
22. Calundann, Gordon W. Presented at the The Robert A. Welch Foundation Conferences on Chemical Research, XXVI, Synthetic Polymers, Houston Texas, Nov. 15-17, 1982.
23. Campbell, F. J., "Hydrolytic Deterioration of Polyimide Insulation on Naval Aircraft Wiring", *Proceedings, IEEE Conference on Electrical Insulation and Dielectric Phenomena* **1988**, 180-188.
24. Campbell, F. J., Naval Research Lab, Washington, D. C., 20375-5000, personal communication.
25. Campbell, F. J., "Temperature Dependence on the Hydrolysis of Polyimide Wire Insulation", *IEEE Transactions on Electrical Insulation* **1985**, E1-20, 111-116.
26. Cassidy, P. E. In *Thermally Stable Polymers*; Marcel Dekker Inc.: New York, 1982; Chap. 5.
27. Clark, J. H.; Owen, N. D. S. *Tetrahedron Letters* **1987**, 28(31), 3627-3630.
28. Collins, P. J. In *Liquid Crystals: Nature's Delicate Phase of Matter*, Princeton University Press: Princeton, NJ, 1990; p 162-180.
29. Collyer, A. A. *Material Science and Technology* **Oct. 1990**, 6, 981-992.
30. Collyer, A. A. *Materials Science and Technology* **April 1989**, 5, 309-322.

31. Connell, J. W.; Siochi, E. J.; Croall, C. I. *High Performance Polymers* **1993**, *5*, 1-14.
32. Cox, M. K. *Mol. Cryst. Liq. Cryst.* **1987**, *153*, 415.
33. Critchley, J. P.; Knight, G. J.; Wright, W. W. *Heat Resistant Polymers, Technologically Useful Materials*; Plenum Press: New York and London, 1983; p 185-321.
34. Croall, C. I.; St. Clair, T. L. *Journal of Plastic Films and Sheeting* **July 1992**, *Vol. 8, No. 3*, 172-190.
35. Croall, C. I.; St. Clair, T. L., NASA Technical Memorandum 104202, January 1992.
36. De Iasi, R.; Russell, J. J. *J. Appl. Polym. Sci.* **1971**, *15*, 2965.
37. Dezern, J. F.; Croall, C. I. In *Advances in Polyimide Science and Technology: Proceedings of the Fourth International Conference on Polyimides*; Ellenville, NY, Oct. 30-Nov 1, 1991; p 468-481.
38. Dezern, J. F.; Croall, C. I., "Structure-Property Study of Keto-ether Polyimides", NASA Technical Memorandum 104178, Dec. 1991.
39. Dine-Hart, R. A. ; Wright, W. W. *J. Appl. Polym. Sci.* **1967**, *11*, 609.
40. Dine-Hart, R. A.; Wright, W. W. *Makromol. Chem.* **1971**, *143*, 189.
41. Doherty, R., "Magellan Blaze Linked to Kapton®", *Electronic Engineering Times* **November 1988**, 6.
42. "DuPont High Performance Films, Kapton® Polyimide Films Summary of Properties"; DuPont, Delaware.
43. DuPont's Kevlar®, product information booklet.
44. DuPont's Technical Information, Properties of Nomex® Aramid Filament yarns, Bulletin NX-17, 1981.
45. E. I. du Pont de Nemours and Co., French Patent 1 239 491, 1960.

46. Dutta, D.; Fruitwala, H.; Kohli, A; Weiss, R. A. *Polym. Eng. Sci.* **Mid-Sept. 1990**, Vol. 30, No. 17, 1005-1018.
47. Edwards, W. M. U.S. Patents 3 179 631 and 31 179 634, 1965; Brit. Pat. 898 651, 1959.
48. Edwards, W. M.; Robinson, I. M. U.S. Patents 2 710 853, 1955; 2 867 609, 1959; 2 900 369, 1959.
49. Eftekhari, A.; St. Clair, A. K.; Stoakley, D. M.; Sprinkle, D. R.; Singh, J. J. In *Polymers For Microelectronics, Resists And Dielectrics*; ACS Symposium Series 537, 1994; Chapter 38, p 535-545.
50. *Encyclopedia of Polymer Science and Engineering*, John Wiley and Sons: 1987; Vol. 5; p 638-641.
51. Endrey, A. L. U.S. Patents 3 179 631 and 3 179 633, 1965; Can. Patent 659 328, 1963.
52. Evans, D.; Morgan, J. T. *Cryogenics* **April 1991**, 31, 220-222.
53. Fay, C. C.; Smith, Jr., J. G.; St. Clair, T. L. *Polymer Preprints* **1994**, 35(1), 541-542.
54. Fay, C. C.; Smith, Jr., J. G.; St. Clair, T. L. Presented at the Gordon Research Polymer Conference, Wolfeboro, NH, July 3-8, 1994.
55. Fein, M. *17th National SAMPE Conference Proceedings* **1985**, Vol. 17, 563-570.
56. Feiring, A. E.; Auman, B. C.; Wonchoba, E. R. *Macromolecules* **1993**, 26(11), 2779-84.
57. Foresman, J. B.; Frisch, A. *Exploring Chemistry with Electronic Structures*, Gaussian, Inc: Pittsburgh, PA; p 1-7.
58. Freilich, Steven C., DuPont Central Research and Development, Experimental Station, Wilmington, DE, personal communication.
59. Frost, L. W.; Kesse, J. J. *J. Appl. Polym. Sci.* **1964**, 8, 1039.

60. Fryd, M. In *Polyimides: Synthesis, Characterization, and Applications*; Mittal, K. L., Ed.; 1984; p 377-383.
61. Funk, J. G.; Sykes, Jr., G. F. *SAMPE Quarterly* **1988**, Vol. 19, No. 3, 19-26.
62. Gerber, M. K.; Pratt, J. R.; St. Clair, A. K.; St. Clair, T. L. *Polym. Prepr.* **1990**, 31 (1), 340.
63. Gerber, M. K.; Pratt, J. R.; St. Clair, T. L. In *Proceedings of the Third Conference on Polyimides*, 1988; p 101.
64. Gibbs, H. H.; Breder, C. V. *ACS Polymer Preprints* **1974**, 15(1), 775.
65. Goff, D. L.; Yuan, E. L. *Polymeric Materials: Science and Engineering* **1988**, 59, 186-189.
66. Gordina, T. A.; Kotov, B. V.; Kolninov, O. V.; Pravednikov, A. N. *Vysok. Soyed 15B* **1977**, 237(3), 612.
67. Gordina, T. A.; Kotov, B. V.; Kolniov, O. V.; Pravednikow, A. N. *Vysokomol Soed*, **1973**, B15, 378.
68. Graff, G. *High Technology* **1985**, 62-63.
69. Harris, F. W. In *Polyimides*, Wilson, D.; Stenzenberger, H. D.; Hergenrother, P. M., Eds.; Blackie: Glasgow and London, 1990; p 1-36.
70. Harris, F. W.; Lanier, L. H. In *Structure-Solubility Relationships in Polymers*, Academic Press: 1977; p 183.
71. Hartman, R. V., "Unsafe Aircraft Wiring Poses Expensive Problem", *Defense Electronics* **January 1983**, 34-38.
72. Havens, S. J., NASA Langley Research Center, Polymeric Materials Branch, Laboratory Notebook 39, December 1987; p 12.
73. Havens, S. J., NASA Langley Research Center, Polymeric Materials Branch, Laboratory Notebook 39, October 1987; p 4.
74. Havens, S. J., NASA Langley Research Center, Polymeric Materials Branch, Laboratory Notebook 69, April 1989; p 46.

75. Havens, S. J., NASA Langley Research Center, Polymeric Materials Branch, Laboratory Notebook 121, July 1991; p 79.
76. Havens, S. J., NASA Langley Research Center, Polymeric Materials Branch, Laboratory Notebook 974, August 1983; p 61.
77. Heacock, J. F. In *Proc. 2nd Int. Conf. on Polyimides*, Ellenville, NY, Oct. 30-Nov. 1, 1985; p 174.
78. Heffelfinger, C. J. *Polym. Eng. and Sci.* **Nov. 1978**, Vol. 18, No. 15, 1163-1173.
79. Heffelfinger, C. J.; Schmidt, P. G. *J. Appl. Polym. Sci.* **1965**, Vol. 9, 2661-2680.
80. Hergenrother, P. M.; Jensen, B. J.; Havens, S. J. *Polymer* **Feb. 1988**, Vol. 29, 358-369.
81. *High Modulus Polymers: Approaches to Design and Development*, Zachariades, A. E.; Porter, R. S. , Eds.; Marcel Dekker: New York, 1988.
82. Hinkley, J. A., NASA Langley Research Center, Composites and Polymers Branch, Polymer Scientist, unpublished results.
83. *IEEE Spectrum* **Oct. 1985**, Vol. 22, 20.
84. Jones, R. J.; O'Rell, M. K. US Patent 4 196 277, 1980.
85. Jones, S., "NASA Wondering if Shuttle is Wired for Disaster", *Fort Worth Star-Telegram* **Sept. 21, 1988**, 1-2.
86. Johnson Control, Inc., Milwaukee, WI, Presented at NASA Langley Research Center; 1994.
87. Keating, J., NASA Contractor Report 195048, "Development of LaRC™-IA Thermoplastic Polyimide Coated Aerospace Wiring", Imitec, Inc.; December 1994.
88. Kinjo, N.; Ogat, M.; Nishi, K.; Kaneda, A. "Epoxy Molding Compounds as Encapsulation Materials for Microelectronic Devices" In *Specialty Polymers/Polymer Physics*; Springer-Verlag: New York, 1989; p 1-83.

89. Kochi, M.; Yokata, R.; Iizuka, T.; Mita, I. *J. Polym. Sci.: Part B: Polymer Physics* **1990**, Vol. 28, 2463-2472.
90. Kochi, M.; Yonezawa, T.; Yokata, R.; Mita, I. In *Advances in Polyimide Science and Technology*, Feger, C.; Kojasteh, M. M.; Htoo, M. S., Eds.; Technomic Publishing: Lancaster, PA, 1991; p 375-387.
91. Kreuz, J. A., E. I. DuPont de Nemours and Company, Electronics Department, Circleville, Ohio, unpublished results.
92. Kreuz, J. A.; Endrey, A. L.; Gay, F. P.; Sroog, C. E. *J. Polym. Sci. A-1* **1967**, 4, 260.
93. Kricheldorf, H. R.; Linzer, V. L. *Polymer* **1995**, Vol. 36, No. 9, 1893.
94. Krigbaum, W. R.; Watanabe, J. *Polymer* **1983**, Vol. 24, 1299.
95. Kwolek, S.; Memeger, W.; Van Trump, J. E. In *International Union of Pure and Applied Chemistry*; Lewin, M., Ed.; VCH Publishers: 1988; p 421-454.
96. La Mantia, F. P. *Thermotropic Liquid Crystalline Polymer Blends*, Technomic: Lancaster, PA, 1993; Chapters 1-6.
97. Landis, G. A.; Bailey, S. G.; Flood, D. J. *Space Power* **1989**, Vol. 8, No. 1/2, 31.
98. Lee, Chung-jen Submitted to the Technical Volume Committee of the Society of Plastics Engineering, 1987; *Macromol. Chem. Phys.* **1989**, C29(4), 431-560.
99. Lee, W. A., Royal Aircraft Establishment Technical Report 66409, August 1966.
100. *Liquid Crystallinity in Polymers: Principles and Fundamental Properties*, Ciferri, A., Ed.; VCH Publishers: New York, 1991.
101. Long, Jr., E. R.; Long, S. A. T., NASA Technical Paper 2429, 1985.
102. Magat, E. E. *Phil. Trans. R. Soc. Lond. A* **1980**, Vol. 294A, 453-469.



103. Maraio, Sharon, Oneida Research Services, Inc., Technical Representative, personal communication.
104. March, J. *Advanced Organic Chemistry, Third Edition*, John Wiley and Sons: 1985.
105. Medtronic, Inc., Technical Services Department, Minneapolis, Minnesota, 1-800-328-2518 (EXT. 8575).
106. Meurisse, P.; Noel, C.; Monnerie, L.; Fayolle, B. *Brit. Polym. J.* **1981**, *13*, 55.
107. Morel, D. L.; Ghosh, A. K.; Feng, T.; Stogryn, E. L.; Purwin, P. E.; Shaw, R. F.; Fishman, C. *Appl. Phys. Lett.* **1978**, *32(8)*, 15.
108. Mundhenke, R. F.; Schwartz, W. T. *High Performance Polymers* **1990**, *2(1)*, 57.
109. Noel, C.; Laupretre, F.; Freidrich, C.; Fayolle, B.; Bosio, L. *Polymer* **1984**, *25*, 808.
110. O'Donnell, J. In *Radiation Effects on Polymers*; Clough, R. L.; Shalaby, S. W., Eds.; ACS Symposium Series, 1991; Chapter 24; p 402-413.
111. O'Neill, J. F., "The Kapton® Question", *Aviation Equipment Maintenance* **February 1989**, 26-32.
112. Pedley, M. D.; Leger, L. J., "Considerations in Using Kapton® Wire Insulation in Shuttle Systems"; NASA, Johnson Space Center, August 1988.
113. Policastro, P.P.; Lupinski, J. H.; Hernandez, P. K. *Preprints Polymer Mat. Sci. and Eng.* **1988**, *59*, 209.
114. *Polyimides*; Wilson, D.; Stenzenberger, H. D.; Hergenrother, P. M., Eds.; Blackie: Glasgow and London, 1990.
115. *Polymer and Plastics Technology and Engineering* **1981**, Vol. 17, 139-191.
116. *Polymeric Liquid Crystals*; Blumstein, A., Ed.; Plenum: New York, 1983.

117. *Polymers: An Encyclopedia Source Book of Engineering Properties*, John Wiley and Sons: New York, 1987; p 319-364, 427-476, 509-569.
118. Pratt, J. R.; Blackwell, D. A.; St. Clair, T. L.; Allphin, N. L. *Polymer Engineering and Science* **1989**, *31(1)*, 63-68.
119. Pravednikov, A. N.; Kardash, I. Ye.; Glukhoyedov, N. P.; Ardashnikov, A. Ya.; *Polym. Sci. USSR* **1973**, *15(2)*, 399.
120. Progar, D. J.; St. Clair, T. L. *Journal of Adhesion Science and Technology* **1990**, *Vol. 4, No. 7*, 527-549.
121. Ralph, E. *Space Power* **1989**, *Vol. 8, Nos. 1/2, 3*.
122. Rausch, A., Medtronic, Inc., verbal and written communication.
123. *Recent Advances in Liquid Crystalline Polymers*; Chapoy, L. L., Ed.; Elsevier Applied Science Publishers: New York, 1986; p 136-139.
124. Research Triangle Institute, "NASA Langley's Colorless and Low Dielectric Polyimide Thin Film Technologies", May 1994.
125. Ronca, G.; Yoon, D. Y. *J. Chem. Physics* **1984**, *80*, 930.
126. Rothman, L. B. *J. Electrochem. Soc.* **1980**, *127*, 2216.
127. Sarlin, J.; Tormala, P. J. *J. Appl. Polym. Sci.* **1990**, *Vol. 40*, 453-469.
128. Schwartz, Jr., W. T. *High Performance Polymers* **1990**, *Vol. 2, No. 2*, 189-196.
129. Schwartz, Jr., W. T. US Patent 4 868 316, September, 1989.
130. *Science and Applications of Conducting Polymers*; Salaneck, W. R.; Clark, D. T.; Samuelsen, E. J., Eds.; Adam Higler Publishers: 1991.
131. Scott, Gary W., "Development of Organic Thin Film Solar Cells for Space Applications", CalSpace Proposal CS-11-92, April 1992; p 3-9.
132. Scott, G. W.; Tran, K. *J. Phys. Chem.* **1994**, *98*, 11563-11569.
133. Senturia, S. D. *Proc. of the ACS Div. of Polym. Mat.: Sci. and Eng.* **1986**, *55*, 385.

134. Siegmann , A; Nir, Y. *Polymer Eng. and Sci.* **Mid Feb. 1987**, Vol. 27, No. 3, 225-230.
135. Sillion, B. In *Comprehensive Polymer Science*, Allen, G.; Bevington, J. C., Eds.; Pergamon Press: Oxford, 1989; Vol. 5, Chap. 30.
136. Singh, J. J.; Eftekhari, A.; St. Clair, T. L. *Nucl. Instrum. Methods. Phys. Res.* **1991**, B53, 342-348.
137. Smith, Jr., Joseph G., NASA Langley Research Center, Composites and Polymers Branch, Polymer Scientist, unpublished results, 1993-94.
138. Sroog, C. E. *Prog. Polym. Sci.* **1991**, Vol. 16, 561-694.
139. Sroog, C. E.; Endrey, A. L.; Abramo, S. V.; Berr, C. E.; Edwards, W. M.; Olivier, K. L. *J. Polym. Sci.* **1965**, A3, 1373.
140. St. Clair, A. K.; St. Clair, T. L.; Winfree, W. P. Presented at the National Meeting of the American Chemical Society, Los Angeles, CA, Sept. 25-30, 1988; *Proceeding of the Division of Polymeric Materials: Science and Engineering* **1988**, Vol. 59, 28.
141. St. Clair, A. K.; Slempe, W. S. *SAMPE Journal* **1985**, Vol. 21(4), 28-33.
142. St. Clair, A. K.; St. Clair, T. L. In *Polymers for High Technology, American Chemical Society Symposium Series*, Bowden, M. J.; Turner, S. R., Eds.; 1987; p 437.
143. St. Clair, A. K.; St. Clair, T. L.; Pratt, J. R. Presented at the SPE ANTEC Conference, New Orleans, LA, May 1993.
144. St. Clair, A. K.; St. Clair, T. L. U.S. Patents 4 595 548 and 4 603 061, 1986.
145. St. Clair, A. K.; St. Clair, T. L. U S Patent 5 428 102, 1995.
146. St. Clair, A. K.; St. Clair, T. L.; Slempe, W. S. In *Recent Advances in Polyimide Science and Technology, Proceedings of the 2nd International Conference on Polyimides*,

- Weber, W.; Gupta, M., Eds.; Society of Plastic Engineers, Poughkeepsie, NY, 1987; p 16-36.
147. St. Clair, A. K.; St. Clair, T. L.; Winfree, W. P. U S Patent 5 338 826, August, 1994.
148. St. Clair, T. L. In *Polyimides*; Wilson, D.; Stenzenberger, H. D.; Hergenrother, P. M., Eds.; Blackie: Glasgow and London, 1990; p 58-78.
149. St. Clair, T. L. Presented at the Symposium on Recent Advances in Polyimides and Other High Performance Polymers, Reno, NV, July 13-16, 1987.
150. St. Clair, T. L.; St. Clair, A. K.; Smith, E. N. In *Structure-Solubility Relationships in Polyimides*; Harris, F. W., Ed.; Academic Press: 1977; p 199.
151. Staniland, P. A.; Wilde, C. J.; Bottino, F. A.; Di Pollicino, G.; Recca, A. *Polymer* **1992**, Vol. 33, No. 9, 1976-1981.
152. Stiegman, A. E.; Brinza, D. E.; Anderson, M. S.; Minton, T. K.; Laue, F. G.; Liang, R. H., Jet Propulsion Laboratory Publication 90-10, 1991.
153. Stoakley, D. M.; St. Clair, A. K.; Baucom, R. M. Presented at the SAMPE Electronic Conference, Los Angeles, CA, June 19-22, 1989.
154. Stoakley, D. M.; St. Clair, A. K.; Croall, C. I. *Journal of Applied Polymer Science* **1994**, Vol. 51, 1479-1483.
155. Stotts, L. J.; Infinger, K. R.; Babka, J.; Genzer, D. *IEEE Journal of Solid State Circuits* **April 1989**, Vol. 24, 292-300.
156. Svelichnyi, V. M.; Kalinish, K. K.; Kudryavtsev, V. V.; Koton, M. M. *Dokl. Akad. Nauk* **1977**, 237(3), 612.
157. T. M. Long Film Stretcher Manual.
158. Tai, H.; Phillips, D. H., NASA Technical Memorandum 101674, June 1990; p 1-97.

159. Takahashi, N.; Yoon, D. Y.; Parrish, W. *Macromolecules* **1984**, *17*, 2583-2588.
160. Takekoshi, T. In *Polyimides*; Wilson, D.; Stenzenberger, H. D.; Hergenrother, P. M., Eds.; Blackie: Glasgow and London, 1990; p 38-57.
161. Takekoshi, T. U.S. Patent 3 847 870, 1974.
162. Tenney, D. In NASA Conference Publication 3035, Part 1, 1989; p 25-52.
163. Thoma, Paul *et. al.* U S patent 5 408 381, April, 1995.
164. Thomas, L. D.; Roth, D. D. *ChemTech* **Sept. 1990**, 546-550.
165. "Upilex® Polyimide Films, Technical DataSheet", ICI Films.
166. Vinogradova, S. V.; Vygodskii, Ya. S.; Korshak, V. V. *Polym. Sci. USSR* **1970**, *12(9)*, 2254.
167. Wong, C. P., "Application of Polymer in Encapsulation of Electronic Parts" In *Electronic Applications*; Springer-Verlag: 1988; p 63-83.
168. Wong, C. P., "Recent Advances in IC Passivation and Encapsulation" In *Polymers for Electronic and Photonic Applications*; Wong, C. P., Ed.; Academic Press, Inc.: 1993; p 167-220.
169. Yamaguchi, K.; Urakami, U.; Tanabe, Y.; Yamazaki, M.; Tamai, S.; Yamaya, N.; Ohta, M.; Yamaguchi, A. Eur. Pat Appl. EP 425 265, May 2, 1991; *Chem. Abstr.* **1992**, *115*, 93782n.
170. Yamaguchi, K.; Urakami, U.; Tanabe, Y.; Yamazaki, M.; Tamai, S.; Yamaya, N.; Ohta, M.; Yamaguchi, A. Eur. Pat Appl. EP 425 265, May 2, 1991; *Chem. Abstr.* **1992**, *115*, 93782n.
171. Yonezawa, T. Masters Thesis, The University of Tokyo, 1990, 71 (reference not obtainable).

172. Zubkov, V. A.; Koton, M. M.; Kudryavtsev, V. V.; Svelichnyi, V. M.; Zh.  
*Org. Khim.* **1981**, *17(8)*, 1682.

**VITA****Catharine Irene Croall Fay**

Born January 28, 1962 in Alexandria, Virginia. She graduated from Menchville High School in June, 1980. She received a B.S. Degree in Chemistry with a minor in Spanish from Virginia Polytechnic Institute & State University in December, 1984. From 1985-1989, she was employed by NASA at Langley Research Center in the Apprentice Program for Engineering Technology. She graduated from the Apprentice Program in October, 1989. From 1990-1994, she was employed by Lockheed Engineering and Sciences Company as a Senior Scientist Associate, during which time she was accepted into the Ph.D. Program in Applied Science at the College of William and Mary. She received a M.S. Degree in Applied Science in August, 1994 and a Ph.D. in Applied Science, Polymer Chemistry in December, 1995. After graduation, she will work at NASA's Langley Research Center as a doctoral fellow with the National Research Council.